

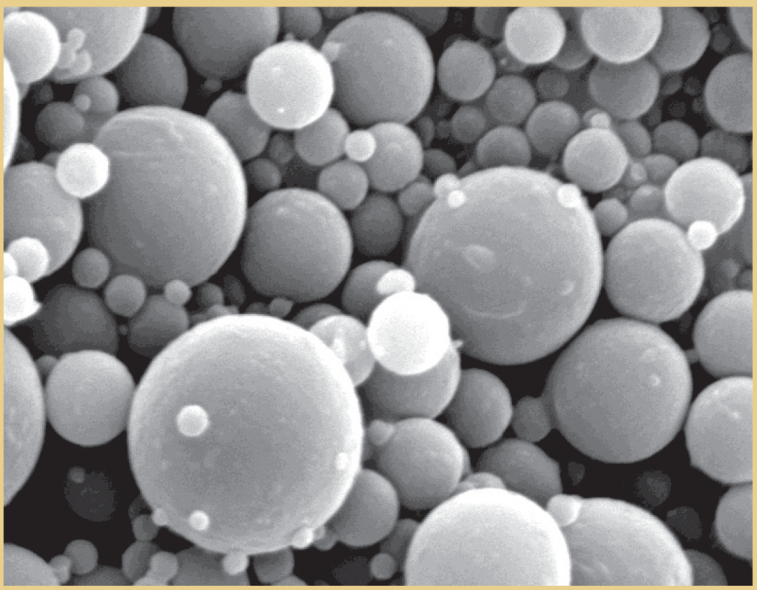
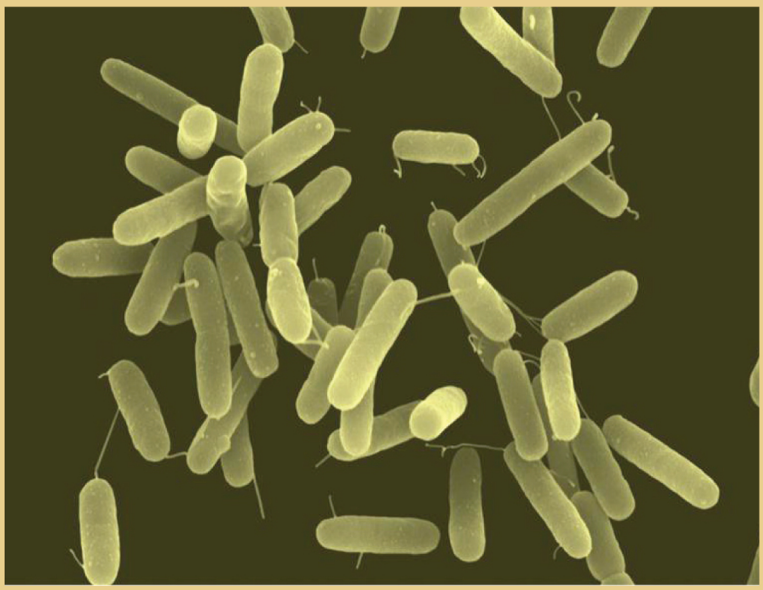

Marisa da Costa Gaspar

PULMONARY TARGETING AND BIOPHARMACEUTICAL EVALUATION OF LEVOFLOXACIN ADMINISTERED AS INNOVATIVE MICROSPHERE AEROSOLS

Tese de Doutoramento em Ciências Farmacêuticas, especialidade de Tecnologia Farmacêutica, orientada pelo Professor Doutor João José Martins Simões de Sousa e pelo Professor Doutor Alberto António Caria Canelas Pais e apresentada à Faculdade de Farmácia da Universidade de Coimbra

Maio 2016

· U C ·

Universidade de Coimbra

Marisa da Costa Gaspar

PULMONARY TARGETING AND BIOPHARMACEUTICAL EVALUATION OF LEVOFLOXACIN ADMINISTERED AS INNOVATIVE MICROSPHERE AEROSOLS

FACULDADE DE FARMÁCIA

UNIVERSIDADE DE COIMBRA

2016

The research work presented in this thesis was developed under the supervision of Professor *JOÃO JOSÉ MARTINS SIMÕES DE SOUSA* from the Pharmaceutical Technology Laboratory, Faculty of Pharmacy, University of Coimbra, Professor *ALBERTO ANTÓNIO CARIA CANELAS PAIS* from the Department of Chemistry, Faculty of Sciences and Technology, University of Coimbra and Professor *JEAN-CHRISTOPHE OLIVIER*, from the Faculty of Pharmacy and Medicine, University of Poitiers, France.

O trabalho experimental apresentado nesta tese foi desenvolvido sob orientação científica do Professor Doutor *JOÃO JOSÉ MARTINS SIMÕES DE SOUSA* do Laboratório de Tecnologia Farmacêutica da Faculdade de Farmácia da Universidade de Coimbra (FFUC), do Professor Doutor *ALBERTO ANTÓNIO CARIA CANELAS PAIS* do Departamento de Química da Faculdade de Ciências e Tecnologia da Universidade de Coimbra (FCTUC) e do Professor Doutor *JEAN-CHRISTOPHE OLIVIER* da Faculdade de Farmácia e Medicina da Universidade de Poitiers, França.

We ourselves feel that what we are doing is just a drop in the ocean.
But the ocean would be less because of that missing drop.

Mother Teresa

ACKNOWLEDGEMENTS

I would like to express my sincere gratitude to everyone who contributed to complete this step of my life, the PhD, a “real adventure” with a number of challenges and obstacles to overcome!

Estou especialmente grata ao meu orientador Professor Doutor JOÃO JOSÉ MARTINS SIMÕES DE SOUSA, da FFUC, por todo o conhecimento que me transmitiu ao longo desta maratona mas também e não só pela confiança que depositou em mim, pela disponibilidade, motivação e energia positiva, e ainda pelas muitas palavras de encorajamento, essenciais para enfrentar as situações mais difíceis!

Ao meu orientador Professor Doutor ALBERTO ANTÓNIO CARIA CANELAS PAIS do Departamento de Química da FCTUC, dotado de uma sabedoria incrível, o meu agradecimento especial pela dedicação, apoio e paciência, mas também pela disponibilidade para analisar as questões que a ciência e a investigação muitas vezes nos colocaram ao longo deste percurso.

Ao Professor Doutor FRANCISCO BAPTISTA VEIGA, expresso a minha gratidão pelas palavras simpáticas, pelo acolhimento na FFUC bem como pela disponibilidade que sempre demonstrou. Agradeço ainda por ter proporcionado todas as condições necessárias ao desenvolvimento do trabalho.

À Professora Doutora Olga Cardoso, da FFUC, estou grata pela disponibilidade imediata demonstrada para colaborar e auxiliar na execução dos estudos *in vitro* de atividade antibacteriana.

Agradeço ainda à Professora Doutora Elisa Serra e à Professora Doutora Dina Murtinho, ambas do Departamento de Química da FCTUC, pela simpatia mas também pelo apoio que sempre manifestaram na resolução de questões específicas da área da química, que surgiram ao longo do trabalho desenvolvido.

Estendo ainda o meu agradecimento aos restantes Professores da FFUC e FCTUC que contribuíram para o culminar desta etapa e pela admiração, simpatia e apoio demonstrados.

Je tiens à exprimer mes profonds remerciements au Professeur JEAN-CHRISTOPHE OLIVIER, pour son aide lors du travail que j'ai développé au sein du laboratoire INSERM U1070, à Poitiers, et pour l'ensemble des discussions et conseils scientifiques sur mon sujet de recherche. Je le remercie également pour son aide durant les moments difficiles et pour ces encouragements qui ont su me remotiver.

Je souhaite exprimer toute ma gratitude au Professeur WILLIAM COUET pour son accueil au sein du laboratoire INSERM U1070, à Poitiers, et pour l'ensemble de ses conseils et sa gentillesse au quotidien.

Un remerciement spécial au Professeur SANDRINE MARCHAND pour la transmission de savoirs concernant les études pharmacocinétiques, et aussi à Madame ISABELLE LAMARCHE pour son aide lors des expérimentations animales et au Docteur NICOLAS GRÉGOIRE pour son aide lors de la modélisation des résultats pharmacocinétiques et pour sa disponibilité. Je souhaite aussi exprimer ma gratitude, au Monsieur PATRICE GOBIN pour son intérêt et aide au travail analytique, au Docteur JULIEN BRILLAUT pour son aide sur les études d'évaluation de cytotoxicité des formulations et au Docteur FRÉDERIC TEWES pour ses suggestions sur le travail de développement galénique.

Je remercie aussi l'ensemble des membres de l'INSERM U1070, et plus particulièrement Madame AGNÈS AUDURIER, Monsieur CHRISTOPHE ADIER, Monsieur JULIAN LAROCHE et Madame MURIEL GOURICHON pour l'accueil, la gentillesse et l'aide précieuse que j'ai reçus au laboratoire. Je remercie les laboratoires IMAGEUP et BIOCYDEX à Poitiers pour leurs collaborations sur mon travail de recherche et pour leur accueil.

Je souhaite aussi exprimer toute ma gratitude à mes collègues et amis de l'INSERM U1070, ALEXIA CHAUZY, ALEXIS VIEL, BARBARA LAMY, ETIENNE MERIGLIER, GUILLAUME AMPLE, MATTHIEU JACOBS, ROMAIN CARREZ et SOPHIE MAGREAULT pour les moments agréables passés au laboratoire, mais aussi pour les autres moments amusants passés en dehors du laboratoire. Un grand merci à mon amie JULIA BERGHOFF, à qui j'ai eu l'opportunité de transmettre quelques savoirs scientifiques, mais surtout pour la grande amitié qui est née, et pour tous les moments de bonheur et de complicité, Danke schön! Merci beaucoup à mon amie SITI NANI NURBAETI pour la bonne humeur et le grand sourire au quotidien, mais aussi surtout pour la grande amitié. Terima kasih!

Merci à tous mes amis "lusophones" et/ou d'électrochimie, particulièrement ISMAIL SEGHIR, MANUEL MORA, ROBERTA ISIDORO, RODRIGO SILVA, SAMUEL DESSOURCES et THOMAS AUDICHON et aussi à BRUNA TERRA, DANILO BEDOR, JACKSON KORCHAGIN, KARINE MELO, LUIZA NUNES, NOELY CAVALCANTI et VANESSA BERTOLAZI, pour l'amitié mais aussi pour avoir ensoleillé ma vie à Poitiers et pour le encouragement, même quand le ciel était trop gris, et pour tous les bons moments passés avec vous.

À minha amiga Cláudia Bispo, agradeço de forma especial, pela amizade, bons momentos e pelo apoio, nomeadamente na adaptação à vida de Poitiers e nos momentos mais difíceis, especialmente nos "tropeços" da saúde! Agradeço também por ser " a amiga que está sempre lá" mesmo que a distância também esteja!

Muito Obrigada aos meus colegas e amigos da FFUC, ANA CLÁUDIA SANTOS, ANA FORTUNA, ANA SERRALHEIRO, CARLA VARELA, DANIELA GONÇALVES, DIOGO FONSECA, DULCE BENTO, EDNA SOARES, FILIPA LEBRE, IVO MÚRIAS, JOANA BICKER, JOANA SEQUEIRA, JOANA SOUSA, JOÃO ABRANTES, MARLENE LOPES, RAQUEL TEIXEIRA, RITA FIGUEIRAS, SANDRA JESUS, SÉRGIO SILVA e SUSANA SIMÕES pela amizade de cada um, de maneira diferente e em momentos distintos, mas também pelo convívio e interajuda durante este percurso. Estou também muito grata à D. GINA pela amizade, palavras simpáticas e disponibilidade que sempre demonstrou. Agradeço ainda à CARLA VITORINO da FFUC pela amizade, mas também pelo incentivo e sugestões que sempre me deu e ainda pela ajuda na obtenção das imagens de microscopia, e à TÂNIA FIRMINO da FCTUC pela incrível disponibilidade para ajudar nas questões de trabalho que envolviam linguagem de programação e pela simpatia.

Muito agradeço aos meus amigos HENRIQUE SOUSA, LUÍS FERREIRA, MARCO PATRÍCIO, PEDRO ALMEIDA, RAQUEL GOMES, STEVEN DA COSTA e VÉRONIQUE GOMES bem como às minhas amigas da "Tertúlia" (ANA RAQUEL ANDRADE, ANA RITA SANTOS, CÁTIA SOUSA, INÊS PEREIRA, JOANA MORAIS, MADALENA RIBEIRO, MARIA INÊS CORREIA, MARIA INÊS LUZIO e TERESA PRIOR) pelo apoio e momentos partilhados mas também pelo perdurar da amizade.

Aos meus PAIS agradeço por tudo! "Tudo" não cabe numa folha de papel mas inclui a paciência, o carinho, o apoio constante, mesmo nos momentos de maior desânimo, a força que sempre me transmitiram, mesmo a muitos quilómetros de distância, e a confiança que sempre depositaram em mim! Obrigada por acreditarem e me fazerem acreditar que tudo

seria possível! Estendo ainda o meu Muito Obrigada ao meu irmão, FLORIAN, pela amizade, pelo seu constante apoio e força, mas também pelos momentos de alegria e cumplicidade partilhados.

Por último, gostaria ainda de agradecer o financiamento da FUNDAÇÃO PARA A CIÊNCIA E TECNOLOGIA (FCT) através da atribuição da Bolsa de Doutoramento com a referência SFRH/BD/80307/2011.

MUITO OBRIGADA A TODOS!

JE TIENS A REMERCIER TOUT LE MONDE!

TABLE OF CONTENTS

Chapter 3

METHODS FOR PREPARATION AND CHARACTERIZATION OF POLYMERIC MICROSPHERES

Chapter 4

OPTIMIZATION OF LEVOFLOXACIN-LOADED CROSSLINKED CHITOSAN MICROSPHERES FOR INHALED AEROSOL THERAPY

Chapter 5

LEVOFLOXACIN-LOADED PLGA MICROSPHERES FOR SUSTAINED RELEASE IN LUNGS: DEVELOPMENT AND CHARACTERIZATION

Chapter 6

PULMONARY PHARMACOKINETICS OF LEVOFLOXACIN IN RATS AFTER AEROSOLIZATION OF IMMEDIATE RELEASE CHITOSAN OR SUSTAINED RELEASE PLGA MICROSPHERES

Chapter 7

CONCLUSIONS AND PERSPECTIVES FOR FURTHER STUDIES

Appendix 1

SCREENING OF CROSSLINKING AGENTS

Appendix 2

HPLC METHOD VALIDATION FOR DETERMINATION OF LEVOFLOXACIN IN MICROSPHERE SYSTEMS

Appendix 3

METHOD VALIDATION FOR LEVOFLOXACIN DETERMINATION IN BRONCHO-ALVEOLAR LAVAGE FLUID BY LC – MS/MS

ABSTRACT

Cystic Fibrosis (CF) is a genetic disease caused by mutations in the CF transmembrane regulator gene on chromosome 7. Thus, function of the chloride channel is compromised leading to thick mucus, which is especially alarming for the respiratory system. The first aim of this thesis was to better understand and characterize both the pulmonary system and the CF disease. Actually, lung damage with declining lung function and presence of infections are common in CF patients. *Pseudomonas aeruginosa* is the main pathogen leading to chronic infection. A number of therapeutic strategies have been developed and usually a combination of intravenous, oral and inhaled antibiotics is conducted. However, the lack of new molecules to improve antibiotic treatment leads to the development of innovative drug delivery systems, which can be especially interesting for direct delivery to the lungs.

In this context, the work described in this thesis aimed at developing new anti-infective biodegradable and biocompatible dry-powder formulations for pulmonary administration. Therefore, innovative microspheres (MS) loaded with levofloxacin (LVX) were prepared from chitosan (immediate release) or PLGA (sustained release), representing promising alternatives to the LVX nebulized solutions.

In a first step, LVX-loaded chitosan MS crosslinked with glutaraldehyde were prepared by the spray-drying method. A factorial design approach was conducted to optimize particle size, a key factor for lung delivery. Safer crosslinking agents, genipin, DL-glyceraldehyde and glutaric acid, were subsequently included in distinct MS, to stabilize the MS structure. A set of analyses for physical and chemical MS characterization, including the swelling behavior, were carried out. *In vitro* studies on antibacterial activity, cytotoxicity evaluation, aerodynamic diameter determination and LVX release were also performed. Similar immediate release profiles were obtained for all formulations and antibacterial activity results were similar to those obtained with free LVX. MS were spherical with smooth surface and LVX in amorphous state and/or molecularly dispersed in the polymeric matrix. Swelling degree was substantially higher for the MS crosslinked with genipin and glutaric acid, being these the best candidates to escape from phagocytosis. They also presented the best aerodynamic and cell viability related-properties.

LVX-loaded PLGA MS were also successfully obtained by double emulsion solvent evaporation method with a premix membrane homogenization step. The preparation method was improved in order to increase drug content, since high soluble drugs such as LVX tend to easily escape to the aqueous phase. PLGA MS were characterized, by several techniques and *in vitro* release studies were also performed. The final selected formulation presented both suitable particle size and drug loading, good incorporation of LVX and spherical morphology. Also, adequate results of biodegradability and biocompatibility were achieved. Promising *in vitro* LVX release behavior was obtained, with sustained release up to 72 hours, which can represent a benefit when compared to LVX /LVX solution by reducing systemic toxicity and increasing lung concentrations.

Finally, a pharmacokinetic study with rats was conducted to evaluate the *in vivo* performance of the selected polymer-based MS after intratracheal administration: an immediate-release formulation (LVX-loaded chitosan MS crosslinked with genipin) and a sustained-release formulation (LVX-loaded PLGA MS). LVX solutions for intravenous administration and intratracheal aerosolization were also included in the study, for comparison. Pharmacokinetic results from plasma and bronchoalveolar lavage samples confirmed the LVX fast release from chitosan MS making them an easy-to-use and more stable alternative to LVX solution for inhalation. For PLGA MS, a sustained release was successfully achieved, with very high LVX pulmonary concentrations, improving antibacterial efficacy. These findings highlight this inhaled formulation as a promising delivery system, improving CF patients' compliance to the therapy due to fewer and faster administrations per day, when compared to nebulized solutions.

RESUMO

A Fibrose Quística (FQ) é uma doença genética causada por mutações no gene regulador da condutância transmembranar da FQ, no cromossoma 7. Desta forma, a função do canal cloreto é comprometida levando à formação de muco espesso, sendo particularmente alarmante no caso do sistema respiratório. O primeiro objetivo desta tese consistiu na melhor compreensão e caracterização quer do aparelho respiratório quer da doença. Os doentes com FQ sofrem frequentemente de danos no pulmão com diminuição da função pulmonar e infeções diversas. A bactéria *Pseudomonas aeruginosa* é o agente patogénico principal, conduzindo habitualmente a infeção crónica. Várias estratégias terapêuticas têm sido desenvolvidas, as quais envolvem normalmente a combinação de antibióticos por via oral, intravenosa e inalatória. No entanto, a escassez de novas moléculas para melhorar a terapia antibacteriana obriga ao desenvolvimento de sistemas inovadores de administração de fármacos, os quais são especialmente interessantes para administração local ao nível pulmonar.

Neste contexto, o principal objetivo do trabalho descrito nesta tese foi o desenvolvimento de novas formulações biodegradáveis e biocompatíveis para administração pulmonar de agentes anti-infecciosos sob a forma de pó seco. Com esta finalidade foram preparadas microsferas (MS) inovadoras com a incorporação de levofloxacina (LVX) usando o quitosano (libertação imediata) ou o PLGA (libertação controlada), em formulações alternativas, promissoras às soluções nebulizadas de LVX.

Numa primeira fase, foram preparadas, pelo método de atomização, MS de quitosano com incorporação de LVX, reticuladas com glutaraldeído. Foi incluída uma abordagem de planeamento fatorial de forma a otimizar o tamanho de partícula, um parâmetro fulcral na administração pulmonar. Reticulantes mais seguros, como o genipin, o DL-gliceraldeído e o ácido glutárico foram depois considerados e incorporados separadamente, com o intuito de estabilizar a estrutura das MS. Efetuaram-se análises de caracterização das MS, incluindo a avaliação do grau de intumescência, e ainda estudos *in vitro*, nomeadamente para avaliação da atividade antibacteriana, citotoxicidade, diâmetro aerodinâmico e libertação da LVX. Foram obtidos perfis de libertação rápida de LVX para todas as formulações e atividades antibacterianas idênticas às encontradas para a LVX propriamente dita. Para além disso, as MS obtidas apresentaram morfologia esférica

com superfície lisa e a LVX no estado amorfo e/ou molecularmente dispersa na matriz polimérica. O grau de intumescência foi substancialmente maior para as MS reticuladas com genipin ou ácido glutárico, permitindo-lhes mais facilmente escapar da fagocitose. Estas MS apresentaram também as melhores propriedades aerodinâmicas e de viabilidade celular.

A incorporação de LVX foi também efetuada em MS de PLGA, as quais foram preparadas pelo método de dupla emulsificação com evaporação de solvente combinado com homogeneização (da emulsão pré-formada) por extrusão através de uma membrana. Incluíram-se algumas alterações de forma a aumentar a quantidade de LVX incorporada, uma vez que fármacos muito hidrossolúveis tendem a escapar para a fase aquosa. As MS foram depois caracterizadas recorrendo a várias técnicas. Foram também efetuados estudos de libertação *in vitro*. A formulação selecionada apresentou tamanho de partícula e dosagem de LVX considerados adequados. Técnicas adicionais revelaram uma apropriada incorporação da LVX, MS de morfologia esférica bem como bons resultados de biodegradabilidade e biocompatibilidade. No que diz respeito ao perfil de libertação, a LVX foi libertada de forma controlada ao longo de 72 h a partir das MS de PLGA, consistindo numa clara vantagem relativamente à LVX e soluções de LVX, devido à redução da toxicidade sistémica e obtenção de elevadas concentrações de fármaco ao nível pulmonar.

Por último, foi realizado um estudo farmacocinético com ratos com o objetivo de avaliar a eficácia das duas formulações poliméricas selecionadas para administração intratraqueal: 1) MS de quitosano reticuladas com genipin e caracterizadas por libertação imediata de LVX; 2) MS de PLGA caracterizadas por libertação controlada de LVX. Duas soluções de LVX, uma para administração intravenosa e outra para nebulização foram também incluídas, para efeitos de comparação. Os resultados obtidos a partir das amostras do plasma e lavagem broncoalveolar confirmaram a libertação rápida da LVX a partir das MS de quitosano, as quais consistem numa alternativa mais estável e fácil de administrar quando comparadas com as soluções de LVX. Relativamente às MS de PLGA, foi obtida uma libertação prolongada com elevados níveis de LVX ao nível pulmonar, potenciando a atividade antibacteriana. Por último, importa salientar que estes resultados indicam que as MS de PLGA são bastante prometedoras, permitindo melhorar a adesão à terapêutica devido ao menor número e mais rápidas administrações por dia, relativamente às soluções nebulizadas.

LIST OF ABBREVIATIONS

ACI	Andersen cascade impactor
ASL	Airway surface liquid
AT I	Alveolar type I
AT II	Alveolar type II
ATR-FTIR	Attenuated total reflectance Fourier transform infrared spectroscopy
AUC	Area under (concentration versus time) curve
BAL	Broncho-alveolar lavage
BCS	Biopharmaceutics classification system
BET	Brunauer, Emmett and Teller
CF	Cystic Fibrosis
CFTR	CF transmembrane conductance regulator
CIP	Ciprofloxacin
COPD	Chronic obstructive pulmonary disease
cp	Centipoise
CV	Coefficient of variation
d_a	Aerodynamic diameter
DCM	Dichloromethane
d_g	Geometric diameter
DL	Drug loading
DMEM/ F-12	Dulbecco's modified Eagle's medium/ F-12 nutrient mixture
DMSO	Dimethyl sulfoxide
DNA	Deoxyribonucleic acid
DNase	Deoxyribonuclease
DPI	Dry-powder inhaler
DPPC	Dipalmitoyl phosphatidylcholine
DSC	Differential scanning calorimetry
DTA/ TGA	Differential Thermal Analysis/ Thermal Gravimetric Analysis
D_v	Mean size of the volume distribution
ED	Emitted dose
EE	Entrapment efficiency

ELF	Epithelial lining fluid
EMA	European Medicines Agency
FBS	Fetal bovine serum
FDA	US Food and Drug Administration
FEV_1	Volume exhaled at the end of the first second of forced expiration
FPD	Fine particle dose
FPF	Fine particle fraction
GA	Glutaric acid
GL	Glutaraldehyde
GLY	DL - glyceraldehyde
GNP	Genipin
GRAS	Generally recognized as safe
GSD	Geometric standard deviation
HBSS	Hanks' balanced salt solution
HIP	Hydrophobic ion pairing
HPLC	High performance liquid chromatography
IS	Internal standard
IT	Intratracheal
IV	Intravenous
LA	Lauric acid
LC - MS	Liquid chromatography – mass spectrometry
LOQ	Lower limit of quantification
LVX	Levofloxacin
MIC	Minimum inhibitory concentration
MMAD	Mass median aerodynamic diameter
MRM	Multiple reaction monitoring
MRSA	Methicillin-resistant staphylococcus aureus
MS	Microspheres
MS/MS	Tandem mass spectrometry
MTS	3-(4,5-dimethylthiazol-2-yl)-5-(3-carboxymethoxyphenyl)-2-(4-sulfophenyl)-2 tetrazolium
NGI	Next generation impactor
NP	Nanoparticles
P. aeruginosa	*Pseudomonas aeruginosa*

PBS	Phosphate buffered saline
PCR	Polymerase chain reaction
PD	Pharmacodynamics
PEG	Polyethylene glycol
PK	Pharmacokinetics
PLA	Polylactic acid
PLGA	Poly (lactic-co-glycolic acid)
pMDI	Pressurized metered dose inhaler
PVA	Polyvinylalcohol
QC	Quality control
RSD	Relative standard deviation
SD	Standard deviation
SEM	Scanning electron microscopy
SPG	Shirasu porous glass
TEM	Transmission electron microscopy
TIP	Tobramycin inhaled powder
TIS	Tobramycin inhalation solution
UV-Vis	Ultraviolet-visible
w/v	Weight/volume
w/w	Weight/weight
XRD	X-ray diffraction

LIST OF FIGURES

LIST OF TABLES

THESIS OUTLINE

In **Chapter 1**, a general introduction with concepts about the pulmonary system and the CF disease is included to present, on one hand, an overview about the anatomophysiological aspects of the lungs and, on the other, the etiology of CF disease and the respective pulmonary changes, highlighting the *P. aeruginosa* infection. The connection between these concepts allows the understanding and conjecture on the behavior of aerosol formulations following lung administration.

Chapter 2 starts with the treatments for CF lung disease, with special emphasis on antibiotic therapy for the different stages of the *P. aeruginosa* infection. The following subsection describes the recent developments in aerosol therapy for the CF lung disease, underlining the liquid and dry powder formulations and some innovative aerosol formulations under investigation. Based on such aerosol advances in the area, the last subsection briefly indicates the motivation and objective of the work included in this thesis, mainly the development of innovative formulations.

Chapter 3 describes the main methods of preparation and characterization of the polymeric microspheres (MS) developed, for fast or slow release of levofloxacin (LVX) after pulmonary administration. In addition to an optimization approach, a set of physicochemical characterization methods are described. *In vitro* and *in vivo* studies, which are essential for confirming the efficacy and advantages of the developed formulations, will be introduced later in the appropriate Chapters.

Chapter 4 reports on the preparation of dry powder crosslinked LVX-loaded chitosan MS with fast release profiles, as an alternative to the nebulized liquid formulations for LVX delivery to the CF patients. An optimization approach by using a factorial design step is applied and the effect of operational variables and formulation parameters on particle size evaluated. Subsequently, and maintaining the fast release profile, the effect of different crosslinking agents on the MS properties, including swelling behavior and cytotoxicity properties, are evaluated.

Chapter 5 explores the potential of LVX-loaded PLGA MS as a dry powder polymeric system for controlled release in the lungs, with high local concentrations and lower risk of

systemic toxicity. Strategies for improving LVX loading are explored. The main characteristics of MS are evaluated and *in vitro* studies included.

In **Chapter 6**, the application of the selected chitosan- and PLGA-based MS is assessed by performing *in vivo* studies with their intratracheal administration into the lungs of rats. Blood and broncho-alveolar lavage (BAL) samples are used to measure the LVX and urea concentrations. Pharmacokinetic parameters are estimated resorting to a modeling approach.

Chapter 7 summarizes the main thesis findings and provides suggestions for future work in the area.

The thesis is complemented by three Appendixes detailing information on crosslinking mechanisms for MS (**Appendix 1**), HPLC method validation for LVX determination in MS systems (**Appendix 2**) and LC-MS/MS method validation for LVX determination in BAL samples (**Appendix 3**).

Scheme 1 presents schematically the thesis structure, sequence and topic inter-relationship, as follows.

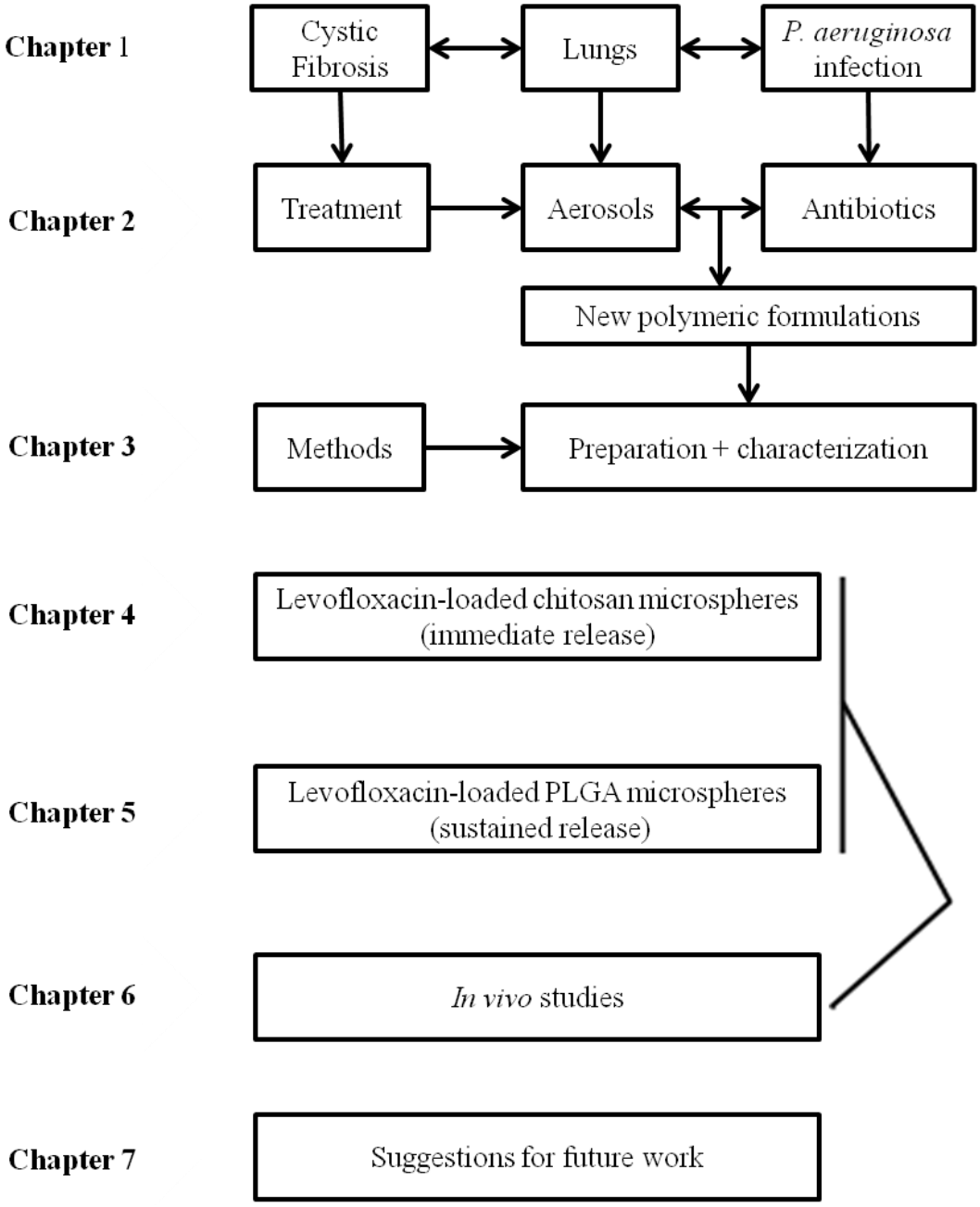

Scheme 1 – Schematic representation of thesis structure, sequence and relationship between chapters.

Chapter 1

GENERAL INTRODUCTION:

PULMONARY SYSTEM AND CYSTIC FIBROSIS

Cystic fibrosis (CF) is a complex inherited disease which affects many organs, including the pancreas and liver, gastrointestinal tract and reproductive system, sweat glands and, particularly, the respiratory system. Therefore, this chapter emphasizes firstly aspects pertaining to the lung architectures and secondly to the CF disease (including the chronic infection by *Pseudomonas aeruginosa*). These concepts allow an overview of the anatomical and physiological aspects involved in the development of the CF lung disease, and provide precious useful tools to predict and understand the dynamics of inhaled drug delivery systems, such as aerosol antibiotics.

1.1 – Pulmonary system

1.1.1 – Anatomy and physiology of airways

General aspects of lung structure are important to understand the changes that occur in the case of CF lung disease, being the basis for the development of new inhaled drug delivery strategies. Briefly, the lungs may be divided in two main zones: conducting zone and respiratory zone [1]. The conducting zone corresponds to the upper airways and is constituted by the trachea, bronchi, bronchioles and terminal bronchioles. It is responsible for the heating, humidification and conduction of the air to the respiratory zone. In the respiratory zone (respiratory bronchioles, alveolar ducts and alveolar sacs) takes place the gas exchange, which is the main function of this zone. Actually, its surface area is about 102 m^2, allowing the ideal contact for gas exchange, while the conducting zone surface area is only around 2-3 m^2 [2]. In addition, the thickness degree of the cell layer is gradually reduced from the conductive zone to the alveoli. A similar situation is observed for the fluid layer that covers the epithelial surface throughout the respiratory tract (Figure 1.1). This fluid in the conducting zone is of mucous nature and mainly constituted of water (95%) and the remaining of solids (mucin glycoproteins, lipids, DNA, actin and minerals), making it looking like a gel.

Pulmonary cells

The conductive zone is mainly constituted of ciliated columnar and goblet cells. Ciliated cells constitute the main part of the conducting airway epithelium with a major role in the mucociliary escalator, allowing removing the foreign particles (Figure 1.1). Goblet cells are nonglandular cells responsible for the mucus secretion. Also participating in the secretions with smaller secretory granules, are Clara cells (predominant in bronchioles) which produce surfactant components and protease inhibitors and participate in the detoxification metabolism. Other cell types make part of the conducting zone and include the basal cells, which are smaller, and pyramidal progenitor cells being responsible for the attachment of the columnar epithelium to the basement membrane, which in fact is an extracellular matrix of several biopolymers to which the epithelial cells attach. The brush cells, pear-shaped and characterized by the presence of microvilli on the apical surface are involved in drug metabolism (Figure 1.1) [3,2,4,5]. Other types include neuroendocrine cells (K cells) that contain and secrete peptide hormones, smooth muscle cells involved in the contraction and relaxation, and mast cells responsible for the antigen recognition and response [2,6]. The most relevant cells of the respiratory zone are the alveolar type I (AT I) and type II (AT II) cells, essential for the gas and material exchange. AT I cells are larger than AT II cells and cover more than 95% of the alveolar surface area, despite the more numerous AT II cells. AT I cells contribute to the alveolar fluid balance by regulating the transport of solutes and water across the blood and alveolar space. AT II cells, which may proliferate into AT II cells or differentiate into AT I cells, are responsible for the production, secretion and recycling of lung surfactant components. Another interesting characteristic is the fact that the partial pressure of oxygen in the alveoli is higher than in the blood of the pulmonary circulation. This characteristic allows the diffusion of oxygen from the alveoli to the blood and the opposite occurs for the carbon dioxide. Some capillary endothelial cells and alveolar macrophages may also be found near the alveolar epithelium [2,3]. Alveolar macrophages are scavenger cells that derived from monocytes and are responsible for the phagocytosis of deposited insoluble particles (e.g. dust, pollutants and allergens) in the alveolar region. This mechanism may include the transport to the mucociliary escalator or to the tracheobronchial lymph, or the degradation by internal enzymes [2].

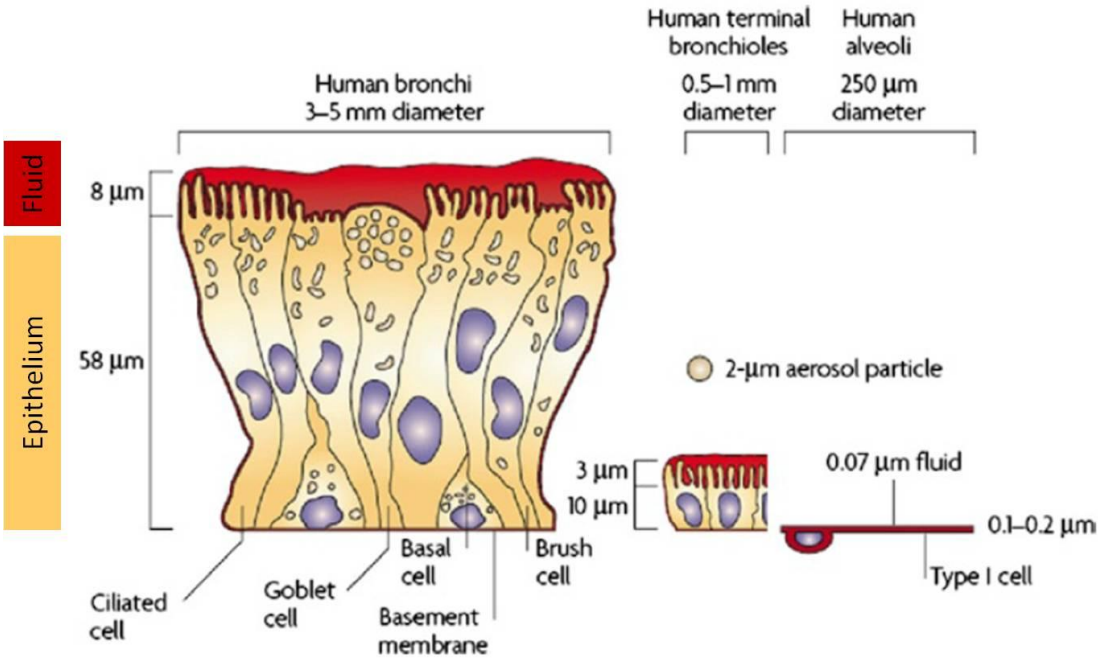

Figure 1.1 – Cell types and different thickness patterns (of cell and fluid layers) across the airways. Adapted from [5], with permission.

1.1.2 – Particle deposition in the respiratory tract

In addition to some anatomical and physiological lung concepts, understanding the process of particle deposition in the respiratory tract is of great value to improve efficiency in drug delivery of inhaled drugs [7].

Mechanisms of particle deposition

The main forces that are involved in the deposition of particles include gravity, inertia and impulse transfer from collisions with gas molecules [8]. Therefore, particles are deposited by three main basic mechanisms: sedimentation, inertial impaction and diffusion toward the surfaces of the respiratory tract [8,7], as represented in Figure 1.2. Gravitational sedimentation and inertial impaction are the main mechanisms of deposition of particles over 0.5 µm and below 5 µm aerodynamic size in the small conducting airways [9]. Impaction occurs principally at the airway bifurcations and it is influenced by particle size, density and velocity [2]. It is the main deposition mechanism in extrathoracic and large conducting airways and for particles with particle size > 5µm.

Diffusion which results from a Brownian motion caused by the impact of surrounding air molecules is the main deposition mechanism in small airways and alveoli and the most common for particles < 0,5 µm [9,1].

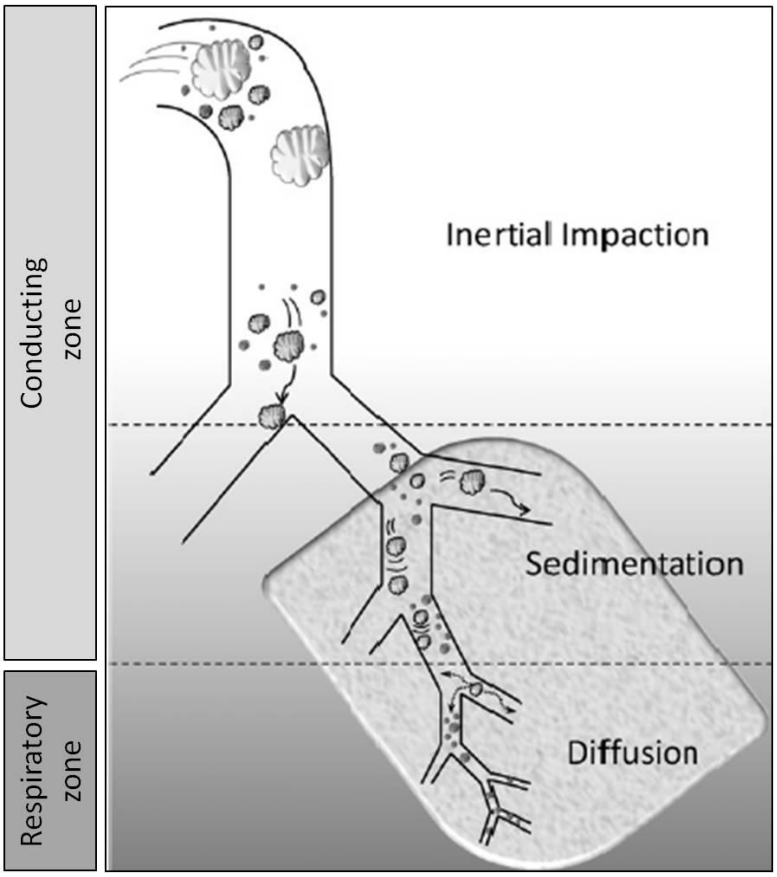

Figure 1.2 – Schematic diagram that represents the particle deposition in the lungs according to the three main mechanisms related to particle size. It is evident that the smaller particles are deposited in the lower airways as opposed to the bigger particles. Adapted from [7], with permission.

Aerodynamic properties of particles

The aerodynamic diameter (d_a) is defined as the diameter of a sphere with a unit density (ρ) that has the same terminal settling velocity in still air as the particle under consideration [10,9,7]. For efficient lung deposition, inhalation aerosols should have d_a in the 1 (or 0.5) to 5 µm range [11,12,9]. Larger particles (> 5 µm) impact in the upper airway and smaller particles (< 1µm) are easily exhaled (Figure 1.3) [11,12]. If particles have a density close to one, d_a and geometric diameter (d_g) are the same, which is the case

of most of the commercialized forms (solid powder or nebulized liquids). However, there might be some advantages in using low-density porous particles of larger d_g (given that $d_a = d_g \sqrt{\rho}$), while keeping the d_a within the optimal range [9], including easier powder dispersion and lower macrophage uptake. This discriminating property of macrophages may be the key for the success of the controlled-release particles development with high porous nature and consequent low density, i.e. ρ) ~0.4 g/cm^3, because of their relatively small d_a and large d_g [13,2]. Regarding the practical aspects, values for d_a of particles can be determined *in vitro* with cascade impactors. MMAD (mass median aerodynamic diameter) is generally reported in the particle characterization in order to estimate the particle deposition in lungs. Several mathematical models are used in predicting the deposition patterns of particles in the lungs, even considering different disease states. Additionally, there are two other mechanisms of particle deposition, known as interception and electrostatic precipitation, which are related to particle shape and electrostatic charges, respectively [7], and are not discussed herein.

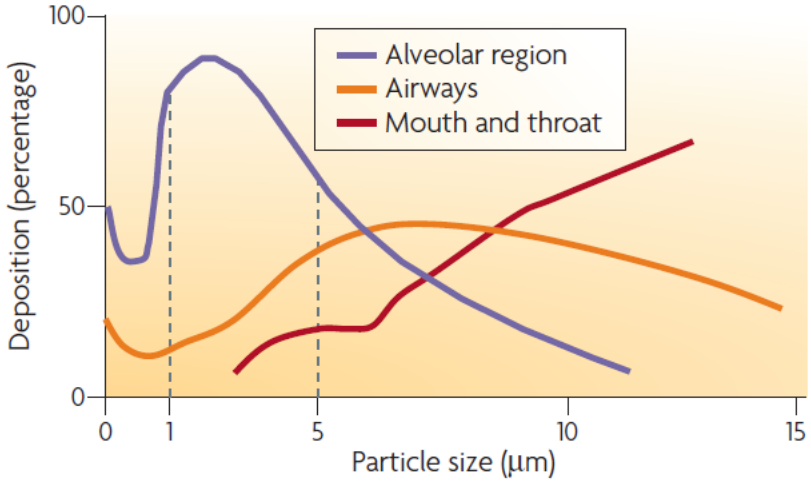

Figure 1.3 – Particle deposition (%) in the respiratory tract according to size. This representation considers for a slow inhalation and a 5-second breath hold. Reproduced from [5], with permission.

Factors influencing particle deposition

Several factors can influence particle deposition in airways including the pattern of inhalation of the patients which is usually device specific and should be adequate to improve the therapeutic dose in deep lungs. Usually a slow and rhythmic inspiration promotes a more homogenous distribution of drug particles, but it depends on the device: nebulizers, metered dose inhalers (MDIs), including the pressurized (pMDIs), and dry-powder inhalers (DPIs). Another two factors include the morphology of oropharynge (geometry influences deposition) and morphological changes due to diseases, such as CF. In this situation, the bacterial colonization (particularly from *P. aeruginosa*) may change the mucosal physiology and the epithelial function and compromises the tidal volume. The impaired mucus clearance complicates the particle diffusion and higher particle deposition in undesired places [2,7,9,14]. Additionally, some formulation-related aspects complicate the pulmonary delivery and include the drug loss during inhalation, dosing difficulties, enzymatic degradation within the lung and high costs of production. To circumvent these aspects, a formulation must be able to be incorporated into an aerosol form, and to remain stable against forces generated during aerosolization. In addition, it should target a specific site or cell population in the lung, protect the compound against aggressive elements in the pulmonary tract and release the compound in a predetermined mode within an acceptable period of time without producing toxic byproducts. It should also be inert to the surrounding tissue and contain no irritating or toxic additives [15].

It should be noted that pulmonary delivery is a route of administration that may be used as a mean of systemic delivery, alternative to parenteral routes, when the drug has poor bioavailability by the oral route of administration [16]. Some lung features, such as the large surface area for absorption, the high solute permeabilities and the limited proteolytic activity make this way as a preferable to administer some drugs (e.g. α2-adrenoceptor agonists, corticosteroids, antibacterials and therapeutic macromolecules such as insulin) [17]. A macromolecule to be absorbed from the lung into the blood must pass through several barriers including the monolayer of surfactant, the surface lining fluid, the epithelium, the interstitium and the basement membrane and the vascular endothelium [18]. The focus here will be on inhalation therapy as a mean to provide high local doses at the site of drug action and limited systemic exposure [16,19,20]. Local delivery of drugs to the lungs is desirable, particularly in patients with specific pulmonary diseases such as

asthma, chronic pulmonary infections and CF lung disease [9]. For CF, antibiotic delivery pulmonary strategies have been developed [21] and will be discussed in Chapter 2.

1.2 – Cystic Fibrosis

1.2.1 – Lung manifestations

CF is an inherited, recessive and autosomal disease which affects approximately one in 2000 newborns in Caucasian populations. It is, however, found in all ethnic groups [12]. This disorder is caused by mutations in the CF transmembrane conductance regulator (CFTR) gene on chromosome 7. A deletion of phenylalanine in the amino acid position 508 is the most common mutation (F508del) [22] but more than 800 different mutations have been identified [23,12]. In addition, CF is a multifunctional disease in which several organs are affected but particularly the respiratory system [12,24-26]. Some carriers of a single CFTR mutation suffer from some pulmonary and gastrointestinal symptoms but not at high level [24]. Because the CFTR protein regulates ion and water movement across the epithelium, these mutations lead to malfunction of the chloride channel in CF patients [12,24,23,27]. Thus, the scenario includes decreased chloride secretion into the airways and increased sodium absorption from the airways that lead to relative dehydration of the airway mucus [28]. Therefore, the volume of the airway surface liquid (ASL), also known as epithelium lining fluid (ELF) [29], decreases leading to accumulation of purulent secretions (expectorated form is known as sputum) [24] and impaired mucociliary clearance [30,31]. Mucociliary clearance is an important defense mechanism against pathogens and foreign substances, being reduced in CF patients [24,32-34], and leading to chronic infections by a variety of pathogens, such as bacteria [14,31]. Concomitantly, CFTR-deficient epithelial cells release proinflammatory cytokines (e.g. IL-1β, IL-6, IL-8) and levels of anti-inflammatory cytokines (e.g IL-10) are decreased leading to a scenario of inflammation [21]. Such inflammatory conditions together with infections and a viscous mucous and reduced mucociliary clearance lead frequently to exacerbations, pulmonary destruction and severe lung function decline. Lung disease in CF is commonly characterized as an endobronchial infection, exaggerated inflammatory response, progressive airway obstruction, bronchiectasis and eventual respiratory failure [35]. In addition, results from *in vitro* studies indicate that mucus adherence to epithelial surfaces are strengthened by the low pH of ASL because of

absent CFTR-dependent HCO_3^- secretion [36]. In CF patients, particle deposition after inhaled therapy is usually non uniform and particle penetration through the viscous mucus is impaired (Figure 1.4).

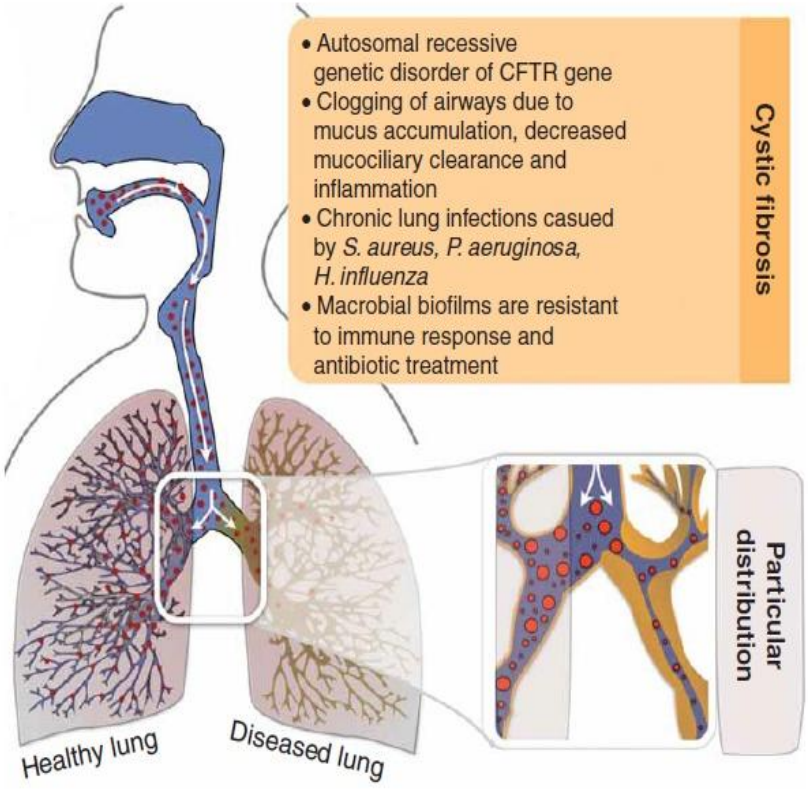

Figure 1.4 – CF lung disease characteristics and pattern distribution of particles administered by inhaled therapy. Adapted with permission from [21].

Airway microbiota in Cystic Fibrosis

Being the main pathogen which leads to chronic infection in CF lung disease, *P. aeruginosa* will be highlighted in the next subsection. In fact, 54.4% of the whole CF patient population are infected with this bacterium, which is found in 70 - 80% of the adult patients [21]. *P. aeruginosa* predominates in the majority of adult CF patients [27,37] whereas *Staphylococcus aureus* (including Methicillin-Resistant *Staphylococcus aureus*, MRSA) [38] and *Haemophilus influenzae* are the main pathogens in children [39,40,31,27], as shown in Figure 1.5. However, it should be kept in mind that other

pathogens, such as *Burkholderia* spp., *Achromobacter* spp. and *Stenotrophomonas maltophilia* also contribute to morbidity and mortality [12,41,14].

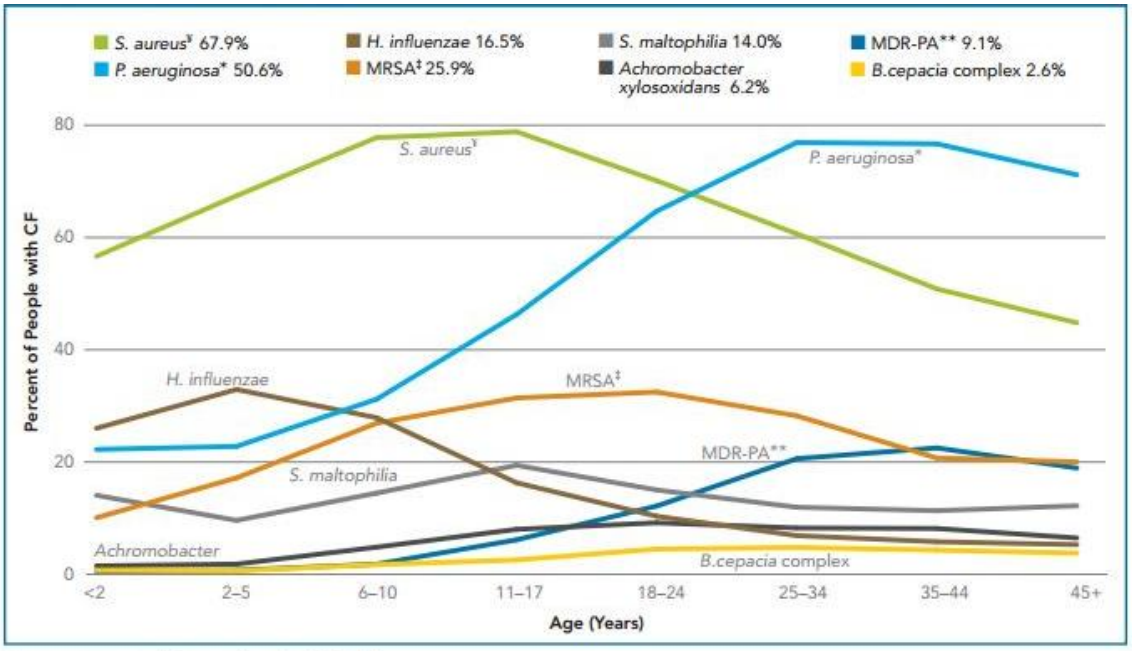

*P. aeruginosa *includes people with MDR-PA.*
***MDR-PA is multi-drug resistant* Pseudomonas aeruginosa (P. aeruginosa).*
¥S. aureus *includes people with MRSA.*
‡*MRSA is methicillin-resistant* Staphylococcus aureus (S. aureus).

Figure 1.5 – Prevalence of pathogens in CF patients according to age. Reproduced from the Cystic Fibrosis Foundation patient registry, 2011 Annual Data Report [42].

Recent studies have shown that the organisms belonging to the *Streptococcus milleri* group may also be an intrinsic component of the CF airway microbiome and have recently been implicated as etiological agents of pulmonary exacerbations in adult CF patients [43]. Besides, fungal and viral infections play also an important role in the development of CF lung disease [37]. In addition, bacterial community in these patients appears to be polymicrobial in nature including several anaerobic species such as the genera *Prevotella*, *Veillonella*, *Propionibacterium* and *Actinomyce*. These anaerobic bacteria are clinically relevant for CF lung disease and consist in a complex issue which is currently under investigation. The clinical significance of these species remains unclear and it is the main reason why clinicians have not specifically treated anaerobes. Nevertheless, some *in vitro* data suggest that *Prevotella intermedia* may contribute to lung disease in CF patients, which if demonstrated *in vivo*, may facilitate the decision for antibiotic therapy [37,44]. Culture-independent microbial profiling methods showed that

microbial communities in airways of CF patients are complex ecosystems with high microbial diversity. Such new methods revealed the infraspecific diversity in *Candida albicans*, *Candida parapsilosis* and *Aspergillus fumigates* and cryptic and new unculturable (or difficult to grow *in vitro*) species, most of them described as human pathogens. They also revealed the complex interaction between typical pathogens and microbiota, such as the association between *P. aeruginosa* and anaerobes. *P aeruginosa* can grow under reduced oxygen tension. Other anaerobic bacteria and *C. albicans* can also grow under anaerobic conditions [45]. Microbial community diversity was shown to evolve with patients' aging. Young CF patients who show less airway inflammation and better pulmonary function possess the greatest diversity of airway bacterial species (including anaerobic community). With aging, the diversity of the microbial communities tends to be substantially reduced [45,46], which might be linked to the gradual decline in the lung function, as suggested by some investigators [47,48]. Some authors suggest that antibiotic treatments contribute to the loss of airway microbiome diversity [48]. Still controversial and requiring further investigations, the management and preservation of the diversity of the lung microbial communities might be a way to prolong lung functions and life expectancies in CF patients and require new treatment strategies beyond the scope of the work described in this thesis [46,47].

1.2.2 – Infection with *P. aeruginosa*

P. aeruginosa is generally considered as the most important pathogen associated with CF in terms of prevalence and pathogenicity and this opportunistic bacterium is the main pathogen leading to advanced CF lung disease [39,35,14]. *P. aeruginosa* is a Gram-negative bacillus (non-capsulate and non-sporing) that affects particularly the lower respiratory tract [49]. Without any treatment, *P. aeruginosa* infection persists in spite of the recruitment of the host´s defense mechanisms, leads to decreased respiratory function [14], and most patients die at a young age due to lung complications. Under intensive treatment, the mean expected lifetime of CF patients is > 35 years, and in some centers it is >50 years [12]. *P. aeruginosa* is transmitted by a direct contact between carriers and via environmental reservoirs. The initial infection usually involves a planktonic, nonmucoid strain of *P. aeruginosa*, which is able to penetrate the mucus by its flagellar activity [22]. The initial infection is not associated with an immediate and rapid decline in lung function and early *P. aeruginosa* isolates appear non-resistant to the antibiotic

treatment [35], presenting an opportunity for an early efficient therapeutic intervention [50]. Aggressive and early antibiotic treatments of *P. aeruginosa* infection were shown to increase the life expectancy of CF patients [39,35]. Transmission between infected CF patients may occur and be favored in communities such as day hospital–like wards where CF patients come into contact with each other, leading to replacement, under antimicrobial pressure, of initially-acquired more antibiotic-sensitive clones to resistant ones [51].

In addition, *P. aeruginosa* was shown to persist and to multiply in hospital equipments and bathroom sinks which suggests that high hygienic standards should be applied to minimize the risk of cross infection [52]. After the initial infection, follows a variable period of "intermittent or transient infection", which refers to patients with less than 50% of the monthly cough swab or sputum cultures found positive to *P. aeruginosa* over a 12-month period, according to the Leeds classification [53]. If left untreated, the starting infection eventually evolves towards a "chronic infection" which, according to the Leeds classification, refers to patients with more than 50% of the monthly cultures found positive over a 12-month period [53]. Chronic infection involves mucoid strains of *P. aeruginosa* which synthesize an exopolysaccharide (alginate) matrix or biofilm that protects bacteria against antibiotics [31] and phagocytosis [35,50,23], as shown in Figure 1.6. Despite the impaired mucociliary clearance, the mucus secretion from goblet cells and glands persists leading to the accumulation of thick mucus plaques where the bacteria can penetrate through flagellar activity. However, defense mechanisms are affected and it is difficult for neutrophils to penetrate into mucus plaques. As aforementioned and though being aerobic, *P. aeruginosa* within biofilm is able to survive in an high hypoxic gradient environment of the CF mucus plug, which diminishes its sensitivity to antibiotics [22]. In most cases, mucoid *P. aeruginosa* infections cannot be eradicated.

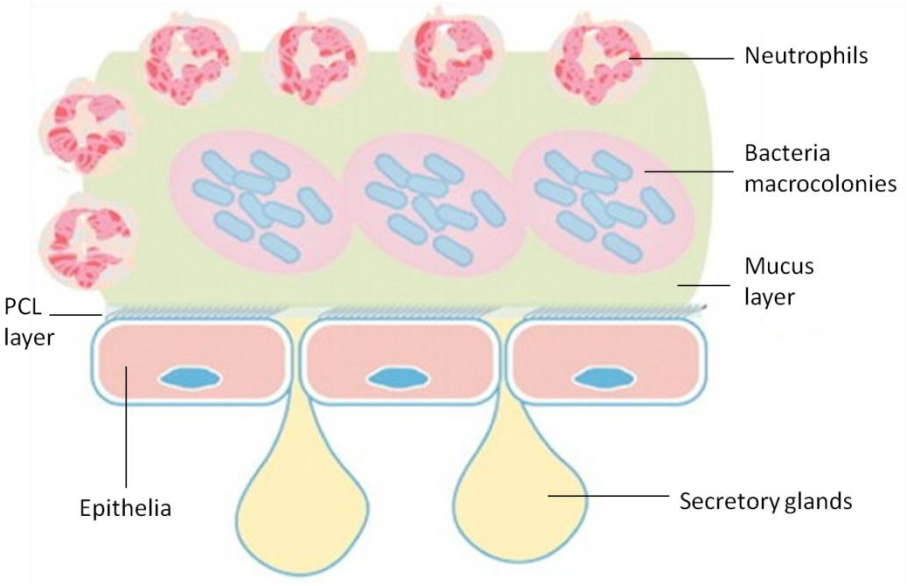

Figure 1.6 – Macrocolonies development in chronic infection by *P. aeruginosa* which resist innate defenses including neutrophils. ASL, which comprises a mucus layer and a periciliary fluid layer (PCL), is also represented. Partially reproduced with modifications from [22].

Early aggressive antibiotic treatment, which is crucial to prevent or at least to delay chronic lung colonization, implies the early diagnosis of initial or recurrent contaminations. *P. aeruginosa* is diagnosed in sputum, hypopharyngeal or endolaryngeal suctions or deep throat culture [23,31]. Routine bacterial cultures appear to have limited sensitivity for detecting the initially very low numbers of bacterial cells. Several molecular assays, generally based on the polymerase chain reaction (PCR) technique, and especially on its quantitative variant, have therefore been proposed for early detection of *P. aeruginosa* and for confirming the respective eradication after antibiotic treatment in young CF patients, but they still require investigations about their clinical significance and relevance before implementation in routine laboratories [54,55].

P. aeruginosa nonmucoid phenotype is located mainly in conductive zone while mucoid strains are located in both respiratory and conductive zones [12]. A study in the Copenhagen CF Center concluded that the intensive antibiotic therapy used by them for chronic *P. aeruginosa* infections appears to restrain but not eradicate the bacteria from the conductive zone, while the remaining healthy respiratory zone may be protected, for a prolonged period, from massive biofilm infection. This strongly suggests that the

conductive zone serves as a bacterial reservoir where the bacteria, organized in mucoid biofilms within the mucus, are protected against host defenses and antibiotics [56]. Other authors concluded that nebulized antibiotics (e.g. colistin and tobramycin) [57] reached high concentrations in the conductive zone (sputum) but the concentrations in the respiratory zone were very low. On the contrary, antibiotics given orally or intravenously reached very low concentrations in sputum and high concentrations in the respiratory zone due to direct transport by the alveolar blood capillaries [12]. Thus, it is easy to understand the importance of combined oral, intravenous (IV) and inhaled therapy to achieve high drug concentrations throughout the respiratory tract. Resistance mechanisms of *P. aeruginosa* to the antibiotic therapy as well as current treatment approaches and new therapeutic strategies for CF management are appropriately discussed in Chapter 2.

1.3 – References

1. Aulton ME (2005) Delineamento de formas farmacêuticas. 2 edn. Artmed, Porto Alegre.

2. Smyth HDC, Hickey AJ (2011) Controlled Pulmonary Drug Delivery. Advances in Delivery Science and Technology. Springer New York.

3. Huh D (2008) Engineering Pulmonary Epithelia and Their Mechanical Microenvironments: Chapter 24 from Micro and Nanoengineering of the Cell Microenvironment. Artech House Publishers, UK.

4. Reid L, Meyrick B, Antony VB, Chang L-Y, Crapo JD, Reynolds HY (2005) The Mysterious Pulmonary Brush Cell: A Cell in Search of a Function. American Journal of Respiratory and Critical Care Medicine 172 (1):136-139.

5. Patton JS, Byron PR (2007) Inhaling medicines: delivering drugs to the body through the lungs. Nature Reviews Drug Discovery 6 (1):67-74.

6. Kim E. Barrett, Scott Boitano, Susan M. Barman, Brooks HL (2012) Ganong's Review of Medical Physiology. 24 edn. McGraw-Hill Companies, Inc., USA.

7. Carvalho TC, Peters JI, Williams RO, III (2011) Influence of particle size on regional lung deposition - What evidence is there? International Journal of Pharmaceutics 406 (1-2):1-10.

8. Heyder J (2004) Deposition of Inhaled Particles in the Human Respiratory Tract and Consequences for Regional Targeting in Respiratory Drug Delivery. Proceedings of the American Thoracic Society 1 (4):315-320.

9. Pilcer G, Amighi K (2010) Formulation strategy and use of excipients in pulmonary drug delivery. International Journal of Pharmaceutics 392 (1-2):1-19.

10. de Boer AH, Gjaltema D, Hagedoorn P, Frijlink HW (2002) Characterization of inhalation aerosols: a critical evaluation of cascade impactor analysis and laser diffraction technique. International Journal of Pharmaceutics 249 (1-2):219-231.

11. Emami J, Hamishehkar H, Najafabadi AR, Gilani K, Minaiyan M, Mahdavi H, Mirzadeh H, Fakhari A, Nokhodchi A (2009) Particle size design of PLGA microspheres for potential pulmonary drug delivery using response surface methodology. Journal of Microencapsulation 26 (1):1-8.

12. Høiby N (2011) Recent advances in the treatment of Pseudomonas aeruginosa infections in cystic fibrosis. BMC Medicine 9 (1):32-38.

13. Mohamed F, van der Walle CF (2008) Engineering biodegradable polyester particles with specific drug targeting and drug release properties. Journal of Pharmaceutical Sciences 97 (1):71-87.

14. Dudley MN, Loutit J, Griffith DC (2008) Aerosol antibiotics: considerations in pharmacological and clinical evaluation. Current opinion in biotechnology 19 (6):637-643.

15. Dailey LA, Kleemann E, Wittmar M, Gessler T, Schmehl T, Roberts C, Seeger W, Kissel T (2003) Surfactant-Free, Biodegradable Nanoparticles for Aerosol Therapy Based on the Branched Polyesters, DEAPA-PVAL-g-PLGA. Pharmaceutical Research 20 (12):2011-2020.

16. Forbes B, Asgharian B, Dailey LA, Ferguson D, Gerde P, Gumbleton M, Gustavsson L, Hardy C, Hassall D, Jones R, Lock R, Maas J, McGovern T, Pitcairn GR, Somers G, Wolff RK (2010) Challenges in inhaled product development and opportunities for open innovation. Advanced Drug Delivery Reviews 63 (1-2):69-87.

17. Sakagami M, Byron PR (2005) Respirable Microspheres for Inhalation: The Potential of Manipulating Pulmonary Disposition for Improved Therapeutic Efficacy. Clinical Pharmacokinetics 44 (3):263-277.

18. John S P (1996) Mechanisms of macromolecule absorption by the lungs. Advanced Drug Delivery Reviews 19 (1):3-36.

19. Zeng XM, Martin GP, Marriott C (1995) The controlled delivery of drugs to the lung. International Journal of Pharmaceutics 124 (2):149-164.

20. Marchand S, Gobin P, Brillault J, Baptista S, Adier C, Olivier J-C, Mimoz O, Couet W (2010) Aerosol Therapy with Colistin Methanesulfonate: a Biopharmaceutical Issue Illustrated in Rats. Antimicrobial Agents and Chemotherapy 54 (9):3702-3707.

21. Klinger-Strobel M, Lautenschläger C, Fischer D, Mainz JG, Bruns T, Tuchscherr L, Pletz MW, Makarewicz O (2015) Aspects of pulmonary drug delivery strategies for infections in cystic fibrosis – where do we stand? Expert Opinion on Drug Delivery 12 (8):1351-1374.

22. Boucher RC (2004) New concepts of the pathogenesis of cystic fibrosis lung disease. European Respiratory Journal 23 (1):146-158.

23. Doring G, Conway S, Heijerman H, Hodson M, Hoiby N, Smyth A, Touw D (2000) Antibiotic therapy against Pseudomonas aeruginosa in cystic fibrosis: a European consensus. European Respiratory Journal 16 (4):749-767.

24. Ibrahim BM, Tsifansky MD, Yang Y, Yeo Y (2011) Challenges and advances in the development of inhalable drug formulations for cystic fibrosis lung disease. Expert Opinion on Drug Delivery 8 (4):451-466.

25. Ramsey BW (1996) Management of Pulmonary Disease in Patients with Cystic Fibrosis. New England Journal of Medicine 335 (3):179-188.

26. Giron Moreno RM, Salcedo Posadas A, Mar Gomez-Punter R (2011) Inhaled antibiotic therapy in cystic fibrosis (Antibioterapia inhalada en la fibrosis quistica.). Archivos de Bronconeumología 47 Suppl 6:14-18.

27. Rogers GB, Hoffman LR, Doring G (2011) Novel concepts in evaluating antimicrobial therapy for bacterial lung infections in patients with cystic fibrosis. Journal of Cystic Fibrosis 10 (6):387-400.

28. George AM, Jones PM, Middleton PG (2009) Cystic fibrosis infections: treatment strategies and prospects. FEMS Microbiology Letters 300 (2):153-164.

29. Parent RA (2015) Section III - Comparative Biochemistry of the Normal Lung. In: Comparative Biology of the Normal Lung. 2 edn. Elsevier Inc., USA.

30. Boucher RC (2007) Airway Surface Dehydration in Cystic Fibrosis: Pathogenesis and Therapy. Annual Review of Medicine 58 (1):157-170.

31. Davies JC, Bilton D (2009) Bugs, Biofilms, and Resistance in Cystic Fibrosis. Respiratory care 54 (5):628-640.

32. Mall MA (2008) Role of cilia, mucus, and airway surface liquid in mucociliary dysfunction: Lessons from mouse models. Journal of Aerosol Medicine and Pulmonary Drug Delivery 21 (1):13-24.

33. Deneuville E, PerrotMinot C, Pennaforte F, Roussey M, Zahm JM, Clavel C, Puchelle E, deBentzmann S (1997) Revisited physicochemical and transport properties of respiratory mucus in genotyped cystic fibrosis patients. American Journal of Respiratory and Critical Care Medicine 156 (1):166-172.

34. King M (1987) The role of mucus viscoelasticity in cough clearance. Biorheology 24 (6):589-597.

35. Geller DE (2009) Aerosol Antibiotics in Cystic Fibrosis. Respiratory care 54 (5):658-670.

36. Coakley RD, Grubb BR, Paradiso AM, Gatzy JT, Johnson LG, Kreda SM, O'Neal WK, Boucher RC (2003) Abnormal surface liquid pH regulation by cultured cystic fibrosis bronchial epithelium. Proceedings of the National Academy of Sciences of the United States of America 100 (26):16083-16088.

37. Bals R, Hubert D, Tümmler B (2011) Antibiotic treatment of CF lung disease: From bench to bedside. Journal of Cystic Fibrosis 10, Supplement 2 (0):S146-S151.

38. Goss CH, Muhlebach MS (2011) Review: Staphylococcus aureus and MRSA in cystic fibrosis. Journal of Cystic Fibrosis 10 (5):298-306.

39. van Westreenen M, Tiddens HAWM (2010) New Antimicrobial Strategies in Cystic Fibrosis. Pediatric Drugs 12 (6):343-352.

40. Harrison F (2007) Microbial ecology of the cystic fibrosis lung. Microbiology 153 (4):917-923.

41. de Vrankrijker AMM, Wolfs TFW, van der Ent CK (2010) Challenging and emerging pathogens in cystic fibrosis. Paediatric Respiratory Reviews 11 (4):246-254.

42. Foundation CF (2012) Cystic Fibrosis Foundation Patient Registry, 2011 Annual Data Report. Available via http://www.cff.org/UploadedFiles/aboutCFFoundation/AnnualReport/2011-Annual-Report.pdf. Accessed 11 March 2015.

43. Grinwis ME, Sibley CD, Parkins MD, Eshaghurshan CS, Rabin HR, Surette MG (2010) Macrolide and Clindamycin Resistance in Streptococcus milleri Group Isolates from the Airways of Cystic Fibrosis Patients. Antimicrobial Agents and Chemotherapy 54 (7):2823-2829.

44. Doering G, Flume P, Heijerman H, Elborn JS, Consensus Study G (2012) Treatment of lung infection in patients with cystic fibrosis: Current and future strategies. Journal of Cystic Fibrosis 11 (6):461-479.

45. Delhaes L, Monchy S, Frealle E, Hubans C, Salleron J, Leroy S, Prevotat A, Wallet F, Wallaert B, Dei-Cas E, Sime-Ngando T, Chabe M, Viscogliosi E (2012) The Airway Microbiota in Cystic Fibrosis: A Complex Fungal and Bacterial Community-Implications for Therapeutic Management. PLoS ONE 7 (4).

46. VanDevanter DR, LiPuma JJ (2012) Microbial diversity in the cystic fibrosis airways: where is thy sting? Future Microbiology 7 (7):801-803.

47. Zemanick ET, Sagel SD, Harris JK (2011) The airway microbiome in cystic fibrosis and implications for treatment. Current Opinion in Pediatrics 23 (3):319-324.

48. Lynch SV, Bruce KD (2013) The cystic fibrosis airway microbiome. Cold Spring Harbor perspectives in medicine 3 (3).

49. Banerjee D, Stableforth D (2000) The Treatment of Respiratory Pseudomonas Infection in Cystic Fibrosis: What Drug and Which Way? Drugs 60 (5):1053-1064.

50. Rosenfeld M, Ramsey BW, Gibson RL (2003) Pseudomonas acquisition in young patients with cystic fibrosis: pathophysiology, diagnosis, and management. Current Opinion in Pulmonary Medicine 9 (6):492-497.

51. Cramer N, Wiehlmann L, Ciofu O, Tamm S, Hoiby N, Tuemmler B (2012) Molecular Epidemiology of Chronic Pseudomonas aeruginosa Airway Infections in Cystic Fibrosis. PLoS ONE 7 (11).

52. Campana S, Taccetti G, Ravenni N, Masi I, Audino S, Sisi B, Repetto T, Döring G, de Martino M (2004) Molecular epidemiology of Pseudomonas aeruginosa, Burkholderia cepacia complex and methicillin-resistant Staphylococcus aureus in a cystic fibrosis center. Journal of Cystic Fibrosis 3 (3):159-163.

53. Lee TWR, Brownlee KG, Conway SP, Denton M, Littlewood JM (2003) Evaluation of a new definition for chronic Pseudomonas aeruginosa infection in cystic fibrosis patients. Journal of cystic fibrosis : official journal of the European Cystic Fibrosis Society 2 (1):29-34.

54. Billard-Pomares T, Herwegh S, Wizla-Derambure N, Turck D, Courcol R, Husson M-O (2011) Application of quantitative PCR to the diagnosis and monitoring of Pseudomonas aeruginosa colonization in 5-18-year-old cystic fibrosis patients. Journal of Medical Microbiology 60 (2):157-161.

55. Deschaght P, Van daele S, De Baets F, Vaneechoutte M (2011) PCR and the detection of Pseudomonas aeruginosa in respiratory samples of CF patients. A literature review. Journal of Cystic Fibrosis 10 (5):293-297.

56. Bjarnsholt T, Jensen PØ, Fiandaca MJ, Pedersen J, Hansen CR, Andersen CB, Pressler T, Givskov M, Høiby N (2009) Pseudomonas aeruginosa biofilms in the respiratory tract of cystic fibrosis patients. Pediatric Pulmonology 44 (6):547-558.

57. Vendrell Relat M, Munoz Castro G, Sabater Talaverano G, De Gracia Roldan J (2011) The future of inhaled antibiotic therapy. New products (El futuro de la antibioterapia inhalada. Nuevos productos.). Archivos de Bronconeumología 47 Suppl 6:30-32.

Chapter 2

CHALLENGES AND NEW APPROACHES IN THE TREATMENT OF CYSTIC FIBROSIS

2.1 – Current treatment and associated barriers

The aim of the CF treatment is to increase life expectancy of patients and decrease the impact of symptoms, attenuating disease progression. Currently, antibiotics (such as aminoglycosides, beta-lactams, polymyxins and fluoroquinolones [1]) and anti-inflammatory drugs are used to control the inflammation and infection of the respiratory tract, particularly by *P. aeruginosa*, as previously remarked. In addition, symptomatic treatment is performed with bronchodilators [2]. Mucolytics (e.g. dornase alfa, which has already proven the respective efficacy) and osmotic agents are administered to improve sputum and airway clearance [3]. These agents will not be detailed here, but several of their features are particularly interesting: (a) osmolytes are not actively transported and are poorly absorbed, being able to restore the volume of the ASL (e.g mannitol) and (b) inhaled hypertonic saline agents are able to draw water to the airway surface [4,5]. However, these agents show difficulties to demonstrate efficacy owing to the short duration of active therapy [5]. In what relates to antibiotics, a number of integrated factors must be taken in consideration to choose the drug and delivery method: pharmacological and pharmacodynamic (PD) considerations, toxicity, cost, patients' characteristics, lung function, symptoms, and others [6]. Thus, there is no standard treatment for patients with the CF lung disease.

2.1.1 – Antibiotics

Although there is no standard treatment, a combination of at least two antibiotics is generally used to treat infection by *P. aeruginosa* in CF patients, especially in cases of bacterial resistance to the antibiotic therapy, as will be discussed later in this Chapter. The treatment with a combination of oral, IV and inhaled antibiotics is a cornerstone of CF therapy and may include aminoglycosides, fluoroquinolones and beta-lactams [3].

Aminoglycosides

Tobramycin is an aminoglycoside which is currently used as an aerosol nebulized antibiotic and accepted as a standard treatment for CF patients [7]. The tobramycin inhalation solution (TIS) was approved in 1998 (TOBI® Novartis Pharmaceuticals, Basel, Switzerland) [8,9] with the Pari LC Plus nebulizer [1] and the administration of 300 mg

(load) twice daily has been investigated alternating 28-day on/off treatment cycles in order to improve lung function measured as FEV_1, volume exhaled at the end of the first second of forced expiration, and to avoid toxicity due to systemic absorption [8]. Recently, a study concluded that the use of TIS was associated with significantly reduced mortality among patients with CF [10]. However, the administration time is extended for almost 20 minutes, which is a problem for patient compliance. Taking into account the development of DPIs and sustained-release formulations, this problem may be solved by faster and less frequently administrations. Actually, a tobramycin inhaled powder (TIP) has recently been approved (TOBI® Podhaler™, Novartis Pharmaceuticals, Basel, Switzerland) and demonstrated similar efficacy to TIS, consisting in a faster and more convenient dosing regimen [2]. However, aminoglycosides have their activity impaired due to low penetration in mucus [7,1]. This appears to result from the binding of cationic moieties on the aminoglycosides to anionic substances present in the sputum of these patients [8].

Fluoroquinolones

Fluoroquinolones are under investigation and may be administered during the "off" cycle of TIS to improve patient outcomes and avoid drug resistance [8]. They are being developed for inhalation, with particular focus on ciprofloxacin (CIP) and LVX, as described below [11,12]. In addition, their antibacterial activity is not impaired by low diffusion into the mucus in contrast to aminoglycosides [8,1]. CIP is a second-generation fluoroquinolone and it is one of the most widely available fluoroquinolone antibiotics with activity against several aerobic Gram-positive and Gram-negative bacteria [13]. Introduced in 1985 as an oral treatment of CF patients, it offered a safe and efficient alternative to standard parenteral therapy for acute pulmonary exacerbations, despite possible side effects such as cartilage toxicity, sunlight sensitivity rash [14] and rapid emergence of resistance [15]. LVX is a third-generation fluoroquinolone with Gram-positive and Gram-negative antibacterial activity. This fluoroquinolone is used for oral and IV administration and a liquid nebulized formulation was recently approved in Europe (Quinsair®) and demonstrated to be effective in improving the lung function of CF patients [16,17].

Beta-lactams

Beta-lactams that are used to fight pseudomonal infections in CF patients include aztreonam, anti-pseudomonal carbapenems (doripenem, imipenem-cilastatin and meropenem), penicillins (piperacillin–tazobactam and ticarcillin–clavulanate) and cephalosporins (ceftazidime and cefepime) [18,19]. In contrast to aminoglycosides and similarly to fluoroquinolones, beta-lactams do not have their antibacterial activity impaired in sputum from CF patients [8,1]. Aztreonam, active against aerobic Gram-negative bacteria is available as IV formulation (for acute pulmonary exacerbations) and aerosolized formulation, aztreonam lysine for inhalation solution, AZLI, (Cayston®; Gilead Sciences, Foster City, CA), currently used against chronic airway *P. aeruginosa* infection, was approved in 2010 by the US Food and Drug Administration (FDA) [20]. Carbapenems, active against anaerobic, aerobic Gram-positive and Gram-negative bacteria are administered by IV route in the treatment of acute pulmonary exacerbations [19]. Among cephalosporins, generally active against both aerobic Gram-positive and Gram-negative bacteria, only ceftazidime and cefepime have activity against *P. aeruginosa*. They are often used to treat *P. aeruginosa*-related exacerbations by IV administration. The penicillins indicated above have also a wide-array of antibacterial activity against anaerobic, aerobic Gram-positive, and Gram-negative bacteria, including *P. aeruginosa* and are administered by the IV route in acute pulmonary exacerbations [13].

Colistin

Colistin, or polymixin E, first marketed in the 1950s, has been neglected up until very recently because of reports of nephrotoxicity and neurotoxicity, but multi-resistance to other antibiotics brought it back on stage as a last-resort anti-infective drug and promoted modern pharmacokinetic investigations and re-evaluation of dosing schemes [21]. Colistin is commercially available as colistin sulfate for topic use (oral tablets) and as an inactive prodrug, colistin methanesulfonate (or colistimethate sodium salt), which is given by IV route or via inhalation, alone or in combination therapy to eradicate early infections and to stabilize chronic infections [22]. Colistin sulfate is not used for inhaled therapy due to throat irritation, cough and severe bronchoconstriction. Colistimethate sodium is usually well tolerated and used to treat chronic endobronchial *P. aeruginosa* infection as

an extemporaneously prepared solution for inhalation with, however, some associated reticence due to the hydrolysis risk and conversion in colistin [23,24,2].

Miscellaneous

Some other antibiotics may be used in specific situations for the treatment of CF lung disease, not only against *P. aeruginosa* but also *S. maltophilia, S. aureus* and other bacteria.

Fosfomycin is an antimicrobial agent with activity against Gram-positive and Gram-negative bacteria, including *Pseudomonas* spp. and, more specifically, multidrug-resistant *Pseudomonas* [25]. This antibacterial agent is available in oral formulations as fosfomycin calcium or fosfomycin trometamol, and in IV formulation as fosfomycin disodium. The repeated use of the same antibiotics usually leads to the development of resistance, patient intolerance and side effects. In these patients, fosfomycin may be co-administered with other antibiotics [26], because its action mode is considered as unique (inhibition of the initial step in cell wall synthesis) [7] and not affected by other classes of antibiotics, thus preventing cross-resistance [25]. IV fosfomycin in combination with other antibiotics for pulmonary exacerbations in CF patients colonized by multi-resistant *P. aeruginosa* resulted in clinical improvement with low side effects [26].

Azithromycin therapy effectively improves lung function and reduces the frequency of pulmonary exacerbations in CF patients chronically colonized with *P. aeruginosa*, but these effects appear to be only temporary. Usually it is used as anti-inflammatory agent. Some authors hypothesized that the mechanism of azithromycin therapy failure could be linked to its antimicrobial properties and the development of resistance in organisms resident in the CF airway microbiome. Studies have shown that the long-term exposure of CF patients to azithromycin leads to significantly increased macrolide resistance in CF pathogens, such as the *Haemophilus* spp. [27].

Minocycline (by oral administration) may have an “adjunct role”, alone or in combination with other antibiotics, in the antimicrobial therapy of multidrug-resistant respiratory pathogens in CF [7]. More specifically, some authors reported that minocycline had *in vitro* activity against isolates of *B. cepacia, S. maltophilia* and, to a lesser extent, *P. aeruginosa* cultured from the respiratory tract of patients with CF lung disease [28].

Clindamycin and rifampicin are recommended for therapy against *S. aureus* by oral or IV route [29]. Linezolid, an oxazolidinone antibiotic, is an optional treatment against MRSA infections in CF patients (with acute exacerbations) [30]. Due to its unique mechanism of action, the probability of cross-resistance with other antibacterial agents is low [31]. In addition, linezolid has a good tissue penetration (especially in the respiratory tract), which is an advantage in the treatment of CF lung disease [32]. However, this antibiotic is expensive and clinical experience is limited [29]. The combination of amoxicillin with clavulanic acid by oral administration may also be used when both *S. aureus* and *H. influenzae* infections are present [29].

2.1.2 – Other therapeutic agents

Gene therapy

Gene therapy is under investigation and innovative approaches are focused on molecules that restore CFTR function or structure [3,33,34]. Although the lung epithelium may be easy to reach by inhaled gene vectors as a targeted treatment, efficient and safe formulations of viral and non-viral vectors are still awaited [3,35]. For the rare mutation G551D, some CFTR modulators (e.g. ivacaftor) have recently been approved. However, for the common mutation F508del, trials are ongoing [36].

Antimicrobial peptides

Antimicrobial peptides such as lysozyme and lactoferrin are present in the ASL and their antimicrobial [5] (and anti-inflammatory) activities have been investigated because the levels of these peptides are increased in CF patients. However, the high salt concentration resulting from the CFTR dysfunction reduces their activity [7,37,38]. Nevertheless, the innate airway defense offers the opportunity for the development of novel therapeutic approaches [38]. Secretary leukocyte proteinase inhibitor and preelafin are other resident lung molecules that demonstrated antimicrobial activity against *P. aeruginosa*. The aim now is to determine the role of protease inhibition in CF lung disease [7,38,39].

Vaccination

The prevention of *P. aeruginosa* infection may have an important role in treatment of CF patients. Some authors concluded that anti-pseudomonal vaccination could be effective in preventing *P. aeruginosa* lung infection [40-42], and some concluded that nasal and oral vaccines are promising candidates for inducing a specific antibody response in the lungs of CF patients [41,40]. Nevertheless, a review of recent trials from the Cochrane CF and Genetic Disorders Group concluded that the use of vaccines against *P. aeruginosa* cannot be recommended in CF patients [43].

2.1.3 – Resistance of *P. aeruginosa* to antibiotic therapy

In spite of intensive antibiotic therapy and defense mechanisms of the immune system, *P. aeruginosa* has the ability to survive and persist for years in the CF patients lungs owing to its adaptive mechanisms [40,15,41,44]. *P. aeruginosa* has the ability to form biofilms [45], to develop a mucoid phenotype and to lack membrane porins (that are important to antibiotic diffusion) [46,3,47,48] or may develop an active drug efflux mechanism [3,49,7,50].

Resistance mechanisms

Different antibiotics display different modes of action (Figure 2.1) and therefore different "rates of resistance":

a) beta-lactams (e.g. carbapenems and the monobactam aztreonam) interfere with bacterial cell wall synthesis [15,14];

b) quinolones inhibit DNA synthesis by acting on topoisomerases, more particularly topoisomerase II (DNA gyrase) and IV (which are essential for maintenance of the appropriate DNA topological state for replication and transcription) [51,52];

c) aminoglycosides (e.g. tobramycin, amikacin and gentamicin) [14,15] inhibit protein synthesis by binding bacterial ribosomal subunits or inhibiting ribosomal enzymes [15].

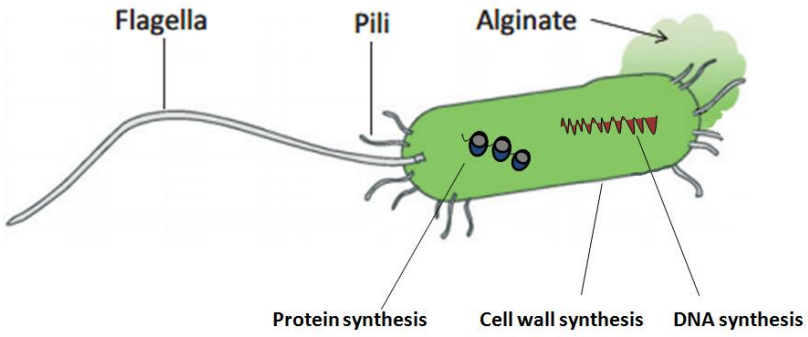

Figure 2.1 – Schematic representation of *P. aeruginosa* morphology detailing the flagella and pili, responsible for the motility and adhesion, and the alginate, involved in the biofilm production. The three main places for antibiotic activity are also indicated. Partially reproduced with modifications from [53], with permission.

In what pertains to the development of resistance to antibiotics, *P. aeruginosa* becomes resistant to fluoroquinolones through two known mechanisms:

1) drug efflux pumps that reduce the accumulation of antibiotics in the cell;

2) point mutations in the genes of the quinolone target enzymes, DNA gyrase and topoisomerase IV, owing to amino acid substitutions in the corresponding genes *gyrA* or *gyrB* (for DNA gyrase) and *parC* or *parE* (for topoisomerase IV) [51,52].

Note that this class of antibiotics is associated with cross-resistance to other antibiotics (e.g. aminoglycosides) and act as selectors for MRSA [54].

With respect to other antibiotic classes, *P. aeruginosa* resists aminoglycosides mainly by reducing their transport through the membrane [55] and reduces the beta-lactam activity by some mechanisms as described in Table 2.1. Recently, a study concluded that resistance to tobramycin in *P. aeruginosa* isolates from CF patients under antimicrobial therapy may occur, while colistin resistance appears to be rare [56].

Table 2.1 – Antibacterial agents used in the treatment of the *P. aeruginosa* infection (mechanism of action and corresponding resistance mechanism).

Antibiotic	Mechanism of action in *P. aeruginosa*	Resistance mechanism
Beta-lactams	Interference with bacterial cell wall synthesis [15,14].	• Mutational derepression of the AmpC chromosomal beta-lactamase; • Acquisition of secondary plasmid or transposon-mediated beta-lactamases; • Reduced permeability; • Multi-drug efflux [57].
Aminoglycosides	Inhibition of protein synthesis: binding to bacterial ribosomes and nhibition of ribosomal enzymes [15].	• Reduction in the active transport through the membrane [55].
Fluoroquinolones	Inhibition of DNA synthesis (action on topoisomerase II and IV) [52,51].	• Drug efflux pumps; • Point mutations in topoisomerases [52,51].

Currently, antibiotic resistance is increasing and new strategies to overcome this reality are needed. As previously suggested [3], the strategy may rely on the combination of antibiotics to avoid antibiotic resistance. Recently, some inhalable particles co-encapsulating two or more antibiotics displayed good results, especially when the microorganism is difficult to kill with a single antibiotic [3,58]. One strategy consists in encapsulating the drugs in liposomes or MS, as will be discussed later [3]. When the resistance is due to the drug efflux mechanism, the alternative consists in the administration of efflux pump inhibitors [7]. With respect to CF, compounds such as broad-spectrum inhibitors efflux pumps in *P. aeruginosa* are in clinical development for use as an aerosol [7,59]. A study has recently evaluated the efficacy of efflux pump inhibitors in reducing CIP and LVX minimum inhibitory concentrations (MICs),

concluding that the activity of these inhibitors cannot be generalized to all bacteria and to all antibiotics of the same class [59]. In what pertains to inhaled antibiotics, there are areas of variable antibiotic concentrations in the airways. The low concentration areas allow the selection of more resistant microbes. Alternating months of antibiotics reduce the selective pressure on the bacteria, and it is necessary to understand whether "drug holidays" or alternating chronic antibiotics may prevent the emergence of multi-resistant organisms in CF. Resistance may be transient, and reverted when antibiotic selective pressure is removed, a process known as adaptive resistance [15]. According to some authors, there is no present definition of *in vitro* resistance relating to the use of aerosolized formulations [60,7] because the analyses are related to systemic administration and not to high concentrations achievable in the pulmonary tract [8].

2.1.4 – Cystic Fibrosis sputum: a barrier to pulmonary administration

Drug delivery to the deep lung may be impeded by changes such as mucus hypersecretion or thickening, fibrosis or poor blood circulation. Thus, a deep understanding on the impact of the CF on lung pathophysiology is required to avoid or reduce the risk of failing to deliver an inhaled particle [61]. Beyond mechanisms of bacterial resistance to the antibiotic therapy, *P. aeruginosa* participates in the sputum development in the CF lung disease. More particularly, the CF sputum is described as a physical, chemical and biological barrier and as a stage for bacterial resistance [3]. Normal mucus consists of a high percentage of water and a small amount of mucins, and it is easily traversed by gas, ions, nutrients and proteins, and can protect the organism against foreign substances such as toxins and pathogens [62,3]. CF sputum has less water (90 %) and intact mucins and more DNA and actin, which provides a higher viscosity to mucus [3]. In addition, mucins have negative charge (carboxyl groups) and form disulphide bonds, physical entanglement and non-covalent interactions [63,3]. *P. aeruginosa* is able to evade antibiotic therapies, changing into mucoid strains and forming biofilms. These biofilms, as mentioned above, are usually resistant to phagocytosis and antibiotics. Their content in oxygen and nutrients is low, which slow down the growth of the bacteria and reduces the susceptibility to some antibiotics. Sputum has to be traversed by some drugs, including gene therapeutics and ion-channel regulators. Other drugs such as aerosolized antibiotics have to penetrate the sputum, where they should be evenly distributed [3]. Thus, it is very important for drug delivery to understand the interaction between the drug and CF

sputum. Some interactions between sputum and drugs are reported such as tobramycin, which provides electrostatic interactions with mucus and biofilms, leading to impaired activity, as previously discussed [7]. In addition, DNA and actin have the ability to form a polymer that increases the sputum viscosity [3,64] and, for example, nanoparticles (e.g. used for the delivery of genetic therapeutics) have difficulty in moving through the viscous sputum. Some authors proposed modifying the nanoparticles' surface with polymers such as polyethylene glycol (PEG) with low molecular mass to reduce the interactions between these particles and sputum, to limit their aggregation and to decrease alveolar clearance [3,65,66]. The administration of mucolytics before nanoparticles administration may reduce the steric hindrance of mucus, but have two types of outcomes [3]: 1) the delivery of particles with deoxyribonuclease (DNAse) and adenoviral genes is enhanced by mucolytics such as N-acetylcysteine [3,67-70]; 2) gene transfection efficiency is, however, not improved [3,70]. Pulmonary co-administration of antibiotics and mucus-thinning agents may also be a good tool for local therapy in CF patients. As reported by some authors, an inhalable dry-powder system co-delivering DNase and CIP may kill the bacteria in sputum more efficiently than particles with CIP alone [3,71]. Some authors proposed the osmotic agent mannitol as an alternative to DNase and observed that it improved antibacterial efficiency of CIP against *P. aeruginosa*. Mannitol has the ability to increase local water content in the mucus and enhances drug penetration into it [72,73]. Other strategies to treat biofilms, and beyond the scope of this thesis, include bacteriophages and efflux pump inhibitors among others, as described elsewhere [74].

2.1.5 – Indications of antipseudomonal inhaled antibiotics

Antibiotic resistance and additional pathogens in this disease lead to new strategies in the life-long treatment of pulmonary infection [7]. Some authors described the airways as the major therapeutic target in this disease. Antibiotics given systemically enter the bronchial secretions from blood by simple passive diffusion and some of them diffuse poorly across lipid membranes and into bronchial secretions [15]. Therefore, some drugs are delivered via inhalation to allow high doses of drug at the site of action and to decrease systemic absorption and side effects [3,7,1]. Thus, inhalational drug formulations are an attractive and interesting mode of delivery of some drugs to treat CF patients [3] and, more

particularly, inhaled antibiotics may be used as prophylaxis, to eradicate early infection, to suppress chronic infection or to treat acute pulmonary exacerbations [1].

Prophylaxis

Regarding prophylactic therapy, paucity of data supports its use and it has also some risks, such as cumulative drug toxicity and the investment of money and time in something unproven [1,75]. Recent guidelines from the CF Foundation recommend against the use of prophylactic antibiotics to prevent the acquisition of *P. aeruginosa* [76]. Nevertheless, CF patients cannot recuperate previous pulmonary function after pulmonary exacerbations and, therefore, aerosolized antibiotics may eventually control this problem [8].

Early eradication

Until now, there are no convincing data showing that the early eradication of *P. aeruginosa* improves the long-term prognosis [1,75]. However, an eradication protocol for first appearance of *P. aeruginosa* has been developed in CF patients between 1995 and 2009 and included 2 weeks of IV piperacilin and tobramycin, followed by oral CIP for 3 weeks and nebulized colistimethate for 6 months. The results showed clinical, economic and resource utilisation benefits [77]. Other studies have been performed, such as inhaled tobramycin alone [78,6], tobramycin with oral CIP [6] and nebulized colistin with oral CIP [79,75,6], and all of them showed good efficacy. Nevertheless, there is a lack of evidence from large randomized trials to define the optimal drug(s), doses, delivery methods and duration of treatment for early *P. aeruginosa* eradication [1]. Although more approaches have been described, there are mainly two prospective multi-center studies (ELITE in Europe, EPIC in USA) that tried to determine the best treatment regime with less adverse effects [79,75]. EPIC compared different regime therapies: participants inhaled tobramycin with either oral CIP or placebo during treatment cycles, but the results showed no significant differences between them [44,80,81]. ELITE concluded that TIS twice daily for 28 days was effective for 56 days, and a well-tolerated therapy for early *P. aeruginosa* infection in CF patients [82]. In this study, almost all of the randomized patients had negative cultures for *P. aeruginosa* one month after the end of treatment and the majority continued to have negative cultures 27 months later, but

clinical outcomes were not compared between patients who did or did not become culture-negative for this bacterium. Nevertheless, a recent 3-year prospective cohort study of adult patients with CF from Canada examined the clearance of *P. aeruginosa* from their sputum and its relationship to the clinical status of patients. The study concluded that changes in the *P. aeruginosa* sputum culture may not reliably predict an improvement in clinical status [83]. Recently, strong recommendations for the use of inhaled antibiotic therapy for the treatment of initial or new growth of *P. aeruginosa* were suggested by the CF Foundation and the favored regimen consisted of inhaled tobramycin, 300 mg twice a day, for 28 days [76].

Chronic infection treatment

The best evidence regarding the indication of antibiotic aerosol is chronic infection with *P. aeruginosa* [75,84]. According to the American CF Foundation, inhaled tobramycin was recommended for chronic use to improve lung function and reduce pulmonary exacerbations but for children less than 6 years, no recommendation was made [1,85,84]. However, European guidelines recommended inhaled antibiotics for CF patients irrespective of age or lung function [1,75,85]. Nebulized colistimethate is also used in Europe against chronic infection but little evidence about its benefits exists [75]. Also nebulized LVX solution was recently approved in Europe (see section 2.2.1 for details).

Treatment of pulmonary exacerbations

These exacerbations in CF are usually treated with oral or, more frequently, IV antibiotics and, as patients recover, inhaled antibiotics are also used to suppress growth of the bacterium [3,85]. Some authors demonstrated that inhaled antibiotics reduce both the frequency of pulmonary exacerbations and the number of hospitalizations [8]. However, due to the risk of toxicity, the CF Foundation concluded that "there is insufficient evidence to recommend for or against continued use of inhaled antibiotics in patients treated with the same antibiotics intravenously for the treatment of an acute exacerbation" [85,15] and, thus, further studies are necessary [1]. Nevertheless, both chronic and airway clearance therapies may be continued during an exacerbation [85]. Different antibiotics are administered according to colonized pathogens in CF patients. As previously described, *P. aeruginosa* is usually eradicated with at least two antibiotics, including IV

aminoglycosides, IV and oral fluoroquinolones and IV beta-lactams [3]. According to the CF Foundation, "once-daily dosing of aminoglycosides is preferable to 3-times daily dosing" [85], as reported for tobramycin [82]. In order to eradicate other pathogens, other antibiotics such as amoxicillin-clavulanic acid, clindamycin, linezolid co-trimoxazole and macrolides are also used [3,15,86].

2.2 – Recent developments and new formulation approaches in the inhaled antibiotic therapy

With respect to the inhaled therapy for treatment of CF patients, some aspects have already been explored and included the administration of different antibiotic classes as inhaled liquid or powder formulations. These two different presentations, dry or wet, will be further discussed next in order to understand the pros and cons for each type of lung delivery, and a brief description of the available inhalers will also be included. Finally, innovative aerosol formulations such as liposomes and polymeric MS will be addressed.

2.2.1 – Liquid antibiotics

Aerosolized antibiotics are generally well tolerated but some adverse effects have been reported such as cough and throat irritation which are, however, more frequently observed with dry-powder formulations (described in the next sub-section). Dysgeusia and a decrease in pulmonary function after administration have also been reported. These effects appear to be more related to aerosolized particles than to the direct pharmacological effect of the drug [8]. Nebulized liquid drugs must be more potent and the time of administration should be reduced to improve compliance to therapy. Concomitant administration of nebulized antibiotics may form precipitates and may lead to antibiotic resistance owing to antibiotic dispersion into the ambient air [58]. Therefore, dry-powder formulations may avoid these problems, as will be discussed herein.

The nebulizers are the devices used to convert the liquid medication into a mist [87]. They do not require from the patient the coordination between the actuation and the inhalation, being less complex than the MDI and DPI devices. However, they are not portable and require long administration times, and cleaning and disinfection procedures, being usually used by the patients who are either too ill or too young to use MDIs or DPIs

[88,12]. Different types of nebulizers are available and include the 1) jet (the most frequent), 2) ultrasonic and 3) vibrating mesh nebulizers, with or without the smart technology (aerosol delivery according to breathing pattern) [88]. Briefly, for the jet nebulizer there is a compressor that sucks air from the environment through a filter, generating airflow through the device, which contains a Venturi tube. In this tube, the air is mixed with the liquid generating the primary aerosol. A baffle in the nebulizer further disintegrates the droplets in smaller aerosol particles. The majority of the formed aerosol particles fall back in the medication cup, being re-nebulized (see Figure 2.2) [87].

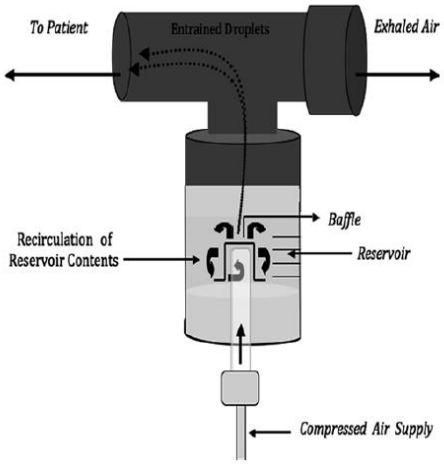

Figure 2.2 – Schematic representation of a jet nebulizer. Reproduced from [88], with permission.

The ultrasonic nebulizers contains a vibrating piezoelectric crystal that is responsible for the aerosol generation, and aerosol droplets are also recycled, as with jet nebulizers [89]. The mesh nebulizers (include the eFlow® technology) are more recent and present several advantages over the jet nebulizers. They can use either a vibrating or a fixed membrane with a piezoelectric element with microscopic holes to generate liquid droplets. These devices are generally portable and silent with optimal particle size for delivery to the small conducting airways and high efficient delivery compared with jet nebulizers [12,87].

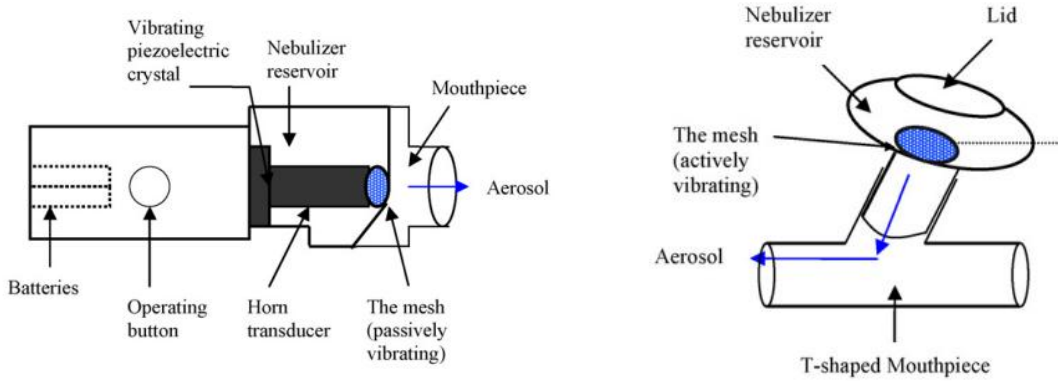

Figure 2.3 – Schematic representation of two examples of mesh nebulizers, "passive" with a vibrating element (left) and "actively" vibrating (right). Reproduced from [89], with permission.

Among the referred nebulizers, the MDI devices are largely used for treatment of pulmonary diseases to deliver, preferentially, corticosteroids and bronchodilators. But, so far, not largely used for drugs which require large doses such as antibiotics. They are portable, but require coordination between actuation and inspiration, making it the most difficult inhaler to use. Usually, there is also a need of an adequate propellant, where the drug is dissolved or dispersed. Detailed features may be found elsewhere [90].

Regarding the inhaled liquid antibiotics for the treatment of CF lung disease, there are two formulations in clinical use for years, the TIS (TOBI®) and the AZLI (Cayston®), respectively corresponding to the nebulized tobramycin and aztreonam (Figure 2.5), as already described in the subsection 2.1.1. Actually, the IV aztreonam appeared to be not appropriate for pulmonary administration because it contains arginine leading to airway inflammation [7]. To overcome this problem, the drug has been reformulated as a lysine salt for inhalation [1] and showed improvements in pulmonary function and reduction in bacterial density in the lungs of CF patients with chronic airway *P. aeruginosa* infection [91,44,92]. This formulation is administered with a vibrating mesh nebulizer, with the Altera® Nebulizer System, over about 2-3 minutes [93,94,92]. For tobramycin, TIS is administered with a jet nebulizer, the PARI LC Plus nebulizer, taking 15-20 min for the administration twice daily and has demonstrated noninferiority when compared with the correspondent dry powder formulation (TIP) [95]. Recently, fosfomycin in combination

with tobramycin [96] has been investigated for inhalation in a phase II study with promising activity against *P. aeruginosa* [1,44,97].

As described previously, thickened mucous secretions result in areas of low oxygen concentrations, that lead to reduced potency/ activity of aminoglycosides, but less so for fluoroquinolones agents. These differences may have important therapeutic implications [5]. Fluoroquinolones result from the addition of a fluorine atom at position 6 of quinolones, a chemical alteration that improves both drug penetration into the bacterial cell and activity against Gram-negative bacteria [52]. With respect to this class of antibiotics, inhaled LVX solution was approved as Quinsair® by the European Medicines Agency (EMA) and is under development in USA as Aeroquin™ [98,1,93,10] for use in the eFlow® mesh nebulizer. A recent study evaluated its pharmacokinetics (PK) and safety and showed high sputum and low serum LVX concentrations [99,1]. Additionally, C_{max}/MIC and AUC/MIC ratios in the airways were substantially larger than with oral or IV administration. A phase 2b trial with inhaled LVX demonstrated a reduction of *P. aeruginosa* in sputum and improvements in lung function. Drug pipeline information from the American CF Foundation indicates that the phase 3 trial is completed (Figure 2.5). However, a relatively long time of administration (5 min) for Quinsair® is required, disadvantage than can be overcome by the preparation of a formulation for a DPI. According to previous information, LVX appears to be more potent against *P. aeruginosa* biofilms than aminoglycosides and aztreonam. Thus, a high level of LVX readily achievable in the lung following aerosol delivery might be useful for the management of pulmonary infections in CF patients [82].

2.2.2 – Dry-powder formulations

Nebulized formulations are particularly useful for potent drugs, as previously reported, but they have also been used for less potent drugs such as antibiotics leading to administration of higher doses which reduce patient tolerance. It may be necessary to administer drugs for several minutes and multiple doses, when higher doses are required [8]. However, dry-powder formulations are more time efficient and more hygienic than nebulized liquid formulations [3]. DPIs are the common devices for pulmonary administration of powders. They are portable, easy to use and breath-activated, being their performance dependent on the inspiration flow rate achieved by the patient and,

therefore, often less suitable for children and elderly [88,90]. Usually, a gelatin capsule is inserted in the DPI before each actuation (Figure 2.4). However, some DPI devices are multiunit dose, which are pre-metered by the device manufacturer and contain enough powder for multiple doses (60-200), being each dose "made as available" by the patient prior to the actuation. The basic operating form consists of three regions: a) an air inlet port for air entering from outside; b) a powder-holding chamber and c) an outlet port designed for delivering the dose to the patient [88]. DPIs may deliver each dose in one-third of the time required for nebulization [44]. Being able to deliver anti-pseudomonal therapeutics with a portable inhaler in a fraction of the time required to deliver the same drug via nebulization is expected to improve quality of life and compliance by CF patients [100]. Currently, inhalable dry-powders of some anti-infective drugs including CIP, tobramycin and colistin have been studied in clinical trials [3]. Inhalable dry-powder is being developed for CIP, alone or in association with recombinant DNase that may be a promising strategy for local anti-pseudomonal therapy [82]. Clinical trials (phase 2) with a lipid-based dry powder formulation (Pulmosphere™ technology) of CIP were carried out in CF and non-CF patients. Despite the reduction in bacterial load for non-CF patients, no significant changes were observed for CF patients and remains unclear whether further trials will be conducted for CF patients and/or if such formulation will be approved for CF [2]. Taking into account that co-encapsulating of two or more antibiotics reduce the amount of powder to be inhaled, particularly if the drugs are synergistic [58], formulations were evaluated containing CIP, doxycycline, or a combination of both, with polyvinylalcohol (PVA) in order to obtain a controlled release pattern. Results demonstrated good particle size distribution, thermal stability, acceptable aerosol performance and modified release profiles [101]. Concomitant administration of antibiotics in the same formulation, such as microparticles with CIP and ceftazidime with dipalmitoyl phosphatidylcholine (DPPC), albumin and lactose as excipients and prepared by the spray-drying method [58], may also avoid the development of antibiotic resistance. In addition, the combination of co-spray-dried mannitol and CIP from a DPI appear to be an attractive approach to promote mucus clearance in the respiratory tract while simultaneously treating local chronic infection in CF patients. In this case, the delivery of both an osmotic agent and an antibiotic in one single dry-powder dose could have many advantages such as physical stability and an efficient aerosol powder, but further studies are required to understand the *in vivo* antibacterial and mucociliary clearance

enhancement of these formulations [73]. With respect to aminoglycosides, TIP received FDA approval in March 2013, based on phase 3 trial results (Figure 2.5) [16]. It demonstrated similar results of FEV_1, bacterial load decrease and adverse effects, with less than one-third of the administration time, when compared with TIS [1,82]. It is administered with a DPI (Figure 2.4) based on the PulmoSphere™ technology, which enable the creation of porous solid microparticles [2,102].

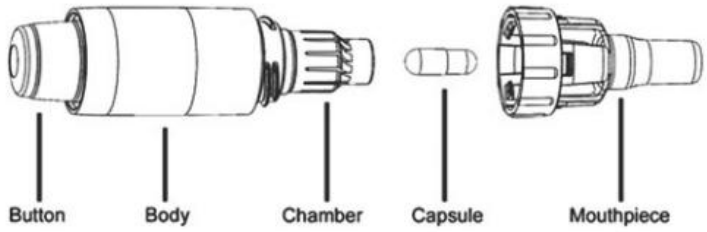

Figure 2.4 – Example of unit dose DPI with the representation of the different portions of the device and the capsule (T-326 Inhaler for TIP). Reproduced from [102], with permission.

Colistin has also been formulated as colistimethate sodium dry-powder for inhalation and showed it was well tolerated by CF patients, being approved in 2012 in Europe as Colobreathe® [103]. Both colistimethate solution and dry-powder for inhalation were found to be as effective against *P. aeruginosa* in chronically-infected CF patients. However, contrary to TIS, inhaled colistimethate solution did not improve lung function and such solution is controversial due to the instability of the prodrug and the spontaneous hydrolysis leading to an increase of colistin, which is nephrotoxic, as aformentioned [104,2]. Colistimethate dry-powder for inhalation was however found to be non-inferior to TIS towards lung function preservation, and is more convenient in terms of administration procedure (1 min twice a day vs. 20 min twice a day) and inhaler maintenance [103]. In spite of the advantages reported for dry-powder formulations, i.e. mainly shorter time of administration over solution of inhalation, there are some issues that need improvement. The deposition of high amounts of dry-powders on pulmonary epithelia may lead to adverse effects, ranging from unpleasant taste, cough, throat irritation, dysphonia to haemoptysis, difficulty of breathing and bronchospasm or even acute toxicity [24,105]. In addition, drug powders are usually immediate-release dosage forms that lead to fluctuations of drug concentrations and necessitate frequent

administrations. To minimize these problems, inhalable innovative drug delivery systems have been under investigation [105,2] and will be discussed in the following section.

2.2.3 – Innovative aerosol formulations

Sustained release of drugs in the lung may be achieved with their incorporation in liposomes and other formulations such as biodegradable microspheres (MS) [106]. Controlled release formulations may increase and sustain lung concentration which contribute to better patient compliance due to decrease of dosing frequency and may reduce systemic and/ or local toxicity. Owing to these characteristics, these formulations appear to be a good vehicle to deliver some anti-infective drugs to treat *P. aeruginosa* lung infection in CF patients. However, the development of controlled release formulations for the lungs may be complicated by the multiple clearance pathways (e.g. mucociliary clearance, macrophages clearance, systemic absorption, cough clearance), and by the concerns relative to the safety and slow clearance of retentive excipients (e.g. polymers) [100].

Lipid-based formulations

Some antibiotic lipid-based delivery systems have been investigated for pulmonary delivery in CF and include the liposomes and solid lipid nano- and microparticles [2]. Liposomes are one of the most investigated systems for controlled pulmonary delivery, since they may be prepared with phospholipids endogenous to the lung as surfactants and may also incorporate both hydrophilic and hydrophobic drugs [106]. Liposomes release the drug overtime and might reduce the dose frequency to once a day or less [1], which may be important for CF patients' compliance. These formulations appear to be able to maintain their integrity following nebulization, can penetrate mucoid biofilms [100,82] and prolong the residence time of the antibiotics in the lungs [1]. Triggering of antibiotic release from liposomes is mediated by the rhamnolipids produced biofilm-localized bacteria [3]. However, some authors consider that nebulization of liposomal formulations can cause structural disruption with consequent release of encapsulated drug and these formulations are unstable during storage (even at low temperature). Thus, dry liposome powder for inhalation may improve stability, which represents an advantage of these forms [107]. Tobramycin liposome has shown both significant increase in drug retention

in the lung and antimicrobial activity compared with classical formulations. However, the clinical demonstration of the sustained release and long-term efficacy could not be demonstrated [7]. Sustained-release lipid formulation of amikacin (Arikace™) is being developed for inhalation (Figure 2.5). It is delivered in 10-13 minutes by Pari eFlow®, and prolonged time intervals between exacerbations was obtained when compared to placebo [1,82]. In a phase 3 trial, both improved lung function and *P. aeruginosa* reduction were observed [16]. The enzymes in sputum and factors associated with *P. aeruginosa* can help amikacin release from the liposomes, thus targeting the drug to the bacterial microenvironment. Some authors developed liposomal gentamicin formulation to compare its activity with free gentamicin against *P. aeruginosa*. Results showed that the liposomal formulation protects the drug from bacterial enzymes and facilitates its diffusion across the bacterial envelope and has MIC significantly lower than those of corresponding free gentamicin [108,109]. Also, a liposomal CIP formulation for nebulization is under development. A study with CF patients treated with liposomal CIP showed both a decrease in sputum density and an increase in lung function [1]. Other lipid-based formulations under development and not addressed in this thesis were reviewed elsewhere [2].

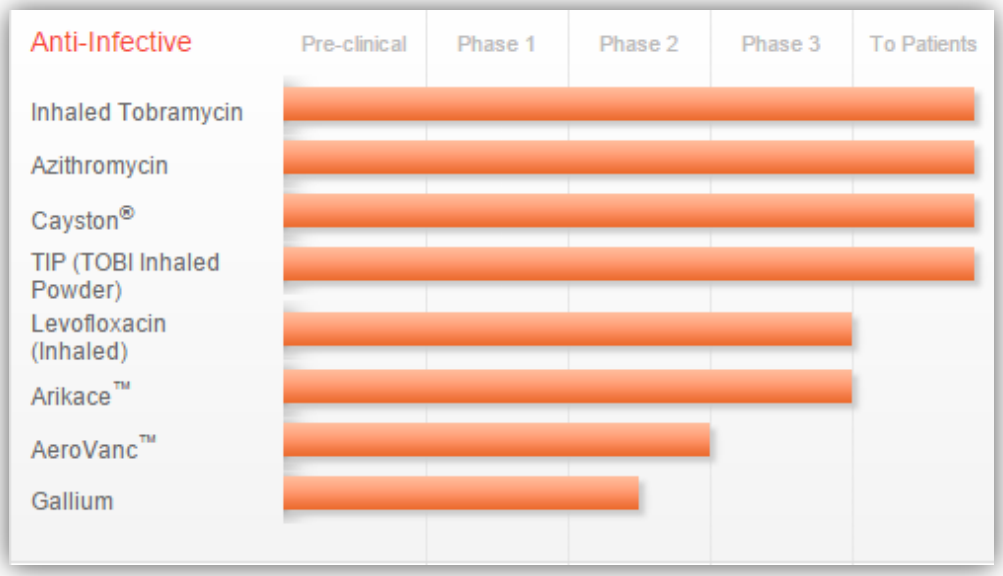

Figure 2.5 – The CF Foundation dynamic 'pipeline' of anti-infective therapy. Reproduced with permission from [16].

Strategies for development of inhaled polymeric microspheres

MS may be an alternative to deliver some of therapeutic agents previously described. In fact they may facilitate the dispersion of drugs in the inhaled air and reduce the deposition in the oropharynx through adequately modulated physical properties, and may target specific regions of respiratory tract by modifying size and density ratios of the particles [110]. Additionally, it is possible to control the kinetics using adequate polymers and formulation additives. These innovative formulations may reduce direct contact of highly concentrated drug formulations with the lung tissue (and reduce the toxicity) and allows a sustained release [105]. Therefore, MS are expected to overcome the problems related to dry-powders inhalers and nebulized solutions of anti-infective drugs for treatment of CF patients. In addition, MS appear to be more stable, from the physic-chemical point of view, with higher shelf-life, in comparison to liposomes and a slower release rate and a longer duration of action may be obtained. Thus, biodegradable MS may be more easily formulated in a suitable pulmonary delivery in comparison with liposomes due to higher stability [106,111]. MS (polymeric or non-polymeric) may be developed to achieve drug targeting and to improve drug absorption and at the same time, with less adverse effects and dosing frequency maintaining the therapeutic effect [112]. Nevertheless, few antibiotic-loaded MS have emerged for pulmonary delivery purposes. Currently, several inhaled MS for lung diseases such as asthma and chronic obstructive pulmonary disease (COPD), pulmonary arterial hypertension, tuberculosis and lung cancer are under research and appear to be a good alternative to lung delivery, as presented in Table 2.2. Thus, we can understand how these controlled-release formulations may represent an interesting mode of drug delivery in CF patients. Some of the methods by which they are formulated (spray-drying technology [3,113], interfacial polymerization [114], emulsion solvent evaporation [114], membrane emulsification [115] or coacervation [116]) will be discussed in the Chapter 3 of this dissertation. Regardless of the method, they should have some characteristics such as easy scale-up, accurate and reproducible control over the size, uniformity of the particles (particularly important in lung administration) and compatibility with the drug (high temperature, organic solvents or physical forces may affect the bioactivity of the drug) [114]. MS may be composed of a biodegradable polymer matrix in which the drug is distributed, presenting some advantages such as possibility of encapsulation of many types of drugs, generally biocompatibility, [117] ability of sustained release for long periods of time. Drug release may be affected by

some factors including type of polymer, polymer molecular weight, copolymer composition, nature of excipients and microsphere size [114]. Sustained drug release properties, high local drug concentrations and less adverse affects make antibiotic-loaded MS an interesting approach for lung delivery in CF disease, with fewer daily administrations and better patient compliance to the therapy. They may be composed of synthetic polymers, such as the poly (lactic-co-glycolic acid) (PLGA) or natural, such as the chitosan.

PLGA inhaled microspheres

Particles prepared from PLGA have generated considerable interest in recent years for their use as delivery vehicles for various therapeutic agents. PLGA is by far the most common biodegradable polymer that is used for the controlled delivery of drugs, due to its well-known biocompatibility [117], and safety in biomedical preparations for parenteral use, which have been approved for human use by the FDA and EMA, as reviewed [118,119]. Its biodegradability is related with the hydrolysis in the respective monomers, lactic and glycolic acids (Figure 2.6), which are endogenous and easily metabolized by the body.

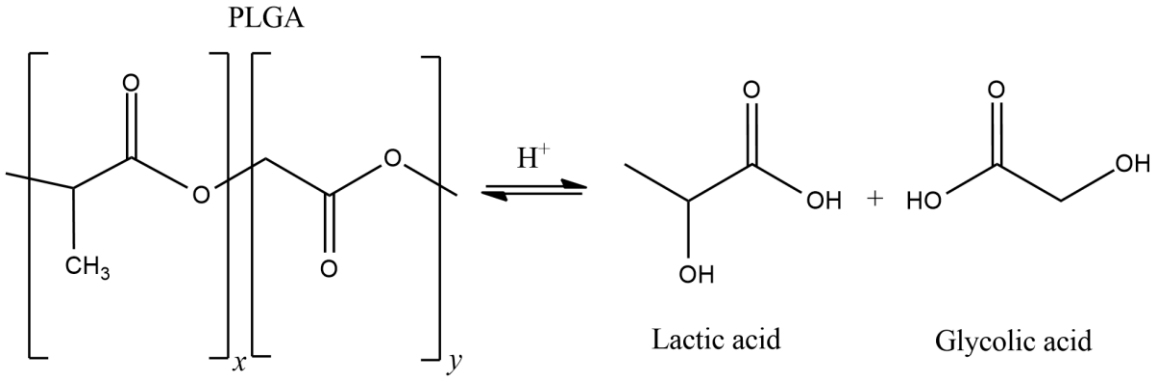

Figure 2.6 – PLGA hydrolysis in the respective monomers (lactic acid and glycolic acid).

However, its use in the lungs is not established yet [120]. Thus, there are some questions about its physiological and immunological toxicity in lungs that should be assessed [112]. PLGA may be not suitable for application in the respiratory tract, especially when frequent administration is necessary due to its prolonged degradation rate [121]. Additionally, PLA (poly (lactic acid)) and PLGA showed significant reduction in cell

viability compared to lipid particles, and long residence due to slow degradation might lead to pulmonary accumulation of polymers [107]. Nevertheless, it was recently concluded that the PLGA nanoparticles (NP) may affect the viability of Calu-3 cells but at concentrations that are too high for clinical use and studies with lung cells (e.g. A549 cell line) confirmed the low cytotoxicity and the absence of inflammation [122]. Therefore, PLGA appears to be a safe ingredient of MS for pulmonary administration in CF patients. As already aforementioned, for effective pulmonary drug delivery, the physical properties of the particles are crucial and the optimal particle size range for inhalation is 1-5μm. However, it is also ideal for phagocytosis and particles tend to agglomerate (due to Van der Waals and electrostatic forces) [123] and flow and disperse poorly [112]. For effective pulmonary drug delivery, particles must avoid phagocytosis by alveolar macrophages and should maintain the appropriate d_a during storage. Large porous microparticles may circumvent the previous problems, owing to their high d_g and low density, and smaller d_a, improving lung deposition [123,112], as previously reported in the Chapter 1. Further engineering of the particle surface may improve dispersion and flow of PLGA MS by minimizing particle-particle contact area. However, such particles are generally inefficient in mucus penetration. Several antibiotic-loaded small mucus-diffusive NP for lung delivery have been prepared but some unclear results were obtained concerning the mucus penetration ability and the deposition in the deep lung and *in vivo* studies are missing, as recently reviewed [2]. For optimization of lung delivery of particles, two considerations should be taken into account: size uniformity and mucoadhesion. PLGA and PLA are both poorly adhesive in comparison to other polymers (e.g. polyanhydrides), possibly due to limited hydrogen bonding potential with mucus glycoproteins. However, they may be coated with polymers with high densities of functional groups (e.g. polyamines) [117] and with polymers such as chitosan, as described below. Such particle coating has, however, shown increased adhesion of NP to the mucus, being controversial for administration in CF patients, once such entanglement does not allow the penetration in the biofilms.

A number of PLGA micro- and nanoparticles have been prepared by distinct methods (e.g. spray drying and emulsion solvent evaporation method) to deliver antibiotics (and other therapeutic agents) to the lungs (see Table 2.2). Also formulations for other administration routes are included in Table 2.2 due to the possibility to “extrapolate”

some concepts to lung delivery. Appropriate aerosol properties and *in vitro* sustained release is frequently successfully obtained, as reported elsewhere [123,117,124,105,125].

Chitosan inhaled microspheres

Natural polymers such as alginate, albumin and chitosan (a natural cationic polysaccharide [113]) have also been used in preparation of MS suitable for pulmonary delivery. They present some advantages including low cost, compatibility with a wide range of drugs, minimal use of organic solvents, bio/mucoadhesion, stability, safety and approval for human use by the FDA [116]. Bioadhesive properties are related to attractive electrostatic forces between the negative charged glycoprotein of mucin and the positive charged amino groups of the polymer [126]. These properties allow an efficient absorption and enhanced bioavailability, a much more intimate contact with the mucus layer and a specific targeting of drug to the absorption [127]. A plethora of published studies with chitosan-based systems for drug delivery exists but none of those products are FDA-approved. However, chitosan is generally recognized as safe (GRAS) material [128]. It exists as a oligosaccharide of D-glucosamine (80%) and *N*-acetyl-D-glucosamine (20%) units, obtained by the chitin deacetylation (Figure 2.7) [129].

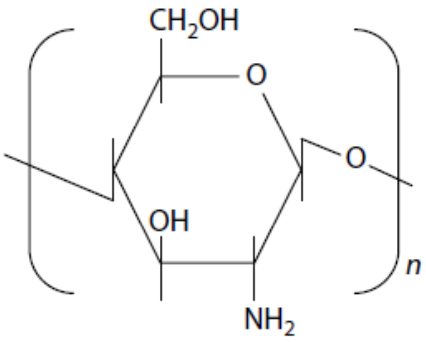

Figure 2.7 – Molecular structure of chitosan.

Chitosan MS were obtained for intrapulmonary administration of moxifloxacin, a fluoroquinolone that may represent an interesting drug for treatment of CF patients [126]. These MS were prepared by spray-drying method using glutaraldehyde (GL) as the crosslinking agent. The produced MS were spherical with suitable sizes for inhalation as detailed in Table 2.2. These authors concluded that formulation parameters such as concentrations of chitosan, moxifloxacin and GL affect the microsphere size. For

example, a higher efficiency of encapsulation was observed for higher chitosan concentrations and the opposite at the highest GL concentrations [126]. As previously described about the strategy of coating polyester polymers with other type of polymers, some authors compared the particle stability during nebulization of PLGA, chitosan and chitosan-coated PLGA microparticles in delivering rifampicin to lung macrophages. Combination of the two polymers leads to the formation of very stable particles, with high loading capacity for rifampicin, lower cytotoxicity towards alveolar epithelial cells, compared to PLGA particles and equivalent to those of chitosan in mucoadhesive properties [116]. Moreover, several antibacterial (including antipseudomonal) MS have been prepared for IV or ocular delivery and may represent an interesting tool for the development of inhaled MS for CF lung disease, by adjusting some formulation parameters. Some of these formulations are present in Table 2.2.

Table 2.2 – MS of antibacterial agents and other drugs used for treatment of lung diseases.

Drug	Disease and/or bacterium	Microsphere material	Method	Size	Appearance	Administration route	Ref.
Rifampicin	Tuberculosis (*M. Tuberculosis*)	PLGA	Double emulsion solvent evaporation	3.45 µm *	Spherical	Pulmonary	[124]
			Spray Drying	2.76 µm *	Shriveled		
		PLGA (PVA)	O/W or W/O/W emulsion solvent evaporation; premix membrane homogenization	3.43-6.26 µm **	Spherical, smooth	Pulmonary	[105]
		PLGA (PVA)	O/W emulsion solvent evaporation	2.58 µm ***	Very smooth	Pulmonary	[116]
		Chitosan	Precipitation	1.47-2.31 µm ***	Crumbled structure		
		PLGA (PVA) Chitosan	Emulsion solvent diffusion	1.41-2.9 µm ***	Very smooth		
Rifampicin/ isoniazid	Tuberculosis (*M. Tuberculosis*)	PLA	Emulsion solvent evaporation	6.2-6.8 µm *	Not evaluated	Pulmonary	[130]
Capreomycin	Tuberculosis	PLGA (PVA or HPMC)	W/O/W double emulsion solvent evaporation	1-20 µm ***	Highly porous interior, rough surface	Pulmonary	[131]
Moxifloxacin	Respiratory infections	Chitosan (GL)	Spray Drying	2.5-6.0 µm ***	Spherical, smooth, distorted	Pulmonary	[126]
Lysozyme	Pulmonary disorders	PLGA Ammonium bicarbonate	W/O/W double emulsion solvent evaporation	4.5 ±0.6 µm **	Porous	Pulmonary	[123]
Doxorubicin			W/O/W double emulsion solvent evaporation	4.6 ±0.4 µm **	Porous	Pulmonary	

Table 2.2 – Continued. (Caption shown on previous page).

Gemcitabine	Lung cancer	Chitosan	Spray-drying	1-5 µm	Porous, spherical	Pulmonary	[132]
Salbutamol sulfate	Asthma and CODP	PCL PVA	O/W emulsion solvent evaporation	Not taken into account	Spherical, rough surface	Pulmonary	[133]
		Chitosan	Spray drying	1-4 µm	Spherical, rough surface	Pulmonary	[134]
Beclometasone dipropionate	Asthma and CODP	Chitosan Leucine Lactose	Spray drying	2.1–3.2 µm **	Amorphous covered in "whisker-like" material low density	Pulmonary	[135]
		HPC	Spray Drying	2.9 µm **	Amorphous (ethanol solution)	Pulmonary	[136]
				2.5 µm **	Crystalline (aqueous solution)		
Prostaglandin E1	Pulmonary arterial hypertension	PLGA (PVA)	W/O/W double emulsion solvent evaporation	1-5 µm **	Spherical, smooth surface	Pulmonary	[137]
Ofloxacin	Pneumonia	Albumin (GL)	W/O emulsion solvent evaporation	11.32 µm ***	Smooth, spherical	IV [ab]	[138]
Ciprofloxacin HCl	*Salmonella typhimurium*	PLGA	O/O emulsion evaporation solvent	10-50 µm ***	Spherical shapes	IV [a]	[139]
Ciprofloxacin HCl	Ocular infections (*P. aeruginosa* and *S. aureus*)	PLGA (PVA)	W/O/W double emulsion solvent evaporation High pressure homogenization	246-309 nm	Amorphous	Ocular [a]	[140]
Tobramycin	CF (*P. aeruginosa*)	PLA (PVA)	W/O/W double emulsion solvent evaporation	0.736 ± 0.180 µm	Not evaluated	IV Intratracheal	[141]

*Volumetric diameter; ** MMAD; *** Mean diameter; [a] Some IV and ocular formulations were considered because they appear to be suitable for inhalation as far as some parameters are adjusted; [b]passive targeted drug delivery system to lungs; HPMC - Hydroxypropyl methyl cellulose; PCL – Polycaprolactone; HPC – Hydroxypropylcellulose.

2.3 – Motivation and objective

The lack of antibiotic-loaded polymeric MS intended to be delivered into the lungs of CF patients motivated most of the research work included in this thesis. As aforementioned, only few formulations have been developed to treat infections such as the *P. aeruginosa* chronic infection in CF. Fluoroquinolones present some advantages over the aminoglycosides, with higher anti-bacterial activity due to the non-impaired penetration in the mucus. LVX (Figure 2.8) was already developed as liquid aerosol for administration in CF patients, as previously detailed.

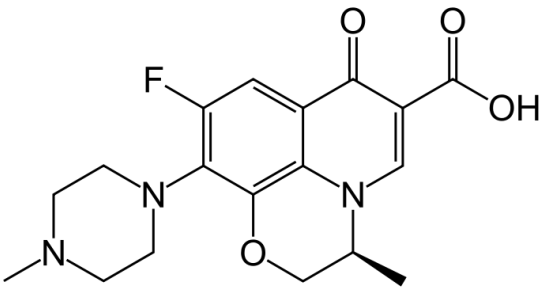

Figure 2.8 – Molecular structure of levofloxacin.

As alternative to this nebulized solution, the work described in this thesis is focused on the development of polymeric formulations for LVX fast and slow release. On the one hand, and prepared from a natural polymer, chitosan MS loaded with LVX and crosslinked with several agents are proposed in order to modulate MS properties (e.g. swelling behavior) and maintaining the immediate drug release and the suitable aerosol properties. In these MS systems, a factorial design was applied in order to optimize the conditions of preparation for the best formulation. On the other hand, and prepared from a synthetic polymer, PLGA MS loaded with LVX are aimed at sustained release in the lungs. Some modifications were performed to increase the drug content, once LVX is highly soluble in water, escaping from the MS core during the preparation. Methods for preparation and characterization of both polymeric systems are detailed next in Chapter 3.

2.4 – References

1. Geller DE (2009) Aerosol Antibiotics in Cystic Fibrosis. Respiratory care 54 (5):658-670.

2. Klinger-Strobel M, Lautenschläger C, Fischer D, Mainz JG, Bruns T, Tuchscherr L, Pletz MW, Makarewicz O (2015) Aspects of pulmonary drug delivery strategies for infections in cystic fibrosis – where do we stand? Expert Opinion on Drug Delivery 12 (8):1351-1374.

3. Ibrahim BM, Tsifansky MD, Yang Y, Yeo Y (2011) Challenges and advances in the development of inhalable drug formulations for cystic fibrosis lung disease. Expert Opinion on Drug Delivery 8 (4):451-466.

4. George AM, Jones PM, Middleton PG (2009) Cystic fibrosis infections: treatment strategies and prospects. FEMS Microbiology Letters 300 (2):153-164.

5. Boucher RC (2004) New concepts of the pathogenesis of cystic fibrosis lung disease. European Respiratory Journal 23 (1):146-158.

6. Rogers GB, Hoffman LR, Doring G (2011) Novel concepts in evaluating antimicrobial therapy for bacterial lung infections in patients with cystic fibrosis. Journal of Cystic Fibrosis 10 (6):387-400.

7. van Westreenen M, Tiddens HAWM (2010) New Antimicrobial Strategies in Cystic Fibrosis. Pediatric Drugs 12 (6):343-352.

8. Dudley MN, Loutit J, Griffith DC (2008) Aerosol antibiotics: considerations in pharmacological and clinical evaluation. Current opinion in biotechnology 19 (6):637-643.

9. Rose LM, Neale R (2010) Development of the First Inhaled Antibiotic for the Treatment of Cystic Fibrosis. Science Translational Medicine 2 (63).

10. Sawicki GS, Signorovitch JE, Zhang J, Latremouille-Viau D, von Wartburg M, Wu EQ, Shi L (2012) Reduced mortality in cystic fibrosis patients treated with tobramycin inhalation solution. Pediatric Pulmonology 47 (1):44-52.

11. Ballmann M, Smyth A, Geller DE (2011) Therapeutic approaches to chronic cystic fibrosis respiratory infections with available, emerging aerosolized antibiotics. Respiratory Medicine 105:S2-S8.

12. Weers J (2015) Inhaled antimicrobial therapy – Barriers to effective treatment. Advanced Drug Delivery Reviews 85:24-43.

13. Stockmann C, Sherwin CMT, Zobell JT, Young DC, Waters CD, Spigarelli MG, Ampofo K (2013) Optimization of anti-pseudomonal antibiotics for cystic fibrosis pulmonary exacerbations: III. fluoroquinolones. Pediatric Pulmonology 48 (3):211-220.

14. Banerjee D, Stableforth D (2000) The Treatment of Respiratory Pseudomonas Infection in Cystic Fibrosis: What Drug and Which Way? Drugs 60 (5):1053-1064.

15. Doring G, Conway S, Heijerman H, Hodson M, Hoiby N, Smyth A, Touw D (2000) Antibiotic therapy against Pseudomonas aeruginosa in cystic fibrosis: a European consensus. European Respiratory Journal 16 (4):749-767.

16. Foundation CF (2015) Drug Development Pipeline. Available via http://www.cff.org/research/DrugDevelopmentPipeline/ Accessed 27 October 2015.

17. EMA (2015) Quinsair - Summary of product characteristics. European Medicines Agency, Science Medicines Health. http://ec.europa.eu/health/documents/community-register/2015/20150326130815/anx_130815_en.pdf. Accessed 26 October 2015 2015.

18. Zobell JT, Young DC, Waters CD, Ampofo K, Cash J, Marshall BC, Olson J, Chatfield BA (2011) A Survey of the Utilization of Anti-Pseudomonal Beta-Lactam Therapy in Cystic Fibrosis Patients. Pediatric Pulmonology 46 (10):987-990.

19. Zobell JT, Young DC, Waters CD, Stockmann C, Ampofo K, Sherwin CMT, Spigarelli MG (2012) Optimization of anti-pseudomonal antibiotics for cystic fibrosis pulmonary exacerbations: I. aztreonam and carbapenems. Pediatric Pulmonology 47 (12):1147-1158.

20. O'Sullivan BP, Yasothan U, Kirkpatrick P (2010) Inhaled aztreonam. Nature Reviews Drug Discovery 9 (5):357-358.

21. Couet W, Gregoire N, Marchand S, Mimoz O (2012) Colistin pharmacokinetics: the fog is lifting. Clinical Microbiology and Infection 18 (1):30-39.

22. Oliveira MS, Prado GVB, Costa SF, Grinbaum RS, Levin AS (2009) Polymyxin B and colistimethate are comparable as to efficacy and renal toxicity. Diagnostic Microbiology and Infectious Disease 65 (4):431-434.

23. Westerman EM, Le Brun PPH, Touw DJ, Frijlink HW, Heijerman HGM (2004) Effect of nebulized colistin sulphate and colistin sulphomethate on lung function in patients with cystic fibrosis: a pilot study. Journal of cystic fibrosis : official journal of the European Cystic Fibrosis Society 3 (1):23-28.

24. Le Brun PPH, de Boer AH, Mannes GPM, de Fraîture DMI, Brimicombe RW, Touw DJ, Vinks AA, Frijlink HW, Heijerman HGM (2002) Dry powder inhalation of antibiotics in cystic fibrosis therapy: part 2: Inhalation of a novel colistin dry powder formulation: a feasibility study in healthy volunteers and patients. European Journal of Pharmaceutics and Biopharmaceutics 54 (1):25-32.

25. Faruqi S, McCreanor J, Moon T, Meigh R, Morice AH (2008) Fosfomycin for Pseudomonas-related exacerbations of cystic fibrosis. International Journal of Antimicrobial Agents 32 (5):461-463.

26. Mirakhur A, Gallagher MJ, Ledson MJ, Hart CA, Walshaw MJ (2003) Fosfomycin therapy for multiresistant Pseudomonas aeruginosa in cystic fibrosis. Journal of cystic fibrosis : official journal of the European Cystic Fibrosis Society 2 (1):19-24.

27. Grinwis ME, Sibley CD, Parkins MD, Eshaghurshan CS, Rabin HR, Surette MG (2010) Macrolide and Clindamycin Resistance in Streptococcus milleri Group Isolates from the Airways of Cystic Fibrosis Patients. Antimicrobial Agents and Chemotherapy 54 (7):2823-2829.

28. Kurlandsky LE, Fader RC (2000) In vitro activity of minocycline against respiratory pathogens from patients with cystic fibrosis. Pediatric Pulmonology 29 (3):210-212.

29. Doering G, Flume P, Heijerman H, Elborn JS, Consensus Study G (2012) Treatment of lung infection in patients with cystic fibrosis: Current and future strategies. Journal of Cystic Fibrosis 11 (6):461-479.

30. Keel RA, Schaeftlein A, Kloft C, Pope JS, Knauft RF, Muhlebach M, Nicolau DP, Kuti JL (2011) Pharmacokinetics of Intravenous and Oral Linezolid in Adults with Cystic Fibrosis. Antimicrobial Agents and Chemotherapy 55 (7):3393-3398.

31. Dotis J, Iosifidis E, Ioannidou M, Roilides E (2010) Use of linezolid in pediatrics: a critical review. International Journal of Infectious Diseases 14 (8):E638-E648.

32. Di Paolo A, Malacarne P, Guidotti E, Danesi R, Del Tacca M (2010) Pharmacological Issues of Linezolid An Updated Critical Review. Clinical Pharmacokinetics 49 (7):439-447.

33. Grasemann H, Ratjen F (2010) Emerging therapies for cystic fibrosis lung disease. Expert Opinion on Emerging Drugs 15 (4):653-659.

34. Anderson P (2010) Emerging therapies in cystic fibrosis. Therapeutic Advances in Respiratory Disease 4 (3):177-185.

35. Boucher RC (1999) Status of gene therapy for cystic fibrosis lung disease. Journal of Clinical Investigation 103 (4):441-445.

36. Boyle MP, Bell SC, Konstan MW, McColley SA, Rowe SM, Rietschel E, Huang X, Waltz D, Patel NR, Rodman D (2014) A CFTR corrector (lumacaftor) and a CFTR potentiator (ivacaftor) for treatment of patients with cystic fibrosis who have a phe508del CFTR mutation: a phase 2 randomised controlled trial. The Lancet Respiratory Medicine 2 (7):527-538.

37. Sagel SD, Sontag MK, Accurso FJ (2009) Relationship between antimicrobial proteins and airway inflammation and infection in cystic fibrosis. Pediatric Pulmonology 44 (4):402-409.

38. Travis SM, Singh PK, Welsh MJ (2001) Antimicrobial peptides and proteins in the innate defense of the airway surface. Current Opinion in Immunology 13 (1):89-95.

39. Albrecht M, Wang W, Shamova O, Lehrer R, Schiller N (2002) Binding of protegrin-1 to Pseudomonas aeruginosa and Burkholderia cepacia. Respiratory Research 3 (1):18.

40. Bumann D, Behre C, Behre K, Herz S, Gewecke B, Gessner JE, von Specht BU, Baumann U (2010) Systemic, nasal and oral live vaccines against Pseudomonas aeruginosa: A clinical trial of immunogenicity in lower airways of human volunteers. Vaccine 28 (3):707-713.

41. Döring G, Meisner C, Stern M, Group ftFVTS (2007) A double-blind randomized placebo-controlled phase III study of a Pseudomonas aeruginosa flagella vaccine in cystic fibrosis patients. Proceedings of the National Academy of Sciences 104 (26):11020-11025.

42. Döring G, Pier GB (2008) Vaccines and immunotherapy against Pseudomonas aeruginosa. Vaccine 26 (8):1011-1024.

43. Johansen HK, Gøtzsche PC (2015) Vaccines for preventing infection with *Pseudomonas aeruginosa* in cystic fibrosis. Cochrane Database of Systematic Reviews Art. No.: CD001399 (8).

44. Høiby N (2011) Recent advances in the treatment of Pseudomonas aeruginosa infections in cystic fibrosis. BMC Medicine 9 (1):32-38.

45. Høiby N, Bjarnsholt T, Givskov M, Molin S, Ciofu O (2010) Antibiotic resistance of bacterial biofilms. International Journal of Antimicrobial Agents 35 (4):322-332.

46. Nicas TI, Hancock REW (1983) Pseudomonas-aeruginosa outer-membrane permeability - isolation of a porin protein-f-deficient mutant. Journal of Bacteriology 153 (1):281-285.

47. Aronoff SC (1988) Outer-membrane permeability in pseudomonas-cepacia - diminished porin content in a beta-lactam-resistant mutant and in resistant cystic-fibrosis isolates. Antimicrobial Agents and Chemotherapy 32 (11):1636-1639.

48. Burns JL, Hedin LA, Lien DM (1989) Chloramphenicol resistance in pseudomonas-cepacia because of decreased permeability. Antimicrobial Agents and Chemotherapy 33 (2):136-141.

49. Nikaido H (1994) Prevention of drug access to bacterial targets - permeability barriers and active efflux. Science 264 (5157):382-388.

50. Davies JC, Bilton D (2009) Bugs, Biofilms, and Resistance in Cystic Fibrosis. Respiratory care 54 (5):628-640.

51. Grégoire N, Raherison S, Grignon C, Comets E, Marliat M, Ploy M-C, Couet W (2010) Semimechanistic Pharmacokinetic-Pharmacodynamic Model with Adaptation Development for Time-Kill Experiments of Ciprofloxacin against Pseudomonas aeruginosa. Antimicrobial Agents and Chemotherapy 54 (6):2379-2384.

52. Maureen K B (2011) The Newer Fluoroquinolones. Medical Clinics of North America 95 (4):793-817.

53. Gellatly SL, Hancock REW (2013) Pseudomonas aeruginosa: new insights into pathogenesis and host defenses. Pathogens and Disease 67 (3):159-173.

54. Goss CH, Muhlebach MS (2011) Review: Staphylococcus aureus and MRSA in cystic fibrosis. Journal of Cystic Fibrosis 10 (5):298-306.

55. Hocquet D, El Garch F, Vogne C, Plésiat P (2003) Mécanisme de la résistance adaptative de Pseudomonas aeruginosa aux aminosides. Pathologie Biologie 51 (8–9):443-448.

56. Valenza G, Radike K, Schoen C, Horn S, Oesterlein A, Frosch M, Abele-Horn M, Hebestreit H (2010) Resistance to tobramycin and colistin in isolates of Pseudomonas aeruginosa from chronically colonized patients with cystic fibrosis under antimicrobial treatment. Scandinavian Journal of Infectious Diseases 42 (11-12):885-889.

57. Chen HY, Yuan M, Livermore DM (1995) Mechanisms of resistance to β-lactam antibiotics amongst Pseudomonas aeruginosa isolates collected in the UK in 1993. Journal of Medical Microbiology 43 (4):300-309.

58. Tsifansky MD, Yeo Y, Evgenov OV, Bellas E, Benjamin J, Kohane DS (2008) Microparticles for inhalational delivery of antipseudomonal antibiotics. AAPS Journal 10 (2):254-260.

59. Sonnet P, Izard D, Mullie C (2012) Prevalence of efflux-mediated ciprofloxacin and levofloxacin resistance in recent clinical isolates of Pseudomonas aeruginosa and its reversal by the efflux pump inhibitors 1-(1-naphthylmethyl)-piperazine and phenylalanine-arginine-beta-naphthylamide. International Journal of Antimicrobial Agents 39 (1):77-80.

60. Govan JRW (2006) Multidrug-resistant pulmonary infection in cystic fibrosis – what does 'resistant' mean? Journal of Medical Microbiology 55 (12):1615-1617.

61. Forbes B, Asgharian B, Dailey LA, Ferguson D, Gerde P, Gumbleton M, Gustavsson L, Hardy C, Hassall D, Jones R, Lock R, Maas J, McGovern T, Pitcairn GR, Somers G, Wolff RK (2010) Challenges in inhaled product development and opportunities for open innovation. Advanced Drug Delivery Reviews 63 (1-2):69-87.

62. Cu Y, Saltzman WM (2009) Mathematical modeling of molecular diffusion through mucus. Advanced Drug Delivery Reviews 61 (2):101-114.

63. Richard A C (2009) Barrier properties of mucus. Advanced Drug Delivery Reviews 61 (2):75-85.

64. Walker TS, Tomlin KL, Worthen GS, Poch KR, Lieber JG, Saavedra MT, Fessler MB, Malcolm KC, Vasil ML, Nick JA (2005) Enhanced Pseudomonas aeruginosa Biofilm Development Mediated by Human Neutrophils. Infection and Immunity 73 (6):3693-3701.

65. Suk JS, Lai SK, Wang Y-Y, Ensign LM, Zeitlin PL, Boyle MP, Hanes J (2009) The penetration of fresh undiluted sputum expectorated by cystic fibrosis patients by non-adhesive polymer nanoparticles. Biomaterials 30 (13):2591-2597.

66. Lai SK, O'Hanlon DE, Harrold S, Man ST, Wang Y-Y, Cone R, Hanes J (2007) Rapid transport of large polymeric nanoparticles in fresh undiluted human mucus. Proceedings of the National Academy of Sciences of the United States of America 104 (5):1482-1487.

67. Sanders NN, De Smedt SC, Van Rompaey E, Simoens P, DeBaets F, Demeester J (2000) Cystic Fibrosis Sputum. American Journal of Respiratory and Critical Care Medicine 162 (5):1905-1911.

68. Sanders NN, Van Rompaey E, De Smedt SC, Demeester J (2002) On the transport of lipoplexes through cystic fibrosis sputum. Pharmaceutical Research 19 (4):451-456.

69. Kushwah R, Oliver JR, Cao H, Hu J (2007) Nacystelyn enhances adenoviral vector-mediated gene delivery to mouse airways. Gene Therapy 14 (16):1243-1248.

70. Ferrari S, Kitson C, Farley R, Steel R, Marriott C, Parkins DA, Scarpa M, Wainwright B, Evans MJ, Colledge WH, Geddes DM, Alton E (2001) Mucus altering agents as adjuncts for nonviral gene transfer to airway epithelium. Gene Therapy 8 (18):1380-1386.

71. Yang Y, Tsifansky MD, Wu C-J, Yang HI, Schmidt G, Yeo Y (2010) Inhalable Antibiotic Delivery Using a Dry Powder Co-delivering Recombinant Deoxyribonuclease and Ciprofloxacin for Treatment of Cystic Fibrosis. Pharmaceutical Research 27 (1):151-160.

72. Yang Y, Tsifansky MD, Shin S, Lin Q, Yeo Y (2011) Mannitol-Guided Delivery of Ciprofloxacin in Artificial Cystic Fibrosis Mucus Model. Biotechnology and Bioengineering 108 (6):1441-1449.

73. Adi H, Young PM, Chan H-K, Agus H, Traini D (2010) Co-spray-dried mannitol-ciprofloxacin dry powder inhaler formulation for cystic fibrosis and chronic obstructive pulmonary disease. European Journal of Pharmaceutical Sciences 40 (3):239-247.

74. Hurley MN, Cámara M, Smyth AR (2012) Novel approaches to the treatment of Pseudomonas aeruginosa infections in cystic fibrosis. The European respiratory journal 40 (4):1014-1023.

75. Giron Moreno RM, Salcedo Posadas A, Mar Gomez-Punter R (2011) Inhaled antibiotic therapy in cystic fibrosis (Antibioterapia inhalada en la fibrosis quistica.). Archivos de Bronconeumología 47 Suppl 6:14-18.

76. Mogayzel PJ, Naureckas ET, Robinson KA, Brady C, Guill M, Lahiri T, Lubsch L, Matsui J, Oermann CM, Ratjen F, Rosenfeld M, Simon RH, Hazle L, Sabadosa K, Marshall BC (2014) Cystic Fibrosis Foundation Pulmonary Guideline. Pharmacologic Approaches to Prevention and Eradication of Initial Pseudomonas aeruginosa Infection. Annals of the American Thoracic Society 11 (10):1640-1650.

77. Lillquist YP, Cho E, Davidson AGF (2011) Economic effects of an eradication protocol for first appearance of Pseudomonas aeruginosa in cystic fibrosis patients: 1995 vs. 2009. Journal of Cystic Fibrosis 10 (3):175-180.

78. Ratjen F, Munck A, Kho P, Angyalosi G, Grp ES (2010) Treatment of early Pseudomonas aeruginosa infection in patients with cystic fibrosis: the ELITE trial. Thorax 65 (4):286-291.

79. Giugno H, Castanos C, Lubatti A, Pinheiro JL, Hernandez C, Pena HG (2010) Early antibiotic treatment for eradication of initial infection by Pseudomonas aeruginosa in patients with cystic fibrosis. Archivos argentinos de pediatría 108 (2):141-147.

80. Treggiari MM, Rosenfeld M, Mayer-Hamblett N, Retsch-Bogart G, Gibson RL, Williams J, Emerson J, Kronmal RA, Ramsey BW, Epic Study G (2009) Early anti-pseudomonal acquisition in young patients with cystic fibrosis: Rationale and design of the EPIC clinical trial and observational study. Contemporary Clinical Trials 30 (3):256-268.

81. Mayer-Hamblett N, Burns JL, Khan U, Retsch-Bogart G, Treggiari M, Ramsey BW (2010) Predictors of pseudomonas aeruginosa recurrence in cystic fibrosis: results from the epic trial. Pediatric Pulmonology:326-327.

82. Bals R, Hubert D, Tümmler B (2011) Antibiotic treatment of CF lung disease: From bench to bedside. Journal of Cystic Fibrosis 10, Supplement 2 (0):S146-S151.

83. Burkett A, Vandemheen KL, Giesbrecht-Lewis T, Ramotar K, Ferris W, Chan F, Doucette S, Fergusson D, Aaron SD (2012) Persistency of Pseudomonas aeruginosa in sputum cultures and clinical outcomes in adult patients with cystic fibrosis. European Journal of Clinical Microbiology & Infectious Diseases 31 (7):1603-1610.

84. Vázquez-Espinosa E, Girón RM, Gómez-Punter RM, García-Castillo E, Valenzuela C, Cisneros C, Zamora E, García-Pérez FJ, Ancochea J (2015) Long-term safety and efficacy of tobramycin in the management of cystic fibrosis. Therapeutics and Clinical Risk Management 11:407-415.

85. Flume PA, Mogayzel PJ, Robinson KA, Goss CH, Rosenblatt RL, Kuhn RJ, Marshall BC, Committee atCPGfPT (2009) Cystic Fibrosis Pulmonary Guidelines. American Journal of Respiratory and Critical Care Medicine 180 (9):802-808.

86. Flume PA, O'Sullivan BP, Robinson KA, Goss CH, Mogayzel PJ, Willey-Courand DB, Bujan J, Finder J, Lester M, Quittell L, Rosenblatt R, Vender RL, Hazle L, Sabadosa K, Marshall B (2007) Cystic Fibrosis Pulmonary Guidelines. American Journal of Respiratory and Critical Care Medicine 176 (10):957-969.

87. Tiddens HAWM, Bos AC, Mouton JW, Devadason S, Janssens HM (2014) Inhaled antibiotics: dry or wet? European Respiratory Journal 44 (5):1308-1318.

88. Smyth HDC, Hickey AJ (2011) Controlled Pulmonary Drug Delivery. Advances in Delivery Science and Technology. Springer New York.

89. Ghazanfari T, Elhissi AMA, Ding Z, Taylor KMG (2007) The influence of fluid physicochemical properties on vibrating-mesh nebulization. International Journal of Pharmaceutics 339 (1–2):103-111.

90. Geller DE (2005) Comparing Clinical Features of the Nebulizer, Metered-Dose Inhaler, and Dry Powder Inhaler. Respiratory care 50 (10):1313-1322.

91. Assael BM (2011) Aztreonam inhalation solution for suppressive treatment of chronic Pseudomonas aeruginosa lung infection in cystic fibrosis. Expert Review of Anti-Infective Therapy 9 (11):967-973.

92. Plosker GL (2011) Aztreonam Lysine for Inhalation Solution in Cystic Fibrosis Profile Report. Pediatric Drugs 13 (2):129-131.

93. Kirkby S, Novak K, McCoy K (2011) Aztreonam (for inhalation solution) for the treatment of chronic lung infections in patients with cystic fibrosis: an evidence-based review. Core evidence 6:59-66.

94. Plosker GL (2010) Aztreonam Lysine for Inhalation Solution In Cystic Fibrosis. Drugs 70 (14):1843-1855.

95. Mazurek H, Chiron R, Kucerova T, Geidel C, Bolbas K, Chuchalin A, Blanco-Aparicio M, Santoro D, Varoli G, Zibellini M, Cicirello HG, Antipkin YG (2014) Long-term efficacy and safety of aerosolized tobramycin 300 mg/4 ml in cystic fibrosis. Pediatric Pulmonology 49 (11):1076-1089.

96. Vendrell Relat M, Munoz Castro G, Sabater Talaverano G, De Gracia Roldan J (2011) The future of inhaled antibiotic therapy. New products (El futuro de la antibioterapia inhalada. Nuevos productos.). Archivos de Bronconeumología 47 Suppl 6:30-32.

97. McColley SA, Trapnell B, Kissner D, McKevitt M, Montgomery B, Rosen J, Grp FTIS (2010) Fosfomycin/tobramycin for inhalation (fti): microbiological results of a phase 2 placebo-controlled trial in patients with cystic fibrosis and pseudomonas aeruginosa. Pediatric Pulmonology:338-338.

98. Stockmann C, Sherwin CMT, Ampofo K, Spigarelli MG (2014) Development of levofloxacin inhalation solution to treat Pseudomonas aeruginosa in patients with cystic fibrosis. Therapeutic Advances in Respiratory Disease 8 (1):13-21.

99. Geller DE, Flume PA, Griffith DC, Morgan E, White D, Loutit JS, Dudley MN (2011) Pharmacokinetics and Safety of MP-376 (Levofloxacin Inhalation Solution) in Cystic Fibrosis Subjects. Antimicrobial Agents and Chemotherapy 55 (6):2636-2640.

100. Weers JG, Bell J, Chan HK, Cipolla D, Dunbar C, Hickey AJ, Smith IJ (2010) Pulmonary Formulations: What Remains to be Done? Journal of Aerosol Medicine and Pulmonary Drug Delivery 23:S5-S23.

101. Adi H, Young PM, Chan H-K, Salama R, Traini D (2010) Controlled release antibiotics for dry powder lung delivery. Drug Development and Industrial Pharmacy 36 (1):119-126.

102. Geller DE, Weers J, Heuerding S (2011) Development of an inhaled dry-powder formulation of tobramycin using PulmoSphere™ technology. Journal of Aerosol Medicine and Pulmonary Drug Delivery 24 (4):175-182.

103. Schuster A, Haliburn C, Döring G, Goldman MH, Group ftFS (2013) Safety, efficacy and convenience of colistimethate sodium dry powder for inhalation (Colobreathe DPI) in patients with cystic fibrosis: a randomised study. Thorax 68 (4):344-350.

104. Hodson ME, Gallagher CG, Govan JRW (2002) A randomised clinical trial of nebulised tobramycin or colistin in cystic fibrosis. European Respiratory Journal 20 (3):658-664.

105. Doan TV, Couet W, Olivier JC (2011) Formulation and in vitro characterization of inhalable rifampicin-loaded PLGA microspheres for sustained lung delivery. International Journal of Pharmaceutics 414 (1-2):112-117.

106. Zeng XM, Martin GP, Marriott C (1995) The controlled delivery of drugs to the lung. International Journal of Pharmaceutics 124 (2):149-164.

107. Cook RO, Pannu RK, Kellaway IW (2005) Novel sustained release microspheres for pulmonary drug delivery. Journal of Controlled Release 104 (1):79-90.

108. Rukholm G, Mugabe C, Azghani AO, Omri A (2006) Antibacterial activity of liposomal gentamicin against Pseudomonas aeruginosa: a time-kill study. International Journal of Antimicrobial Agents 27 (3):247-252.

109. Mugabe C, Azghani AO, Omri A (2005) Liposome-mediated gentamicin delivery: development and activity against resistant strains of Pseudomonas aeruginosa isolated from cystic fibrosis patients. Journal of Antimicrobial Chemotherapy 55 (2):269-271.

110. Heyder J (2004) Deposition of Inhaled Particles in the Human Respiratory Tract and Consequences for Regional Targeting in Respiratory Drug Delivery. Proceedings of the American Thoracic Society 1 (4):315-320.

111. Pilcer G, Amighi K (2010) Formulation strategy and use of excipients in pulmonary drug delivery. International Journal of Pharmaceutics 392 (1-2):1-19.

112. Sakagami M, Byron PR (2005) Respirable Microspheres for Inhalation: The Potential of Manipulating Pulmonary Disposition for Improved Therapeutic Efficacy. Clinical Pharmacokinetics 44 (3):263-277.

113. Re MI (2006) Formulating drug delivery systems by spray drying. Drying Technology 24 (4):433-446.

114. Varde NK, Pack DW (2004) Microspheres for controlled release drug delivery. Expert Opinion on Biological Therapy 4 (1):35-51.

115. Cescutti P, Cuzzi B, Liut G, Segonds C, Di Bonaventura G, Rizzo R (2011) A novel highly charged exopolysaccharide produced by two strains of Stenotrophomonas maltophilia recovered from patients with cystic fibrosis. Carbohydrate Research 346 (13):1916-1923.

116. Manca ML, Mourtas S, Dracopoulos V, Fadda AM, Antimisiaris SG (2008) PLGA, chitosan or chitosan-coated PLGA microparticles for alveolar delivery? A comparative study of particle stability during nebulization. Colloids and Surfaces B-Biointerfaces 62 (2):220-231.

117. Mohamed F, van der Walle CF (2008) Engineering biodegradable polyester particles with specific drug targeting and drug release properties. Journal of Pharmaceutical Sciences 97 (1):71-87.

118. d'Angelo I, Quaglia F, Ungaro F (2015) PLGA carriers for inhalation: where do we stand, where are we headed? Therapeutic Delivery 6 (10):1139-1144.

119. Danhier F, Ansorena E, Silva JM, Coco R, Le Breton A, Préat V (2012) PLGA-based nanoparticles: An overview of biomedical applications. Journal of Controlled Release 161 (2):505-522.

120. Emami J, Hamishehkar H, Najafabadi AR, Gilani K, Minaiyan M, Mahdavi H, Mirzadeh H, Fakhari A, Nokhodchi A (2009) Particle size design of PLGA microspheres for potential pulmonary drug delivery using response surface methodology. Journal of Microencapsulation 26 (1):1-8.

121. Dailey LA, Kleemann E, Wittmar M, Gessler T, Schmehl T, Roberts C, Seeger W, Kissel T (2003) Surfactant-Free, Biodegradable Nanoparticles for Aerosol Therapy Based on the Branched Polyesters, DEAPA-PVAL-g-PLGA. Pharmaceutical Research 20 (12):2011-2020.

122. Mura S HH, Nicolas J, Le Droumaguet B, Gueutin C, Zanna S, Tsapis N, Fattal E (2011) Influence of surface charge on the potential toxicity of PLGA nanoparticles towards Calu-3 cells. International Journal of Nanomedicine 6 (1):2591-2605.

123. Yang Y, Bajaj N, Xu P, Ohn K, Tsifansky MD, Yeo Y (2009) Development of highly porous large PLGA microparticles for pulmonary drug delivery. Biomaterials 30 (10):1947-1953.

124. O'Hara P, Hickey AJ (2000) Respirable PLGA microspheres containing rifampicin for the treatment of tuberculosis: Manufacture and characterization. Pharmaceutical Research 17 (8):955-961.

125. Martin-Banderas L, Holgado MA, Alvarez-Fuentes J, Fernandez-Arevalo M (2012) Use of Flow Focusing(R) technology to produce tobramycin-loaded PLGA microparticles for pulmonary drug delivery. Medical Chemistry 8 (4):533-540.

126. Ventura CA, Tommasini S, Crupi E, Giannone I, Cardile V, Musumeci T, Puglisi G (2008) Chitosan microspheres for intrapulmonary administration of moxifloxacin: Interaction with biomembrane models and in vitro permeation studies. European Journal of Pharmaceutics and Biopharmaceutics 68 (2):235-244.

127. Chowdary KPR, Rao YS (2004) Mucoadhesive microspheres for controlled drug delivery. Biological & Pharmaceutical Bulletin 27 (11):1717-1724.

128. Muzzarelli RAA (2012) Chemical and Technological Advances in Chitins and Chitosans Useful for the Formulation of Biopharmaceuticals. In: Chitosan-Based Systems for Biopharmaceuticals. John Wiley & Sons, Ltd, pp 1-21.

129. Brück WM, Slater JW, Carney BF (2011) The Sources and Production of Chitin and Chitosan Derivatives - Chitin and Chitosan from Marine Organisms. In: Kim S-K (ed) Chitin, Chitosan, Oligosaccharides and Their Derivatives. CRC Press, pp 11-23.

130. Sharma R, Saxena D, Dwivedi AK, Misra A (2001) Inhalable microparticles containing drug combinations to target alveolar macrophages for treatment of pulmonary tuberculosis. Pharmaceutical Research 18 (10):1405-1410.

131. Giovagnoli S, Blasi P, Schoubben A, Rossi C, Ricci M (2007) Preparation of large porous biodegradable microspheres by using a simple double-emulsion method for capreomycin sulfate pulmonary delivery. International Journal of Pharmaceutics 333 (1-2):103-111.

132. Ventura CA, Cannava C, Stancanelli R, Paolino D, Cosco D, La Mantia A, Pignatello R, Tommasini S (2011) Gemcitabine-loaded chitosan microspheres. Characterization and biological in vitro evaluation. Biomedical Microdevices 13 (5):799-807.

133. Tuli RA, Dargaville TR, George GA, Islam N (2012) Polycaprolactone microspheres as carriers for dry powder inhalers: Effect of surface coating on aerosolization of salbutamol sulfate. Journal of Pharmaceutical Sciences 101 (2):733-745.

134. Corrigan DO, Healy AM, Corrigan OI (2006) Preparation and release of salbutamol from chitosan and chitosan co-spray dried compacts and multiparticulates. European Journal of Pharmaceutics and Biopharmaceutics 62 (3):295-305.

135. Learoyd TP, Burrows JL, French E, Seville PC (2008) Modified release of beclometasone dipropionate from chitosan-based spray-dried respirable powders. Powder Technology 187 (3):231-238.

136. Sakagami M, Kinoshita W, Sakon K, Sato J, Makino Y (2002) Mucoadhesive beclomethasone microspheres for powder inhalation: their pharmacokinetics and pharmacodynamics evaluation. Journal of Controlled Release 80 (1-3):207-218.

137. Gupta V, Rawat A, Ahsan F (2010) Feasibility Study of Aerosolized Prostaglandin E(1) Microspheres as a Noninvasive Therapy for Pulmonary Arterial Hypertension. Journal of Pharmaceutical Sciences 99 (4):1774-1789.

138. Harsha S, Chandramouli R, Rani S (2009) Ofloxacin targeting to lungs by way of microspheres. International Journal of Pharmaceutics 380 (1-2):127-132.

139. Jeong Y-I, Kim D-G, Seo D-H, Jang M-K, Nah J-W (2008) Multiparticulation of ciprofloxacin HCl-encapsulated chitosan microspheres using poly(dl-lactide-co-glycolide). Journal of Industrial and Engineering Chemistry 14 (6):747-751.

140. Dillen K, Vandervoort J, Van den Mooter G, Verheyden L, Ludwig A (2004) Factorial design, physicochemical characterisation and activity of ciprofloxacin-PLGA nanoparticles. International Journal of Pharmaceutics 275 (1-2):171-187.

141. Poyner EA, Alpar HO, Almeida AJ, Gamble MD, Brown MRW (1995) A comparative-study on the pulmonary delivery of tobramycin encapsulated into liposomes and pla microspheres following intravenous and endotracheal delivery. Journal of Controlled Release 35 (1):41-48.

Chapter 3

METHODS FOR PREPARATION AND CHARACTERIZATION OF POLYMERIC MICROSPHERES

3.1 – Introduction

This chapter presents the two main methods used for the preparation of chitosan MS and PLGA MS, respectively, the spray drying method and the double emulsion solvent evaporation technique with premix membrane homogenization. For chitosan MS, a factorial design was applied for the optimization of the preparation process and this technique will also be introduced here. A technical description and the basic principles of characterization methods are comprised, including particle size and morphology analysis, thermal and gravimetric analysis, infrared spectroscopy and X-ray diffraction techniques, among others. Additional details, or more specific practical considerations, are given along the thesis in relevant sections.

3.2 – Preparation

Nanospheres and MS usually consist of a polymeric matrix where the drug is entrapped/ distributed throughout the whole particle, while nanocapsules and microcapsules have an external polymeric wall and an inner core, where the drug is dispersed [1]. Several methods are used to prepare polymeric MS and usually the choice of the method is not straightforward. The required size and morphology of MS, the nature of the drug(s) to incorporate and the route of administration are aspects that must be considered before selecting the technique. Emulsion-based methods with evaporation/ extraction of the solvent and nanoprecipitation are widely used to prepare PLA and PLA-copolymers, such as PLGA [1,2]. The spray-drying technology [3,4], interfacial polymerization [2], membrane emulsification [5] or coacervation [6] are also used for polymer formulations development, especially for controlled release purposes. Several types of emulsions (simple oil-in-water, O/W; double (multiple) W/O/W or O/O) are commonly employed in the MS preparation. This thesis will focus on the W/O/W double emulsion solvent evaporation method combined with premix membrane homogenization. Also herein, spray-drying method will be highlighted, in what follows.

3.2.1 – Spray drying

Spray drying is a well established and versatile technique with applications in a number of different areas that include food, cosmetics, ceramics and pharmaceutical industry [7].

It is a technique used to dry aqueous or organic solutions, suspensions or emulsions by atomization. The spray drying process consists mainly of four continuous steps: 1) atomization of the liquid; 2) contact between the air and the spray; 3) evaporation and 4) powder collection by separation of the dried particles from the gas. Briefly, the sample is fed into the drying chamber by a peristaltic pump and through an atomizer or nozzle. Fine droplets are dispersed (mist) in warm air, becoming dried with the solvent evaporation. Such fine particles are further separated from the drying gas through the cyclone by centrifugal and/ or gravitational forces. The product is usually collected in a vessel for further characterization. The main components of a conventional spray dryer and the steps of particle formation, when aqueous solutions are used, are represented in Figure 3.1 and the operation is open-loop with air as the drying gas. When organic solvents are employed, the drying process is a closed-loop operation, with recycling of an inert gas (e.g. nitrogen) in order to avoid the risk of explosion [7,8].

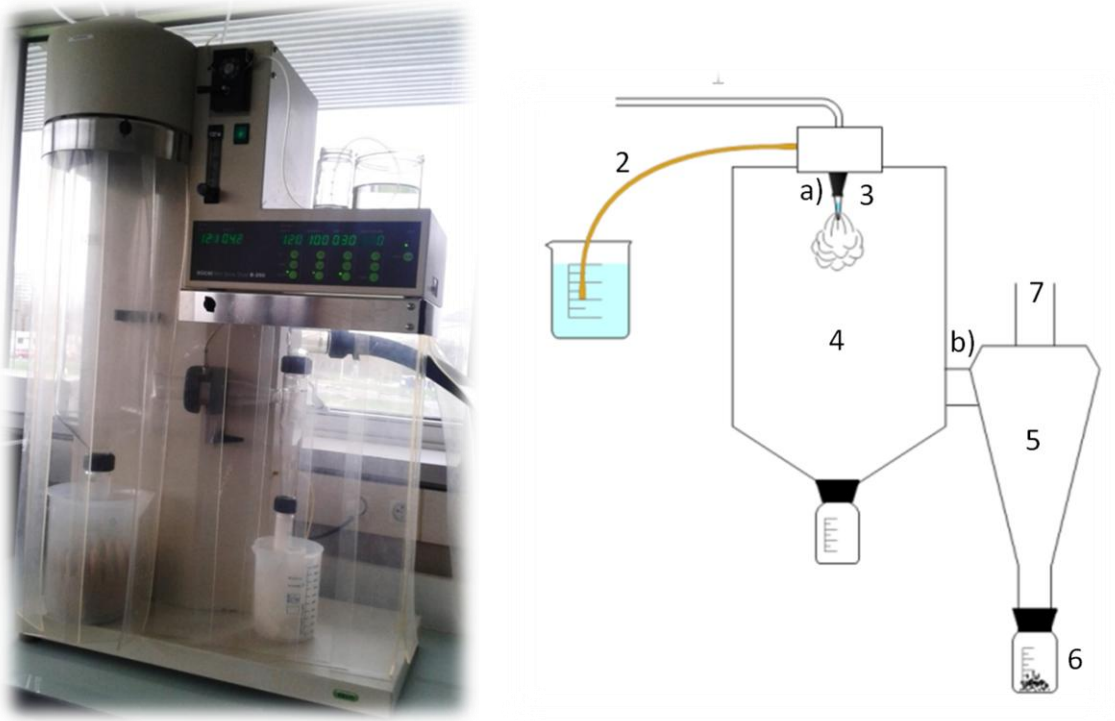

Figure 3.1 – Büchi mini spray dryer B-290 (left) and schematic representation of a conventional spray dryer (right) components and processes: 1. Drying air; 2. Feed; 3. Nozzle; 4. Drying chamber; 5. Cyclone; 6. Collection vessel; 7. Exhaust; a) inlet temperature and b) outlet temperature.

Despite being known as a drying technology, the spray drying method has been successfully used to encapsulate/ incorporate drugs into polymer-based formulations. The strategy of incorporation may protect the drug from degradation, may modulate its release, reducing administration frequency and/ or systemic toxicity and, may also mask drug-related unpleasant taste [8]. The advantages of spray drying technology include an easy scale-up, fast particle formation (generally with size < 10 μm) and the possibility of working in continuous mode [7,9,8]. When compared to other techniques such as the spray freeze drying and the emulsion solvent evaporation, it is less time consuming, once the drying/ encapsulation occurs in one continuous step, and higher drug content and encapsulation efficiency are usually achieved, especially for hydrophilic drugs [10,7,11]. Concerning the yield, it ranges from 20 to 70 % for a laboratory scale spray dryer but values close to 100 % can be reached at the industrial scale [8]. Better flow properties were also obtained for some powders produced by spray drying, when compared with the double emulsion solvent evaporation method [12]. Thermally labile molecules (e.g. proteins) should be, however, carefully used because temperatures higher than 100°C are usually required for the spray drying process [9]. Some strategies including the addition of stabilizers (e.g. sugars) have already been developed to maintain their bioactivity. Nevertheless, the time exposure of droplets to the high temperatures is extremely short (milliseconds or seconds) [8].

Some factors can influence droplet size and consequently, particle size, including feed rate, air flow rate and viscosity of the liquid [7]. Particle formation mechanisms and the corresponding mathematical approaches were explored, [13] but are not in the focus of this thesis. Increase of viscosity or reduction of air flow usually promotes larger particle size. Some other parameters that can influence the properties of the particles (e.g. size, morphology, density) are the inlet and outlet temperatures. Higher temperatures usually allow better powder flow properties, higher process yields, and lower humidity in the final product [14]. The main influences of parameters and process variables on the properties of particles are described elsewhere [14,15], and it should be noted that the specific composition of the spray dried liquid is particularly important in the respective size/ morphology/ shape [9]. In this context, a factorial design arises as an interesting approach to elucidate the effects of some parameters and working conditions on particle size, as will be discussed later in this Chapter.

Among other applications (e.g. oral delivery) of spray dried pharmaceutical products, the pulmonary administration has gained special interest in the last years and a number of formulations have been developed. The majority of them are chitosan-based systems for incorporation of antibiotics or corticosteroids, but other biodegradable polymers such as PLA, PLGA and poly(vinylpyrrolidone) together with PVA, were also used for encapsulation of corticosteroids/ antifungal agents [7].

3.2.2 – Emulsion solvent evaporation and membrane emulsification methods

Solvent evaporation methods have been used in recent years for the drug encapsulation in biodegradable polymers, mainly for controlled release purposes. Several methods are available and the choice is generally based on the solubility nature of the drug(s) to be encapsulated. For insoluble or poorly water-soluble drugs, O/W emulsion is often applied and consists in the dissolution of the drug in the organic phase, where the polymer is also dissolved, followed by its emulsification in a continuous aqueous phase. Solvent evaporation is then performed with the transformation of the organic (dispersed) phase into solid particles, which are then recovered and dried. For hydrophilic drugs it is more difficult to dissolve them in the organic solvent and there is a trend to diffuse into the continuous phase resulting in a great drug loss. Therefore, some other methods have been explored and include the W/O/W double emulsion. In this method, the drug is usually dissolved in the aqueous phase and emulsified with the organic phase (W/O emulsion), and dispersion into a second aqueous phase (W/O/W) is then performed. Concerning the organic solvents, and despite some that are less toxic (e.g. ethyl acetate), the dichloromethane is the most used once its evaporation is fast and the obtained MS present high encapsulation efficiencies and spherical shape. With respect to the surfactants that are used in the dispersed phase, they can be anionic, cationic or non-ionic, such as the partially hydrolyzed PVA, which has been extensively used because it promotes smaller MS size [16,17]. The effectiveness of the method depends mainly on the successful entrapment of the drug [17] but also on other properties, such as particle size and powder flow properties, when a pulmonary administration is required.

Recently, the Shirasu Porous Glass (SPG) membrane emulsification/ homogenization method was developed to prepare PLA and PLGA MS with uniform size. Conventional membrane emulsification technique was firstly developed but being time consuming, the

premix membrane emulsification was developed: it is characterized by high transmembrane flux and size controllability [18,19]. This technique is usually combined with the double emulsion solvent evaporation [18,20]. In a first step, double emulsions are obtained under stirring. Then, they are extruded through a SPG membrane and small uniform droplets obtained due to shear force induced by transmembrane pressure and MS can be obtained following the solidification process (Figure 3.2) [19].

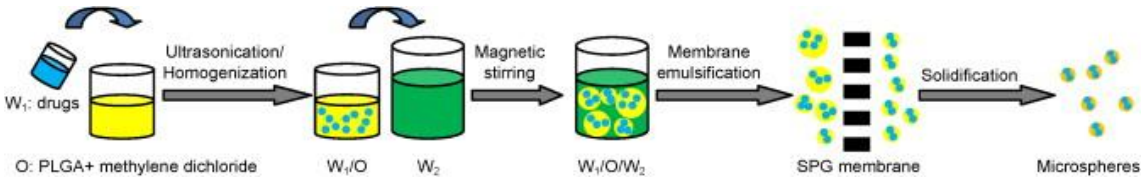

Figure 3.2 – Scheme of MS preparation by double-emulsion with premix membrane emulsification method. Reproduced from [19], with permission.

Several parameters can be adjusted to obtain the desired MS properties including membrane pore size, transmembrane pressure and nature and concentration of the organic and aqueous phases.

3.3 – Characterization

A number of physicochemical analyses are available to characterize the particles obtained by spray drying method or emulsion solvent techniques and are crucial to ensure MS quality and suitability for lung delivery. Some MS characteristics are particularly important, including size and morphology, among others, and will be explored in the following sub-sections.

3.3.1 – Particle size

Although particle size can be measured by several methods, laser diffractometry (also known as static light scattering) is a widely used method and it was selected, in this thesis, for the geometric size analysis of obtained MS. The respective instruments are easy to use and allow fast and reproducible measurements for particle size, usually in the range of 0.04 – 2000 µm [21]. This technique measures particle size distribution, and is based on the angular variation in intensity of the light scattered by a particle. The angle of

the light scattered is inversely proportional to the size of that particle (larger angles correspond to smaller particles). This technique considers the particles as spheres and the scatering pattern as the sum of the individual scattering patterns, with little or no interaction between them. In addition, there is a lack of ability to distinguish between well-dispersed powders and agglomerates [22]. Nevertheless, laser diffraction analysis has been successfully used for size distribution evaluation of pulmonary formulations [23]. Additional methods for morphology evaluation and MMAD determination are of importance to confirm the convenience and the results obtained using this technique.

3.3.2 – Morphology

Morphological evaluation of obtained MS, including shape and size, and also surface characteristics, may be performed by scanning electron microscopy (SEM) and/or by transmission electron microscopy (TEM). Cross-sections of the MS may also be analyzed by these techniques, in order to understand the nature of the MS core.

In SEM, a focused beam of high-energy electrons is produced at the top of the microscope. This beam travels, in vacuum, through electromagnetic fields and lenses, and is responsible for the generation of a variety of signals at the surface of solid specimens. The signals produced can be of three main types: backscattered electrons; secondary electrons; and specimen, absorbed, induced currents [24] and are finally sent to a screen, generating the final image. Non-conductive samples have to be coated with a thin layer of gold or platinum.

In TEM, there is an electron gun responsible for the emission of electrons. Condenser lenses are very important to form a fine electron probe to interact with the sample. The magnification system, composed of intermediate and projection lenses, gives a magnification up to 1.5 million. The data recording system is usually digital [25]. Sample preparation is more complex than in the case of SEM analysis, because the electron beam has to pass through the sample and therefore the specimen has to be thin (in nanometer range).

3.3.3 – Surface area

Surface area of powders is dependent on some factors, such as the particle size, and shape and porosity, with logical larger surfaces areas for materials of porous nature. Several techniques are available to infer about surface area, including mercury porosimetry, thermoporometry or NMR-methods. However, gas adsorption is the most popular method, allowing an assessment of pore sizes in the range of 0.35 nm to values higher than 100 nm, including measurements of the three types of pores: micropores (< 2 nm), mesopores (2 – 50 nm) and macropores (> 50 nm). In the gas adsorption technique, the gas/ solid interface is considered, being the solid, the adsorbent, and the gas, the adsorptive, which is capable of being adsorbed. Among others, the Brunauer, Emmett and Teller (BET) theory has gained special interest for research. It enables the evaluation of the number of molecules that are required to form a monolayer, although such layer is never actually formed. There is an equilibrium between the adsorbed layer and the vapor, even for the second and next layers, but the number of molecules remains constant [26]. Basically, for the BET method, samples are pre-conditioned at a given temperature, and a gas, usually nitrogen, is used to adsorb by weak bonds at the surface of the solid. A desorption can occur by a decrease in pressure at the same temperature [27]. In the context of MS characterization, BET gives information about the surface area of MS and respective porosity, properties that can be related with the measured particle size.

3.3.4 – X-ray diffraction (XRD)

XRD is an interesting technique for understanding the nature of the obtained MS, amorphous or crystalline, and for structure determination of crystals. It requires a well organized material (e.g. crystals and fibers), not providing enough information for amorphous structures. Briefly, when an X-ray beam impinges on a crystal, a number of scattered beams are obtained in specific directions, when conditions satisfy Bragg's Law ($n \times \lambda = 2d \sin \theta$, with d, distance between parallel planes; θ, the reflection angle; λ, the X-ray wavelength and n, an integer) [28]. Actually, this law correlates the radiation wavelength to the reflection angle and the lattice spacing in the sample, and the incident beam is only reflected in the directions for which the Bragg's law is observed. Therefore, a diffractogram with distinct diffraction peaks are obtained for a specific crystalline sample, which compared with standards, may allow its identification [29]. Additionally,

and in the context of this thesis, it may provide information about the drug nature, when incorporated in a polymeric matrix by spray drying or by the emulsion solvent evaporation method.

3.3.5 – Attenuated total reflectance Fourier transform infrared spectroscopy (ATR-FTIR)

FTIR method provides information on the chemical components in the sample by resorting to the vibration modes of specific molecular groups, resulting from the interaction between the IR light and the sample. When using the ATR mode, the IR light is completely reflected at the interface between the sample and the crystal [30], which is composed of a material with high index of refraction. In fact, the radiation penetrates a short distance into the sample (known as evanescent wave). The sample interacts with the evanescent wave, resulting in the absorption of radiation and allowing to obtain the corresponding spectrum [31]. ATR mode has the advantage of minimal or none requirements for sample preparation, because the depth of IR light in the sample is independent of its thickness and therefore, measurements are faster [32]. In addition, ATR-FTIR may consist in a valuable tool for understanding the interactions between all the components of obtained MS, as well as, for confirming the integrity of the drug, after encapsulation.

3.3.6 – Differential Thermal Analysis/ Thermal Gravimetric Analysis (DTA/ TGA)

DTA/ TGA is a combined well established method for simultaneous thermal and gravimetric analysis of pharmaceutical products.

DTA is a technique very similar to differential scanning calorimetry (DSC). Actually, DSC measures the energy changes (heat flow) that occur when a sample is heated, cooled or held isothermally, together with the temperature at which the changes happen.

For DTA, the microvolt signal is not converted to the equivalent heat flow and the temperature difference between the sample and the reference is measured, against temperature or time [33-35]. Generally, instruments capable of heating to temperatures ≥ 1500 °C use this principle.

TGA corresponds to the measurement of mass change, monitored against time or temperature, while the sample temperature is programmed, in a specific atmosphere [36,37]. Typically, the sample is heated at a constant heating rate but it may be held at a constant temperature or other temperature programs may be applied.

Modern thermobalances allow the simultaneous DTA and TGA measurements and enable the user to characterize the materials for melting and decomposition processes, measurement of glass transitions, and other events accompanied or not by mass loss [34,37]. In the context of this work, it provides information about the thermal events of polymers and respective MS, during a temperature program, usually accompanied by weight changes. In addition, DTA/ TGA can be an interesting tool to investigate the physical state of the drug inside the MS, by the presence or absence of the respective melting peak transition. Practical aspects such as the type of pan and atmosphere, the calibration material or the type of plot (representation of endotherm, up or down), as well as the scan temperature rate that were used for MS analysis in this thesis, are indicated in the respective sections.

3.4 – Optimization: factorial design

In the pharmaceutical field, strategies of optimization are procedures that attempt to find the best conditions for an analytical method or to obtain an optimized product, for example. Using experimental design, the factors, which are parameters than can be set at different levels, may be evaluated simultaneously and in a short period of time. In addition, not only the effect of each factor (e.g. concentration or stirring speed) on each response (e.g. property of final formulation) may be evaluated, but also the possible interaction between them. In this context, different procedures can be applied to evaluate the influence of certain factors on the response(s). The classic approach is to vary and optimize one factor at a time. However, the interaction between factors is not considered. To overcome that, a multivariate approach, which varies several factors simultaneously, must be applied. When an experimental set-up is used to simultaneously evaluate several factors at given numbers of levels in a predefined number of experiments, it is called experimental design. Experimental designs can be classified into different categories, including screening designs (e.g. full factorial design), response surface designs and mixture designs. Screening designs are frequently used for optimization of formulations

and, in addition, when the number of factors is small, full factorial design may be applied [38,39]. Actually, a number of approaches, including factorial design, have been applied for optimization of properties of particles obtained by spray drying method [40-43]. In this thesis, a two-level full factorial design was carried out to elucidate the influence of formulation and operational variables of spray drying, as well as their interactions, on chitosan MS particle size, as will be detailed in Chapter 4. Basically, full factorial design with two levels contains all possible combinations between the X_i factors (f) and their L levels, leading to $N=L^f=2^f$ experiments that should be performed. Basically, in order to solve this factorial approach, a table is usually designed, with f columns and 2^f rows. Columns correspond to the influence of each factor X_i and rows to the experiments performed. A common coding with -1 and +1 for the lower and upper level, respectively, for qualitative or quantitative factors, is usually employed to build the table. In an experiment, if the level assigned is -1, it means that the corresponding factor X_i is in the lower level (e.g. lower concentration). The opposite is observed when the level is +1. This table is then expanded to include the interactions between factors (e.g. quadratic terms), which correspond in the table to the multiplication between coded values of the factors. In the simplest example, which corresponds to two factors and two levels, four possible combinations may occur, corresponding to four different experiments (e.g. four formulations), Table 3.1.

Table 3.1 – Two-factor (X_1 and X_2), two-level full factorial design 2^2, and respective interaction of factors.

Factors (*f*) / **Formulations**	X_1	X_2	$X_1 X_2$
1	-1	-1	+1
2	+1	-1	-1
3	-1	+1	-1
4	+1	+1	+1

Results from such experimental design allow the estimation of the effects produced by the factors and their interactions. The effects usually correspond to the average result of changing from -1 to +1 and the interaction between factors influences, when two or more

factors are changed at the same time. In order to evaluate the results and interactions resulted from the experimental design, a multiple linear regression is usually applied, based on a model that can be represented, for a simple case, by

$$y = \beta_0 + \beta_1 x_1 + \beta_2 x_2 + \beta_{12} x_1 x_2 \quad (3.1)$$

where y corresponds to the response, β_0 to the intercept, x_1 and x_2 to the coded factors and β_1 and β_2 to the regression coefficients [39,38]. Mathematical programs are often employed to solve the equations (e.g. GNU octave software) [44]. The estimated coefficients are assessed by statistical methods, commonly by Student's *t*-test, where a *t* value for the factor is compared with a tabulated *t* value (for significance level of 0.05, for example). Therefore, *t* values larger or equal to tabulated *t* values are considered significant, meaning a significant influence of respective factor/ interaction on the response [39,38]. The overall model is also frequently assessed with ANOVA.

3.5 – Analytical methods

3.5.1 – Ultraviolet – Visible (UV-Vis) spectrophotometry

UV-Vis spectrophotometry is a widely used technique for simple and fast analytical determinations. Actually, versatility, simplicity and speed are the main characteristics of spectrophotometers. Briefly, they are based in the Beer-Lambert law, which states that the concentration of the sample is directly proportional to the absorbance, applied when a monochromatic light is used (single wavelength) [45]. This technique is especially important when fast results are needed and it is not straightforward developing and validating a method based on sophisticated techniques. For MS properties evaluation it is a useful method, for example, for drug content evaluation, as will be described in the respective section.

3.5.2 – High performance liquid chromatography (HPLC)

HPLC is a widely used physical separation technique for separation of constituent components in mixtures, including pharmaceuticals samples. There is a flowing liquid (mobile phase), which is pumped at high pressure through a small-particle column, where sorbents are packed and constitute the stationary phase. Different components from a

sample are separated in distinct bands as they migrate down the column (filled with stationary phase). There is a partitioning process of the components between the mobile phase and the stationary phase, according to their affinity. For example, for an analyte with stronger affinity to the stationary phase, the movement is retarded. This method may also infer about the concentration of each separated component with a specific band, being monitored by a detector, which generates a trace called "chromatogram" [46]. The selection of the mobile phase and column to obtain good resolution is not straightforward, and depends on the nature of analytes and immobilized ligands from the stationary phase, and the interaction between them may be based on several forces such as hydrophobic, electrostatic or polar forces, which are usually associated with specific "types" of chromatography (e.g. in reversed-phase chromatography, hydrophobic interactions predominate) [47]. A number of advantages can be highlighted for HPLC and include the automated system, detection with high sensitivity, rapid quantitative analysis with high precision and amenability for a number of compounds [46]. There are, however, some limitations that should also be considered. For instance, identification is based on the retention characteristics and the existence of a large number of compounds does not allow an unequivocal analyte identification and, sometimes, separation of peaks for some analytes is very difficult, even with changes in the method. Nevertheless, the combination of chromatography with mass spectrometry analysis may overcome HPLC disadvantages, [48], as described in the next subsection.

In the pharmaceutical field, HPLC applications include drug discovery, development of dosage forms with optimized delivery, PK profiles of the drug in animal models and quality control [49]. In the context of this work, it was especially useful for drug content evaluation of MS and drug determination in *in vitro* release studies.

3.5.3 – Liquid Chromatography – Mass spectrometry (LC - MS)

The combination of a chromatographic technique, characterized by the separation ability, with mass spectrometry method, with capability of identification, is clearly advantageous for compound differentiation, with particular interest for those with very similar retention properties and different mass spectra [48]. Briefly, an LC – MS system consists of an HPLC (pump, injector and column) system attached to a mass spectrometer through an evaporative ionizing interface, and all the components are coordinated by a computer

system with control of HPLC (flow, solvent gradient, starting of injection, gradient run) and spectrometer parameters (scan range and lens) that accesses and processes data from the ion detector's amplifier [50]. In fact, a mass spectrometer can ionize the separated peak, providing information about the molecular weight for each component from the peak [50]. In addition, a mass spectrometry in combination with mass spectrometry (MS/ MS), also called tandem mass spectrometry, can fragment an ion of interest ("parent" ion) into distinctive fragmentation pattern and separate the "daughter" ions for identification and quantification [48,50], with measurement of their molecular weights, making LC – MS/ MS a powerful tool for analytical purposes. Identification may be performed by comparison of fragmentation pattern from each "parent" ion to standard databases of fragmentation patterns [50,51]. The main advantages of the mass spectrometry systems are the absolute identification of the analyte with information about the molecular weight and, high sensitivity, with identification that can be obtained from pictograms of analyte, and also quantification from low levels with accuracy and precision [51].

Concerning the characteristics of this hybrid method (LC – MS/ MS), it consists of a valuable technique for drug identification and quantification, especially when low amount of analyte is available and when interfere from biological matrixes (e.g. plasma) may exist, such as in the PK studies, described in Chapter 6.

3.6 – *In vitro* aerosol performance: aerodynamic properties

Several *in vitro* methods are described in Pharmacopoeias for measurement of aerosol aerodynamic particle size distribution, using multistage cascade impactors. Basically, the principle of operation is the inertial size fractionation, which allows the direct determination of particle aerodynamic size. Size evaluation can also be determined by quantification of the drug incorporated in the collected particles, excluding the interference of particles only consisting of excipient material. A single-stage impactor comprises a noozle plate with one or more jets (noozles) with a specific diameter located at a fixed distance from a flat collection surface (usually horizontal). Classification of the particles in terms of the respective size is based on their differential inertial behavior, which reflects the resistance to a change in direction of the flow. Actually, the laminar flow streamlines diverge on approach to the collection surface. On the one hand, particles with larger inertia tend to easily cross these streamlines to impact on the substract. On the

other hand, finer particles (with less inertia) follow the streamlines and remain airbone as they pass the obstruction. For an impactor with several stages and progressively smaller jets, the particle velocity (and inertia) is increased. Thus, it allows the fractioning of the incoming aerosol into distinct size ranges. In addition to the stages, seven or more, the compendial apparatuses are usually used with an induction port, corresponding to the throat, which possesses well-defined entry and exit profiles and a right-angle bend to simulate the human oropharynx [52]. Among other apparatuses included into the European Pharmacopoeia and into the United States Pharmacopoeia, the Andersen cascade impactor (ACI) is still the most used impactor for testing performance of inhaled aerosols. However, it requires some stages replacement when a flow of 60L/min and 100 L/min are used. Recently, the Next generation impactor (NGI, Figure 3.3) has gained special interest, becoming more widely used. It does not require stage replacement and provides excellent size resolution [52]. In addition, lower interstage deposition/ wall losses were found for NGI, when compared with ACI [53]. Actually, the NGI has been successfully used to evaluate aerodynamic properties of a number of pulmonary systems for drug delivery [54-57]. Therefore, it was the choice for MMAD and other parameters evaluation of obtained MS as will be detailed in respective sections. Some apparatus' details will be given here, in what follows.

A

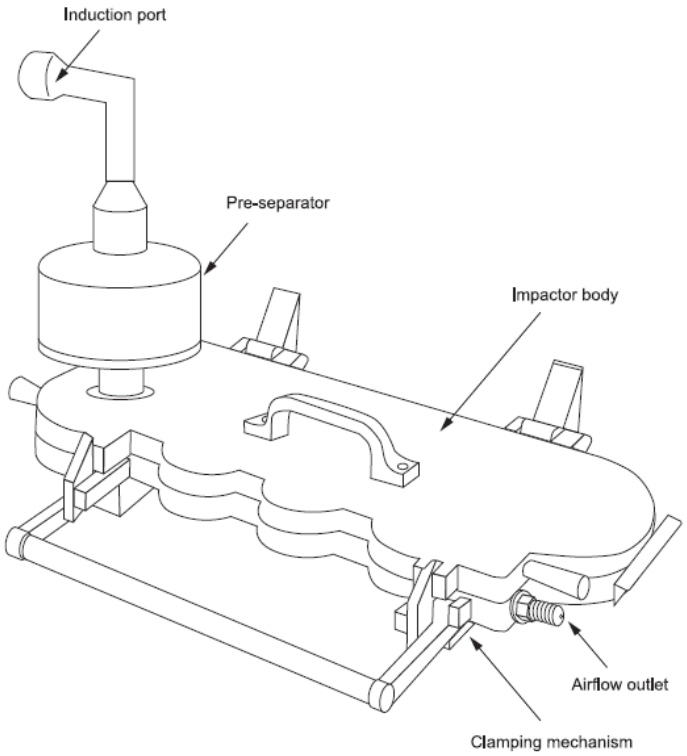

B

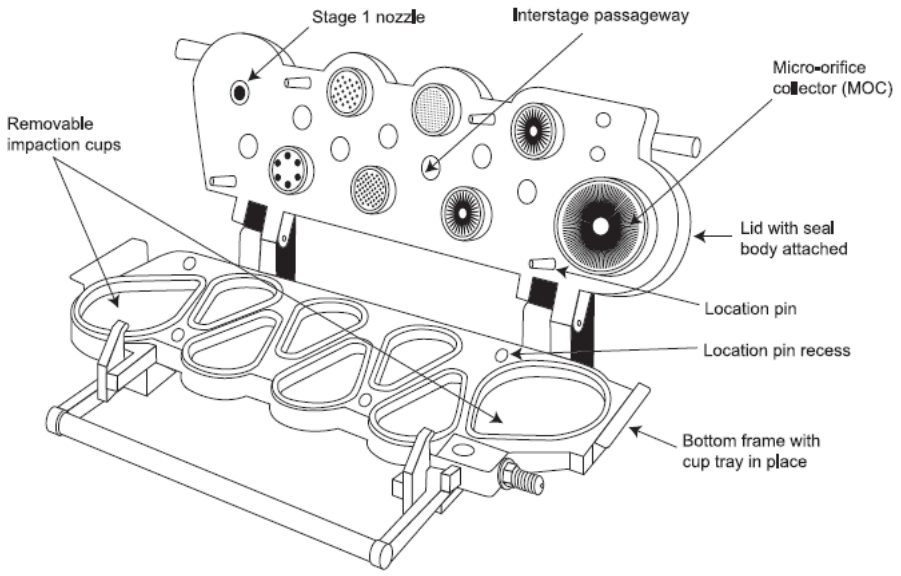

Figure 3.3 – NGI apparatus with the induction port and pre-separator connected (A) and the component parts (B). Reproduced from [58].

The NGI apparatus contains seven stages with progressively finer holes and the last stage, the micro-orifice collector. It is made of three main sections: the bottom frame that holds the impaction cups, the seal that holds the jets and the lid that contains the interstage passageways (Figure 3.3 B). For investigating the aerodynamic properties of a powder

formulation, the induction port is connected to impactor inlet and sometimes, a pre-separator is also used to catch non-inhalable particles (Figure 3.3 A). An inhaler, containing the formulation, is connected to the induction port by using a mouthpiece adapter and a vacuum pump to the outlet of the NGI, allowing the air to be drawn through the apparatus in order to simulate the inhalation. The cut-off points for each stage depend on the flow rate applied and are comprised in the range 0.24 – 11.7 µm. For a volumetric flow rate of 60 L/min, the cut-offs for stages 1 to 7 are respectively, 8.06, 4.46, 2.82, 1.66, 0.94, 0.55 and 0.34 µm. The particles deposited in each stage and retained in the induction port, pre-separator, adapter, capsule and inhaler are recovered and the drug dissolved in an appropriate solvent to be next analyzed by an adequate analytical method [59,58].

Aerosolization studies included in this thesis were performed with the NGI for the chitosan MS and PLGA MS developed. Known amount of MS was introduced into capsules and using a breath-activated inhaler, the HandiHaler® (Figure 3.4).

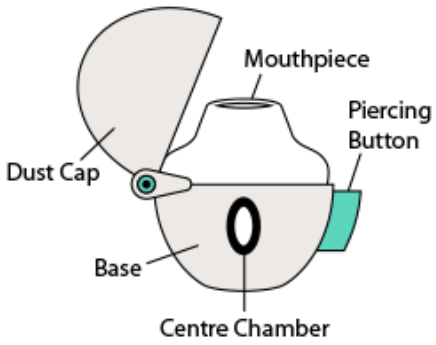

Figure 3.4 – HandiHaler® (Boehringer Ingelheim International GmbH) inhaler with main constituents. The capsule is inserted in the centre chamber by opening the mouthpiece. Before actuation, the capsule is pierced by using the piercing button.

Practical aspects and specific conditions are detailed in Chapters 4 and 5.

Additional analyses and studies performed with the obtained MS will be adequately introduced in the respective sections and include *in vitro* studies such as antibacterial and cytotoxicity evaluation and *in vivo* studies, among others.

3.7 – References

1. Lassalle V, Ferreira ML (2007) PLA Nano- and Microparticles for Drug Delivery: An Overview of the Methods of Preparation. Macromolecular Bioscience 7 (6):767-783.

2. Varde NK, Pack DW (2004) Microspheres for controlled release drug delivery. Expert Opinion on Biological Therapy 4 (1):35-51.

3. Ibrahim BM, Tsifansky MD, Yang Y, Yeo Y (2011) Challenges and advances in the development of inhalable drug formulations for cystic fibrosis lung disease. Expert Opinion on Drug Delivery 8 (4):451-466.

4. Re MI (2006) Formulating drug delivery systems by spray drying. Drying Technology 24 (4):433-446.

5. Cescutti P, Cuzzi B, Liut G, Segonds C, Di Bonaventura G, Rizzo R (2011) A novel highly charged exopolysaccharide produced by two strains of Stenotrophomonas maltophilia recovered from patients with cystic fibrosis. Carbohydrate Research 346 (13):1916-1923.

6. Manca ML, Mourtas S, Dracopoulos V, Fadda AM, Antimisiaris SG (2008) PLGA, chitosan or chitosan-coated PLGA microparticles for alveolar delivery? A comparative study of particle stability during nebulization. Colloids and Surfaces B-Biointerfaces 62 (2):220-231.

7. Bowey K, Neufeld R (2010) Systemic and Mucosal Delivery of Drugs within Polymeric Microparticles Produced by Spray Drying. BioDrugs 24 (6):359-377.

8. Sosnik A, Seremeta KP (2015) Advantages and challenges of the spray-drying technology for the production of pure drug particles and drug-loaded polymeric carriers. Advances in Colloid and Interface Science 223:40-54.

9. Ameri M, Maa Y-F (2006) Spray Drying of Biopharmaceuticals: Stability and Process Considerations. Drying Technology 24 (6):763-768.

10. Giunchedi P, Conte U, Alpar HO (1998) PDLLA microspheres containing steroids: Spray-drying, o/w and w/o/w emulsifications as preparation methods. Journal of Microencapsulation 15 (2):185-195.

11. S. Zgoulli VGGBGGPTSZ (1999) Microencapsulation of erythromycin and clarithromycin using a spray-drying technique. Journal of Microencapsulation 16 (5):565-571.

12. Anish C, Upadhyay AK, Sehgal D, Panda AK (2014) Influences of process and formulation parameters on powder flow properties and immunogenicity of spray dried polymer particles entrapping recombinant pneumococcal surface protein A. International Journal of Pharmaceutics 466 (1–2):198-210.

13. Vehring R (2008) Pharmaceutical Particle Engineering via Spray Drying. Pharmaceutical Research 25 (5):999-1022.

14. Patel BB, Patel JK, Chakraborty S, Shukla D (2015) Revealing facts behind spray dried solid dispersion technology used for solubility enhancement. Saudi Pharmaceutical Journal 23 (4):352-365.

15. Nandiyanto ABD, Okuyama K (2011) Progress in developing spray-drying methods for the production of controlled morphology particles: From the nanometer to submicrometer size ranges. Advanced Powder Technology 22 (1):1-19.

16. Li M, Rouaud O, Poncelet D (2008) Microencapsulation by solvent evaporation: State of the art for process engineering approaches. International Journal of Pharmaceutics 363 (1–2):26-39.

17. O'Donnell PB, McGinity JW (1997) Preparation of microspheres by the solvent evaporation technique. Advanced Drug Delivery Reviews 28 (1):25-42.

18. Wei Q, Wei W, Tian R, Wang L-y, Su Z-G, Ma G-H (2008) Preparation of uniform-sized PELA microspheres with high encapsulation efficiency of antigen by premix membrane emulsification. Journal of Colloid and Interface Science 323 (2):267-273.

19. Qi F, Wu J, Fan Q, He F, Tian G, Yang T, Ma G, Su Z (2013) Preparation of uniform-sized exenatide-loaded PLGA microspheres as long-effective release system with high

encapsulation efficiency and bio-stability. Colloids and Surfaces B: Biointerfaces 112:492-498.

20. Doan TVP, Olivier JC (2009) Preparation of rifampicin-loaded PLGA microspheres for lung delivery as aerosol by premix membrane homogenization. International Journal of Pharmaceutics 382 (1–2):61-66.

21. Blott SJ, Croft DJ, Pye K, Saye SE, Wilson HE (2004) Particle size analysis by laser diffraction. Geological Society, London, Special Publications 232 (1):63-73.

22. Jillavenkatesa A, Dapkunas SJ, Lum L-SH (2001) Particle size characterization. NIST special publication ; no. 960-1. U.S. Dept. of Commerce, Technology Administration, National Institute of Standards and Technology, Washington, D.C.

23. Pilcer G, Vanderbist F, Amighi K (2008) Correlations between cascade impactor analysis and laser diffraction techniques for the determination of the particle size of aerosolised powder formulations. International Journal of Pharmaceutics 358 (1–2):75-81.

24. Goldstein J, Newbury DE, Joy DC, Lyman CE, Echlin P, Lifshin E, Sawyer L, Michael JR (2003) Scanning Electron Microscopy and X-ray Microanalysis. 3 edn. Springer US, New York.

25. Wang ZL (2000) Transmission Electron Microscopy of Shape-Controlled Nanocrystals and Their Assemblies. The Journal of Physical Chemistry B 104 (6):1153-1175.

26. Lowell S, Shields JE, Thomas MA, Thommes M (2004) Characterization of Porous Solids and Powders: Surface Area, Pore Size and Density. Particle Technology Series, vol 16, 1 edn. Springer Netherlands.

27. Arvaniti E, Juenger MG, Bernal S, Duchesne J, Courard L, Leroy S, Provis J, Klemm A, De Belie N (2015) Determination of particle size, surface area, and shape of supplementary cementitious materials by different techniques. Materials and Structures 48 (11):3687-3701.

28. Bragg W (1913) The diffraction of short electromagnetic waves by a crystal. Proceedings of the Cambridge Philosophical Society:43-57.

29. Drenth J (2001) X-ray Diffraction: Principles. John Wiley & Sons, Ltd., The Netherlands.

30. Chan KLA, Hammond SV, Kazarian SG (2003) Applications of Attenuated Total Reflection Infrared Spectroscopic Imaging to Pharmaceutical Formulations. Analytical Chemistry 75 (9):2140-2146.

31. Wartewig S, Neubert RHH (2005) Pharmaceutical applications of Mid-IR and Raman spectroscopy. Advanced Drug Delivery Reviews 57 (8):1144-1170.

32. Kazarian SG, Chan KLA (2006) Applications of ATR-FTIR spectroscopic imaging to biomedical samples. Biochimica et Biophysica Acta (BBA) - Biomembranes 1758 (7):858-867.

33. Haines PJ (1995) Introduction to thermal methods. In: Thermal Methods of Analysis. Springer Netherlands, pp 1-21.

34. Gabbott P (2008) A Practical Introduction to Differential Scanning Calorimetry. In: Principles and Applications of Thermal Analysis. Blackwell Publishing Ltd, pp 1-50.

35. Haines PJ, Wilburn FW (1995) Differential thermal analysis and differential scanning calorimetry. In: Thermal Methods of Analysis. Springer Netherlands, pp 63-122.

36. Haines PJ (1995) Thermogravimetry. In: Thermal Methods of Analysis. Springer Netherlands, pp 22-62.

37. Bottom R (2008) Thermogravimetric Analysis. In: Principles and Applications of Thermal Analysis. Blackwell Publishing Ltd, pp 87-118.

38. Dejaegher B, Vander Heyden Y (2011) Experimental designs and their recent advances in set-up, data interpretation, and analytical applications. Journal of Pharmaceutical and Biomedical Analysis 56 (2):141-158.

39. Lewis GA, Mathieu D, Phan-Tan-Luu R (1998) Pharmaceutical Experimental Design. Informa Healthcare, New York.

40. Naikwade S, Bajaj A, Gurav P, Gatne M, Singh Soni P (2009) Development of Budesonide Microparticles Using Spray-Drying Technology for Pulmonary

Administration: Design, Characterization, In Vitro Evaluation, and In Vivo Efficacy Study. AAPS PharmSciTech 10 (3):993-1012.

41. Kulkarni AD, Bari DB, Surana SJ, Pardeshi CV (2016) In vitro, ex vivo and in vivo performance of chitosan-based spray-dried nasal mucoadhesive microspheres of diltiazem hydrochloride. Journal of Drug Delivery Science and Technology 31:108-117.

42. Narayan P, Marchant D, Wheatley MA (2001) Optimization of spray drying by factorial design for production of hollow microspheres for ultrasound imaging. Journal of Biomedical Materials Research 56 (3):333-341.

43. Pardeshi CV, Rajput PV, Belgamwar VS, Tekade AR (2012) Formulation, optimization and evaluation of spray-dried mucoadhesive microspheres as intranasal carriers for Valsartan. Journal of Microencapsulation 29 (2):103-114.

44. Eaton JW (2009) GNU Octave Software. Version 3.2.3.

45. Harris DC (2007) Fundaments of spectrophotometry. In: Quantitative Chemical Analysis. 8th edn. NY: W.H. Freeman and Company, New York, pp 399-404.

46. Dong MW (2006) Introduction. In: Modern HPLC for Practicing Scientists. John Wiley & Sons, Inc., pp 1-14.

47. Hanai T (2000) HPLC: A Practical Guide. Journal of the American Chemical Society, vol 122 (12). Royal Society of Chemistry, Cambridge, UK.

48. Ardrey RE (2003) Introduction. In: Liquid Chromatography – Mass Spectrometry: An Introduction. John Wiley & Sons, Ltd, pp 1-5.

49. Dong MW (2006) Pharmaceutical Analysis. In: Modern HPLC for Practicing Scientists. John Wiley & Sons, Inc., pp 135-156.

50. McMaster MC (2005) Introduction to LC/MS. In: LC/MS. John Wiley & Sons, Inc., pp 1-8.

51. Ardrey RE (2003) Mass Spectrometry. In: Liquid Chromatography – Mass Spectrometry: An Introduction. John Wiley & Sons, Ltd, pp 33-74.

52. Smyth HDC, Hickey AJ (2011) Controlled Pulmonary Drug Delivery. Advances in Delivery Science and Technology. Springer New York.

53. Kamiya A, Sakagami M, Hindle M, Byron PR (2004) Aerodynamic sizing of metered dose inhalers: an evaluation of the Andersen and Next Generation pharmaceutical impactors and their USP methods. Journal of Pharmaceutical Sciences 93 (7):1828-1837.

54. El-Sherbiny IM, Smyth HDC (2010) Biodegradable nano-micro carrier systems for sustained pulmonary drug delivery: (I) Self-assembled nanoparticles encapsulated in respirable/swellable semi-IPN microspheres. International Journal of Pharmaceutics 395(1-2):132-41.

55. Amaro MI, Tewes F, Gobbo O, Tajber L, Corrigan OI, Ehrhardt C, Healy AM (2015) Formulation, stability and pharmacokinetics of sugar-based salmon calcitonin-loaded nanoporous/nanoparticulate microparticles (NPMPs) for inhalation. International Journal of Pharmaceutics 483 (1–2):6-18.

56. Donovan MJ, Smyth HDC (2010) Influence of size and surface roughness of large lactose carrier particles in dry powder inhaler formulations. International Journal of Pharmaceutics 402 (1–2):1-9.

57. Kuttler A, Dimke T (2015) Extent of inhaled drug deposition in mouth-throat and pulmonary airways: A novel biophysical modelling approach for inhaled therapeutics. European Respiratory Journal 46 (suppl 59).

58. Preparations for inhalation (2007). In: European Pharmacopoeia. vol 1, 6 edn. Council of Europe, Strasbourg, pp 287-300.

59. Quality Solutions for Inhaler Testing (2012). Copley Scientific, MSP Corporation, 2012 Edition edn., USA.

Chapter 4

OPTIMIZATION OF LEVOFLOXACIN-LOADED CROSSLINKED CHITOSAN MICROSPHERES FOR INHALED AEROSOL THERAPY

4.1 – Introduction

Being a genetic disease, CF is caused by various mutations in the CFTR gene resulting in multiple organ failure. In the lungs, the consequence is a viscid mucus which is responsible for the dysfunction of the lung microorganism clearance system and for the clinical symptoms, i.e. chronic inflammation and bacterial infection that eventually leads to respiratory failure [1]. *P. aeruginosa* chronic infection is considered the main cause of mortality in adult CF patients [2]. Treatment consists of intensive antibiotherapy to prevent the onset of chronicity and the occurrence of resistance. Tobramycin, aztreonam and colistimethate, a prodrug of colistin, are available in efficient products for inhalation and represent a valuable alternative to solution for injection or oral therapy. For LVX, a nebulized solution exists in Europe (Quinsair®) and demonstrated reduction of *P. aeruginosa* in sputum as well as improvements in lung function [3,4]. However, the compliance to inhaled therapy has to be improved and some innovative formulations have appeared in recent years, including nanospheres, MS and liposomes [5,6]. In addition, dry-powders inhalers were reported to possess some advantages over liquid aerosols, among the main ones on compliance: quicker administration and a simpler, more hygienic procedure [7].

In this context, this chapter focuses on the development of immediate-release formulations of dry powder LVX for inhalation, based on polymeric MS. It should be recalled that for appropriate deposition in the lungs, aerosolized MS should possess an aerodynamic size between 1 and 5 µm [8]. MS of this size are, however, phagocytosed by the lung macrophages, which in turn may induce toxicity to macrophages or modify the bioavailability of the drug. In order to avoid such phagocytosis, some authors proposed to formulate "swelling" MS, i.e. MS able to swell upon hydration after deposition in the ELF [9,10]. Chitosan is an example of polymer with swelling capacity, biodegradability, biocompatibility, nontoxicity, as well as antibacterial and anti-inflammatory properties and it has been extensively investigated for the preparation of microsphere-based drug delivery systems [11-14]. However, their biocompatibility with specific cell lines has been evaluated for chitosan itself or for certain drug delivery systems [13,15,16]. Therefore, it is important to assure the absence of toxicity in other formulations. Besides, MS made of chitosan possess bioadhesive properties, promoting adhesion to the pulmonary system [17].

The aim of this work is, therefore, the preparation of LVX-loaded chitosan MS by the spray drying method. A factorial planning was applied for MS crosslinked with glutaraldehyde (GL) in order to evaluate the influence of some parameters (chitosan and crosslinker concentration, inlet temperature and presence of drug) on the MS size. After the optimization process, other chemical crosslinkers were also considered to control the swelling magnitude of the MS, to maintain/stabilize the microsphere structure [18,19,9,10] and to facilitate the spray-drying process [15,20,6]. Such properties allow the drug to be delivered directly to the lungs avoiding phagocytosis after lung deposition. The additional crosslinkers studied included genipin (GNP), glutaric acid (GA) and DL-glyceraldehyde (GLY). GL is a widely-used and the most common crosslinker and has already been applied to chitosan MS [21,17,22]. However, some toxicity has been reported [17,23,24] . The three other crosslinking agents present lower toxicity. GNP demonstrated levels of toxicity 5,000 - 10,000 times lower than GL and is a natural agent obtained from geniposide, a compound isolated from the fruits of the *Gardenia jasminoides* Ellis plant. Cytotoxicity studies on A549 and Calu-3 cells have shown significant lower cytotoxicity of GNP when compared with GL and sodium tripolyphosphate [25,26,17,27]. GA is found in plant and animal tissues and considered to be non-toxic. Cell viability assays with GA-crosslinked chitosan suggested no significant difference with the polymer itself [23,28]. GLY is also nontoxic and biocompatible, being found in the human organism as a metabolic product of fructose [24,29,30]. Analyses of the obtained MS included aerodynamic size, morphology, swelling properties, drug loading, thermal and chemical characteristics, *in vitro* antibacterial and drug release studies. Cytotoxicity of the differently crosslinked chitosan MS on the human airway epithelial Calu-3 cells was also assessed.

4.2 – Materials and methods

4.2.1 – Materials

Chitosan low molecular weight (20,000 cps, 75-85% deacetylated), Glutaraldehyde (GL) 50% (w/w) aqueous solution, Phosphate buffered saline (PBS) tablets, Whatman® qualitative filter paper, Grade 1 (11-µm pore size), DL-glyceraldehyde (≥ 90% by GC) and Dulbecco's modified Eagle's medium/F-12 nutrient mixture (DMEM/F-12) and fetal bovine serum (FBS) were obtained from Sigma-Aldrich® (France). Glacial

acetic acid was obtained from Panreac® (Spain). Levofloxacin hemihydrate was kindly provided by Tecnimede S.A. (Portugal). PIC B7 was obtained from Waters® (France). Formic acid 99-100% AnalaR (NormaPur) was obtained from VWR® (France) and acetonitrile of HPLC grade was purchased from Carlo Erba reagents (France). Genipin (98% purity) was obtained from Challenge Bioproducts Co., Ltd. (Taiwan). Glutaric acid (99% purity) was purchased from Merck® (Portugal). Hanks' Balanced Salt Solution (HBSS) was obtained from GIBCO® Thermo Fisher Scientific™ (France). 3-(4,5-dimethylthiazol-2-yl)-5-(3-carboxymethoxyphenyl)-2-(4-sulfophenyl)-2 tetrazolium (MTS) CellTiter 96® AQueous One Solution Cell Proliferation Assay was purchased from Promega (France). All other chemicals were of analytical grade or equivalent. Purified water was produced using a MilliQ gradient® Plus Millipore system.

4.2.2 – Preparation

The formulations and operational parameters were firstly optimized using GL as a standard crosslinker and resorting to a factorial design approach (see Table 4.1). For the MS preparation, chitosan was dissolved under magnetic stirring (300 rpm) in 150 ml of 1% (w/v) acetic acid solution (3 h at 50°C, then overnight at room temperature) and solutions were paper-filtered. LVX was added according to the specified weight ratios and solutions were stirred for 30 min. After addition of GL, the crosslinking reaction was performed under stirring for 15 min [15]. The mixtures were then spray dried using a Büchi® Mini Spray Dryer B-290 (Switzerland) set up in blowing mode and equipped with a 0.7 mm nozzle. Constant settings were as follows: 10 mL/min pump rate, 473L/h air flow rate and aspiration rate of 100 %. The two inlet temperatures studied, 120°C or 175°C, resulted in outlet temperatures of 45-60°C and 65-80°C, respectively. Table 4.1 details the formulations and conditions for the factorial planning.

The optimized conditions and formulation were deduced from the factorial planning and were finally applied to other crosslinkers. Conditions during the crosslinking step were however adapted to the crosslinker chemical reactivity, based on literature's reports and viscosity screening (see Appendix 1). For GNP (0.2 mmol per g chitosan), crosslinking reaction was carried out at 50°C for 3h under magnetic stirring (300 rpm) (adapted from [17]). For GLY (1 mmol/g), crosslinking was carried out at room temperature for 30 min (same stirring conditions) [24] and for GA (1 mmol/g) crosslinking was carried out at

60°C for 2 h (same stirring conditions) [28,23,31]. MS were collected and stored at 5 ± 3°C in vacuum desiccators on silica gel.

4.2.3 – Optimization

Factorial design

The factorial approach was performed for MS crosslinked with GL in order to optimize geometric size, for which determination is faster than aerodynamic size in the formulation development stage. This experimental design included four independent variables (x_1 to x_4) and two coded levels (-1, +1) (Table 4.1). The values at each level were chosen considering acceptable domains for each variable and according to therapeutic approach and published works [15,20,32,33]. Programs developed by the authors with GNU Octave software [34] were used to solve the polynomial multilinear model: $D = \beta_0 + \beta_1 x_1 + \beta_2 x_2 + \beta_3 x_3 + \beta_4 x_4 + \beta_{12} x_1 x_2 + \beta_{13} x_1 x_3 + \beta_{14} x_1 x_4 + \beta_{23} x_2 x_3 + \beta_{24} x_2 x_4 + \beta_{34} x_3 x_4$, where β_0 was the arithmetic mean response, β_1- β_4 the coefficients of the respective independent variables and β_{12}, β_{13}, β_{14}, β_{23}, β_{24} and β_{34} the interaction between variables. The response D (dependent variable) corresponded to the mean diameter of the MS from the volume distribution. This model was applied to evaluate the effects and interactions of the variables. For the statistical analysis, Student's *t*-test was performed with a significance level of 95%.

Table 4.1 – Coding of independent variables *x* for MS preparation.

		Coded levels of independent variables *x*			
		x_1	x_2	x_3	x_4
Description of variables and coding		Presence of LVX*	Chitosan concentration	GL amount	Inlet temperature
		-1 (No)	*-1 (0.25% (w/v))*	*-1 (5 mmol per g chitosan)*	*-1 (120°C)*
		+1 (Yes)	*+1 (0.5 % (w/v))*	*+1 (10 mmol per g chitosan)*	*+1 (175°C)*
Formulations	F1	- 1	- 1	- 1	- 1
	F2	- 1	- 1	+1	- 1
	F3	- 1	- 1	- 1	+1
	F4	- 1	- 1	+1	+1
	F5	- 1	+1	- 1	- 1
	F6	- 1	+1	+1	- 1
	F7	- 1	+1	- 1	+1
	F8	- 1	+1	+1	+1
	F9	+1	- 1	- 1	- 1
	F10	+1	- 1	+1	- 1
	F11	+1	- 1	- 1	+1
	F12	+1	- 1	+1	+1
	F13	+1	+1	- 1	- 1
	F14	+1	+1	+1	- 1
	F15	+1	+1	- 1	+1
	F16	+1	+1	+1	+1

* 1:1 LVX:chitosan weight ratio

Particle size

MS were dispersed in purified water, sonicated for 10 min and analyzed using laser light diffraction (Microtrac® X100 particle size analyzer), as previously described [35]. Three measurements were carried out for each sample and particle size expressed as the mean diameter ± SD of the volume distribution (D_v) calculated using the Microtrac Particle Size Analyzer application program (version 9.0g).

4.2.4 – Scanning electron microscopy

Samples were dispersed on double-sided adhesive carbon tapes that were fixed on aluminum stubs. They were then sputter coated with a gold film making them conducting. SEM images were taken using a Jeol JSM 6010 LV electron microscope (Tokyo, Japan) with the primary electrons accelerated under a voltage of 15 kV. The images were obtained from the collection of secondary electrons at a working distance of 11 mm.

4.2.5 – X-ray diffraction

Samples were placed in a low background silicon holder in Bragg-Brentano configuration, with a copper tube powered at 45 kV and 40 mA. They were scanned in the range $5° < 2\theta < 145°$ at a step of 0.066° and time/step of 10 seconds in an Empyrean PANalytical (The Netherlands) diffractometer with the detector Xcelerator in scanning mode and opened at 2°. A nickel filter was installed in a secondary optic in order to eliminate the Kβ component.

4.2.6 – Differential Thermal Analysis/ Thermal Gravimetric Analysis

MS were analyzed by combined DTA/ TGA that were performed on a SDT Q600 Instrument (TA, USA) from 30º C to 300º C with a 10°C/min heating rate and under a 100 mL/min air flow rate. The calibration procedure was performed with sapphire, using empty platinum pans as reference.

4.2.7 – Attenuated total reflectance Fourier transform infrared spectroscopy

ATR infrared spectra were recorded using a FT-IR 6700 spectrometer (Thermo Scientific Nicolet^{TM}, USA) equipped with an ATR accessory. Samples were placed in the ATR device and measurements were made by using 16 scans between 4000 and 650 cm^{-1} for each spectrum with a resolution of 4 cm^{-1}.

4.2.8 – Swelling properties

Studies concerning the swelling behavior of MS were also conducted. A known amount (20 mg ± 1 mg) of MS was added to 1 mL of PBS (pH 7.4). After dispersion with a vortex, the MS suspensions were mixed at 350 rpm and 37 ± 0.5 °C by using a

Thermomixer (Thermomixer® Comfort, Eppendorf AG., Hamburg, Germany). At predetermined points, samples were centrifuged at 10,000 rpm for 5 minutes (Eppendorf® Centrifuge 5418R, Germany) and supernatants were removed. Weight of swollen MS was determined. The percentage of swelling was calculated as follows: Swelling (%) = (W_t / W_i) x 100, where W_t corresponds to the weight of swollen MS at time *t* and W_i to the initial weight [10]. Experiments were done in triplicate and results expressed as mean ± SD.

4.2.9 – Drug loading and entrapment efficiency

LVX-loaded MS (10 ± 1mg) were submitted to an extraction process with 20 mL of 0.1M hydrochloric acid [36] for 3 h at room temperature, under magnetic stirring (300 rpm). An aliquot (1 mL) of each suspension was collected and centrifuged at 3500 rpm for 5 min (Hettich® Zentrifugen Universal 320R, Germany). Supernatants were collected and appropriately diluted in PBS prior to HPLC quantification. Drug loadings (DL) (%) were expressed as the amount of LVX (mg) per mg of MS (including entrapped LVX). Entrapment efficiencies (EE) (%) were calculated as the percent ratios of the determined contents to the theoretical contents calculated considering a 100% EE [6]. All the experiments were done in triplicate.

4.2.10 – Levofloxacin determination by HPLC

The chromatographic system consisted of an L-2200 autosampler unit (Lachrom Elite®, Hitachi), an L-2130 pump (Lachrom Elite®, Hitachi) and an Intelligent Fluorescence Detector JASCO FP-920. It was equipped with a C18 X-Bridge™ HPLC column (5 µm, 2.1x100 mm, Waters). The mobile phase was run at a 0.25 mL/min flow rate and was composed of a 20:80 (v/v) acetonitrile: water mixture supplemented with 0.1% (v/v) formic acid and 0.2% (v/v) PIC B7. The injection volume was 10 µL and the run time was 8 min. LVX was detected by fluorometry (λ_{ex} = 290 nm; λ_{em} = 460 nm). The calibration curve was constructed by linear regression of the peak areas versus the added concentrations (0.156 - 5 µg/mL in PBS (pH 7.4)), and appropriate quality controls were included to monitor the performance of the method (See appendix 2 for details and method validation results).

4.2.11 – Aerodynamic properties

The aerodynamic diameter was measured using a Next Generation Impactor (NGI, Copley Ltd., Nottingham, UK), equipped with a TPK 2000 critical flow controller and a HCP5 vacuum pump (Copley HCP5, Nottingham, UK). For each measurement, a size-three hard gelatin capsule was filled with 20 ± 1 mg of LVX-loaded MS powder, inserted in a dry-powder inhaler Handihaler® (Boehringer-Ingelheim, Germany) and pierced. The inhaler was tightly connected to the NGI induction port via a silicone adapter. The pump was turned on, allowing a constant air flow of 60 ± 5% L/min for 4 seconds (twice) in order to obtain 4L of air from the adapter and through the NGI. The powder remaining in the capsule and deposited in the inhaler, the adapter, the induction port, all the stages and the filter was collected with 0.1 M hydrochloric acid solution allowing extraction for LVX determination (see Appendix 2). The emitted dose (ED), i.e. the mass of LVX deposited in the induction port, the stages and the filter, was expressed as the percentage (ED %) of the total recovered LVX mass (i.e. from the induction port, the stages and the filter NGI *plus* from the adapter, the inhaler and capsule). The fine particle dose (FPD), i.e. the fraction of LVX in particles with aerodynamic diameters below 5.0 µm, was calculated by interpolation, from the inverse of the standard normal cumulative mass percentage distribution, and considering stages 1 to 3. The MMAD of the particles was calculated from a similar plot as the particle aerodynamic diameter at which the line crosses the 50% mark [37-39]. The fine particle fraction (FPF) was calculated by converting the FPD mass as the percentage of the ED.

4.2.12 – *In vitro* release studies

Release studies were performed at 37 ± 0.5 °C in PBS (pH 7.4) under sink conditions. The LVX-loaded MS powder (15 ± 1 mg) was dispersed in 150 mL PBS and the release medium was maintained under a uniform shaking of 250 rpm using a VWR® incubating mini shaker. At pre-determined time points 1 mL aliquots were taken and centrifuged at 3500 rpm for 5 min (Hettich® Zentrifugen Universal 320R, Germany). Then, 50 µL of supernatant were collected for LVX HPLC determination (see Appendix 2 for details about method validation). The remaining 950 µL were vortex-mixed and added back to the flasks. Experiments were conducted in triplicate.

4.2.13 – *In vitro* antibacterial activity

Antibacterial activity of free LVX was compared with chitosan and LVX-loaded chitosan MS by measuring the MICs. Two *P. aeruginosa* strains (CF2_2004 and CF7_2005) isolated from sputum of two CF patients (Pediatric Unit, Coimbra Hospital Centre, CHC, Portugal) were used. Identification was made by both MicroScan WalkAway® (Dade Behring, West Sacramento, CA) and API® 20NE (Biomérieux Vitek, Inc. Hazelwood, Mo., USA) systems. The bacteria were incubated on Trypticase soy agar for 24 h at 37 °C. Few colonies were transferred to physiological saline in order to obtain a 0.5 McFarland standard (1.5 x 10^8 CFU/mL) inoculum, as described for the broth microdilution method [40,41]. In 96-well plates, Mueller-Hinton broth (100 µl) and LVX solution or MS/ chitosan suspensions in a 40% (v/v) ethanol-water mixture (100 µl) were added per well. These solutions/suspensions were then sequentially diluted (from 5 to 0.078 mg/L LVX). Then, 100 µl of inoculum were added. Negative controls with MS suspensions (in all the concentrations) and growth controls were also included. After 24h of incubation at 37 °C and under 100 rpm, optical density was measured at 600 nm in a Synergy™ HT microplate reader (BioTek Instruments®, Inc.,Winooski, VT, USA). Values lower than 0.1 were considered as zero bacterial growth and the lowest concentration that yields an optical density value < 0.1 indicated the MIC [42]. As a complementary study, the bacterial susceptibility was also evaluated by the disk diffusion test in Mueller-Hinton agar, measuring the diameter of the inhibition zone (mm) [41]. Experiments were done in three different occasions.

4.2.14 – Cytotoxicity study

Human airway epithelial Calu-3 cells were obtained from the American Type Culture Collection (Rockville, MD) and used between passages 40 to 60. Cell growth was maintained in plastic tissue culture flasks of 75 cm^2 (Nunc, Roskilde, Denmark) in 95 % relative humidity with 5% CO_2/95% atmospheric air at 37°C. The cells were cultured in DMEM/F-12 nutrient mixture supplemented with L-glutamine (2 mM) and FBS (10% (v/v)).

The *in vitro* cytotoxicity of MS was studied using the MTS assay. For that, the Calu-3 cells were seeded in 96-well plates (1 x 10^4 cells per well in 100 µL culture medium) and

incubated for 24h in the conditions described above. The medium was then replaced with 100 µL of fresh pre-warmed medium containing unloaded MS, LVX-loaded MS or LVX. The starting suspensions of unloaded MS (2 mg/mL chitosan), LVX-loaded MS (4 mg/mL, corresponding to 2 mg/mL of chitosan and 2 mg/mL of LVX) or solution of LVX (2 mg/ml) were prepared in culture medium and then diluted following a sequential two-fold dilution ranging from 1 to 0.0156 mg/ml of chitosan and/or LVX. The cells were then incubated with these dilutions for 24 h. After incubation, the medium was replaced with 120 µL of pre-warmed MTS reagent diluted in HBSS (20 % (v/v)), allowing the reduction of the tetrazolium compound by living cells into a soluble formazan product during the plate incubation for 2 hours. After transfer of the samples into new plates to avoid absorbance interference of adhered MS to the cells, the absorbance was spectrophotometrically measured at 490 nm wavelength (A_{490nm}) using a microplate reader (Varioskan^{TM}, Thermo Scientific^{TM}). Background measurements were carried out at 650 nm (A_{650nm}). Experiments were done in six different occasions. The cell viability (%) was calculated according to

$$\text{Cell viability (\%)} = \frac{A_{490nm} - A_{650nm}}{A_{control\ 490nm} - A_{control\ 650nm}} \times 100 \qquad (4.1)$$

where $A_{control\ 490nm}$ and $A_{control\ 650nm}$ correspond to the absorbance measured in the control wells (Calu-3 cells alone).

Cell viability (%) versus log concentration curves were fitted with GraphPad software (GraphPad Prism version 5.00 for Windows, San Diego California USA), for each experiment, using

$$\text{Cell viability (\%)} = 100/(1+10^{((LogIC50-X)*H)}) \qquad (4.2)$$

where IC50 is the concentration that inhibits 50 % of cell growth, i.e. cell viability decreased in 50% [13], X the logarithmic concentration of the formulation and H the Hillslope number. For fitting the curves, concentrations were transformed to the corresponding logarithm.

Statistical analysis of cell viability was performed from IC50 values (n=6) by one-way ANOVA followed by post hoc Dunnett's multiple comparison test. All analyses were

carried out resorting to the GraphPad software. The differences were considered to be statistically significant at a level of $p < 0.05$.

4.3 – Results and discussion

4.3.1 – Optimization

The first step of the process optimization was carried out with GL as crosslinker using factorial design. Some formulation parameters (presence of drug, x_1, chitosan concentration % (w/v), x_2 and GL concentration (mmol/g), x_3) and one operating condition (inlet temperature (°C), x_4) were investigated as their effect on the geometric diameter of MS, a crucial parameter for lung delivery using solid particles. Actually, the geometric size was useful in the screening step to foreseen the aerodynamic properties and it is much quicker to perform than the impactor measurements. The response function obtained from the factorial planning was as follows: $D = 7.78 + 1.43x_1 + 0.26x_2 – 0.33x_3 + 0.63x_4 + 0.27x_1x_2 – 0.01x_1x_3 + 0.55x_1x_4 + 0.09x_2x_3 – 0.09x_2x_4 – 0.11x_3x_4$. The β coefficient with the higher value corresponds to the higher effect on particle size. A positive coefficient means an increasing effect in particle size and a negative one the opposite. In this case, the presence of drug ($\beta_1 = 1.43$) and the inlet temperature ($\beta_4 = 0.63$) were the main factors affecting MS size, both in an increasing way with an increasing level of the variable. This result can be explained by the higher temperature that leads to a faster droplet evaporation and to polymer precipitation at the liquid-air interface, resulting in larger MS [43]. The presence of drug represents an amount of material that the chitosan matrix has to incorporate, resulting also in larger particles, which is in accordance with some results already published that state that a higher amount of solute leads to larger particles [44-46,43]. In addition, the β_{14} coefficient of interaction between these two factors shows a synergistic effect for particle growth (Figure 4.1). The coefficients for the other variables corresponded to lower values and were not statistically significant (see *t*-values, Table 4.2). However, higher chitosan concentrations tend to be associated with larger particles ($\beta_2 = 0.26$). Similar results have already been observed and were attributed to larger droplets formed when higher concentrations of the polymer increase the viscosity of the nebulized phase [37]. A slight decrease of size was also observed for MS crosslinked with a higher concentration of GL ($\beta_3 = – 0.33$), which can be attributed to the tightly covalently bonded structure [47].

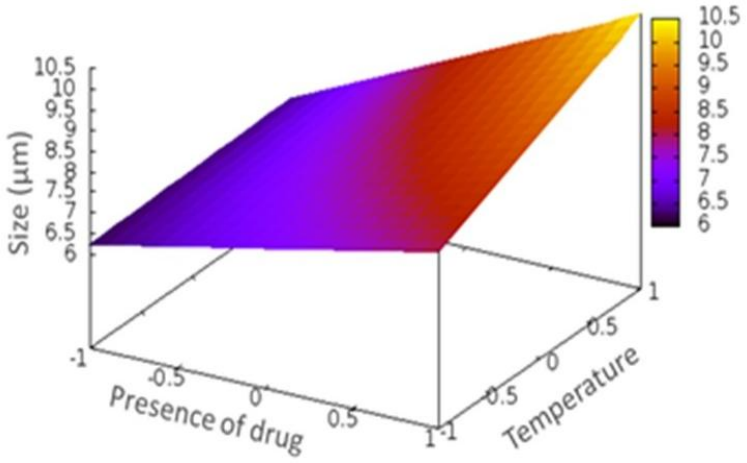

Figure 4.1 – Response surface for the main factors affecting the geometric size of MS: presence of drug and temperature (the other factors were set to zero in terms of codified values).

Table 4.2 – Coefficients obtained for model from the factorial design and respective *t* value and significance level.

Coefficients	β_0	β_1	β_2	β_3	β_4	β_{12}	β_{13}	β_{14}	β_{23}	β_{24}	β_{34}
Values	7.78	1.43	0.26	- 0.33	0.63	0.27	- 0.01	0.55	0.09	- 0.09	- 0.11
***t* value**	37.5	6.9	1.3	- 1.6	3.0	1.3	- 0.1	2.7	0.4	- 0.4	- 0.5
Significance level	100.0	100.0	76.9	86.7	99.0	77.5	3.9	97.9	33.6	33.5	38.1

The geometric size of the MS prepared according to the experimental design ranged from 4.70 ± 0.45 µm to 12.65 ± 2.82 µm, as indicated in Table 4.3. The results from the factorial planning allowed the selection of parameters for MS with a suitable geometric size, also allowing a rapid preparation and good yield (Table 4.3), i.e. 0.5 % (w/v) chitosan, 120°C inlet temperature, and 5 mmol/g GL concentration. Although 10 mmol/g concentration tends to reduce the size of MS by intermolecular tightening, it was observed that some powder adhered to the cyclone during the preparation process (leading to lower yield), and it was difficult to spray dry those formulations owing to their high viscosity. Therefore, the formulation that was selected was F13 (Table 4.1). After the optimization step, MS were prepared with alternative crosslinking agents, i.e. GNP, GA or GLY, using the same operating conditions as for F13, but adapting their

concentrations to their reactivity. These formulations and F13 were further analyzed by different techniques, whose results are described below. For clarity purposes, F13 is also referred to as MS_LVX_GL in the text that follows. For comparison, unloaded and uncrosslinked 0.5 % (w/v) chitosan MS (MS_uncross), as well as unloaded MS crosslinked with GL (MS_GL), GNP (MS_GNP), GA (MS_GA) and GLY (MS_GLY) were also prepared using the same operating conditions.

Table 4.3 – Particle size of MS for formulations used in factorial planning and corresponding values of yield (%), DL (%) and EE (%). Results are expressed as mean ± SD, n=3, except for yield, n=1.

Formulations	D_v **(µm)**	**Yield (%)**	**DL (%)**	**EE (%)**
F1	7.3 ± 1.1	58	-	-
F2	4.7 ± 0.4	51	-	-
F3	6.4 ± 2.4	64	-	-
F4	7.0 ± 2.6	45	-	-
F5	6.6 ± 2.7	66	-	-
F6	6.5 ± 1.8	50	-	-
F7	6.4 ± 1.2	66	-	-
F8	5.8 ± 1.2	50	-	-
F9	7.4 ± 2.6	75	43.2 ± 0.5	108 ± 1
F10	8.5 ± 4.2	67	39.8 ± 0.8	120 ± 3
F11	9.9 ± 3.6	67	42.5 ± 0.8	106 ± 2
F12	8.8 ± 4.2	58	42.4 ± 0.3	128 ± 1
F13	8.2 ± 2.6	79	43.2 ± 0.5	108 ± 1
F14	8.0 ± 2.8	59	40.7 ± 0.6	123 ± 2
F15	12.6 ± 2.8	72	46.7 ± 1.1	117 ± 3
F16	10.1 ± 3.7	51	41.4 ± 0.8	125 ± 2

4.3.2 – Scanning electron microscopy

The crystalline nature of LVX alone was confirmed by SEM analysis, with the presence of pointed and rod-shaped powder (Figure 4.2 A). In turn, spherical structures were observed for all the spray dried formulations. The LVX-loaded MS appear to have sizes

up to 5 µm and are spherical with a uniformly smooth surface, without visible free LVX crystals on the surface (Figure 4.2 C-J). The appearance is not affected by the crosslinking agents or by the entrapment of LVX. However, results of geometric size for MS crosslinked with GL were higher than those obtained with SEM images which were attributed to the possible agglomeration of MS when dispersed in water.

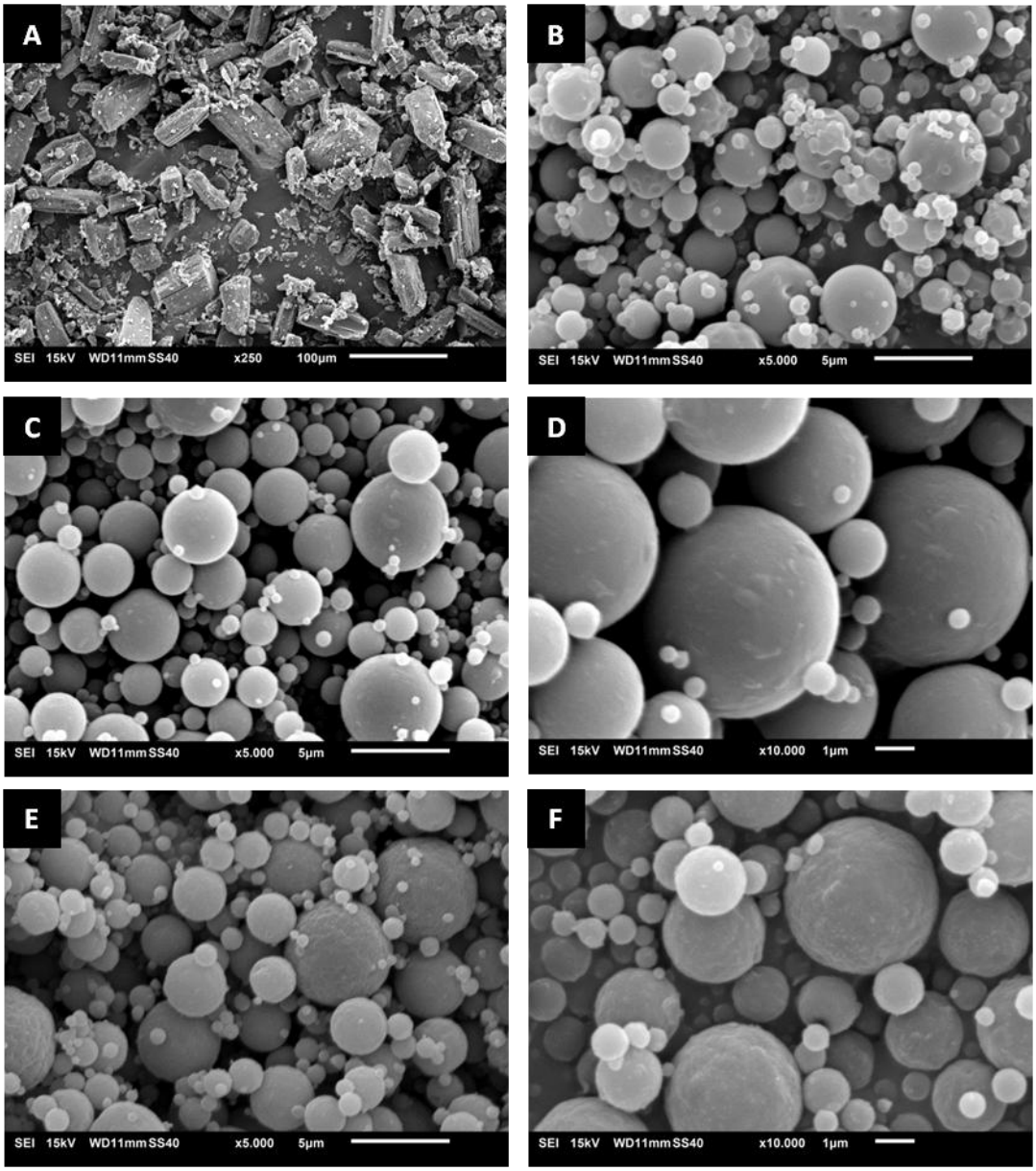

Figure 4.2 – SEM images of LVX crystals (A), unloaded uncrosslinked MS (B) and LVX-loaded MS crosslinked with GL (C,D), GLY (E,F), GA (G,H) or GNP (I,J).

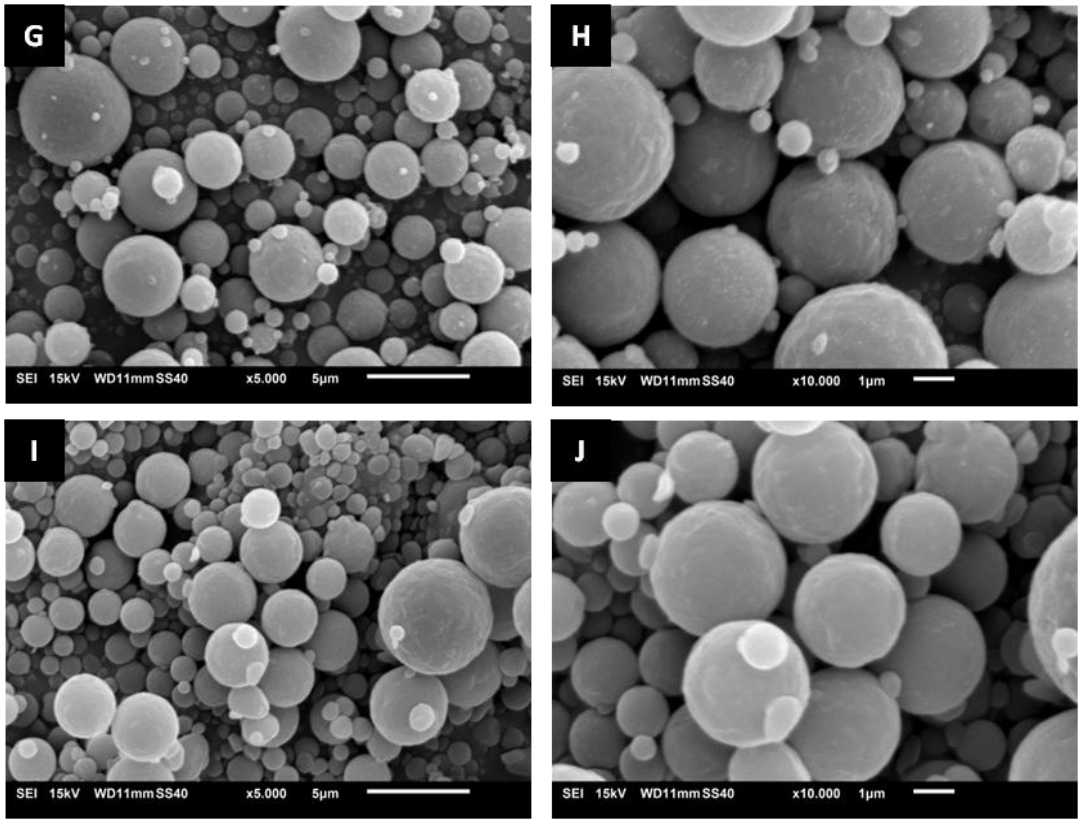

Figure 4.2 – Continued. (Caption shown on previous page).

4.3.3 – X-ray diffraction

Sharp diffraction peaks of raw materials denoted their crystalline nature. The absence of the sharp peaks of LVX in the XRD spectra of corresponding MS (Figure 4.3) indicated that LVX was in amorphous state and/ or molecularly dispersed in the MS, irrespective of the crosslinking agent.

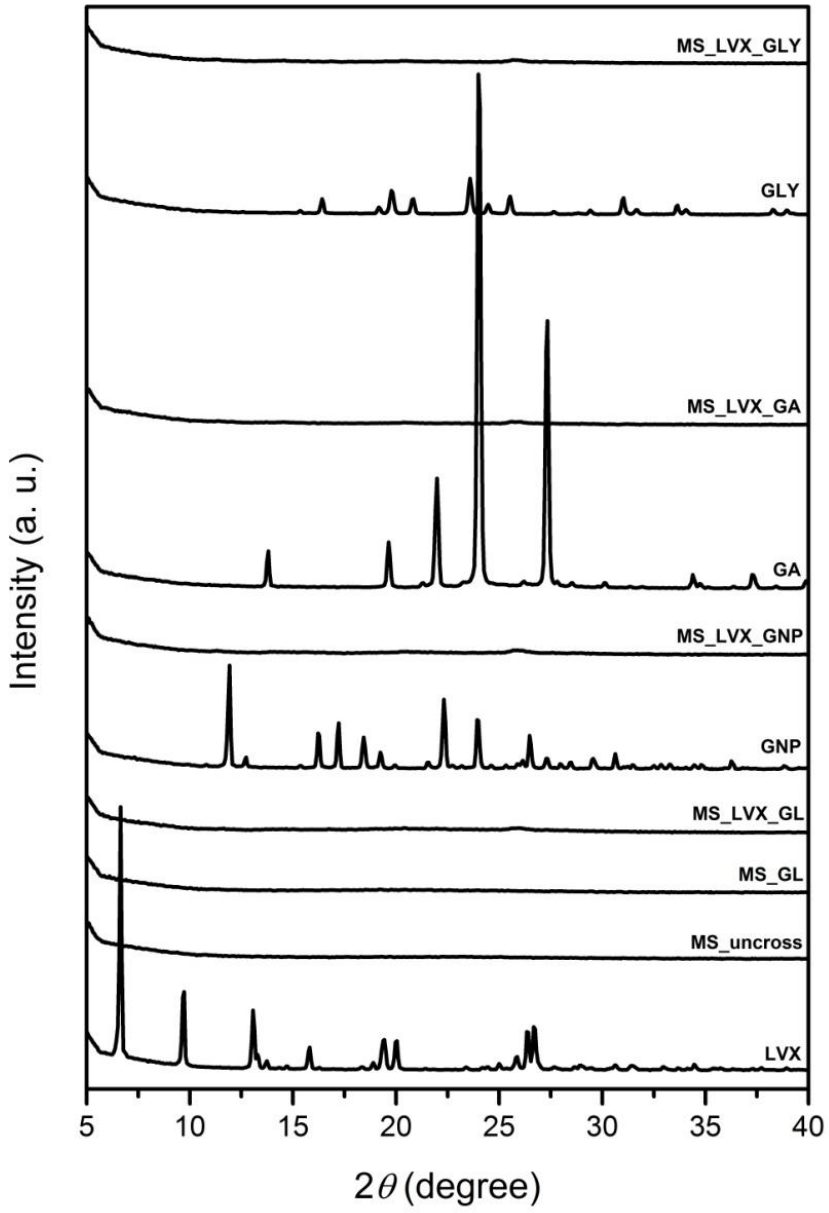

Figure 4.3 – XRD patterns of raw materials (LVX, GLY, GNP, GA), of unloaded uncrosslinked MS (MS_uncross), of unloaded MS crosslinked with GL (MS_GL = F5), and of LVX-loaded MS crosslinked with GL (MS_LVX_GL = F13), GNP (MS_LVX_GNP), GA (MS_LVX_GA) or GLY (MS_LVX_GLY).

4.3.4 – Differential Thermal Analysis/ Thermal Gravimetric Analysis

DTA/ TGA measurements (Figure 4.4) were performed to further characterize the MS formulated with different crosslinking agents.

On the LVX thermogram, an endothermic event was observed at 78°C corresponding to a weight loss of 2.35 % (w/w) measured by TGA, that agrees with the theoretical water content (2.43 %) from the LVX hemihydrate. The endothermic peak at 225°C corresponds to the anhydrate LVX melting [48]**.** For GNP, GA and GLY, the melting temperatures were observed at 125°C [49,50], 100°C and 140°C, respectively. The GA boiling point was observed at 265°C [28].

Concerning uncrosslinked and unloaded chitosan MS (MS_uncross), the endothermic peak near 60°C corresponds to the absorbed water loss [22]. An exothermic peak was observed above 225°C, which was attributed to the chemical degradation of chitosan [17,51]. Independently of the crosslinking agent, these two previously mentioned thermal events were observed for LVX-loaded MS with some differences in the shape of peaks and different values of weight loss (TGA, Figure 4.4 B). Therefore, the dispersion of LVX in the MS was confirmed by the absence of the respective melting peak, being in accordance with the results from XRD [22,17].

With respect to the gravimetric analysis, non-crosslinked MS tend to lose ca. 60% of the mass up to 300°C. If the MS are crosslinked, the weight loss is slightly lower. Upon addition of the drug, the percentage weight loss drops to values close to 40%. However, this value indicates a total weight loss somewhat exceeding what would be predictable from the separate components of the MS (ca. 33%) [49].

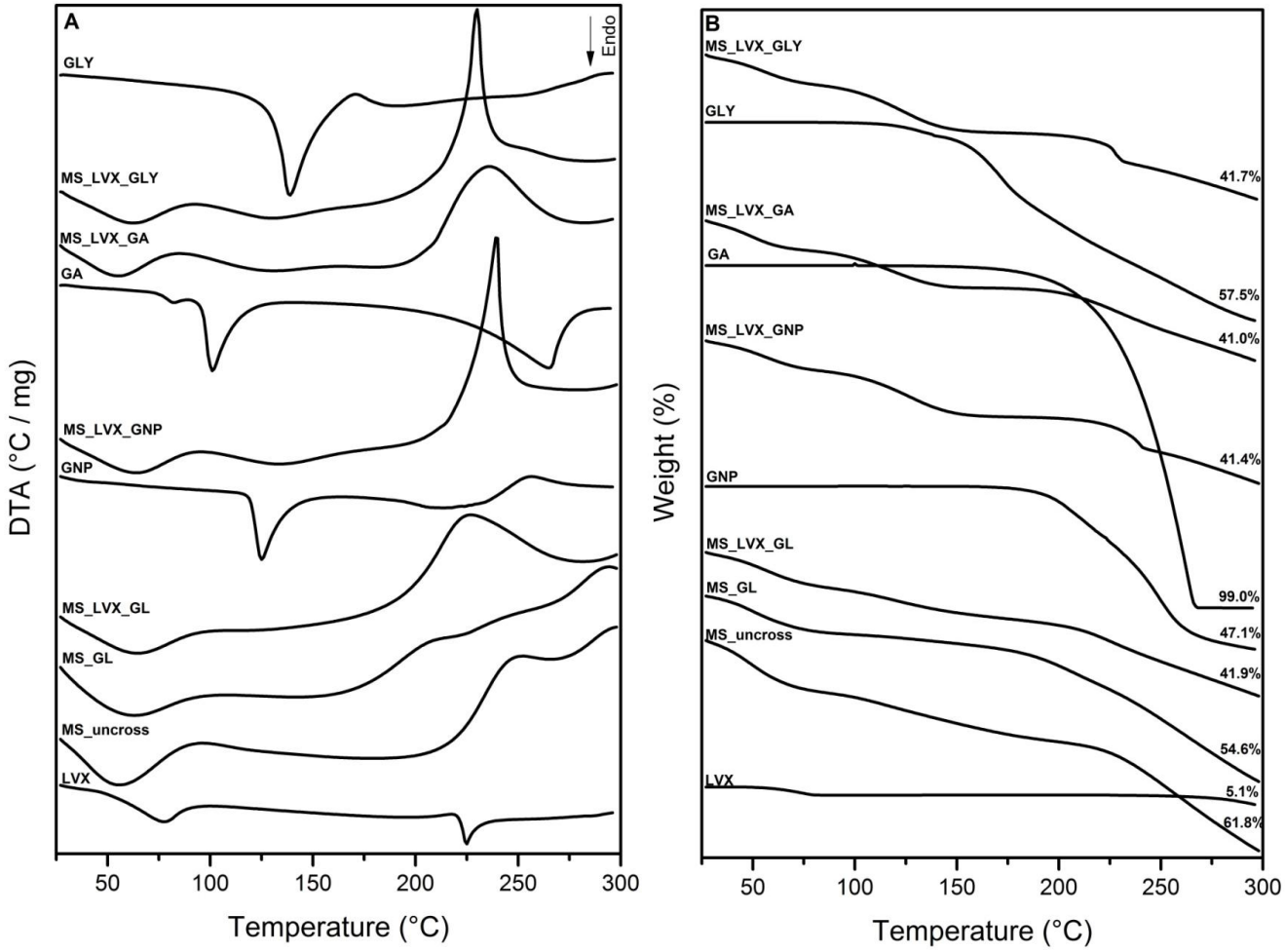

Figure 4.4 – DTA (A) and TGA (B) thermograms of raw materials (LVX, GLY, GNP, GA), of unloaded uncrosslinked MS (MS_uncross), of unloaded MS crosslinked with GL (MS_GL = F5), and of LVX-loaded MS crosslinked with GL (MS_LVX_GL = F13), GNP (MS_LVX_GNP), GA (MS_LVX_GA) or GLY (MS_LVX_GLY). Total weight loss (%) is indicated on TGA curves.

4.3.5 – Attenuated total reflectance Fourier transform infrared spectroscopy

ATR-FTIR studies were conducted in order to analyze the potential LVX chemical modification in the MS and to evaluate the chemical interactions developed by the crosslinking agents.

The LVX spectrum presented the characteristic peaks at 1724 (C=O acid), 1618 (C=O carbonyl) and 1289 cm^{-1} (C-O acid) [52,53]. These three peaks were present in all the LVX-loaded MS, confirming there was no change in the functional groups of LVX after

its incorporation, suggesting that no chemical reactions occurred between LVX and other components of the MS (Figure 4.5).

Concerning unloaded and uncrosslinked MS (MS_uncross), characteristic bands of chitosan were present in the region 3000-3500 cm^{-1} for amino and hydroxyl groups. Other characteristic absorption peaks were found at 1633 cm^{-1} corresponding to amide I (C=O) and 1547 cm^{-1} to amide II (NH) [49,54]. The band observed at 1400 cm^{-1} may be attributed to the C-N or C-OH stretch. The two bands at 1064 and 1018 cm^{-1} correspond to C-O-C, C-O and C-N stretchings. For unloaded MS, crosslinked with GL, MS_GL, the change in intensity of the band at 1633 cm^{-1} may be due to the presence of the C=N group (Figure 4.5) that confirmed the crosslinking reaction, responsible for the formation of the imine, resulting from the reaction of the amine group of chitosan with GL (see Appendix 1) [28].

With respect to the MS crosslinked with GNP (MS_GNP, Figure 4.5), this crosslinking agent reacts with the amine groups of chitosan (Appendix 1), which is accompanied by a change in colour to dark blue. This is due to the formation of a heterocyclic amine by the nucleophilic substitution by the amino group of chitosan on the C-3 carbon atom of GNP, followed by a ring opening [49,25]. GNP showed two intense bands at 1680 and 1620 cm^{-1} corresponding to the C=O and C=C stretchings. The change in the profile in this region in the MS crosslinked with GNP is an indication that the crosslinking actually took place. For MS crosslinked with GA (Figure 4.5) no significant changes were observed when comparing uncrosslinked MS (MS_uncross) with MS crosslinked with GA, MS_GA. However, the band at 1696 cm^{-1} in the GA IR spectrum is no longer present in the MS crosslinked with GA, which could be an indication that a transformation occurred. It has been reported in the literature that ionic interactions between chitosan and GA as well as the hydrogen bond between the carboxylic group of GA and amino group of chitosan are possible (see Appendix 1) [28]. There is paucity of data with respect to the crosslinking reaction of GLY with polymers such as chitosan. Only the interpretation from swelling behavior and release studies have been used to demonstrate its efficacy as a crosslinking agent [24,29]. In this case, no significant information can be obtained by comparing the IR spectra (Figure 4.5).

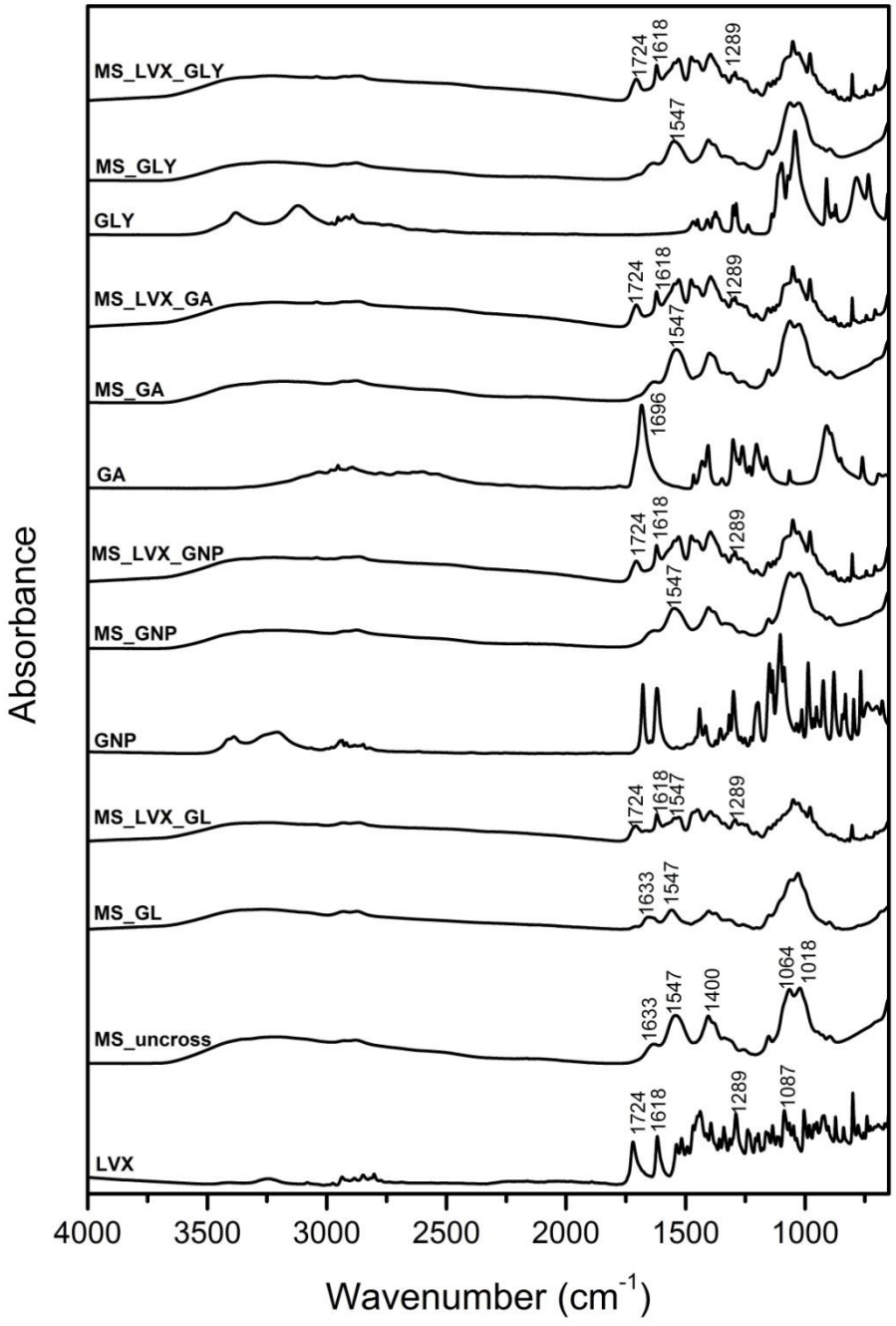

Figure 4.5 – ATR-FTIR spectra of raw materials (LVX, GLY, GNP, GA, GL), of unloaded uncrosslinked MS (MS_uncross), of unloaded MS crosslinked with GL (MS_GL = F5), GNP (MS_GNP), GA (MS_GA) or GLY (MS_GLY), and of LVX-loaded MS crosslinked with GL (MS_LVX_GL) (=F13), GNP (MS_LVX_GNP), GA (MS_LVX_GA) or GLY (MS_LVX_GLY).

4.3.6 – Swelling properties

LVX-loaded MS crosslinked with GL presented the lowest swelling value, which was constant over time (Table 4.4). MS crosslinked with the other crosslinkers swelled to a larger extent. For GLY as crosslinker the swelling value was close to 500 %. In the case of GNP or GA, swelling values were the highest (around 1000 %) and a dark blue solid-like gel and a slight yellow weak gel were observed, respectively. The higher swelling of GNP- or GA-crosslinked MS compared to GL-crosslinked MS was attributed to lower degrees of crosslinking [55]. An *in vitro* study about the relationship between the swelling properties of MS and their phagocytosis by macrophages showed that MS of swelling values ≥ 1000 % were dramatically less phagocytosed than nonswellable particles [10]. Therefore, the GNP- and GA-crosslinked MS have a great potential to escape from macrophages once deposited in the lungs.

Table 4.4 – MS degree of swelling (%) at two time points. Results are expressed as mean ± SD, n=3.

Formulations	**Crosslinkers and concentrations (mmol/g chitosan)**		**Swelling (%)**	
			30 min	**16 h**
MS_LVX_GL (=F13)	Glutaraldehyde	5	243 ± 23	247 ± 51
MS_LVX_GNP	Genipin	0.2	935 ± 14	1154 ± 47
MS_LVX_GA	Glutaric acid	1	991 ± 67	1097 ± 113
MS_LVX_GLY	DL–Glyceraldehyde	1	458 ± 24	535 ± 9

4.3.7 – Drug loading and entrapment efficiency

EE values were around 110% and 120%, respectively for MS crosslinked with 5 mmol or 10 mmol GL per g of chitosan (Table 4.3). Taking into account that the GL boiling point is 101°C in aqueous solution [56], we hypothesize that a fraction of GL did not react and evaporated during the spray-drying process, which can explain the high values of the EE (%). Using GNP, GA and GLY as crosslinkers, the EE were around 100% (Table 4.5). Such high EE values allow also concluding that LVX did not appreciably react with the crosslinkers in the preparation process. In what pertains to the DL (%), the aim was to maximize the content of LVX in order to minimize the amount of powder material to be

administered into the lungs. DL ranged from 40.7 to 55.8 % (w/w) (Tables 4.3 and 4.5). An efficient dose with inhaled LVX solution was shown to range from 120 to 240 mg (once or twice a day) [57,58]. With the present MS, the amount of material to administer such a dose would range from 250 to 500 mg a day, considering a therapeutic efficiency equivalent to the aerosolized LVX solution. This deserves to be evaluated in terms of safety. Alternatively, the present LVX-loaded MS may be used as a short-term therapeutic option for out-of-home patients, as an alternative to fastidious and demanding aerosol therapy with liquid formulations [59].

Table 4.5 – Values of yield (%), DL (%) and EE (%) for MS prepared after the optimization process. Results are expressed as mean ± SD, n=3. All formulations include LVX with LVX:chitosan preparation ratio of 1:1 (w/w).

Formulations	Yield (%)	DL (%)	EE (%)
MS_LVX_GNP	89	48.4 ± 5.8	99 ± 12
MS_LVX_GA	91	50.5 ± 0.3	107 ± 1
MS_LVX_GLY	88	50.8 ± 0.9	106 ± 2

4.3.8 – Aerodynamic properties

The experimental conditions for aerodynamic determinations were selected to ensure high aerosol performance. The 60 L/min flow rate was higher than that considered to be attainable by patients using a Handihaler® device, but it provided a high pressure drop through the inhaler (around 8 kPa) [60], thus a high energy input to disperse efficiently the microsphere powder [61]. In addition, the pump was turned on twice to ensure complete emptying of the capsules. Results of the selected formulations are presented in Table 4.6. All the formulations showed a high dispersibility with ED values around 90%, indicating that the microsphere powder was efficiently emitted from the DPI. MMAD values were dependent on the crosslinker used. For MS crosslinked with GNP and GA, MMAD values were found around 5 µm, a value satisfactory for delivery to the conductive zone of the lungs (trachea, bronchi and terminal bronchioles) where the *P. aeruginosa* infection is mainly present [2]. These results were consistent with SEM analyses (Figure 4.2). However, for MS crosslinked with GL and GLY, MMAD values were close to 8 µm. For MS prepared with GL, MMAD mean values exceeding the range

of the higher aerodynamic cut-off plate consist of extrapolated values established from the cumulated mass percentage distribution. Since SEM images revealed an MS diameter close to 5 µm (Figure 4.2 C and D, and E and F respectively), the MS may not fully de-aggregate in the inhaler despite the high pressure drop applied [62]. For MS crosslinked with GNP, GA and GLY, FPF was high (around 30%), Table 4.6, i.e. in the upper values reported for marketed powder formulations for inhalation [63]. For MS crosslinked with GL, FPF was slightly lower. Thus, in general, the MS obtained in the present work should be efficient to deliver LVX into the lungs.

Table 4.6 – *In vitro* aerosolization properties of MS (values are expressed as mean ± SD, n=3).

Formulations	ED (%)	FPF (%)	FPD (mg)	MMAD (µm)
MS_LVX_GL (= F13)	89.8 ± 1.1	23.7 ± 5.3	1.2 ± 0.2	8.4 ± 2.3
MS_LVX_GNP	89.5 ± 0.7	31.8 ± 1.3	2.2 ± 0.5	5.4 ± 0.2
MS_LVX_GA	91.9 ± 1.9	32.3 ± 4.0	2.3 ± 0.3	5.9 ± 1.2
MS_LVX_GLY	88.0 ± 3.2	27.3 ± 1.1	1.6 ± 0.1	7.4 ± 1.1

4.3.9 – *In vitro* levofloxacin release

All the formulations resulted in an almost immediate release of LVX (Figure 4.6). This allows concluding that chitosan crosslinking has no impact upon LVX release. This was attributed to the high solubility in water of LVX associated with the high drug content and with the large surface area developed by the micrometric-sized particles, which allowed the rapid diffusion of the drug from the MS matrix. In addition, the amorphous state of LVX, evidenced by XRD and DTA analyses, is usually associated with a higher dissolution rate compared to crystalline state [38]. Similar results were obtained by the preparation of salbutamol sulphate loaded in formaldehyde-crosslinked chitosan MS [64] with no difference between crosslinked and non-crosslinked systems. Despite some authors having reported drug controlled release with crosslinked chitosan matrices, it is usually observed for drugs with low hydrophilicity and/or at low drug content values [17,22]. In this work, we found that with a hydrophilic high soluble drug as LVX, and with high values of drug content it is not possible to obtain a controlled release profile using a crosslinked chitosan system.

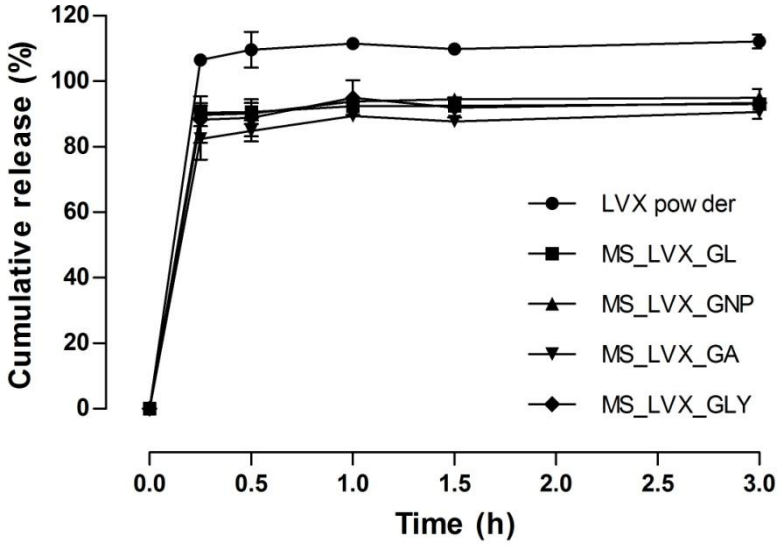

Figure 4.6 – *In vitro* release profiles of LVX-loaded MS. MS_LVX_GL corresponds to F13.

4.3.10 – Antibacterial activity

Antibacterial activity of free LVX, chitosan and selected LVX-loaded MS was evaluated for two bacterial isolates of *P. aeruginosa* (CF2_2004 and CF7_2005) by the broth microdilution method. The aim was to investigate whether the LVX activity is altered by encapsulation in MS, and to understand whether there is some antibacterial synergistic effect due to chitosan and LVX in loaded MS. The MIC value for LVX was 0.625 mg/L for both bacterial isolates. Regarding the MS, the MIC value of 0.625 mg/L was observed for CF2_2004, regardless of the crosslinking agent that was used. Very similar results were obtained from CF7_2005, but MS crosslinked with GNP demonstrated a lower MIC value (0.312 mg/L), see Table 4.7. This effect may be due to the presence of some uncrosslinked GNP, taking into consideration that this crosslinker has already been reported as an antimicrobial and anti-inflammatory agent [50,65]. Chitosan alone did not exhibit any antibacterial activity against the two isolates that were used (bacterial growth was observed for all the concentrations in the range 0.078 – 5 mg/L). Actually, some antibacterial activity has been recently reported for chitosan, but it was observed only at higher concentrations such as 0.0125 % (w/v) [66] and 0.05 % (w/v) [11] for *P. aeruginosa*. The similarity between the results from LVX and loaded MS is in accordance

with the fast drug release that was already explored and it is apparent that LVX can be safely encapsulated in MS without losing its antibacterial activity. Concerning the results from the disk diffusion test, which was used to evaluate bacterial susceptibility, very similar diameters of the inhibition zone were obtained for free LVX and all the MS. In fact, all the values were in excess of 17 mm (Table 4.7 and Figure 4.7), meaning that the bacterial isolates CF2_2004 and CF7_2005 may be classified as "sensitive" to LVX [41]. No inhibition zone was observed for chitosan.

Table 4.7 – MIC and disk diffusion test results from LVX, chitosan and loaded MS crosslinked with GL, GNP, GA and GLY.

Formulation or Compound	**MIC (mg/L)**		**Inhibition zone diameter (mm)***	
	CF2_2004	CF7_2005	CF2_2004	CF7_2005
Chitosan	-	-	0	0
LVX	0.625	0.625	26	22
MS_LVX_GL (= F13)	0.625	0.625	20	24
MS_LVX_GNP	0.625	0.312	20	23
MS_LVX_GA	0.625	0.625	20	24
MS_LVX_GLY	0.625	0.625	18	25

*values obtained from theoretical value of 0.5 µg/µl LVX.

A- CF2_2004

B- CF7_2005

Figure 4.7 – Inhibition zones for LVX, chitosan and loaded MS crosslinked with GL, GNP, GA and GLY, for the bacterial isolates CF2_2004 (A) and CF7_2005 (B).

4.3.11 – Cytotoxicity study

The cytotoxicity results are presented on Figure 4.8 and Table 4.8. In Figure 4.8, for the legibility of the curves, data were plotted as mean ± SEM of the six different experiments and the curve for each formulation was fitted with Equation 4.2. On the other hand, in Table 4.8, each experiment was analyzed independently with Equation 4.2 in order to obtain an IC50 value for each set of data. Finally, data were plotted as mean ± SEM of six IC50 values for each formulation and analyzed with statistical test.

The results showed that unloaded uncrosslinked MS were the less toxic formulation to the Calu-3 cells, at all the tested concentrations with cell viability values close to 80% at the highest concentration tested (1mg/mL), Figure 4.8 A, being in agreement with previously published work in chitosan systems [13,14]. In addition, and despite some variability, a

value of IC50 close to 3.0 mg/mL (Table 4.8) corroborates this finding and corresponds to the highest IC50 value obtained. Furthermore, this value is close to the already described range of 0.2 - 2 mg/mL for chitosan IC50. Note that the respective cytotoxicity varies with molecular weight and degree of deacetylation. However, it also depends on chitosan modifications and on the assessed cells, as well as on incubation time [67,68,14].

LVX was well tolerated up to 0.25 mg/mL, but at the highest concentration (1mg/mL) reached a value close to 50 % of cell viability (Figure 4.8 A), being in accordance with the obtained IC50 of 1.10 ± 0.30 mg/mL.

The unloaded MS crosslinked with GL decreased the cell viability to values close to 30% at the highest concentration (Figure 4.8 B) and presented an IC50 equal to 0.48 ± 0.08 mg/mL (Table 4.8), which was the lowest among the unloaded MS, and significantly different from the uncrosslinked MS ($p< 0.01$), suggesting that the formulation with the GL crosslinker is the most toxic to pulmonary cells. Actually, in spite of the wide use of GL as crosslinker, some toxicity has been reported [23], in accordance with our results. The other unloaded crosslinked MS tend to be safer, with cytotoxicity in the order GLY > GA > GNP (Figure 4.8 C-E), with higher IC50 values (Table 4.8). It should be noted that for GNP, no significant difference was obtained for IC50, when it was compared with uncrosslinked MS, confirming its safety when incorporated in the chitosan matrix. In addition, GNP crosslinked MS were about five times less toxic than GL crosslinked MS, by comparison of IC50 values. Significant difference was also observed in cell viability at the highest concentration tested (1 mg/mL), with 63% and 30% of cell viability, for GNP and GL crosslinked MS, respectively. GNP is a natural compound isolated from the fruit *Gardenia jasminoides Ellis* plant and some *in vitro* studies on pulmonary cell lines have already demonstrated the much lower toxicity of GNP, when compared to GL, as already described [17]. For both unloaded GA and GLY crosslinked MS, a cell viability close to 45% was obtained at 1mg/mL. As previously indicated, GLY is a metabolic product of fructose but there is lack of data for this crosslinking agent. For GA, it can be found in plant and animal tissues and some studies suggested this crosslinker as a suitable alternate to the more toxic GL [23].

For the LVX-loaded MS, that crosslinked with GL presented the most adverse effects by reducing the cell viability to 20 % (Figure 4.8 B) at the highest concentration, which is consistent with the lowest IC50 value (0.22 ± 0.04 mg/mL), Table 4.8. Being loaded in

the range 1:1 (LVX:chitosan matrix), this means that 0.22 mg of LVX incorporated in 0.22 mg of GL-crosslinked chitosan, per mL, are enough to reduce to one half the number of living cells. When compared to LVX itself, the IC50 of this formulation was significantly lower ($p< 0.01$), denoting the higher GL toxicity, even if incorporated in the polymeric matrix (Table 4.8). A lower toxicity was found for LVX loaded MS crosslinked with GLY, GNP or GA (Figure 4.8 C-E), with IC50 values of 0.46 ± 0.16, 0.47 ± 0.08 and 0.83 ± 0.15 mg/mL, respectively (Table 4.8). However, for all LVX-loaded formulations, lower IC50 values are found than for LVX alone. LVX is rapidly released, as shown with the *in vitro* release results [69], thus not minimising the respective intrinsic toxicity to which the toxicity of crosslinked chitosan is added. The results for GNP crosslinked MS are somewhat surprising, since the toxicity of the LVX-loaded GNP formulation was expected to be at the level of that found for LVX, according to the very low toxicity of the unloaded formulation. However, it should be noted that some viability profiles may be influenced by the different conformation of chitosan chains when loaded with LVX and crosslinked, because some groups that interact with the MTS product may be not exposed, leading to underestimated values for cell viability [67]. In conclusion, a lower toxicity for Calu-3 cells is found by using LVX-loaded chitosan MS crosslinked with GNP, GA or GLY, when compared with LVX-loaded GL crosslinked MS. This is an interesting finding, that stresses the fact that cytotoxicity cannot be established without considering the whole system, and interactions therein.

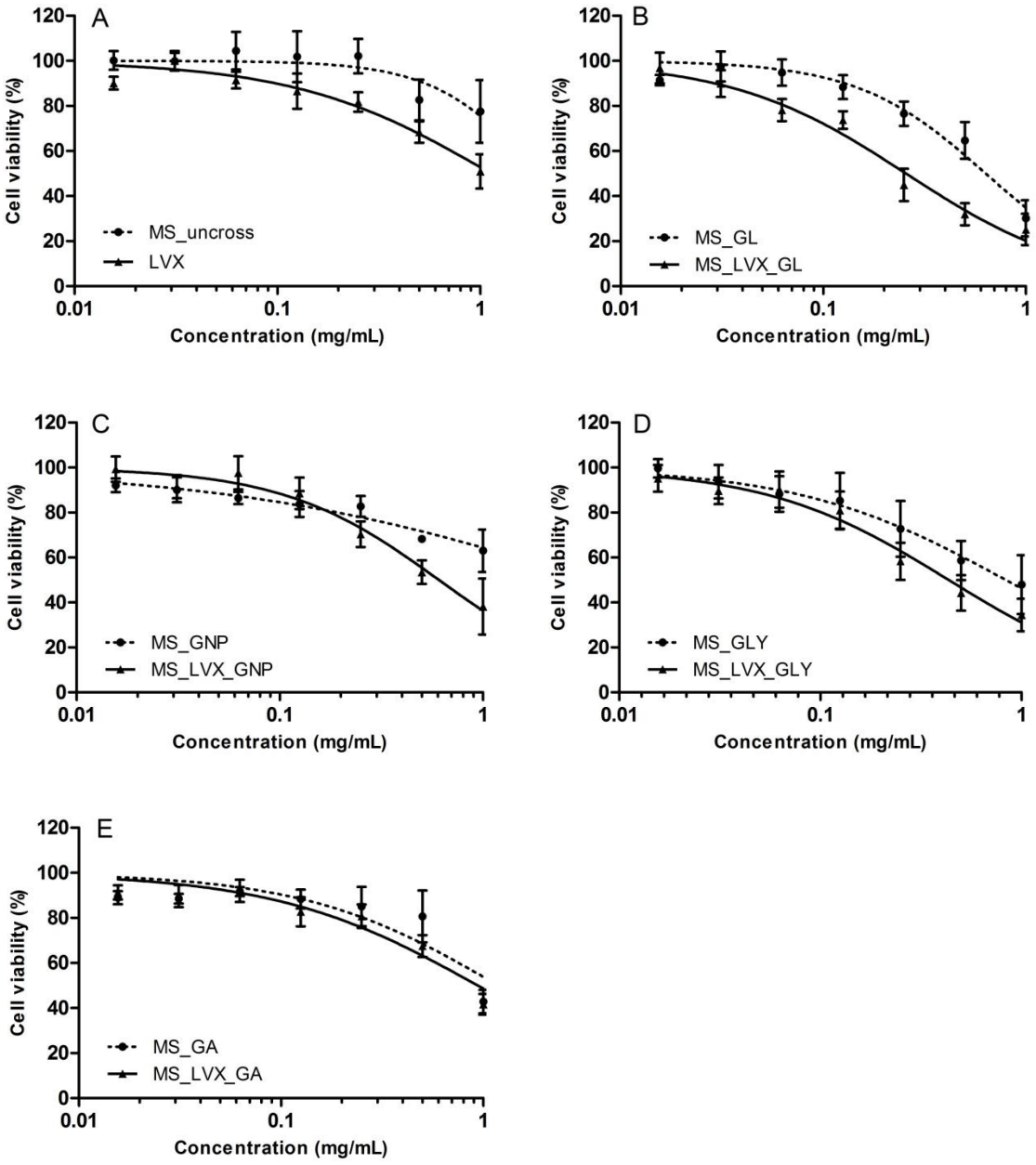

Figure 4.8 – Calu-3 cell viability measured with MTS assay and after 24h of incubation with increasing concentrations of LVX or unloaded uncrosslinked chitosan MS (MS_uncross) (A), unloaded and LVX-loaded chitosan MS crosslinked with GL (B), GNP (C), GLY (D) and GA (E). The concentrations correspond to mg of LVX and/or of chitosan matrix (ratio 1:1 in loaded MS). Viability results are shown on log scale, as mean ± SEM of six different experiments and the curves were fitted according to Equation 4.2.

Table 4.8 – IC50 values after 24 h of incubation for all formulations: unloaded MS crosslinked with GL (MS_GL), GNP (MS_GNP), GLY (MS_GLY) or GA (MS_GA) were compared with unloaded and uncrosslinked MS (MS_uncross) and LVX-loaded MS crosslinked with GL (MS_LVX_GL), GNP (MS_LVX_GNP), GLY (MS_LVX_GLY) and GA (MS_LVX_GA) were compared with LVX itself. Results expressed as mean ± SEM (n=6), * p <0.05 and ** p < 0.01.

Crosslinker	Unloaded MS		LVX-loaded MS	
	Formulation name	**IC50 (mg/mL)**	**Formulation name**	**IC50 (mg/mL)**
without	MS_uncross	3.00 ±0.80	-	-
GL	MS_GL	0.48 ± 0.08**	MS_LVX _GL	0.22 ± 0.04**
GNP	MS_GNP	2.60 ± 0.70	MS_LVX_GNP	0.47 ± 0.08*
GLY	MS_GLY	0.51 ± 0.17**	MS_LVX_GLY	0.46 ± 0.16*
GA	MS_GA	0.87 ± 0.05*	MS_LVX _GA	0.83 ± 0.15

4.4 – Conclusions

MS crosslinked with GL were prepared by spray drying and according to a factorial design for size optimization. After this step, MS with high LVX loading and using less toxic crosslinking agents (GNP, GA and GLY) were successfully prepared to control swelling properties. Entrapped LVX was shown to be in an amorphous or well dispersed state within the polymeric matrix. All the MS formulations produced similar immediate *in vitro* release profiles. Their antibacterial activities against bacterial isolates of *P. aeruginosa* were equivalent to free LVX. The highest degree of swelling was obtained with MS crosslinked with GNP and GA, which make these MS the best candidates to escape from phagocytosis. In addition, these MS possess satisfactory aerodynamic properties for lung delivery as dry powder and in terms of cytotoxicity. Therefore these polymeric systems may offer an easy-to-use alternative to LVX solution for inhalation.

4.5 – References

1. Ng MY, Flight W, Smith E (2014) Pulmonary complications of cystic fibrosis. Clinical Radiology 69 (3):e153-e162.

2. Høiby N (2011) Recent advances in the treatment of Pseudomonas aeruginosa infections in cystic fibrosis. BMC Medicine 9 (1):32-38.

3. EMA (2015) Quinsair - Summary of product characteristics. European Medicines Agency, Science Medicines Health. http://ec.europa.eu/health/documents/community-register/2015/20150326130815/anx_130815_en.pdf. Accessed 26 October 2015.

4. Foundation CF (2015) Drug Development Pipeline. Available via http://www.cff.org/research/DrugDevelopmentPipeline/ Accessed 27 October 2015.

5. Zeng XM, Martin GP, Marriott C (1995) The controlled delivery of drugs to the lung. International Journal of Pharmaceutics 124 (2):149-164.

6. Saigal A, Ng WK, Tan RBH, Chan SY (2013) Development of controlled release inhalable polymeric microspheres for treatment of pulmonary hypertension. International Journal of Pharmaceutics 450 (1–2):114-122.

7. Gaspar MC, Couet W, Olivier JC, Pais AACC, Sousa JJS (2013) Pseudomonas aeruginosa infection in cystic fibrosis lung disease and new perspectives of treatment: a review. European Journal of Clinical Microbiology & Infectious Diseases 32 (10):1231-1252.

8. Loira-Pastoriza C, Todoroff J, Vanbever R (2014) Delivery strategies for sustained drug release in the lungs. Advanced Drug Delivery Reviews 75 (0):81-91.

9. Du J, El-Sherbiny I, Smyth H (2014) Swellable Ciprofloxacin-Loaded Nano-in-Micro Hydrogel Particles for Local Lung Drug Delivery. AAPS PharmSciTech 15 (6):1535-1544.

10. El-Sherbiny IM, McGill S, Smyth HD (2010) Swellable microparticles as carriers for sustained pulmonary drug delivery. Journal of Pharmaceutical Sciences 99 (5):2343-2356.

11. Benhabiles MS, Salah R, Lounici H, Drouiche N, Goosen MFA, Mameri N (2012) Antibacterial activity of chitin, chitosan and its oligomers prepared from shrimp shell waste. Food Hydrocolloids 29 (1):48-56.

12. Raafat D, von Bargen K, Haas A, Sahl H-G (2008) Insights into the Mode of Action of Chitosan as an Antibacterial Compound. Applied and Environmental Microbiology 74 (12):3764-3773. doi:10.1128/aem.00453-08.

13. Anderson JM, Shive MS (2012) Biodegradation and biocompatibility of PLA and PLGA microspheres. Advanced Drug Delivery Reviews 64, Supplement:72-82.

14. Kean T, Thanou M (2010) Biodegradation, biodistribution and toxicity of chitosan. Advanced Drug Delivery Reviews 62 (1):3-11.

15. Ventura CA, Tommasini S, Crupi E, Giannone I, Cardile V, Musumeci T, Puglisi G (2008) Chitosan microspheres for intrapulmonary administration of moxifloxacin: Interaction with biomembrane models and in vitro permeation studies. European Journal of Pharmaceutics and Biopharmaceutics 68 (2):235-244.

16. Grenha A, Gomes ME, Rodrigues M, Santo VE, Mano JF, Neves NM, Reis RL (2010) Development of new chitosan/carrageenan nanoparticles for drug delivery applications. Journal of Biomedical Materials Research Part A 92A (4):1265-1272.

17. Feng H, Zhang L, Zhu C (2013) Genipin crosslinked ethyl cellulose–chitosan complex microspheres for anti-tuberculosis delivery. Colloids and Surfaces B: Biointerfaces 103 (0):530-537.

18. Bigi A, Cojazzi G, Panzavolta S, Rubini K, Roveri N (2001) Mechanical and thermal properties of gelatin films at different degrees of glutaraldehyde crosslinking. Biomaterials 22 (8):763-768.

19. Bigi A, Cojazzi G, Panzavolta S, Roveri N, Rubini K (2002) Stabilization of gelatin films by crosslinking with genipin. Biomaterials 23 (24):4827-4832.

20. Abdel Mouez M, Zaki NM, Mansour S, Geneidi AS (2014) Bioavailability enhancement of verapamil HCl via intranasal chitosan microspheres. European Journal of Pharmaceutical Sciences 51 (0):59-66.

21. Dhanaraju MD, Elizabeth S, Gunasekaran T (2011) Triamcinolone-loaded glutaraldehyde cross-linked chitosan microspheres: prolonged release approach for the treatment of rheumatoid arthritis. Drug Delivery 18 (3):198-207.

22. Ramachandran S, Nandhakumar S, Dhanaraju MD (2011) Formulation and Characterization of Glutaraldehyde Cross-Linked Chitosan Biodegradable Microspheres Loaded with Famotidine Tropical Journal of Pharmaceutical Research 10 (3):309-316.

23. Mitra T, Sailakshmi G, Gnanamani A (2014) Could glutaric acid (GA) replace glutaraldehyde in the preparation of biocompatible biopolymers with high mechanical and thermal properties? Journal of Chemical Sciences 126 (1):127-140.

24. Oliveira BF, Santana MHA, Ré MI (2005) Spray-dried chitosan microspheres cross-linked with d, l-glyceraldehyde as a potential drug delivery system: preparation and characterization. Brazilian Journal of Chemical Engineering 22:353-360.

25. Mi F-L, Shyu S-S, Peng C-K (2005) Characterization of ring-opening polymerization of genipin and pH-dependent cross-linking reactions between chitosan and genipin. Journal of Polymer Science Part A: Polymer Chemistry 43 (10):1985-2000.

26. Nishi C, Nakajima N, Ikada Y (1995) In vitro evaluation of cytotoxicity of diepoxy compounds used for biomaterial modification. Journal of Biomedical Materials Research 29 (7):829-834.

27. Sung HW, Huang RN, Huang LL, Tsai CC (1999) In vitro evaluation of cytotoxicity of a naturally occurring cross-linking reagent for biological tissue fixation. Journal of Biomaterials Science, Polymer Edition 10 (1):63-78.

28. Sailakshmi G, Tapas M, Suvro C, Gnanamani A (2013) Chemistry behind the Elastic Nature of the Biomaterial Prepared Using Oxidized Form of Glutaraldehyde and Chitosan - An Approach at 2D and 3D Level. International Journal of Life Science and Medical Research 4 (2):64-75.

29. Vandelli MA, Rivasi F, Guerra P, Forni F, Arletti R (2001) Gelatin microspheres crosslinked with d,l-glyceraldehyde as a potential drug delivery system: preparation,

characterisation, in vitro and in vivo studies. International Journal of Pharmaceutics 215 (1–2):175-184.

30. Conti B, Modena T, Genta I, Perugini P, Pavanetto F (1998) A proposed new method for the crosslinking of chitosan microspheres. Drug Delivery 5 (2):87-93.

31. Piyakulawat P, Praphairaksit N, Chantarasiri N, Muangsin N (2007) Preparation and evaluation of chitosan/carrageenan beads for controlled release of sodium diclofenac. AAPS PharmSciTech 8 (4).

32. Muzzarelli C, Stanic V, Gobbi L, Tosi G, Muzzarelli RAA (2004) Spray-drying of solutions containing chitosan together with polyuronans and characterisation of the microspheres. Carbohydrate Polymers 57 (1):73-82.

33. Elzoghby A, Samy W, Elgindy N (2013) Novel Spray-Dried Genipin-Crosslinked Casein Nanoparticles for Prolonged Release of Alfuzosin Hydrochloride. Pharmaceutical Research 30 (2):512-522.

34. Eaton JW (2009) GNU Octave Software. Version 3.2.3.

35. Doan TV, Couet W, Olivier JC (2011) Formulation and in vitro characterization of inhalable rifampicin-loaded PLGA microspheres for sustained lung delivery. International Journal of Pharmaceutics 414 (1-2):112-117.

36. Osman R, Kan PL, Awad G, Mortada N, El-Shamy A-E, Alpar O (2013) Spray dried inhalable ciprofloxacin powder with improved aerosolisation and antimicrobial activity. International Journal of Pharmaceutics 449 (1–2):44-58.

37. Jain V, Prasad D, Jain D, Mishra SK, Singh R (2011) Factorial design-based development of measlamine microspheres for colonic delivery. Biomatter 1 (2):182-188.

38. Tewes F, Paluch KJ, Tajber L, Gulati K, Kalantri D, Ehrhardt C, Healy AM (2013) Steroid/mucokinetic hybrid nanoporous microparticles for pulmonary drug delivery. European Journal of Pharmaceutics and Biopharmaceutics 85 (3, Part A):604-613.

39. Amaro MI, Tewes F, Gobbo O, Tajber L, Corrigan OI, Ehrhardt C, Healy AM (2015) Formulation, stability and pharmacokinetics of sugar-based salmon calcitonin-loaded

nanoporous/nanoparticulate microparticles (NPMPs) for inhalation. International Journal of Pharmaceutics 483 (1–2):6-18.

40. Matuschek E, Brown DF, Kahlmeter G (2014) Development of the EUCAST disk diffusion antimicrobial susceptibility testing method and its implementation in routine microbiology laboratories. Clinical Microbiology and Infection 20 (4):O255-O266.

41. CLSI (2014) Performance Standards for Antimicrobial Susceptibility Testing Twenty-Fourth Informational Supplement. CLSI document M100-S24.

42. Cheow WS, Chang MW, Hadinoto K (2010) Antibacterial efficacy of inhalable levofloxacin-loaded polymeric nanoparticles against E. coli biofilm cells: the effect of antibiotic release profile. Pharmaceutical Research 27 (8):1597-1609.

43. Adi H, Young PM, Chan H-K, Agus H, Traini D (2010) Co-spray-dried mannitol-ciprofloxacin dry powder inhaler formulation for cystic fibrosis and chronic obstructive pulmonary disease. European Journal of Pharmaceutical Sciences 40 (3):239-247.

44. Vehring R (2008) Pharmaceutical Particle Engineering via Spray Drying. Pharmaceutical Research 25 (5):999-1022.

45. Elversson J, Millqvist-Fureby A, Alderborn G, Elofsson U (2003) Droplet and particle size relationship and shell thickness of inhalable lactose particles during spray drying. Journal of Pharmaceutical Sciences 92 (4):900-910.

46. Belotti S, Rossi A, Colombo P, Bettini R, Rekkas D, Politis S, Colombo G, Balducci AG, Buttini F (2014) Spray dried amikacin powder for inhalation in cystic fibrosis patients: A quality by design approach for product construction. International Journal of Pharmaceutics 471 (1–2):507-515.

47. Patel KS, Patel MB (2014) Preparation and evaluation of chitosan microspheres containing nicorandil. International Journal of Pharmaceutical Investigation 4 (1):32-37.

48. Gorman EM, Samas B, Munson EJ (2012) Understanding the Dehydration of Levofloxacin Hemihydrate. Journal of Pharmaceutical Sciences 101 (9):3319-3330.

49. Kawadkar J, Chauhan MK (2012) Intra-articular delivery of genipin cross-linked chitosan microspheres of flurbiprofen: Preparation, characterization, in vitro and in vivo studies. European Journal of Pharmaceutics and Biopharmaceutics 81 (3):563-572.

50. Zhao X, Song K, Wang S, Zu Y, Li N, Yu X (2013) Micronization of the Pharmaceutically Active Agent Genipin by an Antisolvent Precipitation Process. Chemical Engineering & Technology 36 (1):33-42.

51. Dhanikula AB, Panchagnula R (2004) Development and characterization of biodegradable chitosan films for local delivery of paclitaxel. The AAPS Journal 6 (3):88-99.

52. Rojanarat W, Nakpheng T, Thawithong E, Yanyium N, Srichana T (2012) Levofloxacin-Proliposomes: Opportunities for Use in Lung Tuberculosis. Pharmaceutics 4 (3):385-412.

53. Shahwal Vk, Dubey BK, Bhoumick M (2012) Preformulation study of Levofloxacin. International Journal of Advances in Pharmaceutics 1 (1):8.

54. Bulut E (2014) In-Vitro Evaluation of Ibuprofen-Loaded Microspheres Prepared from Novel Chitosan/Poly(vinyl alcohol) Interpenetrating Polymer Network. Polymer-Plastics Technology and Engineering 53 (4):371-378.

55. Gonçalves VL, Laranjeira MCM, Fávere VT, Pedrosa RC (2005) Effect of crosslinking agents on chitosan microspheres in controlled release of diclofenac sodium. Polímeros 15:6-12.

56. O'Neil MJ (ed) (2006) The Merck Index - An Encyclopedia of Chemicals, Drugs, and Biologicals. Merck and Co., Inc, Whitehouse Station, NJ.

57. Geller DE, Flume PA, Staab D, Fischer R, Loutit JS, Conrad DJ (2011) Levofloxacin Inhalation Solution (MP-376) in Patients with Cystic Fibrosis with Pseudomonas aeruginosa. American Journal of Respiratory and Critical Care Medicine 183 (11):1510-1516.

58. Foundation CF (2012) Drug Development Pipeline. Available via http://www.cff.org/research/DrugDevelopmentPipeline/ Accessed 07 January 2015.

59. Fiel SB (2014) Aerosolized antibiotics in cystic fibrosis: an update. Expert Review of Respiratory Medicine 8 (3):305-314.

60. Shur J, Lee S, Adams W, Lionberger R, Tibbatts J, Price R (2012) Effect of Device Design on the In Vitro Performance and Comparability for Capsule-Based Dry Powder Inhalers. The AAPS Journal 14 (4):667-676.

61. Donovan MJ, Kim SH, Raman V, Smyth HD (2012) Dry powder inhaler device influence on carrier particle performance. Journal of Pharmaceutical Sciences 101 (3):1097-1107.

62. Learoyd TP, Burrows JL, French E, Seville PC (2008) Chitosan-based spray-dried respirable powders for sustained delivery of terbutaline sulfate. European Journal of Pharmaceutics and Biopharmaceutics 68 (2):224-234.

63. Smith IJ, Parry-Billings M (2003) The inhalers of the future? A review of dry powder devices on the market today. Pulmonary Pharmacology & Therapeutics 16 (2):79-95.

64. Corrigan DO, Healy AM, Corrigan OI (2006) Preparation and release of salbutamol from chitosan and chitosan co-spray dried compacts and multiparticulates. European Journal of Pharmaceutics and Biopharmaceutics 62 (3):295-305.

65. Koo H-J, Lim K-H, Jung H-J, Park E-H (2006) Anti-inflammatory evaluation of gardenia extract, geniposide and genipin. Journal of Ethnopharmacology 103 (3):496-500.

66. Kong M, Chen XG, Xing K, Park HJ (2010) Antimicrobial properties of chitosan and mode of action: A state of the art review. International Journal of Food Microbiology 144 (1):51-63.

67. Susana R, Marita D, Carmen Remuñán L, Ana G (2012) Biocompatibility of Chitosan Carriers with Application in Drug Delivery. Journal of Functional Biomaterials 3 (3).

68. Garcia-Fuentes M, Alonso MJ (2012) Chitosan-based drug nanocarriers: Where do we stand? Journal of Controlled Release 161 (2):496-504.

69. Gaspar MC, Sousa JJS, Pais AACC, Cardoso O, Murtinho D, Serra MES, Tewes F, Olivier J-C (2015) Optimization of levofloxacin-loaded crosslinked chitosan

microspheres for inhaled aerosol therapy. European Journal of Pharmaceutics and Biopharmaceutics 96:65-75.

Chapter 5

LEVOFLOXACIN-LOADED PLGA MICROSPHERES FOR SUSTAINED RELEASE IN LUNGS: DEVELOPMENT AND CHARACTERIZATION

5.1 – Introduction

The antibiotic therapy directly to the site of infection became in the last few years an interesting alternative to IV therapy, especially for infections in CF lung disease. Several nebulized formulations have recently emerged to deliver the drug directly to the lungs, allowing high local concentrations and a reduction of the systemic toxicity risk [1,2]. Among other formulations, the nebulized solution of LVX demonstrated to enhance lung function, as previously referred along this thesis [3,4]. However, solutions for inhalation require hygienic procedures for the devices, and longer administration times compared to the dry powder systems. In what pertains to the work described in this thesis, we have already developed LVX-loaded chitosan MS for inhalation as a dry powder for immediate drug release (Chapter 4).

The incorporation of LVX in biodegradable and biocompatible polymer-based MS, administered in a dry powder inhaler, is a promising approach, particularly for a controlled-release purpose. In this chapter, the work carried out aims at the development of LVX-loaded polymeric MS for lung delivery as a dry powder formulation with controlled release properties. The hydrophobic copolymer PLGA is of particular relevance for the preparation of drug sustained release systems, since it is biodegradable and biocompatible. Processes for the preparation of PLGA-based carriers for hydrophilic drugs include the double W/O/W emulsion-solvent evaporation method, the W/O phase separation, and the Hydrophobic Ion Pairing (HIP) technique. However, poor incorporation efficiency for water soluble drugs (such as LVX) has been reported due to the rapid migration, and consequent loss of drug into the aqueous phase [5]. There is no consensus for selecting the optimal technique, and advantages and disadvantages of the various options have been reviewed [6,7]. Despite being a well established method for incorporation of water-soluble drugs, the W/O/W solvent evaporation method generally results in low drug contents. Although considered as a more efficient method, W/O phase separation is a difficult technique and requires a large amount of organic solvent. In turn, the HIP technique is based on the use of toxic compounds [6]. The LVX incorporation in PLGA MS with high drug content and sustained release properties is therefore a clear challenge.

The aim of this work is, therefore, to prepare LVX-loaded PLGA MS using the double emulsion solvent evaporation technique for the controlled release of LVX in the lungs administered as dry powder. The premix membrane homogenization technique was included in the preparation method in order to obtain narrowly size-distributed MS [8]. After a preliminary procedure for the selection of the polymer grade, emulsions were modified in order to increase the drug content by saturating the aqueous phases with LVX in order to avoid drug escaping. The effect of adding a fatty acid (lauric acid) on drug content was also addressed [5].

5.2 – Materials

Resomer® RG 502 H (PLGA 50:50, MW: 7000-17000, acid terminated), Resomer® RG 503 (PLGA 50:50, MW: 24000-38000, ester terminated), Resomer® RG 502 (PLGA 50:50, MW: 7000-17000, alkyl ester terminated), lauric acid, dimethyl sulfoxide (DMSO), Dulbecco's modified Eagle's medium (DMEM) nutrient mixture F-12 and fetal bovine serum (FBS) were obtained from Sigma-Aldrich® (France). PLGA Purasorb® PDLG 5002 (50:50, MW: 17000, ester terminated) was purchased from PURAC Biomaterials (The Netherlands). Rhodoviol 4/125 (polyvinylalcohol (PVA)), degree of hydrolysis of 88% was purchased from Prolabo (France). Levofloxacin hemihydrate was kindly provided by Tecnimede S.A. (Portugal). Dichloromethane (DCM) HipPerSolv™ Chromanorm for HPLC was purchased from BDH® (VWR analytical, France). Formic acid 99–100% AnalaR (NormaPur) was obtained from VWR® (France) and acetonitrile of HPLC grade was purchased from Carlo Erba reagents (France). 3-(4,5-dimethylthiazol-2-yl)-5-(3-carboxymethoxyphenyl)-2-(4-sulfophenyl)-2 tetrazolium (MTS) CellTiter 96® AQueous One Solution Cell Proliferation Assay was purchased from Promega (France). Hanks' Balanced Salt Solution (HBSS) was obtained from GIBCO® Thermo Fisher Scientific™ (France). All other chemicals were of analytical grade or equivalent. Purified water was produced using a MilliQ Gradient® Plus Millipore system.

5.3 – Selection of polymer grade

A preliminary step for PLGA MS preparation consisted of testing different PLGA polymer grades (see Table 5.1) and concentrations to obtain a formulation with both

suitable size and LVX content. Briefly, LVX-loaded PLGA MS were prepared by a double emulsion - solvent evaporation method with a premix membrane homogenization step [9,8]. A volume of 0.6 mL of a LVX solution (250 mg/mL, adjusted to pH=6 with hydrochloric acid) was emulsified into 3 ml of a solution of PLGA (300 or 600 mg) in DCM using a Polytron® PT 3100D homogenizer equipped with a 7 mm homogenizing accessory (Kinematica AG, Switzerland) and set at 30000 rpm for 30 s. The obtained W_1/O emulsion was dispersed in 7 mL of a solution W_2 of PVA (3% w/v) in PBS at pH 7.4 under magnetic stirring (400 rpm). The resulting $W_1/O/W_2$ emulsion was subjected to three homogenization cycles through a SPG membrane (19.9 µm porosity) under 25 kPa transmembrane pressure using an external pressure-type micro kit emulsification device (SPG Technology, Sadowara, Japan). It was immediately poured into 25 ml of a solution of 0.4 % (w/v) PVA in PBS under magnetic stirring (400 rpm). Then DCM was evaporated under vacuum at room temperature during 10 minutes using a rotatory evaporator. MS were then washed through three cycles of centrifugation (3500 rpm, 5 min) and resuspended in purified water and finally freeze-dried. MS size was determined by laser light diffraction and LVX content by spectrophotometry (see section 5.6 for details). Table 5.1 presents the conditions of preparation and the characteristics of size, and drug loading (DL).

Table 5.1 – Characteristics of MS obtained in the preliminary method for polymer grade selection, based on particle size and drug content values.

PLGA type	LVX (mg)	PLGA (mg)	D_v (µm)*	DL (%)
PDLG 5002	150	600	7.0	0.21
RG 502H	150	300	4.6	3.30
RG 502	150	600	5.8	0.27
RG 503	150	300	4.3	0.30

*Mean particle size of the volume distribution (D_v) evaluated by laser light diffraction

The MS mean size was satisfactory for lung delivery, but the DL values were very low, ranging from 0.2 to 3.3 % (w/w). This can be ascribed to the high water solubility of LVX, making the incorporation in a hydrophobic polymer difficult, as already reported for other water soluble drugs [5]. Nevertheless, the PLGA RG 502H presented the highest

LVX content, 3.3% (w/w), similar to the LVX content in MS of the same polymer type, 3.6 % (w/w), previously reported for different conditions of preparation [10]. This type, having more free carboxylic end groups has promoted higher drug encapsulation than esterified PLGA, owing to the best combination of physicochemical interactions between the polymer and the drug [10,11]. Taking into account these results, PLGA RG 502H was the choice for the modified MS preparation, next detailed. Some changes were added to the initial method of double emulsion solvent evaporation with premix membrane homogenization, in order to further increase LVX content, as follows.

5.4 – Increasing the drug content

The preparation of three LVX-loaded PLGA MS with the RG 502H type was based on the method described above, with the following alterations and tests aiming at enhancing drug content:

a) 100 mg of LVX were additionally added in the O phase;

b) the W_2 was constituted of PVA (3% w/v) saturated with LVX (35 mg/mL) in PBS at pH 7.4, trying to avoid the LVX escape from the O phase;

c) the double $W_1/O/W_2$ emulsion was added to 0.4 % (w/v) PVA, which was also saturated with LVX (32 mg/mL) in PBS;

d) In one formulation, 200 mg of LVX were added to the O phase (instead of 100 mg);

e) Lauric acid (LA) was added to another formulation, together with 100 mg of LVX in the O phase, in a molar ratio of 1:1 (LVX:LA), following previous work with other drugs [5].

5.5 – Characterization

5.5.1 – Particle size

The mean size of the volume distribution (D_v) was evaluated by dispersing the MS in purified water using laser light diffraction (Microtrac® X100 particle size analyzer) [12].

5.5.2 – Drug loading

The amount of LVX in the MS was determined by spectrophotometry at 300 nm using a Varian Cary 50 UV-Visible spectrophotometer after MS dissolution in DMSO (LVX calibration curve 0.625 – 10 µg/mL). DL (%) values are expressed as the amount of LVX in the MS (w/w, similarly to what was presented in Chapter 4).

5.5.3 – *In vitro* release studies

The LVX *in vitro* release study was performed by dispersion of LVX-loaded MS (5 mg) in PBS (10 mL) at 600 rpm of magnetic stirring, pH=7.4 and 37 °C, ensuring the sink conditions. For the HPLC LVX determination, aliquots of 1 mL were collected at pre-determined points and subjected to centrifugation for 5 min at 3500 rpm (Hettich® Zentrifugen Universal 320R, Germany). 100 µL of the obtained supernatant were kept to allow the determination of the released LVX (see Appendix 2 for validation details). The remaining 900 µL were mixed after and added back to the flasks [12].

In vitro release data were firstly inspected using different models, after which the conjunction of a first order model (from 0 to 0.5 h), for a burst release regime, followed by the Weibull model (from 0.5 h to 72 h), for slower release, was deemed the more adequate for a non-linear fit of the data (Equation 5.1 and 5.2). For some release profiles, a first order model may be enough to adequately describe the release (see results section). Such models were expressed as:

$$f_t = f1\left(1 - \exp\left(-kt\right)\right) \qquad 0\ \text{h} \le t \le 0.5\ \text{h} \qquad (5.1)$$

$$f_t = f_{0.5h} + f2\left(1 - \exp\left(-\left(\frac{t\text{-}0.5\text{h}}{a}\right)^{b}\right)\right) \qquad 0.5\ \text{h} \le t \le 72\text{h} \qquad (5.2)$$

where f_t is the fraction (in percentage) released at time t, $f_{0.5h}$ is the fraction released at 0.5 h, *f1* and *f2* are the asymptotic released fractions predicted by the first order and Weibull functions, respectively. These account for release rates differing from the standard 100% value [13]. In the case of the latter, only the portion released after 0.5 h is estimated with

this parameter. Parameter *k* corresponds to an apparent first-order kinetic constant, *a* defines the time scale of the process and *b* is a shape parameter. Note that the fraction at the 0.5 h time point is used for both functions, thus promoting the interconnection between the two regimes. The correlation between the experimental data and the model was evaluated using the correlation coefficient R^2 [14].

5.5.4 – Scanning electron microscopy

Morphology and surface appearance of MS were analyzed by SEM after gold-sputtering the MS in argon atmosphere. It was performed using a Jeol JSM 6010 LV electron microscope (Tokyo, Japan) at 15 kV. The appearance of MS after 1 week of incubation in the *in vitro* release conditions was also observed to obtain information about the degree of MS degradation.

5.6 – Additional evaluation of final formulation

The optimized formulation was further analyzed by several techniques as described in what follows.

5.6.1 – X-ray Diffraction

For XRD analysis, samples were placed in a low background silicon holder in Bragg-Brentano configuration, with a copper tube powered at 45 kV and 40 mA. The scanning was made in the range $5° < 2\theta < 45°$ at a step of 0.066° and time/step of 10 seconds in an Empyrean PANalytical (The Netherlands) diffractometer with the detector Xcelerator in scanning mode and opened at 2°.The Kβ component was eliminated by using a nickel filter in a secondary optic.

5.6.2 – Differential Thermal Analysis/ Thermal Gravimetric Analysis

A SDT Q600 Instrument (TA, USA) was used to perform DTA/TGA analysis of the selected MS. It was operated from 30º C to 300º C with a 10°C/min heating rate and under a 100 mL/min air flow rate. Aluminum empty pans were used as reference, and calibration resorted to sapphire.

5.6.3 – Attenuated total reflectance Fourier transform infrared spectroscopy

A FT-IR 6700 spectrometer (Thermo Scientific Nicolet™, USA) equipped with an ATR accessory was use to perform the IR analysis. Samples were placed in the ATR device and measurements made by using 16 scans between 4000 and 650 cm^{-1} for each spectrum (4 cm^{-1} of resolution).

5.6.4 – Aerodynamic properties

For the selected LVX-loaded PLGA MS, the ED (%), MMAD and FPF (%) were also evaluated, using a NGI (Copley Ltd., Nottingham, UK) and according to the method described in Chapter 4. Briefly, a size-three transparent gelatin capsule was filled with 20 ± 1 mg of MS powder, inserted in a dry-powder inhaler Handihaler (Boehringer-Ingelheim, Germany) and pierced. The pump was turned on for 4 seconds (twice) at 60L/min of flow rate [12]. The powder remaining in the device, capsule, induction port and all the stages was collected with DMSO allowing the LVX extraction for quantification by spectrophotometry with the method described in the section 5.5.2.

5.6.5 – Cross-section analysis

In order to understand the internal structure of MS, they were incorporated in a resin (at 35 °C, for 24 h, avoiding the MS melting) and cross-sections were after obtained with the Microtome Leica EM UC6 (Leica Co, Austria), before observation. For SEM analyses, MS were incorporated in Spurr's resin (Spurr low-viscosity embedding kit, Sigma-Aldrich®, Germany), and cross-sections of 1.5 µm of thickness then observed (SEM, Jeol ISM 5600 LV microscope), after platinum-sputtering the samples in argon atmosphere. In the case of TEM, incorporation in epoxy resin (epoxy embedding resin kit, Fluka analytical, Sigma-Aldrich®, Germany) was carried and cross-sections of 80 nm obtained, being stained with aqueous lead citrate solution (0.2% (w/v), 10 min) before observation (TEM, FEI-Tecnai™ G2 Spirit BioTwin; AnalySIS 3.2 acquisition software).

5.6.6 – Specific surface area and density

In addition to cross-sections analysis, the specific surface area of the selected PLGA MS was evaluated and compared with that of a chitosan formulation (genipin-crosslinked

LVX-loaded chitosan MS, referred as MS_LVX_GNP). It was determined by the N_2 adsorption BET multipoint method, with 6 points in the relative pressure range of 0.1 – 0.3, using a Micrometrics ASAP 2020 v 2.04, [15]. Samples were prepared by purging under N2 overnight at room temperature.

Also, the density was measured by helium pycnometry using a Micrometrics AccuPyc 1330 v 2.01 [10].

5.6.7 – Cytotoxicity study

The *in vitro* cytotoxicity of PLGA MS on Calu-3 cell line was determined by the MTS assay using a similar procedure to that described in Chapter 4. Briefly, Calu-3 cells were cultured in DMEM/F-12 nutrient mixture supplemented with L-glutamine (2 mM) and FBS (10% (v/v)). The cells were seeded at a density of 1 x 10^4 cells/well in 96-well plates in 100 µL of the same medium used for the culture and at the same atmosphere conditions for 24h, before the incubation with formulations. LVX-loaded PLGA MS, respective unloaded MS or the LVX powder were mixed with the same medium for cell culture to obtain solutions/suspensions with the LVX concentration of 2 mg/mL and the PLGA concentration was close to 20 mg/mL [16]. In the 96-well plates, the medium was aspirated and replaced by 100 µL of the same pre-warmed medium. 100 µL of LVX solution/MS suspensions were added to obtain the highest tested concentration (1mg/mL of LVX). Successive dilutions were conducted to obtain a concentration range of LVX in the 0.0156 – 1mg/mL range [16]. Positive control wells of cell growth were also included. After 24h of incubation, the medium was replaced by 120 µL of pre-warmed MTS diluted in HBSS (20 % (v/v)). The absorbance was measured at 490 nm and 650 nm [17] and experiments were done at five different times. The cell viability (%) and IC 50 values were calculate as detailed in Chapter 4, section 4.2.14.

5.7 – Results and discussion: comparing formulations

After the preliminary procedure for MS preparation and selection of PLGA type (RG 502H), several MS were prepared. These have taken into account the alterations described in section 5.4, and aiming at increasing the drug content. These were subsequently analyzed and results obtained are described next.

5.7.1 – Particle size and drug loading

Data are presented in Table 5.2 for drug content imposed in each phase, for each formulation, and the results of size and MS drug loading. See also Figure 5.1 for particle size distribution.

MS_LVX_1 and MS_LVX_2 presented very similar and suitable D_v values (close to 5 µm), since the optimal size range for pulmonary administration is usually assumed to be within 1-5 µm. A larger D_v (17.5 ± 1.0 µm) was obtained for MS with the incorporation of LA (MS_LVX_LA).

The DL values were ca. 10% for both MS_LVX_1 and MS_LVX_2, meaning that the addition of 100 or 200 mg of LVX to the O phase did not have influence on the final LVX content. These values of DL were substantially higher than the values obtained by the preliminary procedure, meaning that changing the aqueous phases by using high concentrations of LVX, and adding LVX also in O phase, was effective. They were considered satisfactory taking into account that highly water soluble drugs, such as LVX, are generally poorly entrapped within the hydrophobic PLGA polymer matrix. For MS with the incorporation of LA, still higher values of DL were obtained. This effect of enhancing drug content by using LA in the molar ratio 1:1 (fatty acid:drug) was previously observed for water soluble drugs [5].

Table 5.2 – Characteristics of LVX-loaded PLGA MS, including particle size (D_v) and DL (%) values. Results are expressed as mean ± SD (n=3).

Formulation code	**LVX (mg)**		***D_v* (µm)**	**DL (%)**
	W_1 phase	**O phase**		
MS_LVX_1	150	100	5.0 ± 1.7	10.5 ± 1.4
MS_LVX_2	150	200	4.5 ± 0.1	9.3 ± 0.7
MS_LVX_LA*	150	100	17.5 ± 1.0	18.4 ± 0.2

*Lauric acid was added in a molar ratio to LVX of 1:1.

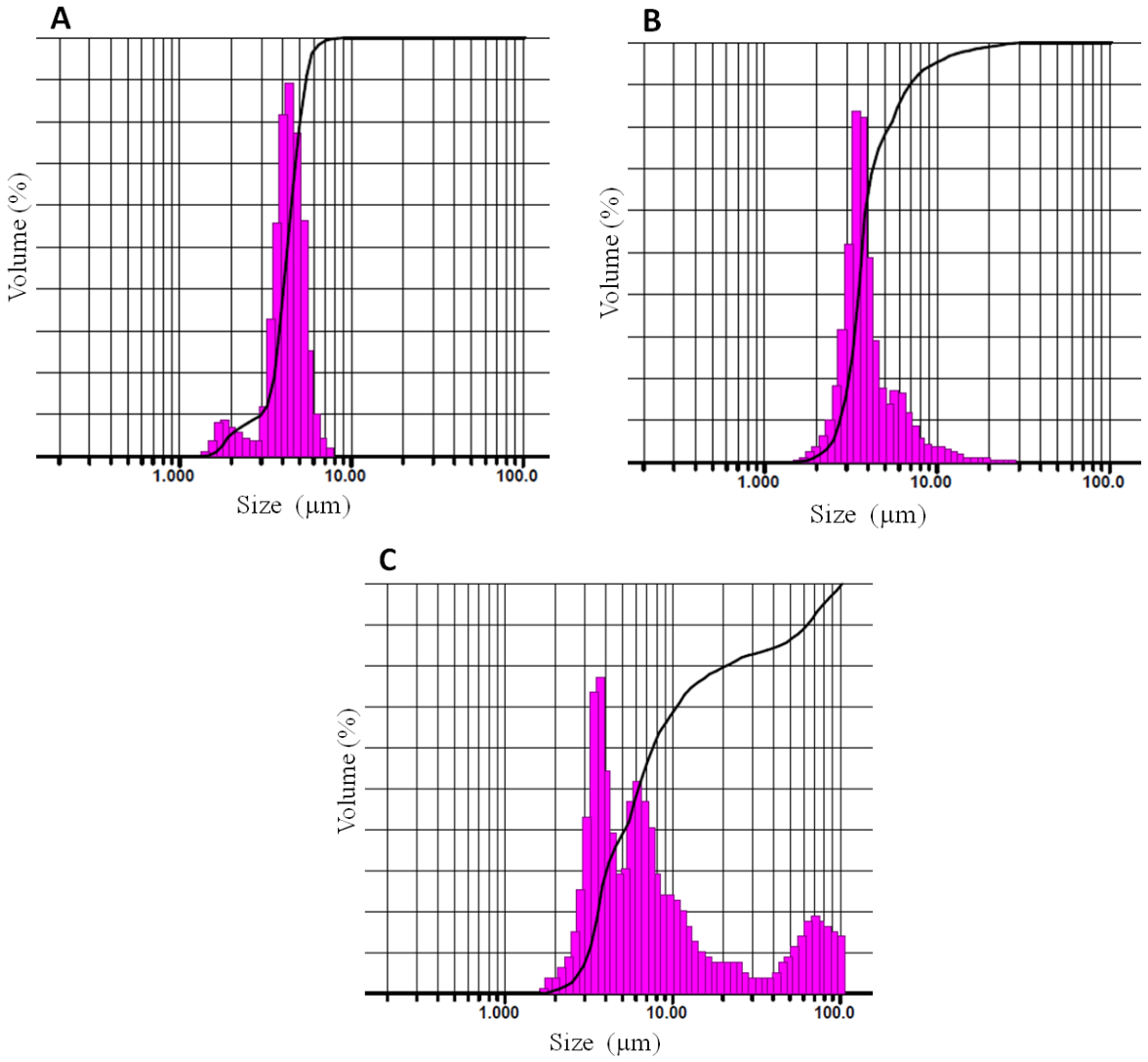

Figure 5.1 – Particle size expressed as volume distribution (D_v) for MS_LVX_1 (A); MS_LVX_2 (B) and MS_LVX_LA (C).

5.7.2 – Scanning electron microscopy

The SEM images corresponding to MS_LVX_1 and MS_LVX_2 formulations (Figure 5.2 A and 5.2 B) revealed spherical shape, with an apparent diameter in agreement with the determined D_v. The surface was smooth with no visible pores, though some small "specks" were visible, which can be ascribed to residual PVA. For the MX_LVX_LA (Figure 5.2 C), MS appear aggregated and despite the overall spherical shape, some of them are distorted with wrinkled surface and also containing "specks" with different dimensions (probably PVA and lauric acid not incorporated). This aggregation is apparently responsible for the larger D_v obtained.

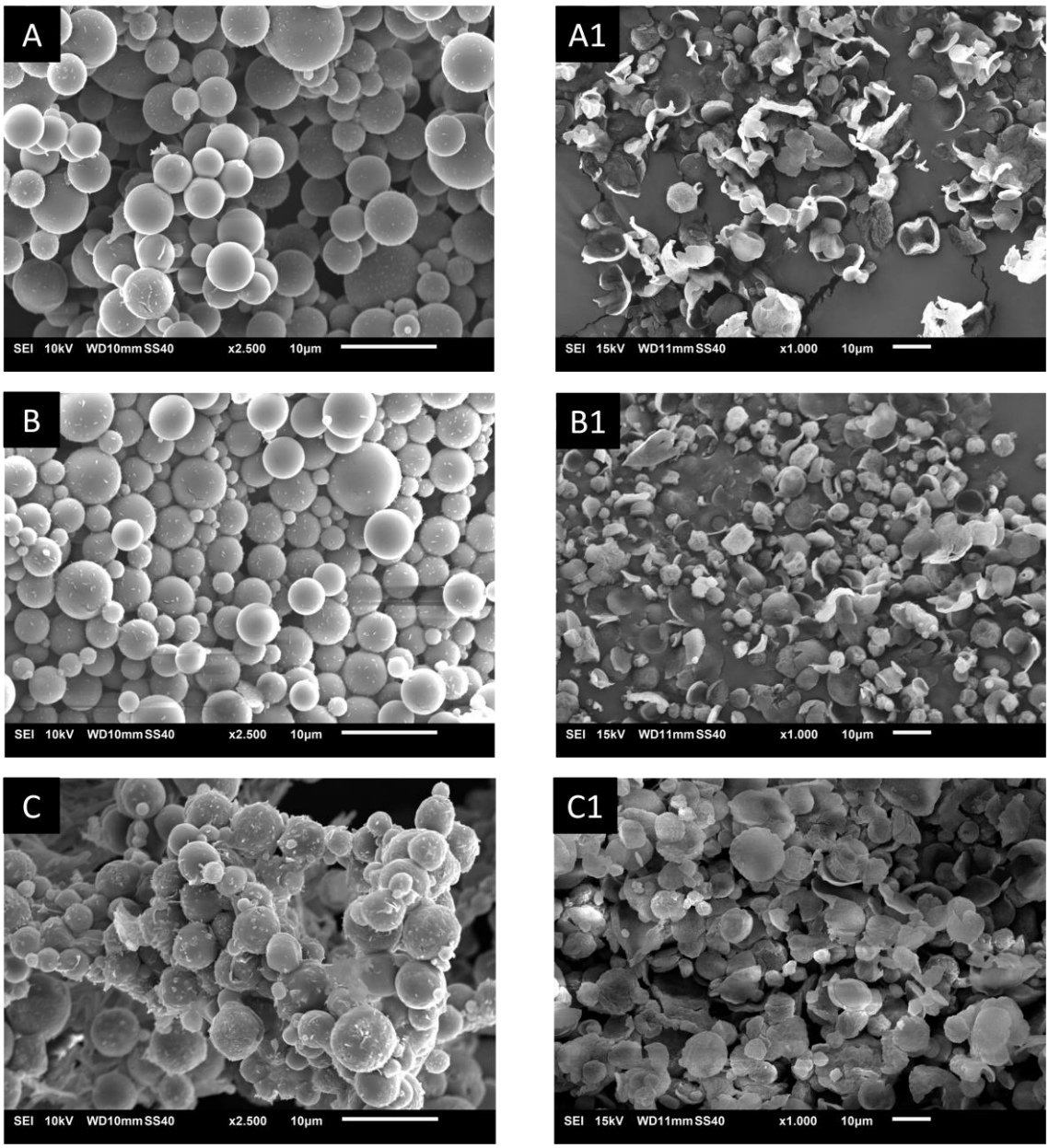

Figure 5.2 – SEM images of PLGA MS observed after preparation: MS_LVX_1 (A); MS_LVX_2 (B) and MS_LVX_LA (C) and after one week of incubation in PBS at 37°C and pH 7.4 under magnetic stirring of 600 rpm, respectively: (A1); (B1) and (C1).

5.7.3 – *In vitro* levofloxacin release

Results from *in vitro* release studies performed with the three PLGA formulations are included in Figure 5.3, as follows.

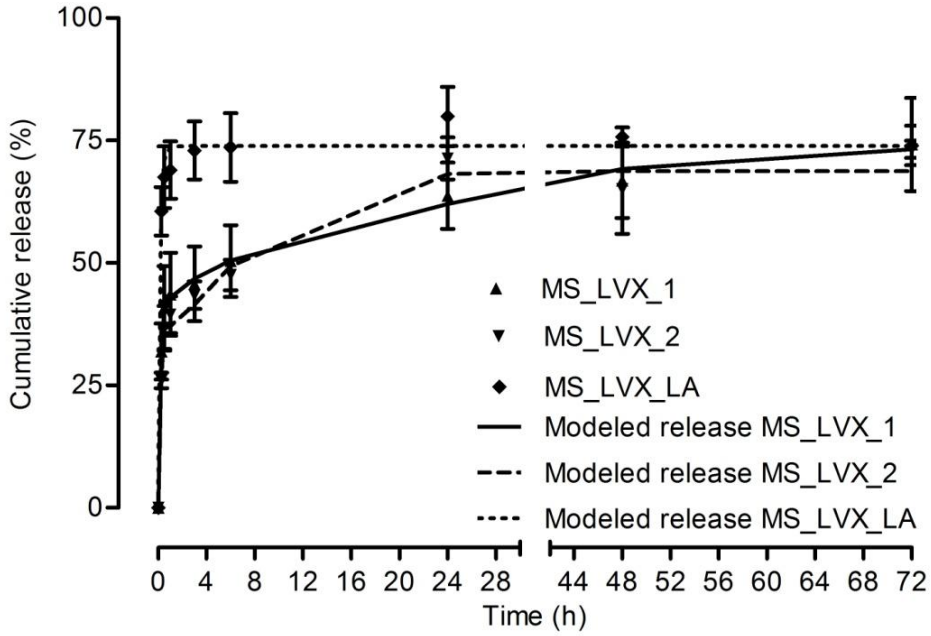

Figure 5.3 – LVX *in vitro* release profile from PLGA MS in PBS, at pH=7.4 and 37°C. Results are expressed as mean ± SEM (n=3). Modeled curves are also presented with the following parameters: MS_LVX_1 (*f1*=44.4, *k*=5.1, *f2*=40.7, *a*=37.1, *b*=0.69); MS_LVX_2 (*f1*=43.9, *k*=3.58, *f2*=32.0, *a*=8.87, *b*=1.44) and MS_LVX_LA (*f1*=73.9, *k*=6.4). See text.

Very similar profiles were obtained for MX_LVX_1 and MS_LVX_2 with a "burst" effect of 35 - 40 % in the first 30 minutes and a slow release up to a maximum of 75 % at 72 h and up to at least one week (not shown). For the LVX-loaded MS with the incorporation of LA, a more pronounced "burst effect" was observed with 70% of LVX released at 30 minutes.

The modeling approach describes well this behavior (with R^2= 0.99). The dissolution profiles rise steeply in the beginning, displaying a burst release that is subsequently replaced by a more controlled behavior as time point 0.5 h is approached. Between 0 and 0.5 h the profile is well represented by the steeper component of a first order release model, while the sequential part of the curve closely follows a Weibull function from 0.5 h to 72 h, corresponding to a parabolic curve (MS_LVX_1 and MS_LVX_2) [14]. There is one exception (MS_LVX_LA), where burst release clearly dominates, and the first order model is sufficient to describe the whole profile.

Usually, the drug release from polymeric systems occurs by diffusion of the drug through the polymer matrix but also due to particle erosion and other mechanisms [18]. Interestingly, in this case, 25 % of the initial LVX content remained in the MS matrix of all the formulations. This was observed despite the extensive MS degradation after one week of incubation observed in the SEM images (Figure 5.2 A1, B1 and C1). MS surface alterations and deformed structures were found for all the formulations (planar form for the MS with LA and shell form for the others). This extensive degradation with obvious signs of surface alteration is in agreement with already published data [19]. Therefore, this PLGA type (RG 502H) is expected to minimize pulmonary accumulation of polymer after MS lung deposition, especially in the case of repeated administrations.

Overall, although the incorporation of LA increased the LVX content, it did not bring definite advantages in terms of formulation once it distorted the microsphere shape, substantially increased the *Dv* and LVX sustained release is absent. Both MS_LVX_1 and MS_LVX_2 showed adequate drug content and particle size results, as well as adequate morphology, and sustained release profiles. Due to the lower amount of LVX needed for preparation of MS_LVX_1, discussion will focus on that formulation, in what follows.

5.8 – Results and discussion: the final formulation

Results of additional analyses performed in the final formulation (MS_LVX_1) are described below.

5.8.1 – X-ray diffraction

The XRD spectra of LVX, PVA, PLGA and selected LVX-loaded MS (MS_LVX_1) are shown in Figure 5.4. LVX presented sharp peaks at several diffraction angles (6.5°, 9.7°, 13.1°, 15.7°, 19.3°, 19.9° and 26.6°) denoting its crystalline form [20]. Diffuse scattering and a broad small peak was observed at 19.3° for PVA confirming its semi-crystalline nature [21]. For PLGA and LVX-loaded MS, no diffraction peaks were observed indicating LVX molecular dispersion in the polymer matrix or its amorphous nature, similarly to PLGA.

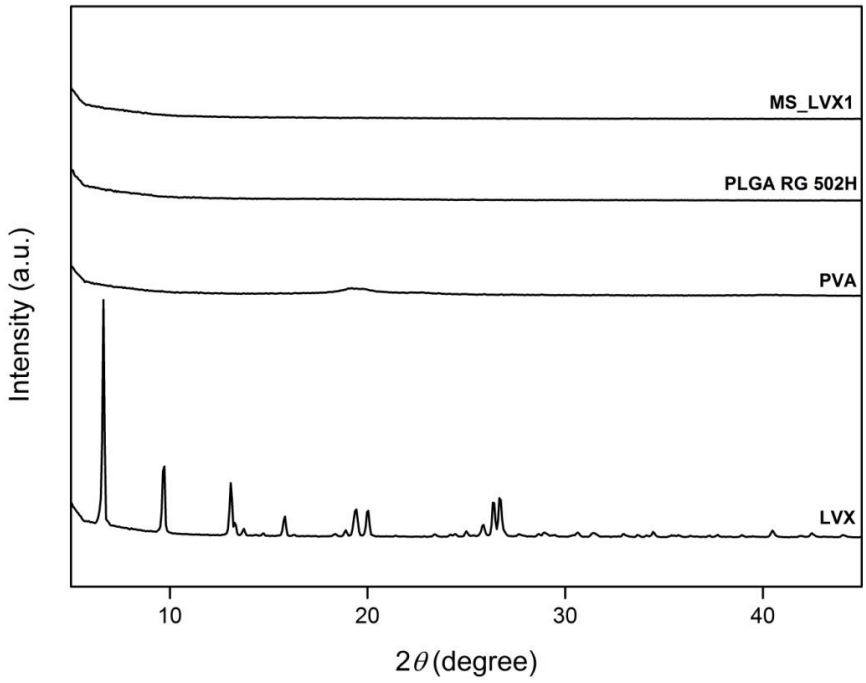

Figure 5.4 – XRD of LVX, PVA, PLGA RG 502H and MS_LVX_1.

5.8.2 – Differential Thermal Analysis/ Thermal Gravimetric Analysis

Samples of LVX, PLGA, PVA and MS_LVX_1 were also evaluated by thermal analysis, for which the results are presented in Figure 5.5 A-D.

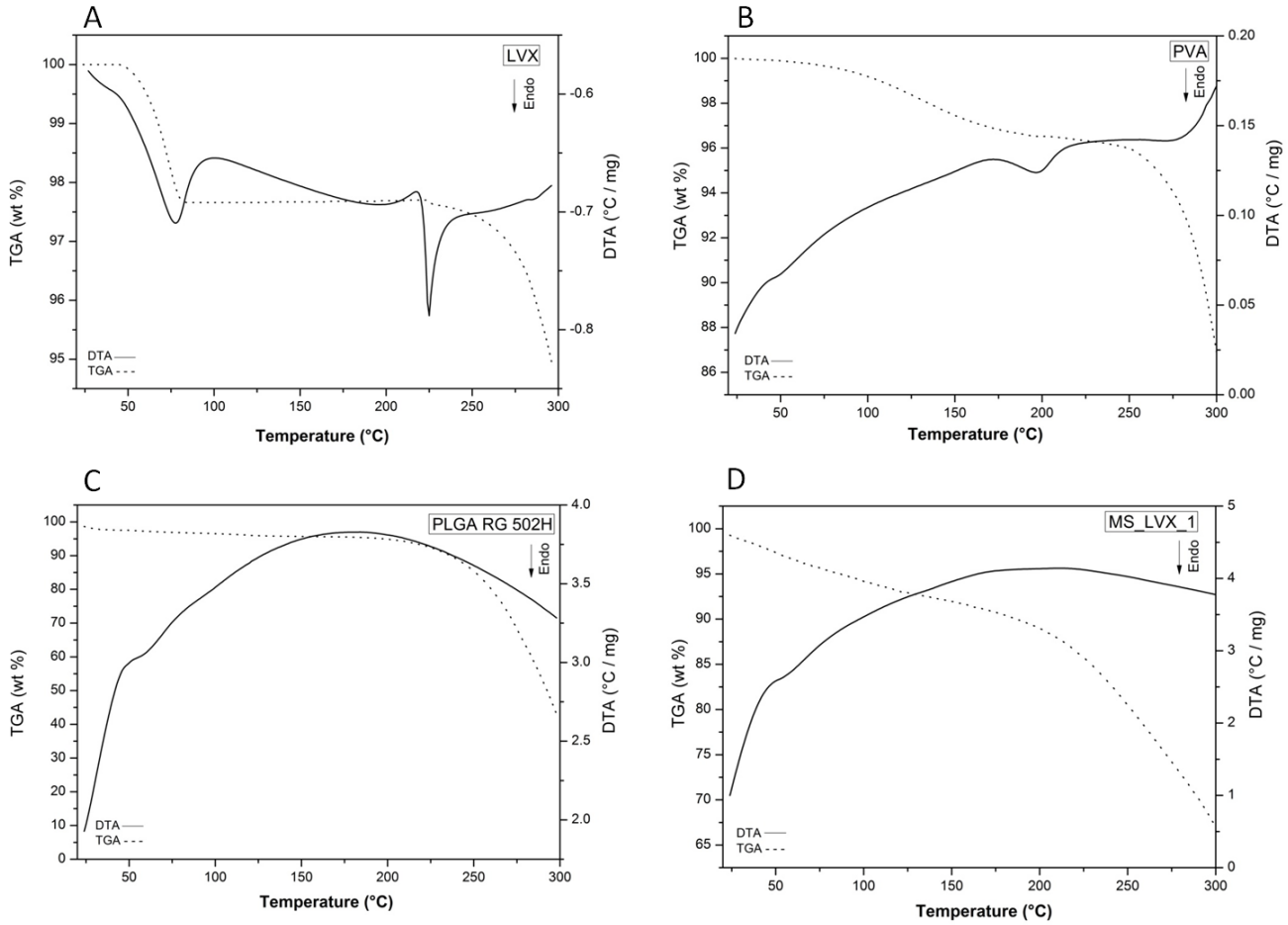

Figure 5.5 – DTA/TGA thermograms of LVX (A); PVA (B); PLGA RG 502H (C) and MS_LVX_1 (D).

For LVX, the two endothermic peaks observed at 78°C and 225°C were respectively attributed to water loss (corresponding to the LVX hemihydrate) and to LVX melting, confirming that it exists as a crystal (Figure 5.5 A) [12]. Such events were accompanied by slight weight loss events. For PVA, the melting point was observed close to 200°C, as reported (Figure 5.5 B) [22]. However, melting for both LVX and PVA disappeared when these components were incorporated in PLGA MS, indicating their amorphous nature and/or molecular dispersion in the polymer matrix, thus confirming the results from the XRD analysis (Figure 5.5 C). In fact, the thermograms from PLGA and MS_LVX_1 are very similar, and only a low peak close to 50°C was detected (Figure 5.5 C and 5.5 D). This is probably due to the glass transition temperature of PLGA [18]. In addition, the total weight loss for LVX-loaded MS was lower than for the PLGA itself, suggesting a more stable structure when LVX and PVA are incorporated.

5.8.3 – Attenuated total reflectance Fourier transform infrared spectroscopy

ATR-FTIR analyses were performed to evaluate the potential chemical alterations or interactions of LVX when incorporated in the MS. Figure 5.6 shows the characteristic bands of LVX, PVA, PLGA and MS_LVX_1. The LVX spectrum includes bands at 1724, 1618 and 1289 cm^{-1} corresponding respectively to the C=O acid, C=O carbonyl and C-O acid groups [12]. For PVA, the main observed bands are related to hydroxyl and acetate groups. A large band was obtained at 3300 cm^{-1} corresponding to O-H stretching. The band observed at 2940 cm^{-1} was attributed to the C-H stretching from alkyl groups and at 1731 cm^{-1} to the stretching from C=O and C-O from the acetate group [20]. The PLGA spectrum presented the main peaks at 1750 and 1090 cm^{-1} corresponding respectively to the C=O and C-O stretching vibrations [18]. For the LVX-loaded PLGA MS, the main peaks from LVX were observed, meaning that LVX suffers no alterations when it is incorporated in the polymer matrix.

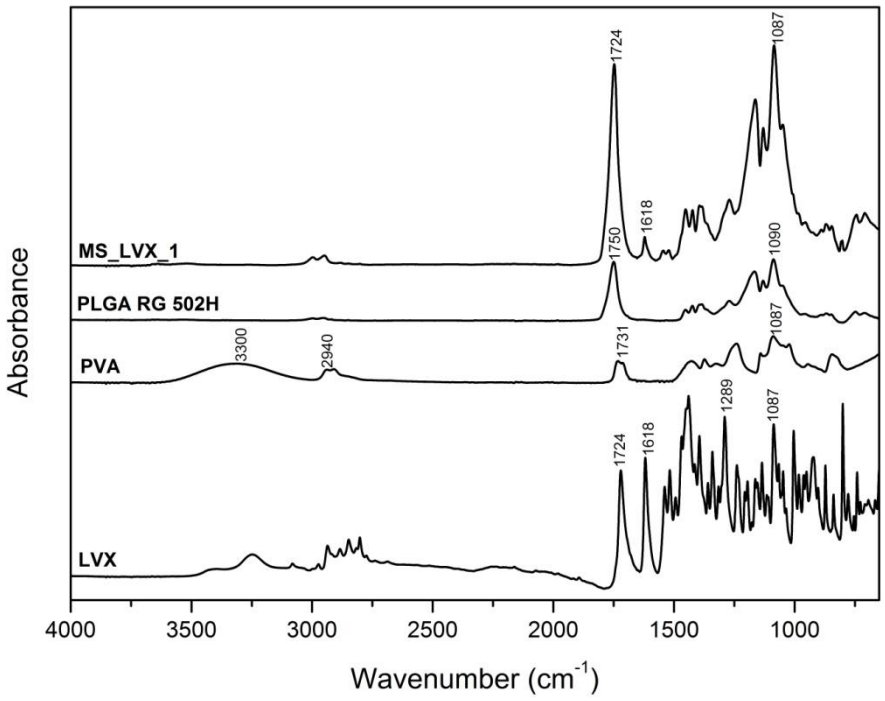

Figure 5.6 – FTIR spectra of LVX, PVA, PLGA RG 502H and MS_LVX_1.

5.8.4 – Aerodynamic properties

Using the Handihaler® DPI to aerosolize the powder, the ED value was determined to be 85.0 ± 3.6 %, the FPF was 30.2 ± 2.3 % and the MMAD 7.1 ± 0.2 µm (mean± SD). The MMAD was slightly higher than D_v, fact that can be explained by particle agglomeration during the aerosolization step, leading to overestimated values for the aerodynamic size of individual particles.

5.8.5 – Cross-section analysis

Cross-sections from the final formulation (MS_LVX_1) were also analyzed by SEM (Figure 5.7 A) and TEM (Figure 5.7 B) in order to inspect the internal morphology of the MS. Both images showed that the MS were filled with polymer, and also that some pores appear to be present (more evident in TEM image, Figure 5.7 B). These pores may be responsible for the initial "burst" effect observed in the *in vitro* release studies.

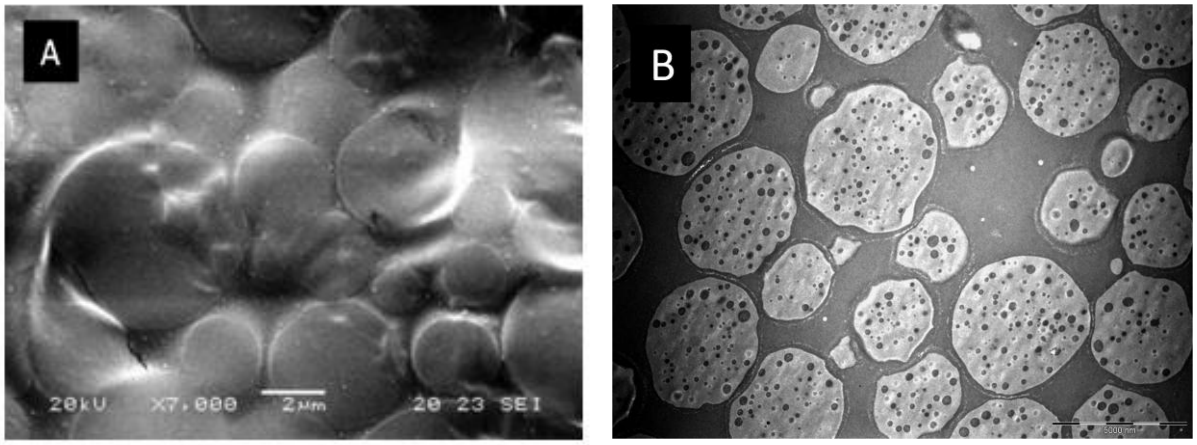

Figure 5.7 – Cross-sections of MS_LVX_1, observed by SEM (A) and TEM (B). Note that the scale bar is 2 µm for (A) and 5 µm for (B).

5.8.6 – Specific surface area and density

BET and density results from selected PLGA formulation (MS_LVX_1) and chitosan formulation (MS_LVX_GNP) are included in Table 5.3.

Table 5.3 – BET surface area and density results for MS_LVX_1 and MS_LVX_GNP formulations. Results are expressed as mean ± SD (n=6).

Formulation	BET surface area (m^2/g)	Density (g/cm^3)
MS_LVX_1	19.67 ± 0.315	1.30 ± 0.18
MS_GNP_LVX	6.85 ± 0.202	1.32 ± 0.03

Although similar density results were obtained for both formulations, a larger value of porosity was observed for the PLGA MS, in accordance with the cross-section observations.

5.8.7 – Cytotoxicity study

Biocompatibility of the final formulation was also evaluated by the MTS assay and using Calu-3 cells as the respiratory cell line tested. Results are expressed as the cell viability percentage, as a function of LVX concentration (Figure 5.8). LVX (powder) demonstrated to be relatively well tolerated once it decreased the cell viability to 50% at the highest concentration tested which was attributed to the intrinsic toxicity [23], (Figure 5.8), as already indicated in Chapter 4. Unloaded PLGA MS (MS_blank), prepared in a similar way but without using LVX, were not cytotoxic to the Calu-3 cells at all the concentrations tested, with values of cell viability close to 100 % and IC50 = 3.0 ± 0.7 mg/mL (Figure 5.8 and 5.9). Slightly lower values of cell viability were obtained for LVX-loaded PLGA MS (MS_LVX_1), with IC50 of 2.3 ±0.8 mg/mL (Figure 5.9), being in accordance with the biocompatibility of PLGA, already found for other PLGA formulations [24]. This characteristic of the LVX-loaded MS is in agreement with the sustained LVX release obtained. Otherwise, lower cell viability values would be obtained, due to free LVX.

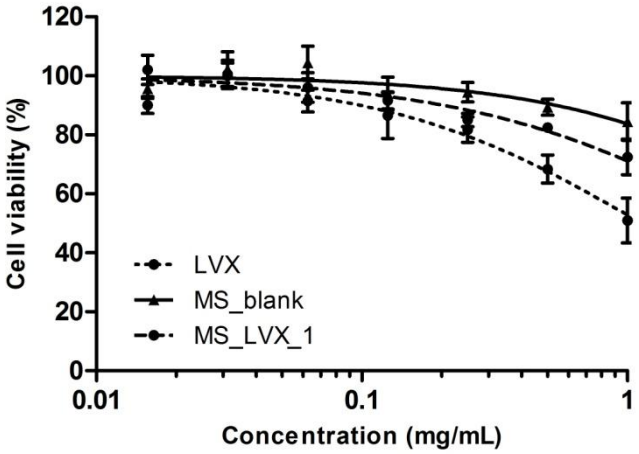

Figure 5.8 – Calu-3 cell viability measured with MTS assay and after 24 h of incubation with increasing concentrations of LVX, unloaded PLGA MS (MS_blank) and MS_LVX_1. Results are on log scale and expressed as mean ± SEM (n=5).

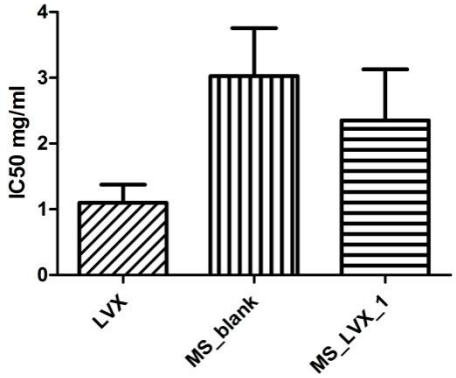

Figure 5.9 – IC50 values after 24 h of incubation for LVX, MS_blank and MS_LVX_1. Formulations were compared with LVX itself. Results expressed as mean ± SEM (n=5).

5.9 – Conclusions

The incorporation of a drug with high water solubility, such as LVX, in a hydrophobic polymer is of high relevance, but also a challenge in MS preparation. A preliminary method allowed choosing the PLGA RG 502H as the more adequate in terms of drug loading and particle size results. In order to further increase LVX content, some modifications were assessed. A DL close to 10%, suitable mean particle size together with spherical morphology and controlled release properties allowed choosing the MS_LVX_1, as an interesting formulation for further analyses. Several techniques demonstrated the good incorporation of LVX in the polymer matrix, without visible changes in the structural drug integrity. The selected formulation also demonstrated to have an acceptable aerodynamic diameter and high biocompatibility with respiratory cells, which are clearly advantageous when compared to LVX itself, by reducing toxicity risk and increasing local concentrations. Being administered in a dry powder inhaler, it may avoid the disadvantages of nebulized solutions, and consists of a promising formulation to achieve high lung concentrations for a prolonged time.

5.10 – References

1. Tiddens HAWM, Bos AC, Mouton JW, Devadason S, Janssens HM (2014) Inhaled antibiotics: dry or wet? European Respiratory Journal 44 (5):1308-1318.

2. Gaspar MC, Couet W, Olivier JC, Pais AACC, Sousa JJS (2013) Pseudomonas aeruginosa infection in cystic fibrosis lung disease and new perspectives of treatment: a review. European Journal of Clinical Microbiology & Infectious Diseases 32 (10):1231-1252.

3. EMA (2015) Quinsair - Summary of product characteristics. European Medicines Agency, Science Medicines Health. http://ec.europa.eu/health/documents/community-register/2015/20150326130815/anx_130815_en.pdf. Accessed 26 October 2015.

4. Foundation CF (2015) Drug Development Pipeline. Available via http://www.cff.org/research/DrugDevelopmentPipeline/ Accessed 27 October 2015.

5. Govender T, Stolnik S, Garnett MC, Illum L, Davis SS (1999) PLGA nanoparticles prepared by nanoprecipitation: drug loading and release studies of a water soluble drug. Journal of Controlled Release 57 (2):171-185.

6. Sah E, Sah H (2015) Recent Trends in Preparation of Poly(lactide-co-glycolide) Nanoparticles by Mixing Polymeric Organic Solution with Antisolvent. Journal of Nanomaterials 2015:22.

7. Yang Y, Bajaj N, Xu P, Ohn K, Tsifansky MD, Yeo Y (2009) Development of highly porous large PLGA microparticles for pulmonary drug delivery. Biomaterials 30 (10):1947-1953.

8. Doan TVP, Olivier JC (2009) Preparation of rifampicin-loaded PLGA microspheres for lung delivery as aerosol by premix membrane homogenization. International Journal of Pharmaceutics 382 (1–2):61-66.

9. Doan TV, Couet W, Olivier JC (2011) Formulation and in vitro characterization of inhalable rifampicin-loaded PLGA microspheres for sustained lung delivery. International Journal of Pharmaceutics 414 (1-2):112-117.

10. Kumar G, Sharma S, Shafiq N, Khuller GK, Malhotra S (2012) Optimization, in vitro–in vivo evaluation, and short-term tolerability of novel levofloxacin-loaded PLGA nanoparticle formulation. Journal of Pharmaceutical Sciences 101 (6):2165-2176.

11. Lecaroz C, Gamazo C, Renedo MJ, Blanco-Prieto MJ (2006) Biodegradable micro- and nanoparticles as long-term delivery vehicles for gentamicin. Journal of Microencapsulation 23 (7):782-792.

12. Gaspar MC, Sousa JJS, Pais AACC, Cardoso O, Murtinho D, Serra MES, Tewes F, Olivier J-C (2015) Optimization of levofloxacin-loaded crosslinked chitosan microspheres for inhaled aerosol therapy. European Journal of Pharmaceutics and Biopharmaceutics 96:65-75.

13. Costa FO, Sousa JJS, Pais AACC, Formosinho SJ (2003) Comparison of dissolution profiles of Ibuprofen pellets. Journal of Controlled Release 89 (2):199-212.

14. Costa P, Sousa Lobo JM (2001) Modeling and comparison of dissolution profiles. European Journal of Pharmaceutical Sciences 13 (2):123-133.

15. Tewes F, Paluch KJ, Tajber L, Gulati K, Kalantri D, Ehrhardt C, Healy AM (2013) Steroid/mucokinetic hybrid nanoporous microparticles for pulmonary drug delivery. European Journal of Pharmaceutics and Biopharmaceutics 85 (3, Part A):604-613.

16. Osman R, Kan PL, Awad G, Mortada N, El-Shamy A-E, Alpar O (2013) Spray dried inhalable ciprofloxacin powder with improved aerosolisation and antimicrobial activity. International Journal of Pharmaceutics 449 (1–2):44-58.

17. Adi H, Young PM, Chan H-K, Agus H, Traini D (2010) Co-spray-dried mannitol-ciprofloxacin dry powder inhaler formulation for cystic fibrosis and chronic obstructive pulmonary disease. European Journal of Pharmaceutical Sciences 40 (3):239-247.

18. Nath SD, Son S, Sadiasa A, Min YK, Lee BT (2013) Preparation and characterization of PLGA microspheres by the electrospraying method for delivering simvastatin for bone regeneration. International Journal of Pharmaceutics 443 (1–2):87-94.

19. Díez S, Tros de Ilarduya C (2006) Versatility of biodegradable poly(d,l-lactic-co-glycolic acid) microspheres for plasmid DNA delivery. European Journal of Pharmaceutics and Biopharmaceutics 63 (2):188-197.

20. Hema M, Selvasekarapandian S, Arunkumar D, Sakunthala A, Nithya H (2009) FTIR, XRD and ac impedance spectroscopic study on PVA based polymer electrolyte doped with NH4X (X = Cl, Br, I). Journal of Non-Crystalline Solids 355 (2):84-90.

21. Guirguis OW, Moselhey MTH (2012) Thermal and structural studies of poly (vinyl alcohol) and hydroxypropyl cellulose blends. Natural Science Vol.04No.01:11.

22. Sudhamani SR, Prasad MS, Udaya Sankar K (2003) DSC and FTIR studies on Gellan and Polyvinyl alcohol (PVA) blend films. Food Hydrocolloids 17 (3):245-250.

23. Bezwada P, Clark LA, Schneider S (2008) Intrinsic cytotoxic effects of fluoroquinolones on human corneal keratocytes and endothelial cells. Current Medical Research and Opinion 24 (2):419-424.

24. Anderson JM, Shive MS (2012) Biodegradation and biocompatibility of PLA and PLGA microspheres. Advanced Drug Delivery Reviews 64, Supplement:72-82.

Chapter 6

PULMONARY PHARMACOKINETICS OF LEVOFLOXACIN IN RATS AFTER AEROSOLIZATION OF IMMEDIATE RELEASE CHITOSAN OR SUSTAINED RELEASE PLGA MICROSPHERES

6.1 – Introduction

The pulmonary administration of antibiotics as aerosols has gained increasing interest in the last years since it allows high lung concentrations, improving the antibacterial efficacy. In addition, a lower systemic exposure is usually observed, decreasing the risk of toxicity [1]. For the CF lung disease, inhaled antibiotics represent alternatives to systemic oral and IV treatments in the prevention and management of *P. aeruginosa* infection and several products have been marketed or are in the drug development pipeline [2]. Among them, a LVX solution for inhalation (Quinsair® in Europe or Aeroquin™ in EUA) [3-6] promoted improvements in lung function and lower systemic exposure when compared to similar oral and IV doses and also reduced the bitter taste of LVX [7,8]. LVX formulations present potent activity against *P. aeruginosa*, and are not inactivated by the CF sputum [9]. As a liquid solution for inhalation, Quinsair® requires relatively long administration times (5 min) to deliver the therapeutic dose and hygienic procedures to clean the inhaler. In addition, being an immediate-release dosage form and due to LVX's high mucosal permeability [10], Quinsair® requires two administrations a day to maintain efficient concentrations in the lungs [8,11]. Alternatives to both long administration times and short efficiency of solutions for inhalation are drug powders for inhalation combined with sustained release properties. Actually, some studies demonstrated that with "low permeability" antibiotics, pulmonary concentrations obtained after nebulization into the lungs were much higher than after systemic administration, which was not the case with "high permeability" antibiotics. In the case of "high permeability" antibiotics optimizing formulations for inhalation may therefore solve this issue. LVX is a Class I drug, i.e. a drug with high solubility and high mucosal permeability according to the biopharmaceutics classification system (BCS) [10]. These properties make LVX a challenging drug to incorporate in sustained-release formulations. Among other biodegradable polymers, PLGA was recently proposed for the formulation of several sustained release MS for inhaled therapy, including the antibiotic class [12-15]. Being a well-known biocompatible and biodegradable polymer, PLGA is a good candidate for producing MS for pulmonary delivery by minimizing the impact on the lung function and accumulation [16].

In this context, the aim of the work described in this chapter is to conduct a PK study with LVX-loaded PLGA MS as dry powder for inhalation with LVX sustained release properties (referred as MS_LVX_1 in Chapter 5). The study was conducted in rats to assess systemic and pulmonary LVX exposures after intratracheal (IT) aerosolization.

For PK modeling and for comparison, the study included IV administration and IT aerosolization of a LVX solution, as well as IT aerosolization of immediate-release LVX-loaded and GNP-crosslinked chitosan MS dry powder formulation (MS_GNP_LVX in Chapter 4). The broncho-alveolar lavage (BAL) method was used to evaluate the LVX distribution in the lungs. However, other techniques exist and some PK considerations should be addressed here before methods section, as follows.

6.1.1 – Pulmonary pharmacokinetic considerations

Determination of the lung distribution of anti-infective drugs is a difficult task, since the measurement of concentration in the whole lung is not recommended and methods such as the lung microdialysis are not used as a routine [17,18]. The BAL method is probably the more adequate technique to evaluate the drug distribution in the lungs. It allows the measurement of drug concentrations in the ELF [17,19,20]. The measurement of concentrations in lung homogenates and their comparison with those derived from the corresponding blood samples should be used carefully because the tissues are made of distinct compartments, in which the drug may not be homogenously distributed. Therefore, the concentrations obtained may not represent the antibiotic concentration at the site of infection [17,21]. Thus, efforts have been made to measure the concentration of antibiotics at infection sites [22]. In diseases such as CF, antibiotic concentration in the ELF could represent antibacterial activity and is often determined by the BAL method. This fluid is measured on the interior surface of the alveolar wall, which is a component of the blood-alveolar barrier. The route of administration has also importance in such measurement because antibiotics administered by oral or IV routes need to cross the blood-alveolar barrier but inhaled antibiotics do not. The concentration ratio of ELF to plasma is different between antibiotics. The reasons are not clear, but it is known that some confounding factors may affect the measures, such as physicochemical characteristics intrinsic to the molecules and technical factors or errors in the method of

measurement. ELF is a mixture of components, including cells, which may be lysed during the measurement and artificially increase or decrease the measured antibiotic concentration. This error will vary with the antibiotic concentration in cells and with the number of cells in the ELF [22]. The volume of ELF sampled by BAL and the amount of antibiotic contained in the sample are corrected for drug-free saline added during the BAL procedure. This correction is frequently performed with urea because it is used as an endogenous marker that can easily cross the membranes (for details, see section 6.2.7). Thus, it is assumed that the concentration of urea in the ELF is the same in the serum. The "dwelling time" of fluid during the measurement can be a source of error because some additional urea appears to diffuse from some tissues when it is prolonged, and the ELF volume may therefore be overestimated [23,22]. Some authors developed simulations to estimate ELF concentrations of different antibiotics considering the impact of protein binding, different lipid solubilities and molecular weights, and lysis of cells. However, in lung diseases such as CF, these studies have to be performed taking into account the modifications in cells, tissues and fluids of these patients [22]. These are interesting approaches but PK parameters are usually expressed taking into account the plasma and ELF concentrations.

In this study, plasma and BAL sampling were performed at predetermined time points. As described before, two LVX-loaded formulations were compared by IT aerosolization: PLGA MS and chitosan MS. In order to better understand the plasma and ELF PK of LVX, a modeling approach was applied to fit the measured concentrations.

6.2 – Materials and methods

6.2.1 – Materials

Levofloxacin hemihydrate was kindly provided by Tecnimede S.A. (Portugal). Sodium chloride (0.9% NaCl injectable) was obtained from C.D.M. Lavoisir (Laboratoires Cbaix et Du Marais, France). Isoflurane (Forène®) was purchased from AbbVie (France). Dichloromethane (DCM) BDH® HipPerSolv™ Chromanorm for HPLC and formic acid 99–100% AnalaR (NormaPur) were purchased from VWR® (France). Acetonitrile of HPLC grade was obtained from Carlo Erba reagents (France). All other chemicals were

of analytical grade or equivalent. Purified water was produced using a MilliQ Gradient® Plus Millipore system.

6.2.2 – Animals

The animal experiments were conducted in compliance with EC Directice 2010/63/EU after approval by the local ethic committee (COMETHEA) and were registered by the French Ministry of Higher Education and Research under the authorization number 2015042116017243. Male Sprague Dawley® rats, RjHan:SD, (300 - 400 g, 8-9 weeks of age) were obtained from Janvier Laboratories (Le Genest-St-Isle, France). They were housed in ventilated, temperature-controlled wire cages under a 12-h light-dark cycle for a minimum of 5 days before experiments, with ad libitum access to food (Product reference: 4RF21- PF1610; FLASH Aptitude, Gif-sur-Yvette, France) and water. The same conditions were maintained after the drug administration.

6.2.3 – Preparation of the levofloxacin solution for intravenous administration

On the day of the experiment, LVX was dissolved in 0.9 % NaCl solution assuring the physiological conditions. The final concentration (1.5 - 2 mg/mL) was adapted to the rat weight in order to administer a maximum volume of 1 mL through the tail vein and to achieve 5 mg LVX per kg body weight. This dose was calculated to be in the range of the LVX inhalation solution (Aeroquin®) doses administered in the CF patients [24].

6.2.4 – Preparation of the levofloxacin solution for intratracheal aerosolization

In the day of the IT administration to the lungs of rat, LVX was dissolved in 0.9% NaCl solution at 20 mg/mL final concentration in order to administer a fixed volume of 100 µL containing a targeted dose close to the IV route (5mg/kg).

6.2.5 – Chitosan microspheres for intratracheal aerosolization

Chitosan MS crosslinked with GNP and loaded with LVX were prepared by the spray drying method and characterized as previously described (Chapter 4) [25]. Briefly, chitosan (0.5 % w/v) was dissolved under magnetic stirring (300 rpm) in 150 ml of 1%

(w/v) acetic acid solution and LVX (1:1 ratio). Solutions were stirred for 30 min and genipin (0.2 mmol per g chitosan) crosslinking reaction was carried out at 50°C for 3h under magnetic stirring (300 rpm). The mixtures were then spray dried using a Büchi® Mini Spray Dryer B-290.

Drug loading was 48.4 ± 5.8 % (w/w) and MMAD 5.4 ± 0.2 µm. *In vitro* release studies showed more than 90% release within 15 min in phosphate buffer saline (PBS), pH 7.4 at 37°C.

6.2.6 – PLGA microspheres for intratracheal aerosolization

LVX-loaded PLGA MS (MS_LVX_1) were prepared by a double emulsion - solvent evaporation method with premix membrane homogenization [12]. Briefly, 0.6 mL of a LVX solution (250 mg/mL) was emulsified into 3 ml of a solution of PLGA (300 mg) and LVX (100 mg) in DCM using a Polytron® PT 3100D homogenizer (30000 rpm, 30 s). The obtained W_1/O emulsion was dispersed in 7 ml of a solution W_2 of PVA (3% w/v) saturated with LVX (35 mg/mL) in PBS at pH 7.4 (400 rpm). The resulting $W_1/O/W_2$ emulsion was subjected to three homogenization cycles through a SPG membrane. It was immediately poured into 25 ml of a solution of 0.4 % (w/v) PVA and saturated LVX (32 mg/mL) in PBS under magnetic stirring (400 rpm). Then DCM was evaporated off and MS washed through three cycles of centrifugation (3500 rpm, 5 min), resuspended in purified water and finally freeze-dried.

The drug loading was 10.5 ± 1.4 % (w/w) and MMAD 7.1 ± 0.2 µm. *In vitro* LVX release (PBS, pH = 7.4, at 37°C) was characterized by a “burst” release of 40 % of the LVX MS content within the first 30 min, followed by a gradual release up to at least 72 h. At 72 h, around 75% of the DL was released.

6.2.7 – Pharmacokinetic study

For the PK studies, the rats (n=80) were divided in four groups. Rats were anaesthetized with inhaled isoflurane for the administration of each formulation. The targeted LVX dose was 5 mg per kg body weight.

Group 1 (n=15) received an IV bolus injection of a LVX solution in saline in a tail vein (Figure 6.1).

Figure 6.1 – IV administration of LVX in 0.9 % NaCl solution by a tail vein of the rat with a syringe of 1 mL.

Group 2, 3 and 4 were treated intratracheally with nebulized solution (Group 2) and aerosolized MS (Group 3 for chitosan MS and Group 4 for PLGA MS), as schematically represented in Figure 6.2.

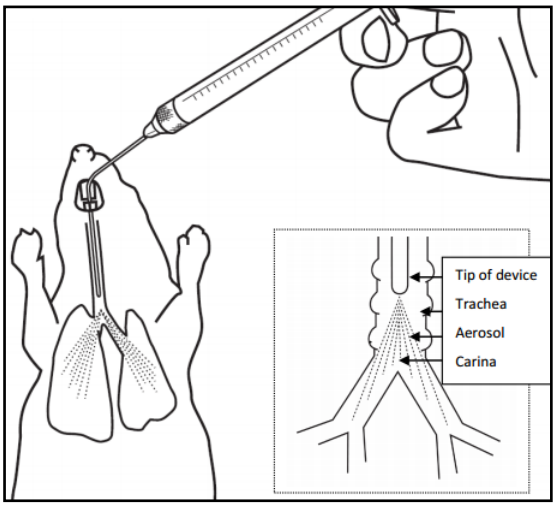

Figure 6.2 – Representation of IT administration of nebulized solutions or aerosolized dry-powder formulations with the aerosolizer or insufflator device, respectively. Partially reproduced from [26].

To perform the IT administrations, anaesthetized rats were placed on a rodent work stand inclined at an angle of 45° (Tem, Lormont, France) and the tip of the microsprayer or of the powder insufflator was introduced into the rat's trachea using an otoscope to visualize the vocal cords (Figure 6.3 and 6.4) [27].

Group 2 (n=15) was treated intratracheally with aerosolized 20 mg/mL LVX solution in saline (100 µL) using a IA-1C liquid Microsprayer® Aerosolizer (Penn-Century Inc., Wyndmoor, PA, USA) [28], Figure 6.3, as previously described [20].

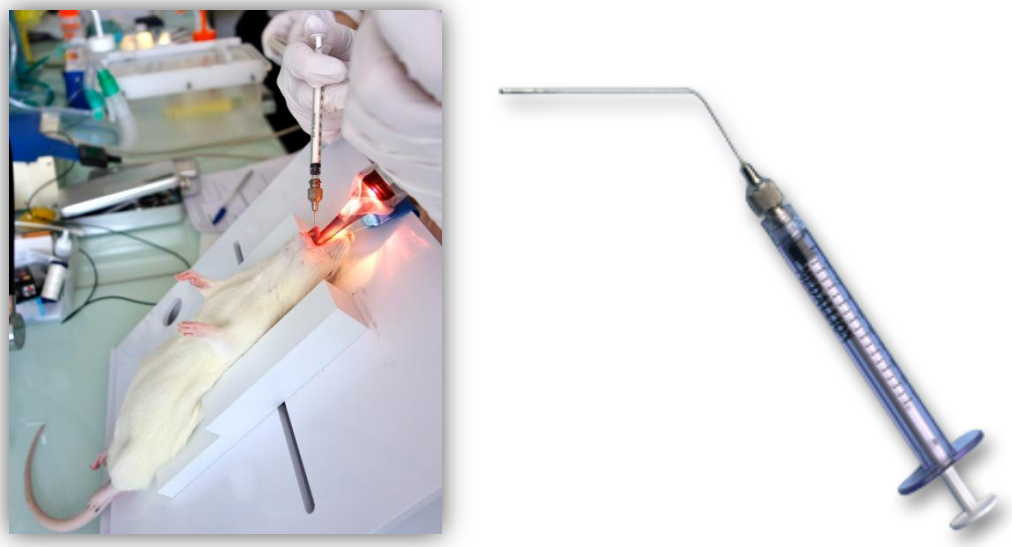

Figure 6.3 – IT aerosolization of 100 µL of LVX in 0.9 % NaCl solution to the rat (left) using the liquid Microsprayer® Aerosolizer (right, partially reproduced from [26]).

The immediate-release chitosan MS (4 mg, corresponding to 2 mg of LVX, Group 3, n=15) or the sustained release PLGA MS (20 mg, corresponding to 2 mg LVX, Group 4, n=35) were aerosolized intratracheally using a Dry powder Insufflator™ DP-4 (Penn-Century Inc., Wyndmoor, PA, USA) [29], device that was weighed before and after the IT administration in order to measure the real administered dose (Figure 6.4).

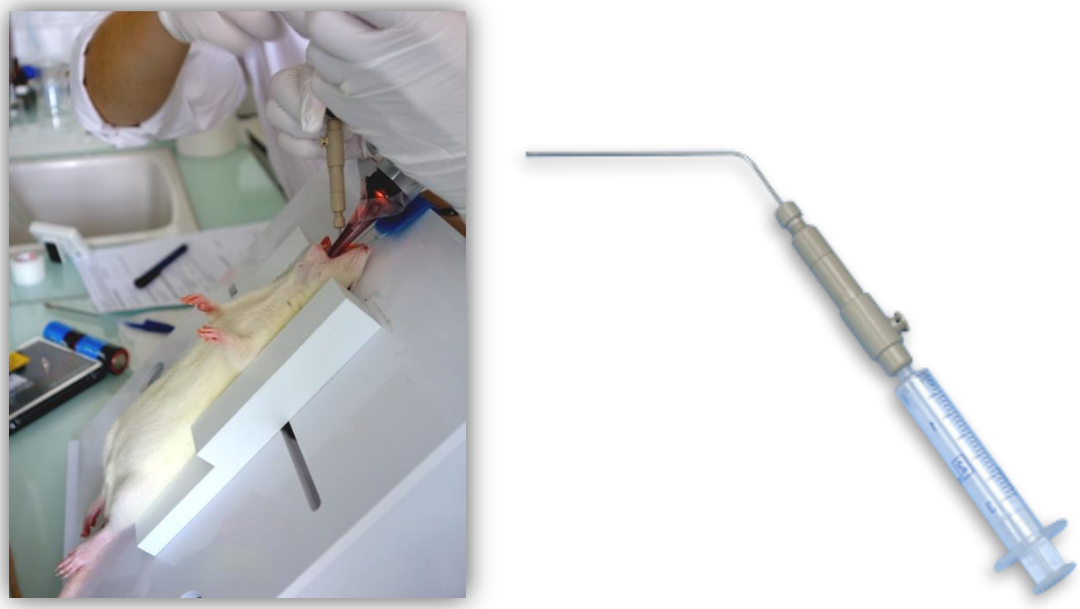

Figure 6.4 – IT aerosolization of chitosan MS or PLGA MS to the rat (left) using the dry powder Insufflator (right, partially reproduced from [30]).

After the IV or the IT aerosol administrations, rats were returned to individual cages with free access to food and water. At pre-determined time points, rats (3 to 5 per time point) were re-anesthetized with inhaled isoflurane for BAL fluid and blood sampling. After rat immobilization in a supine position with cervical hyperextension, the trachea was exposed and incised between two rings. A polyethylene catheter (0.58 mm i.d. and 0.96 mm o.d.; Harvard, Les Ulis, France) connected to a syringe filled with 1 mL of saline at 37°C was inserted into the trachea (50 mm deep). After injection of saline, BAL samples (300 to 800 µl) were immediately collected by aspiration via the same catheter (Figure 6.5).

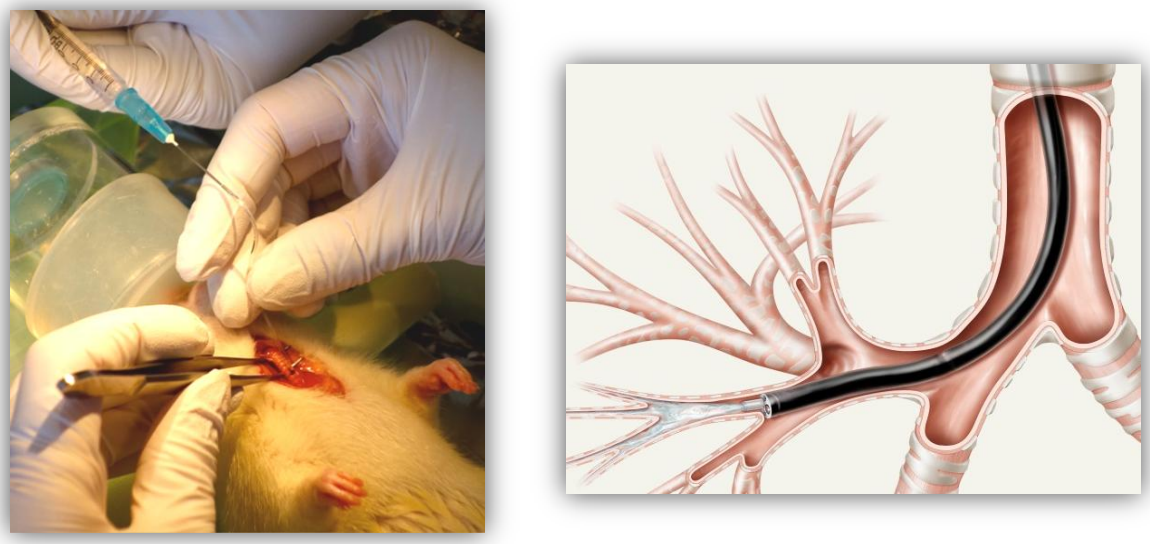

Figure 6.5 – BAL sampling procedure applied to the rat with injection of 1 mL saline at 37 °C followed by immediate aspiration (left) and representation of the catheter tip in the bronchus during the BAL procedure (right, reproduced from [31]).

A blood sample was then collected by cardiac puncture. Blood and BAL samples were centrifuged (3000 rpm for 10 min and 3500 rpm for 5 min, respectively, at 4°C) and supernatants stored at –20 °C until LVX and urea assays. For BAL fluid sampling, conditions for centrifugation were optimized in a preliminary study in order to ensure that all the MS potentially withdrawn during the BAL procedure were sedimented. For Group 4, lungs were collected at time 48 h and 72 h, washed with saline, weighed and frozen at -20 °C until LVX LC-MS/MS determination. Also for Group 4, the pellets obtained after the BAL sample centrifugation were freeze-dried and analyzed by LC-MS/MS to determine LVX.

Concentrations of LVX in ELF (LVX_{ELF}) were estimated from the BAL sample LVX concentrations (LVX_{BAL}) using a dilution factor calculated from the equation

$$LVX_{ELF} = LVX_{BAL} (Urea_{plasma}/ Urea_{BAL}) \quad (6.1)$$

where $Urea_{plasma}$ and $Urea_{BAL}$ are the urea concentrations, respectively, in plasma and BAL samples.

6.2.8 – Levofloxacin determination

Sample preparation

For plasma samples, 50 µL of plasma were mixed with 200 µL of the ciprofloxacin internal standard (IS) solution (0.1 µg/mL) in acetonitrile. Protein precipitate was separated by centrifugation at 14000 rpm for 15 min and 200 µL of supernatant were collected and vortex-mixed with 400 µL of 0.1 % (v/v) formic acid prior to analysis. The same procedure was applied to LVX calibration standards (2 to 400 ng/mL) prepared in blank rat plasma samples. For BAL samples, 20 µL of supernatant were mixed with 80 µL of IS (0.05 µg/mL) in 0.1% (v/v) formic acid before analysis. The freeze-dried pellet samples were treated with 300 µL of acetonitrile in order to extract LVX. After vortex-mixing, 20 µL were collected and diluted with 80 µL of 0.9 % NaCl. For BAL or pellet sample analysis, LVX calibration standards (2 to 400 ng/mL) were prepared in 0.9 % NaCl solution. For lung tissue samples, the whole lungs were defrosted and homogenized in water (10 mL per g of tissue), using a Polytron® PT 3100D for 2 min at 25000 rpm. Then, 100 µL of tissue homogenate were added to 1.1 mL of DCM and 25 µL of IS (0.4 µg/mL). After vortex-mixing for 30 s, the samples were centrifuged at 14000 rpm for 10 min and the DCM phase was collected and evaporated off at 40ºC under a nitrogen flow. Then, 150 µL of a mixture of mobile phase and 10 mM ammonium formiate solution (50:50 (v:v)) were added to the dry residue. After mixing, the samples were centrifuged at 3000 rpm during 5 min and the supernatants collected for analysis. The same procedure was applied to calibration standards, prepared with blank lung tissues (0.1 g) which were homogenized with 1 mL of LVX standard solutions (6.25 to 400 ng/mL).

LC-MS/MS

LVX concentrations were determined by LC-MS/MS in plasma, pellets and lung tissue samples using validated LC-MS/MS methods. For BAL, a new method of LVX determination was developed and validated (as detailed in Appendix 3). The system consisted of a Waters Alliance 2695 separations module equipped with a binary pump and an autosampler thermostatically controlled at 4°C, and of a Waters Micromass® Quattro micro API triple quadrupole tandem mass spectrometer. Reversed-phase chromatography was performed on a Phenomenex Jupiter™ C18 300 Å column (5.0 µm,

50 x 2.1 mm). The mobile phase was composed of 0.1% (v/v) formic acid in acetonitrile and 0.1% (v/v) formic acid in water (25:75 (v:v)). The flow rate was 0.20 mL/min and the injection volume 20 µl. The mass spectrometer was operated in the positive-ion mode. Ions were analyzed via multiple reaction monitoring (MRM) employing the transition of the $[M + 2H]^{2+}$ precursor to the product ions for analyte and IS. Transition ions were 362.2 to 318.2 m/z for LVX and 332.2 to 314.2 m/z for IS. Optimal MS/MS set up parameters were: +3.25 kV ion spray voltage, 600 L/h and 350°C desolvation gas (N_2) flow and temperature respectively, 10 L/h cone gas (N_2) flow, 120°C source temperature, 25 V cone potential for LVX and IS, 20 V collision energy for LVX and IS, 500 ms dwell time.

6.2.9 – Urea determination

For urea determination in plasma, a photometric detection was applied using a modular automatic analyzer (Cobas c kit, Roche, France). For BAL fluid, the urea concentration was evaluated by LC-MS/MS using a calibration range of 2.5 – 100 µg/mL in 0.9% NaCl, as previously described [18].

6.2.10 – Pharmacokinetic analysis and modeling strategy

LVX concentration in plasma and BAL fluid versus time data were analyzed according to a non-linear mixed effects method with S-ADAPT software (v 1.52) using MC-PEM (Monte-Carlo Parametric Expectation Maximization) estimation algorithm and S-ADAPT TRAN translator [32]. Observed concentrations were log-transformed for the analysis. Various structural models were tested and compared based on likelihood ratio tests ($p < 0.05$) of their objective functions and on visual inspection of diagnostic plots. LVX concentrations below the limit of quantification (LOQ) were handled by using the Beal M3 method [33].

6.3 – Results and discussion

The administration of IV and IT LVX solutions as well as IT chitosan or PLGA MS to the rats did not cause apparent signs of toxicity. Moreover, the rats that were maintained up to 72 h after the IT treatment with aerosolized PLGA MS showed normal weight gain.

6.3.1 – Pharmacokinetic model

Through the IV route, rats were dosed accurately with 5 mg LVX per kg body weight, but through the IT route, due to the fixed volume of liquid administered with the microsprayer or the variable dosing efficiency of the powder insufflators, the targeted LVX dose was not achieved and real doses are presented in Table 6.1.

Table 6.1 – PK parameter estimates of exposure.

PK parameters for LVX	**IV solution**	**IT solution**	**IT chitosan MS**	**IT PLGA MS**
LVX dose (mg/kg)	5	5.79 ± 0.5	4.73 ± 2.0*	3.06 ± 1.5*
Plasma total $AUC_{0.5\text{-}72h}$ (h.mg/L) (CV)**	1.45 (0%)	1.69 (12%)	0.98 (19%)	1.05 (21%)
Plasma unbound $AUC_{0.5\text{-}72h}$ (h.mg/L) (CV)	0.79 (0%)	0.92 (12%)	0.53 (19%)	0.57 (21%)
ELF $AUC_{0.5\text{-}72h}$ (h.mg/L) (CV)	1.64 (56%)	1.87 (108%)	1.20 (181%)	167 (104%)
ELF-to-plasma total $AUC_{0.5\text{-}72h}$ ratios (CV)	1.14 (56%)	1.21 (103%)	1.25 (174%)	169 (97%)
ELF-to-plasma unbound $AUC_{0.5\text{-}72h}$ ratios (CV)	2.09 (56%)	2.22 (103%)	2.30 (174%)	311 (97%)

*dose estimated by weighing the powder insufflator before and after the dosing

**corresponding to free and protein bound LVX

A population PK approach was used to characterize mainly the intra-pulmonary PK of LVX after IT aerosolization of the two dry MS powder formulations. The study design

included the IV and IT administrations of a LVX solution in order to get comparators and to improve the modeling output since the population PK approach allows simultaneous analysis of various data sets. It is also the most appropriate modeling procedure when only one data set (i.e., simultaneous plasma and ELF concentrations) can be collected in each individual. The PK model is presented with PK parameter estimates in Figure 6.6 and it was derived from an initial generic hybrid compartment model, with a mono-compartmental model for systemic PK and a bi-compartment model for ELF PK. The model for LVX systemic PK was monocompartmental with a volume V and a total clearance CL. The distribution between plasma and ELF was described by two different processes, on the one hand by a bi-directional transfer characterized with a clearance Cl_{dif} and on the other hand by a unidirectional transfer from plasma to ELF characterized with a clearance Cl_{out}. Only the unbound fraction of LVX in plasma (55%) [34] was assumed to distribute between plasma and ELF. A bi-compartmental PK of LVX in the ELF was necessary for a good fitting of the observed data, with the ELF compartment characterized with a volume V_{ELF} estimated by the modeling and directly linked to the plasma compartment, and a peripheral compartment of volume V_p characterized with a distribution clearance Cl_{dist}. Both V_{ELF} and V_p were estimated through modeling. The release process of LVX from the intratracheally-aerosolized formulations was divided into two components: a fraction of the dose F_{ELF} that was immediately released into the ELF compartment (burst release), and a fraction of the dose F_{Weib} that was released according to a Weibull release model, expressed as a differential equation for PK modeling,

$$\frac{dQ}{dt} = Q \times \left(\frac{b}{a}\right) \times \left(\frac{t}{a}\right)^{(b-1)} \qquad (6.2)$$

where Q is the amount of LVX not yet released, *t* is time, *a* is the time-scale parameter and *b* the shape parameter. Inter-individual variabilities were expressed as coefficient of variation (CV) and modeled as log-normal. The residual variability was estimated with an additive error model on the log scale, back-transformed into a proportional error model on normal scale for both plasma and ELF data.

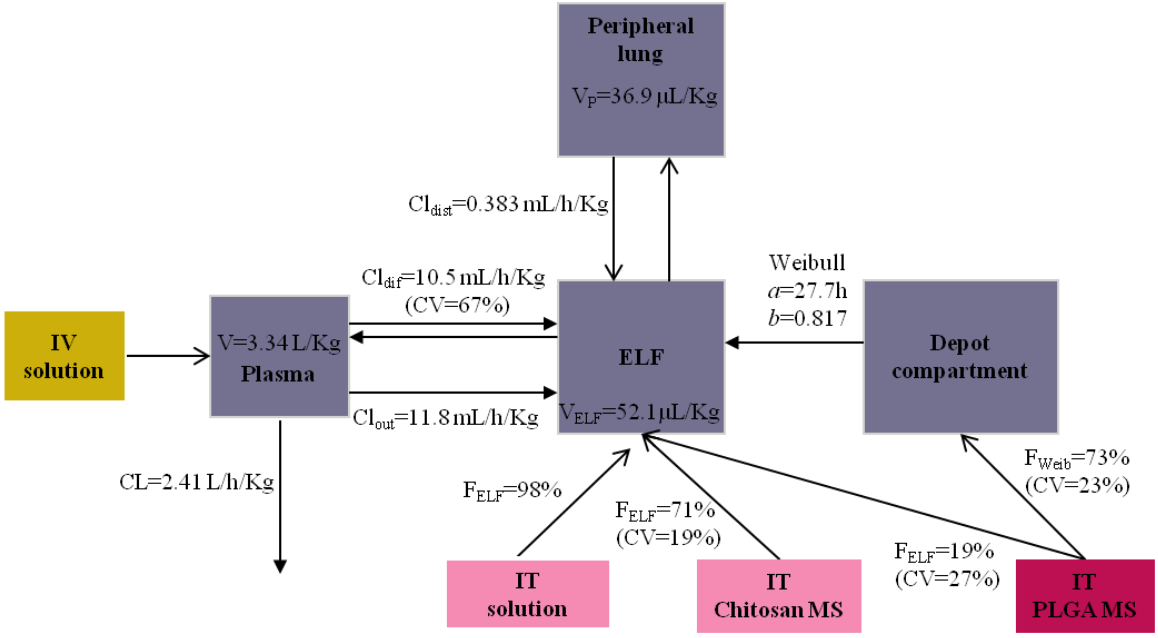

Figure 6.6 – Structural PK model for IV and IT solutions, IT chitosan MS and IT PLGA MS, with typical parameter estimates (see results for comments): V, LVX distribution volume; V_{ELF}, volume of ELF compartment; V_p, volume of peripheral compartment; CL, LVX total clearance; Cl_{dif}, bidirectional transfer of LVX clearance between plasma and ELF; Cl_{out}, unidirectional transfer of LVX clearance from plasma to ELF; Cl_{dist}, LVX distribution clearance; $F_{ELF,}$ fraction of dose immediately released into the ELF compartment; F_{Weib}, fraction of dose released according to a Weibull release model; *a*, time scale parameter; *b*, curve shape parameter, and CV, estimable inter-individual variabilities.

No inter-individual variability could be estimated for CL, V and V_p. The selected PK model provided a reasonably good description of the experimental data over time, both in plasma and ELF, after IV administration or IT aerosolization with the various formulations, as illustrated on Figure 6.7. Residual errors of the model were 13% in plasma and 18% and 21% in ELF depending on whether LVX was administered IV or IT (all formulations taken together), respectively. The much higher ELF exposure after LVX-loaded PLGA MS aerosolization with high concentrations sustained over time was adequately reported by the model. However, the analysis of the PK study needs to take into account some limitations. Rapid initial absorption or distribution phases are often difficult to characterize in PK, especially when sampling procedures are not instantaneous

(which is the case of the BAL sampling method). Early ELF concentrations after IT aerosolization of the dry MS powders may indeed depend on multiple uncontrolled parameters, including the depot characteristics and the onset of drug release from the MS or/ and of LVX solubilization within the small volume of the ELF (Figure 6.6). In addition, the invasive IT aerosolization procedure may induce by itself a transient alteration of the lung physiology which may affect LVX disposition. All these factors would result in a high variability of the data at early sampling times, which would require extensive data, and therefore a large number of animals, in order to interpret properly and to computerize the initial resorption and distribution phases. Therefore, it was decided not to collect plasma and BAL samples earlier than 30 min post administration. As a consequence, the PK model with an early burst release is probably a crude description of a more complex reality and the very high initial ELF concentrations of LVX predicted by the model (between 20 mg/mL and 100 mg/mL, depending on the administered formulation), together with the ELF AUC between time 0 and 0.5 h which contributed dramatically to the total AUC should be taken with caution. Accordingly, AUC from 30 min to 72 h only were considered in order to compare LVX exposures (Table 6.1).

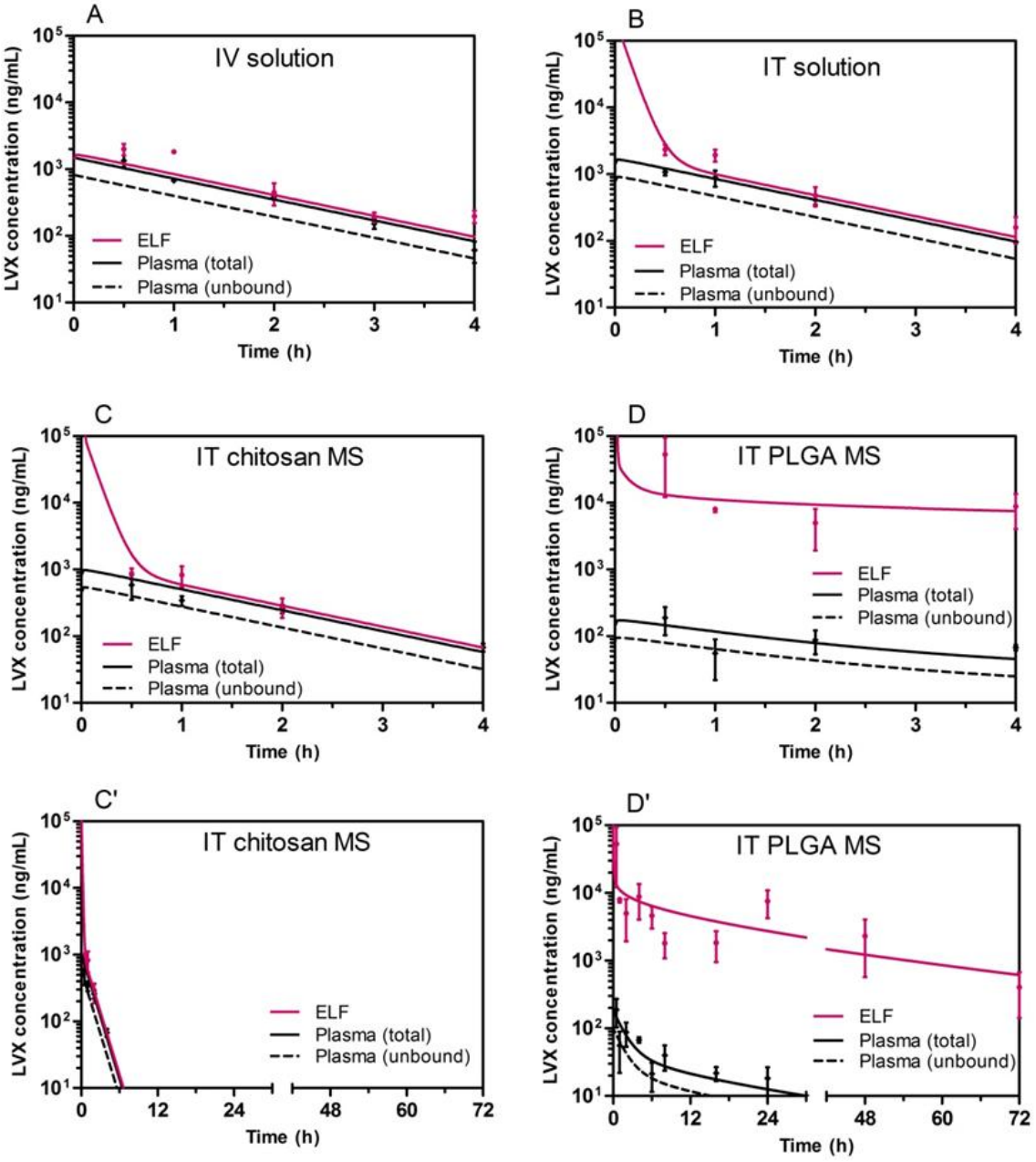

Figure 6.7 – Observed (mean ± SEM) LVX plasma and ELF concentrations (on log scale) versus time (symbols) and the respective PK model-predicted curves (solid lines, in pink for ELF and in black for total LVX in plasma) after administration of IV solution (A); IT solution (B), 5.79 ± 0.5 mg/kg dose; IT chitosan MS (C) and (C'), 4.73 ± 2.0 mg/kg dose, and IT PLGA MS (D) and (D'), 3.06 ± 1.5 mg/kg dose. Dotted lines correspond to the unbound plasma concentration curves. Note that for (C') and (D') panels the abscissa (time) scale is extended to 72 h.

6.3.2 – Intravenous and nebulized solutions

IV or IT administration of the LVX solutions resulted in similar experimental LVX concentrations in plasma and ELF (Figure 6.7 A and B) with an elimination half-life of 0.96 h. The bioavailability for the IT LVX solution was estimated to be 98%, with a direct release of LVX into the ELF compartment. The distribution between the ELF and plasma compartments was very rapid, with an estimated half-life of transfer between the two compartments lower than 1 min. The LVX estimated passive distribution clearance (clearance of diffusion, Cl_{dif}, Figure 6.6) was found to be close to the value determined for moxifloxacin [18], in consistency with their similar log D values [35] and their reported high permeability [36]. For both routes of administration of the LVX solutions, the ELF-to-plasma $AUC_{0.5\text{-}72h}$ ratios were slightly above 1 (Table 6.1). The Cl_{out} term, which improved the modeling, reflects the higher ELF LVX concentrations than the LVX unbound plasma concentrations, independently of the route of administration. It is of note that the ELF-to-plasma $AUC_{0.5\text{-}72h}$ ratio is ca. 2.1 when considering unbound concentrations in plasma, which reflected the ratio of clearances going from plasma towards ELF to clearances going from ELF to plasma, *i.e.* $(Cl_{out}+ Cl_{dif})/Cl_{dif}$.

Considering that LVX intracellular accumulation into macrophages was reported to be low and intermediate between those of ciprofloxacin and moxifloxacin [37], a systematic overestimation of LVX concentrations in ELF due to a potential lysis of alveolar macrophages [18] was excluded. The Cl_{out} term may therefore characterize a LVX efflux transport mechanism as previously reported *in vitro* [35] and *in vivo* [38]. However, as predicted by *in vitro* permeability studies on a Calu-3 lung epithelial model [35] the impact of efflux transport was modest compared to what was reported with moxifloxacin, and the Cl_{out} value estimated for LVX (11.8 ml/h/kg) was much lower than the one estimated for moxifloxacin (57.1 mL/h/kg [18]).

6.3.3 – Chitosan microspheres

Soon after IT aerosolization of the chitosan MS (Figure 6.7 C and C'), plasma and ELF concentrations were similar. Considering that LVX was shown *in vitro* to be almost immediately released from the chitosan MS [25] and was predicted by the PK model to be immediately released into the ELF compartment after IT administration (Figure 6.6), the

low bioavailability of LVX compared to the IT solution or to the PLGA MS powder was attributed to the loss of chitosan MS powder during the IT administration step. During the administration with the insufflator, the generated aerosol was indeed observed to be partly dispersed back into the environment. The ELF-to-plasma $AUC_{0.5\text{-}72h}$ ratio was above 1 (Table 6.1), in consistency with IV or IT administrations of the LVX solution. Therefore, the immediate release MS did not substantially differ, in terms of ELF concentration or systemic exposure to LVX, from IV or aerosolized administration of the LVX solution.

6.3.4 – PLGA microspheres

After IT aerosolization of the LVX-loaded PLGA MS (Figure 6.7 D and D'), PK profiles dramatically differed from profiles obtained after IV or IT administration of the LVX solution or after the IT administration of the chitosan MS. ELF concentrations were much higher than plasma concentrations, resulting in a very high ELF-to-plasma $AUC_{0.5\text{-}72h}$ ratio (Table 6.1). Moreover, plasma concentrations declined much more slowly than after IV administration or IT aerosolization of the LVX solution and could be measured up to 24 h versus 4 h after dosing. They declined in parallel to ELF concentrations with an approximate half-life of 18 h (vs. 0.96 h after IV administration), thus illustrating a flip-flop phenomenon (Figure 6.7 D and D'). This flip-flop observed in plasma corroborated the sustained release of LVX in ELF that followed the IT aerosolization of the LVX-loaded PLGA MS. On the one hand, the sustained LVX release from PLGA MS allows a long time high concentration in ELF due to the continuous slow release from MS and also due to the small volume of ELF (~ 17 µL), i.e., a low amount of LVX corresponds to a high concentration in ELF. On the other hand, lower plasma concentrations were observed due to the lower administered mean dose (3.06 mg/kg) and the lower fraction immediately available (only 19% of dose is estimated to be of immediate release). In addition, the continuous LVX slow release from MS contribute to the maintenance of plasma concentrations for longer but at levels subsequently lower due to the very large volume of plasma compared to ELF and to the high total clearance. Such a result confirmed previous works where ELF concentrations that were modelled from plasma concentrations after IT administration of sustained release rifampicin-loaded PLGA MS were predicted to be much higher than plasma concentrations [39]. The bioavailability was 92%, with 19% of the dose released immediately (burst release) into

the ELF and 73% released slowly over more than 72 h into the ELF from a depot compartment, the PLGA MS, according to a Weibull model (a = 27.7 h; b = 0.817).

LVX release: in vitro and in vivo

The *in vivo* release profile of LVX from the PLGA MS that was estimated by the model is presented on Figure 6.8 for comparison with the *in vitro* release profile.

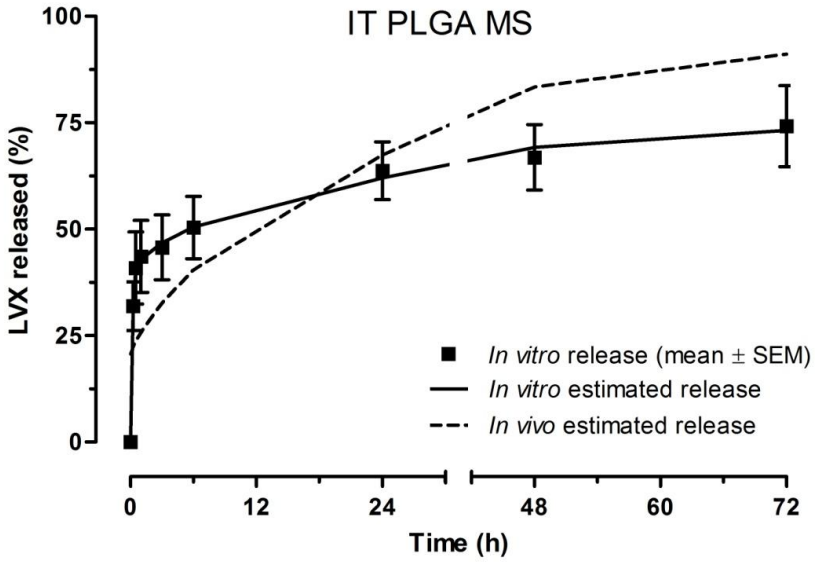

Figure 6.8 – Experimental *in vitro* release data of LVX-loaded PLGA MS in PBS, pH 7.4, at 37ºC (mean ± SEM (square), n=3) with the curve (solid line) corresponding to the model (a = 37.1 and b = 0.69, see Chapter 5 for details), superimposed. Also represented is the *in vivo* release kinetic curve (dashed line) predicted by the PK model after PLGA MS IT administration and cumulating the immediate release (F_{ELF} = 19% of administered dose) and the slow release according to a Weibull model (F_{Weib} = 73%, a = 27.7 and b = 0.817).

The "burst" release was lower *in vivo* than *in vitro* (19% (= F_{ELF} =) vs. 40 %). This difference may be explained by the fact that the *in vitro* release was performed in sink conditions under stirring and at constant pH (7.4), whereas *in vivo* LVX saturation concentration may be reached rapidly due to the small volume of the ELF compartment (Figure 6.6). Subsequently, the release became faster *in vivo* than *in vitro*. Beyond 18

hours, the cumulated *in vivo* released amount overpassed the *in vitro* results. It should be recalled that the *in vitro* LVX release profile was described using a first order model followed by a Weibull model. The *in vivo* LVX release modeling also combined an immediate release with a slow release according to a Weibull model (Figure 6.8). In both cases, a "burst" release was observed, followed by a slower release, given by the Weibull model, with scale factors *a* of the same order of magnitude, indicating that the release processes were similar *in vitro* and *in vivo* in terms of process time. The shape factors *b* were below 1 and corresponded to a parabolic curve, with a higher initial slope followed by an exponential behavior. An additional consideration is that inhaled MS with diameter below 10 µm are likely to be phagocytosed by lung macrophages [40]. The LVX release from the PLGA MS may be impacted by the MS accumulation in intracellular compartments like phagolysosomes, characterized by an acidic pH where LVX is more soluble than at pH 7.4. In addition, in the case of the biodegradable polymeric PLGA MS, it is assumed that after the initial burst release the sustained release process results from the combination of drug diffusion within the polymer matrix and of the polymer matrix erosion [41]. Polymer erosion *in vitro* was demonstrated by SEM analysis, by comparison with the morphology after preparation (Figure 6.9 A and 6.9 B), as already indicated in Chapter 5. Polymer erosion may be faster *in vivo* than *in vitro*, thus explaining the higher LVX amount released between 18 and 72 hours.

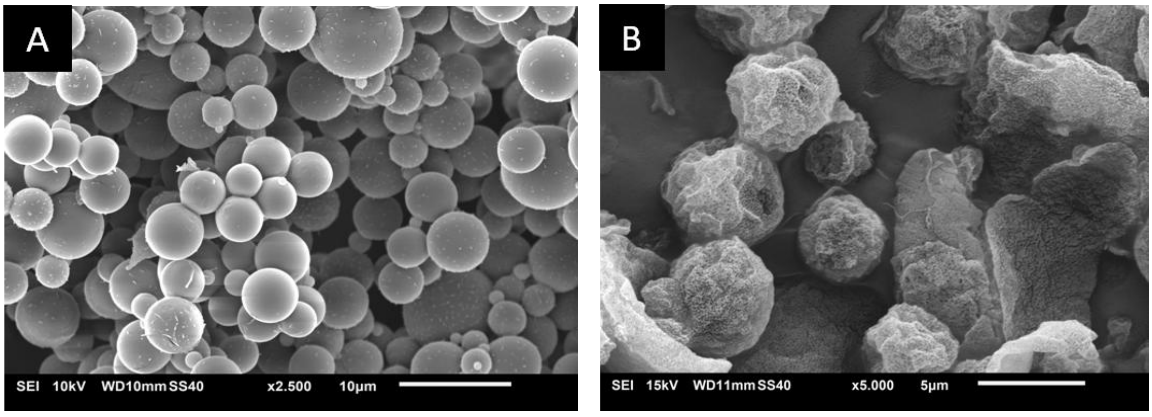

Figure 6.9 – SEM images of PLGA MS after preparation (A) and after a 1 week incubation at 37°C in PBS pH 7.4 under magnetic stirring of 600 rpm (B).

Antibacterial action

Concerning the expected antibiotic efficiency of the LVX-loaded PLGA MS, *P. aeruginosa* strains are considered to be sensitive to the therapy with LVX when MIC is lower than 2 µg/mL and to be resistant when MIC is equal to or above 8 µg/mL [42,24]. With the IT aerosolization of LVX-loaded PLGA MS at a dose of 3 mg/kg in rats, LVX concentrations in ELF were higher than 8 µg/mL up to 3.5 hours and higher than 2 µg/mL up to 30 hours. This finding represents a promising approach in the management of *P. aeruginosa* infections in CF patients, by demonstrating that sustained release MS would permit higher ELF concentrations of Class I 'high solubility and high permeability', and potentially less frequent administration drugs than an aerosolized solution or an aerosol of pure drug powder.

Lung homogenates and pellets

For the IT PLGA MS group, the percentages of LVX recovered from the lung homogenates at 48 h and 72 h, are presented in Table 6.2, together with the values estimated by the model.

Table 6.2 – Recovered LVX in homogenized lung tissue from rats at 48 h and 72 h post-treatment with IT PLGA MS and respective values predicted by the PK model.

IT PLGA MS (time)	Recovered LVX (%)*	Predicted unreleased LVX (%)*
48 h	2.30 ± 1.5**	17
72 h	0.14***	10

*expressed as the percentage (%) of the bioavailable dose

**mean ± SD (n=3)

*** n=1

Results from lung homogenates (Table 6.2) confirm that even after 72 h, some LVX-loaded PLGA MS remain in the lungs, being in accordance with predictions by the model. At 48 h values around 2% of LVX of the available dose were recovered vs. 17 % from the predicted unreleased LVX (and at 72 h it was 0.14 % vs. 10 %, respectively). These

differences can be attributed to the inherent experimental errors and/ or to some uncertainty of the modelling approach.

Results from pellets (obtained after the BAL centrifugation) from the IT PLGA MS group indicate that the LVX determined in pellets was in the range 81-99 %, when compared to the LVX determined in BAL plus pellets. This means that a small fraction of LVX was in the BAL samples (supernatant). Thus, even if some LVX escaped from the MS and/ or has been released from macrophages during the BAL sampling/ centrifugation, this phenomenon would correspond to negligible amount of LVX in the supernatant, due to the much higher LVX concentrations found in pellets. In addition, the BAL sampling procedure was performed only once (1mL) in order to avoid lung damage/ cell disruption. Therefore, these results confirm the sustained release of LVX from the PLGA MS, with high levels of LVX in ELF, as also predicted by the *in vivo* modeling approach.

6.4 – Conclusions

The IT administration of the immediate release chitosan MS formulation provided PK profiles comparable to the IV or the IT LVX solutions, with the benefits inherent to dry powder formulations. The IT administration of LVX-loaded PLGA MS resulted in a prolonged release of LVX within the lungs and in much higher LVX concentrations in the ELF than in plasma. Such a sustained-release formulation is expected to reduce the frequency of administrations compared to a LVX solution for inhalation, and to increase anti-infectious treatment efficiency while reducing systemic toxicity. More generally, these results highlight the benefit of using sustained-release MS administered as aerosols to provide and to maintain high pulmonary concentrations of a highly water soluble antibiotic characterized by a high permeability profile through the broncho-alveolar barrier. The sustained-release MS dry powder aerosol may therefore provide a promising alternative to the solutions or to pure drug dry powders for inhalation in terms of ease and frequency of administration, which should have a positive impact on the compliance of patients to treatments.

6.5 – References

1. Hoppentocht M, Hagedoorn P, Frijlink HW, de Boer AH (2014) Developments and strategies for inhaled antibiotic drugs in tuberculosis therapy: A critical evaluation. European Journal of Pharmaceutics and Biopharmaceutics 86 (1):23-30.

2. Gaspar MC, Couet W, Olivier JC, Pais AACC, Sousa JJS (2013) Pseudomonas aeruginosa infection in cystic fibrosis lung disease and new perspectives of treatment: a review. European Journal of Clinical Microbiology & Infectious Diseases 32 (10):1231-1252.

3. Stockmann C, Sherwin CMT, Ampofo K, Spigarelli MG (2014) Development of levofloxacin inhalation solution to treat Pseudomonas aeruginosa in patients with cystic fibrosis. Therapeutic Advances in Respiratory Disease 8 (1):13-21.

4. Geller DE (2009) Aerosol Antibiotics in Cystic Fibrosis. Respiratory care 54 (5):658-670.

5. Kirkby S, Novak K, McCoy K (2011) Aztreonam (for inhalation solution) for the treatment of chronic lung infections in patients with cystic fibrosis: an evidence-based review. Core evidence 6:59-66.

6. Sawicki GS, Signorovitch JE, Zhang J, Latremouille-Viau D, von Wartburg M, Wu EQ, Shi L (2012) Reduced mortality in cystic fibrosis patients treated with tobramycin inhalation solution. Pediatric Pulmonology 47 (1):44-52.

7. Foundation CF (2015) Drug Development Pipeline. Available via http://www.cff.org/research/DrugDevelopmentPipeline/ Accessed 27 October 2015.

8. EMA (2015) Quinsair - Summary of product characteristics. European Medicines Agency, Science Medicines Health. http://ec.europa.eu/health/documents/community-register/2015/20150326130815/anx_130815_en.pdf. Accessed 26 October 2015.

9. King P, Lomovskaya O, Griffith DC, Burns JL, Dudley MN (2010) In Vitro Pharmacodynamics of Levofloxacin and Other Aerosolized Antibiotics under Multiple

Conditions Relevant to Chronic Pulmonary Infection in Cystic Fibrosis. Antimicrobial Agents and Chemotherapy 54 (1):143-148.

10. Koeppe MO, Cristofoletti R, Fernandes EF, Storpirtis S, Junginger HE, Kopp S, Midha KK, Shah VP, Stavchansky S, Dressman JB, Barends DM (2011) Biowaiver monographs for immediate release solid oral dosage forms: levofloxacin. Journal of Pharmaceutical Sciences 100 (5):1628-1636.

11. Traini D, Young PM (2009) Delivery of antibiotics to the respiratory tract: an update. Expert Opinion on Drug Delivery 6 (9):897-905.

12. Doan TV, Couet W, Olivier JC (2011) Formulation and in vitro characterization of inhalable rifampicin-loaded PLGA microspheres for sustained lung delivery. International Journal of Pharmaceutics 414 (1-2):112-117.

13. Ramazani F, Chen W, Van Nostrum CF, Storm G, Kiessling F, Lammers T, Hennink WE, Kok RJ (2015) Formulation and characterization of microspheres loaded with imatinib for sustained delivery. International Journal of Pharmaceutics 482 (1–2):123-130.

14. Feng T, Tian H, Xu C, Lin L, Xie Z, Lam MH-W, Liang H, Chen X (2014) Synergistic co-delivery of doxorubicin and paclitaxel by porous PLGA microspheres for pulmonary inhalation treatment. European Journal of Pharmaceutics and Biopharmaceutics 88 (3):1086-1093.

15. Sah E, Sah H (2015) Recent Trends in Preparation of Poly(lactide-co-glycolide) Nanoparticles by Mixing Polymeric Organic Solution with Antisolvent. Journal of Nanomaterials 2015:22.

16. Anderson JM, Shive MS (1997) Biodegradation and biocompatibility of PLA and PLGA microspheres. Advanced Drug Delivery Reviews 28 (1):5-24.

17. Mouton JW, Theuretzbacher U, Craig WA, Tulkens PM, Derendorf H, Cars O (2008) Tissue concentrations: do we ever learn? Journal of Antimicrobial Chemotherapy 61 (2):235-237.

18. Gontijo AVL, Brillault J, Grégoire N, Lamarche I, Gobin P, Couet W, Marchand S (2014) Biopharmaceutical Characterization of Nebulized Antimicrobial Agents in Rats: 1. Ciprofloxacin, Moxifloxacin, and Grepafloxacin. Antimicrobial Agents and Chemotherapy 58 (7):3942-3949.

19. Kiem S, Schentag J (2008) Interpretation of antibiotic concentration ratios measured in epithelial lining fluid. Antimicrob Agents Chemother 52 (1):24-36.

20. Marchand S, Gobin P, Brillault J, Baptista S, Adier C, Olivier J-C, Mimoz O, Couet W (2010) Aerosol Therapy with Colistin Methanesulfonate: a Biopharmaceutical Issue Illustrated in Rats. Antimicrobial Agents and Chemotherapy 54 (9):3702-3707.

21. Ryan DM, Cars O (1983) A problem in the interpretation of beta-lactam antibiotic levels in tissues. Journal of Antimicrobial Chemotherapy 12 (3):281-284.

22. Kiem S, Schentag JJ (2008) Interpretation of antibiotic concentration ratios measured in epithelial lining fluid. Antimicrobial Agents and Chemotherapy 52 (1):24-36.

23. Conte JE, Golden J, Duncan S, McKenna E, Lin E, Zurlinden E (1996) Single-dose intrapulmonary pharmacokinetics of azithromycin, clarithromycin, ciprofloxacin, and cefuroxime in volunteer subjects. Antimicrobial Agents and Chemotherapy 40 (7):1617-1622.

24. Geller DE, Flume PA, Staab D, Fischer R, Loutit JS, Conrad DJ (2011) Levofloxacin Inhalation Solution (MP-376) in Patients with Cystic Fibrosis with Pseudomonas aeruginosa. American Journal of Respiratory and Critical Care Medicine 183 (11):1510-1516.

25. Gaspar MC, Sousa JJS, Pais AACC, Cardoso O, Murtinho D, Serra MES, Tewes F, Olivier J-C (2015) Optimization of levofloxacin-loaded crosslinked chitosan microspheres for inhaled aerosol therapy. European Journal of Pharmaceutics and Biopharmaceutics 96:65-75.

26. Instructions for use - MicroSprayer® Aerosolizer – Model IA-1B. Penn Century, Inc. http://penncentury.com/support/instructions/. 2016.

27. Gagnadoux F, Pape AL, Lemarie E, Lerondel S, Valo I, Leblond V, Racineux JL, Urban T (2005) Aerosol delivery of chemotherapy in an orthotopic model of lung cancer. European Respiratory Journal 26 (4):657-661.

28. Bivas-Benita M, Zwier R, Junginger HE, Borchard G (2005) Non-invasive pulmonary aerosol delivery in mice by the endotracheal route. European Journal of Pharmaceutics and Biopharmaceutics 61 (3):214-218.

29. Morello M, Krone CL, Dickerson S, Howerth E, Germishuizen WA, Wong Y-L, Edwards D, Bloom BR, Hondalus MK (2009) Dry-powder pulmonary insufflation in the mouse for application to vaccine or drug studies. Tuberculosis 89 (5):371-377.

30. Instructions for use - Dry Powder Insufflator™ – Model DP-4 & DP-4M. Penn Century, Inc. http://penncentury.com/support/instructions/. 2016.

31. Bronchoscopic Alveolar Lavage (BAL). Olympus Europa SE & CO. KG. http://www.olympus-europa.com/medical/en/medical_systems/applications/pulmonology/diagnostic_bronchoscopy/bronchoscopic_alveolar_lavage__bal_/bronchoscopic_alveolar_lavage__bal_.html . 2016.

32. Bulitta JB, Bingölbali A, Shin BS, Landersdorfer CB (2011) Development of a New Pre- and Post-Processing Tool (SADAPT-TRAN) for Nonlinear Mixed-Effects Modeling in S-ADAPT. The AAPS Journal 13 (2):201-211.

33. Beal SL (2001) Ways to fit a PK model with some data below the quantification limit. Journal of Pharmacokinetics and Pharmacodynamics 28 (5):481-504.

34. Hurtado FK, Weber B, Derendorf H, Hochhaus G, Dalla Costa T (2014) Population Pharmacokinetic Modeling of the Unbound Levofloxacin Concentrations in Rat Plasma and Prostate Tissue Measured by Microdialysis. Antimicrobial Agents and Chemotherapy 58 (2):678-686.

35. Brillault J, De Castro WV, Couet W (2010) Relative Contributions of Active Mediated Transport and Passive Diffusion of Fluoroquinolones with Various

Lipophilicities in a Calu-3 Lung Epithelial Cell Model. Antimicrobial Agents and Chemotherapy 54 (1):543-545.

36. Saelim N, Suksawaeng K, Chupan J, Techatanawat I (2015) Biopharmaceutics classification system (BCS)-based biowaiver for immediate release solid oral dosage forms of moxifloxacin hydrochloride (moxiflox GPO) manufactured by the government pharmaceutical organization (GPO). Asian Journal of Pharmaceutical Sciences.

37. Seral C, Barcia-Macay M, Mingeot-Leclercq MP, Tulkens PM, Van Bambeke F (2005) Comparative activity of quinolones (ciprofloxacin, levofloxacin, moxifloxacin and garenoxacin) against extracellular and intracellular infection by Listeria monocytogenes and Staphylococcus aureus in J774 macrophages. Journal of Antimicrobial Chemotherapy 55 (4):511-517.

38. Zimmermann ES, Laureano JV, dos Santos CN, Schmidt S, Lagishetty CV, de Castro WV, Dalla Costa T (2015) A simultaneous semi-mechanistic population analysis of levofloxacin in plasma, lung and prostrate to describe the influence of efflux transporters on drug distribution following intravenous and intratracheal administration. Antimicrobial Agents and Chemotherapy.

39. Doan TVP, Grégoire N, Lamarche I, Gobin P, Marchand S, Couet W, Olivier JC (2013) A preclinical pharmacokinetic modeling approach to the biopharmaceutical characterization of immediate and microsphere-based sustained release pulmonary formulations of rifampicin. European Journal of Pharmaceutical Sciences 48 (1–2):223-230.

40. Hirota K, Kawamoto T, Nakajima T, Makino K, Terada H (2013) Distribution and deposition of respirable PLGA microspheres in lung alveoli. Colloids and Surfaces B: Biointerfaces 105:92-97.

41. Shen J, Burgess DJ (2012) Accelerated in vitro release testing methods for extended release parenteral dosage forms. The Journal of pharmacy and pharmacology 64 (7):986-996.

42. Lee CKK, Boyle MP, Diener-West M, Brass-Ernst L, Noschese M, Zeitlin PL (2007) Levofloxacin Pharmacokinetics in Adult Cystic Fibrosis. Chest 131 (3):796-802.

Chapter 7

CONCLUSIONS AND PERSPECTIVES FOR FURTHER STUDIES

7.1 – Conclusions

This dissertation aimed at the development of polymeric formulations loaded with LVX and intended for pulmonary delivery in CF lung disease. Both immediate and sustained release systems were respectively prepared with chitosan and PLGA, and appropriately characterized in order to comply with the properties required for lung administration. Further studies, particularly, *in vitro* and *in vivo* approaches were carried out for selected microsphere-based systems. The main goals and achievements obtained are summarized in what follows.

The development of LVX-loaded chitosan MS, differently crosslinked and obtained by spray drying, was the initial focus of this thesis. A first step in the optimization was carried out resorting to factorial planning, shedding light on the influence of some parameters on MS size, a key point when pulmonary delivery is intended. Inlet temperature of spray dryer, chitosan and GL concentrations and presence of LVX were considered in two different levels. Higher temperature and/or the presence of LVX promoted an increased MS size.

Crosslinkers with favorable toxicity profiles (GNP, GLY and GA) were subsequently considered for chitosan MS in order to stabilize the polymeric structure, but maintaining the immediate release profile, which was also obtained for the usual GL-crosslinked MS. In general, a promising drug content ranging from 39.8% to 50.8% was obtained. Techniques such as ATR-FTIR, DTA/ TGA and XRD confirmed the amorphous state and/or molecular dispersion of LVX in MS. Interesting values of swelling were especially obtained for GNP- and GA- crosslinked MS, which also presented the best aerodynamic diameters (close to 5 μm) and cytotoxicity profiles. Such formulations represent a promising alternative to the nebulized LVX solution, by reducing the time of administration, avoiding cleaning of the devices and promoting stability due to the powder state.

Subsequently, sustained-release systems based on LVX-loaded PLGA MS were developed. These were prepared by a modified double emulsion solvent evaporation method, combined with premix membrane homogenization. Incorporating a high hydrophilic drug into a hydrophobic polymer is a challenge. Several types of PLGA polymers were firstly addressed and the influence of lauric acid and high concentrations

of LVX in aqueous phases after evaluated. LVX-loaded PLGA MS prepared from the RG 502H polymer type with saturated levels of LVX in aqueous phases were successfully obtained with both adequate values of MMAD (7.1 ± 0.2 μm) and drug content (10.5 ± 1.4 %). In addition, a clear sustained release was obtained and investigated by appropriate mathematical models. A first order ("burst" release) followed by a Weibull model (sustained release) fitted well the data. In addition, these MS demonstrated a good incorporation of LVX, by several techniques, promoted high Calu-3 cell viability values and a fast rate of biodegradability (1 week).

The work also included *in vivo* studies with rats, carried out with one selected immediate-release dosage form (LVX-loaded chitosan MS crosslinked with GNP) and one sustained-release formulation (LVX-loaded PLGA MS). IV administration and IT nebulization of a LVX solution were also considered in the PK study, for comparison purposes.

The fast LVX release from chitosan MS was confirmed, combined with improved stability and usability relative to LVX solutions. It may be used as a short-term therapeutic option for out-of-home patients.

Concerning the PLGA MS, sustained release up to at least 72 h was obtained with high pulmonary concentrations, strongly improving the antibacterial activity, particularly important for *P. aeruginosa* infections. In fact, LVX concentrations in the ELF were very high, for an extended time, while those in plasma were low. These results clearly indicate a promising alternative to nebulized solutions of LVX to CF disease, with the advantages of fewer administrations per day and better compliance to the therapy.

7.2 – Perspectives for further studies

Further formulation development is especially warranted for PLGA MS, to increase even further the LVX content, and decreasing the total amount of powder to be administered.

Additional *in vitro* release studies with a medium simulating the lung fluid may lead to narrow the distances between *in vitro* and *in vivo* approaches.

Co-encapsulation of LVX with other drugs such as mucolytics (e.g. dornase alpha) may contribute to the improvement of MS penetration in thick mucus, commonly present in CF patients. Efficacy of MS penetration and of anti-infective drugs in *P. aeruginosa*

biofilms may be assessed by preparing artificial medium (containing DNA, mucin, aminoacids and salts, among others) and using bacteria cultures.

In this context, bioluminescence imaging studies would be useful to elucidate the MS distribution along the "pulmonary tree".

Finally, it would be very important to develop an animal model of the CF disease, preferentially chronically infected by *P. aeruginosa*, in order to evaluate the performance of selected MS.

Appendix 1

SCREENING OF CROSSLINKING AGENTS

A 1.1 – Introduction

Different crosslinking agents can be considered for chitosan delivery systems. However, they react differently with chitosan, and a comparison in terms of molar ratio between them may not be appropriate, being a comparison of the amount of crosslinker to the amount of chitosan preferred. In addition, for some crosslinkers, if used in high amounts, too viscous solutions are obtained, not allowing the spray drying process. Therefore, a screening of viscosity from chitosan solutions with different amounts of a crosslinking agent was carried out in order to choose the crosslinker concentration for the chitosan MS preparation. Also data from literature were taken into account, as indicated below in the section A 1.4.

The combined results from viscosity evaluation together with literature information allowed choosing the concentration for each crosslinker that was used for the preparation of chitosan MS (Chapter 4). It should be recalled that Glutaraldehyde (GL), DL-glyceraldehyde (GLY), glutaric acid (GA) and genipin (GNP) were the crosslinking agents assessed.

A 1.2 – Understanding the crosslinking mechanisms

The chitosan MS structure can be stabilized resorting to crosslinking agents, which can also model other MS properties, as investigated in Chapter 4.

With respect to GL, it is known as the most common crosslinking agent for polymers such as chitosan. For this crosslinker, the typical crosslinking reaction results in covalent bonds and occurs between the amino groups of chitosan with aldehyde groups of GL, leading to imine bonds formation (Figure A 1.1) [1,2].

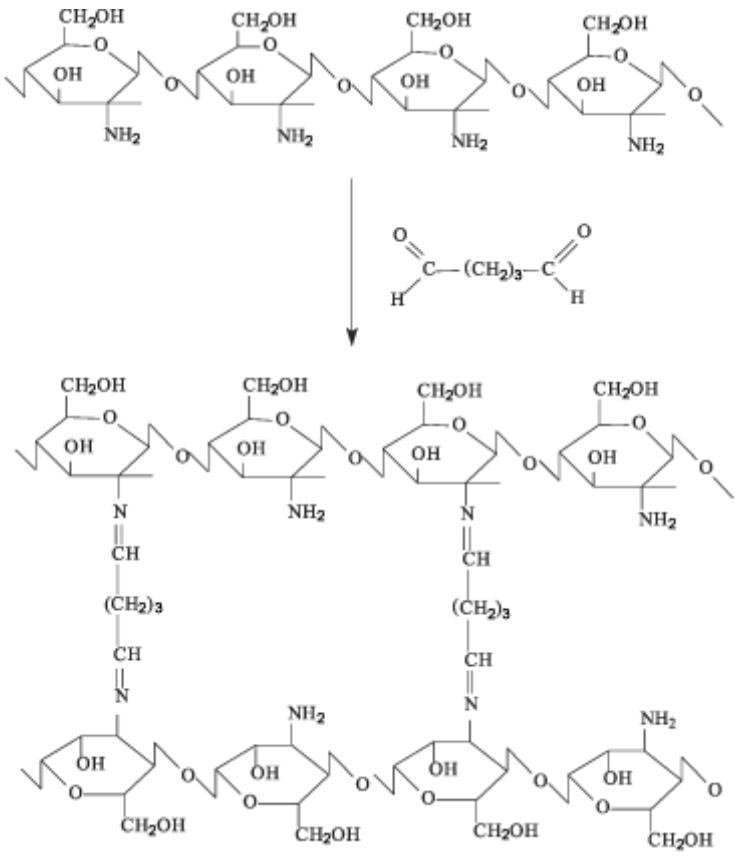

Figure A 1.1 – Structure resulted from the crosslinking reaction of GL with chitosan Reproduced from [2].

Due to some toxicity reported for GL, other more biocompatible crosslinkers were considered, as already explained in Chapter 4, and included GNP, GA and GLY.

Concerning the crosslinking mechanism of GNP with chitosan, several possibilities exist, depending on the pH of the medium, as investigated elsewhere [3]. Once the GNP-crosslinked chitosan MS described in this thesis were prepared in acidic conditions, few details of the respective reaction of GNP with chitosan are here included [4]. Actually, at neutral and acidic pH, GNP reacts covalently with amino groups of chitosan forming heterocyclic amines (Figure A 1.2).

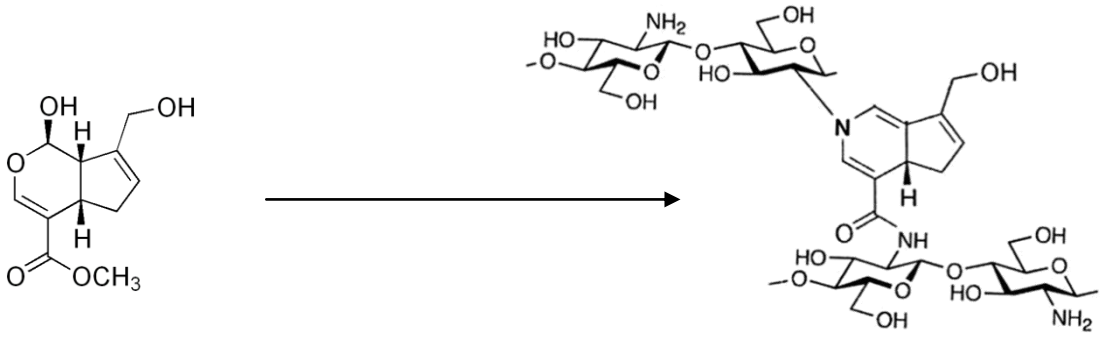

Figure A 1.2 – GNP structure (left) and crosslinked structure resulted from the reaction of GNP with chitosan (right).

In what pertains to GA, some interactions between this crosslinking agent and chitosan chains take place. Actually, non-covalent interactions (ionic interaction and multiple intermolecular hydrogen bonding) between amine groups of chitosan and carboxylic groups of dicarboxylic acids, such as the GA (Figure A 1.3), have already been reported [5-7].

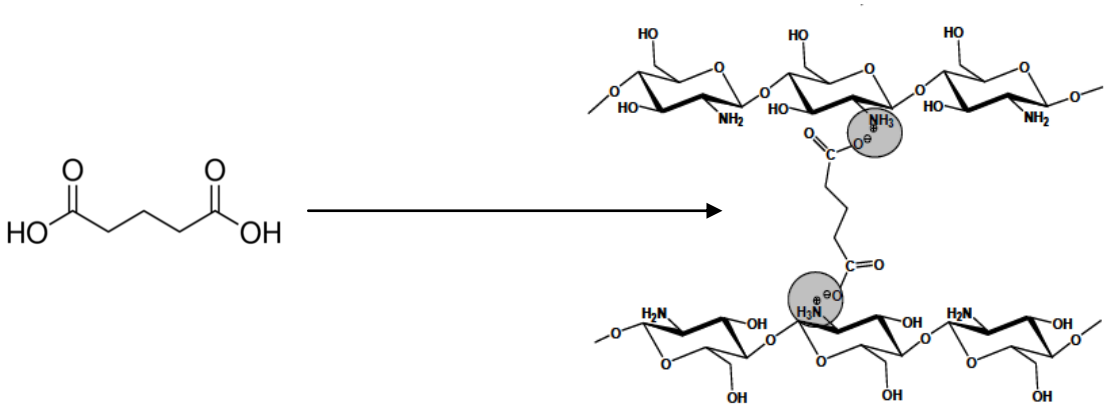

Figure A 1.3 – GA structure (left) and representation of the interaction between GA and chitosan (right).

For GLY (Figure A 1.4), few studies have investigated this compound as a crosslinker [8,9]. Nevertheless, being a nontoxic compound reinforces its investigation as a crosslinking agent. Despite the paucity of data about the interactions between GLY and chitosan, some considerations are here included. There is the possibility of the reaction of

GLY with the amine groups of chitosan leading to imines, and therefore, no crosslinking reaction occurs. Nevertheless, reaction between aldehyde groups from GLY and hydroxyl groups of chitosan are possible, resulting in a crosslinked structure, with ether bonds.

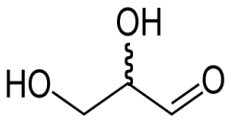

Figure A 1.4 – GLY structure.

A 1.3 – Materials

Chitosan low molecular weight (20,000 cps, 75–85% deacetylated), Glutaraldehyde (GL) 50% (w/w) aqueous solution and DL-glyceraldehyde (≥ 90% by GC) were obtained from Sigma-Aldrich® (France). Genipin (98% purity) was obtained from Challenge Bioproducts Co., Ltd. (Taiwan). Glutaric acid (99% purity) was purchased from Merck® (Portugal). Glacial acetic acid was obtained from Panreac® (Spain). Purified water was produced using a MilliQ Gradient® Plus Millipore system. All other chemicals were of analytical grade or equivalent.

A 1.4 – Viscosity screening

For the viscosity screening, chitosan solutions (0.5 % (w/v) and 1% (w/v)) were prepared in 1% (w/v) acetic acid solution. Each crosslinking agent was added in different amounts (mmol) per g of chitosan, as detailed in Table A 1.1. Also distinct temperature and time conditions were applied based on and/ or adapted from previous work detailed in literature [10,11,8,7]. For GL-crosslinked chitosan MS, in spite of GL being used in a wide range of concentrations, special attention was given to very similar chitosan MS that have already been described with 0.25 to 4 mL of 50 % GL by 200 mL of 1% acetic acid with chitosan concentrations ranging from 0.1 to 0.5 % (w/v) [11]. In the case of GNP, 0.1 g for 1 % (w/v) chitosan and 1 % (w/v) GNP for 1.5 % (w/v) of chitosan have been used for MS and membranes preparation, and also concentrations of 0.5 to 2 % (w/w) were reported [10,3,12]. For GA, 0.05 to 0.5 % (w/v) concentrations have already been considered in literature [7]. In the case of GLY, some authors have already prepared GLY-crosslinked MS (0.15 g GLY per g of chitosan) [8].

Table A 1.1 – Results from the viscosity study with different crosslinking agents for chitosan dissolved in diluted acetic acid.

Crosslinking agent	**Conditions of crosslinking reaction**	**Concentration (mmol per g of chitosan)**	**Viscosity (cp)**	
			0.5 % (w/v) chitosan	**1 % (w/v) chitosan**
No crosslinker	n/a	n/a	59	108
Glutaraldehyde (GL)	15 min, 300 rpm, RT*	2.5	59	108
		5	58	111
		10	58	149
Genipin (GNP)	3 h, 300 rpm, 50°C	0.2	57	147
		0.8	69	Too viscous
DL-glyceraldehyde (GLY)	30 min, 300 rpm, RT	0.5	57	92
		1	56	97
Glutaric acid (GA)	2 h, 300 rpm, 60°C	0.5	56	93
		1	56	92

RT = room temperature; n/a = not applicable

For viscosity measurements, a rotational viscometer (Visco Star *plus* R, Fungilab SA., Barcelona) was used by immersing the appropriate disc spindle into the obtained solutions-filled cup. The motor torque that is required for turning the spindle against the fluid's viscous forces is proportional to the viscosity, read as centipoise (cp), and corresponding to mPa.s. The rotational speed should not be too high in order to avoid a turbulent flow (Figure A 1.5). For choosing the correct spindle and rotational speed, a specific table (provided by the supplier) should be consulted to know the maximum viscosity that can be measured with the selected conditions. For the work described here, measurements were made with the R2 Spindle at 200 rpm, conditions that allow the measurement of a maximum of 200 cp. Viscometer calibration was performed with the standards 5000 cp and 12500 cp [13].

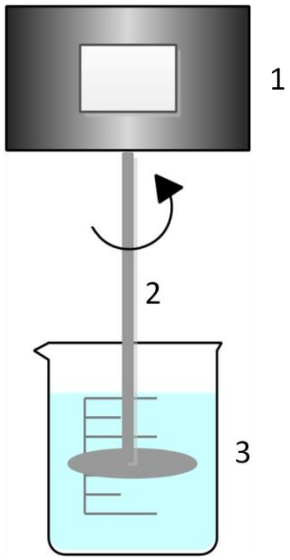

Figure A 1.5 – Schematic representation of a rotational viscometer with the 1) motor, measuring unit and user interface; 2) spindle and 3) sample-filled cup.

A 1.5 – Discussion and conclusion

Distinct crosslinking mechanisms between the crosslinkers and chitosan were reported or suggested (in the case of paucity of data). The choice of crosslinkers' concentration and conditions of crosslinking reaction was based on some published work but also taking into account the results from a viscosity screening study. Such results indicated that GL and GNP promoted a concentration-dependent viscosity. For GL it was observed that an increase in the concentration, from 2.5 mmol to 10 mmol, resulted in an increase of the viscosity from 108 to 149 cp (in the case of 1 % (w/v) chitosan). For GNP, an increase of viscosity was observed for both chitosan concentrations. For GLY and GA, no differences in the viscosity were observed for all the concentrations tested and also between the viscosity of the crosslinked and uncrosslinked chitosan solutions (Table A 1.1). Taking into account the results from viscosity screening and literature references, the selected concentrations of crosslinkers for the preparation of chitosan MS were: 5 and 10 mmol of GL per g of chitosan. For GNP it was 0.2 mmol/g and for both GLY and GA, 1 mmol/g. The obtained solutions were then spray dried and MS obtained appropriately characterized, as described in Chapter 4.

A 1.6 – References

1. Dini E, Alexandridou S, Kiparissides C (2003) Synthesis and characterization of cross-linked chitosan microspheres for drug delivery applications. Journal of Microencapsulation 20 (3):375-385.

2. Gonçalves VL, Laranjeira MCM, Fávere VT, Pedrosa RC (2005) Effect of crosslinking agents on chitosan microspheres in controlled release of diclofenac sodium. Polímeros 15:6-12.

3. Mi F-L, Shyu S-S, Peng C-K (2005) Characterization of ring-opening polymerization of genipin and pH-dependent cross-linking reactions between chitosan and genipin. Journal of Polymer Science Part A: Polymer Chemistry 43 (10):1985-2000.

4. Muzzarelli RAA, El Mehtedi M, Bottegoni C, Aquili A, Gigante A (2015) Genipin-Crosslinked Chitosan Gels and Scaffolds for Tissue Engineering and Regeneration of Cartilage and Bone. Marine Drugs 13 (12):7314-7338.

5. Sailakshmi G, Mitra T, Chatterjee S, Gnanamani A (2013) Engineering Chitosan Using α, ω-Dicarboxylic Acids—An Approach to Improve the Mechanical Strength and Thermal Stability. Journal of Biomaterials and Nanobiotechnology 4 (2):14.

6. Gong R, Li C, Zhu S, Zhang Y, Du Y, Jiang J (2011) A novel pH-sensitive hydrogel based on dual crosslinked alginate/N-α-glutaric acid chitosan for oral delivery of protein. Carbohydrate Polymers 85 (4):869-874.

7. Mitra T, Sailakshmi G, Gnanamani A (2014) Could glutaric acid (GA) replace glutaraldehyde in the preparation of biocompatible biopolymers with high mechanical and thermal properties? Journal of Chemical Sciences 126 (1):127-140.

8. Oliveira BF, Santana MHA, Ré MI (2005) Spray-dried chitosan microspheres cross-linked with d, l-glyceraldehyde as a potential drug delivery system: preparation and characterization. Brazilian Journal of Chemical Engineering 22:353-360.

9. Conti B, Modena T, Genta I, Perugini P, Pavanetto F (1998) A proposed new method for the crosslinking of chitosan microspheres. Drug Delivery 5 (2):87-93.

10. Feng H, Zhang L, Zhu C (2013) Genipin crosslinked ethyl cellulose–chitosan complex microspheres for anti-tuberculosis delivery. Colloids and Surfaces B: Biointerfaces 103 (0):530-537.

11. Ventura CA, Tommasini S, Crupi E, Giannone I, Cardile V, Musumeci T, Puglisi G (2008) Chitosan microspheres for intrapulmonary administration of moxifloxacin: Interaction with biomembrane models and in vitro permeation studies. European Journal of Pharmaceutics and Biopharmaceutics 68 (2):235-244.

12. Kawadkar J, Chauhan MK (2012) Intra-articular delivery of genipin cross-linked chitosan microspheres of flurbiprofen: Preparation, characterization, in vitro and in vivo studies. European Journal of Pharmaceutics and Biopharmaceutics 81 (3):563-572.

13. Daubert CR, Farkas BE (2010) Viscosity Measurement Using a Brookfield Viscometer. In: Nielsen SS (ed) Food Analysis Laboratory Manual. Food Science Texts Series. Springer US, NC, USA, pp 165-169.

Appendix 2

HPLC METHOD VALIDATION FOR DETERMINATION OF LEVOFLOXACIN IN MICROSPHERE SYSTEMS

A 2.1 – Introduction

For characterization purposes of obtained chitosan MS or PLGA MS, there is a need for an analytical method to assess drug content, the LVX released from the MS in the *in vitro* release studies and, the LVX deposited in each stage of the NGI (for MMAD determination).

Some methods for LVX quantification have already been developed and validated by other authors [1-3] and an HPLC method with fluorescence detection developed and validated by INSERM U1070 (FTALAB 28, Poitiers).

LVX content and LVX from NGI experiments of PLGA MS were determined by spectrophotometry. Therefore, the reversed-phase HPLC method, with fluorescence detection described here, was applied for evaluation of LVX content and LVX from NGI experiments of chitosan MS as well as of LVX released in *in vitro* release studies with the prepared chitosan MS and PLGA MS. The method was based on FTALAB 28 method with some chromatographic changes. A partial validation was performed and a number of parameters assessed (suitability, selectivity, precision, accuracy and linearity), according to EMA and FDA regulations [4-6].

A 2.2 – Materials and methods

A 2.2.1 – Materials

LVX hemihydrate was kindly provided by Tecnimede S.A. (Portugal). Phosphate buffered saline (PBS) tablets were obtained from Sigma-Aldrich® (France). PIC B7 was purchased from Waters® (France). Formic acid (99–100%, AnalaR, NormaPur) was obtained from VWR® (France). Acetonitrile of HPLC grade was purchased from Carlo Erba reagents (France). All other chemicals were of analytical grade or equivalent. Purified water was produced using a MilliQ Gradient® Plus Millipore system.

A 2.2.2 – Instrumentation and chromatographic conditions

HPLC analyses of LVX were performed with a chromatographic system consisted of an L-2200 autosampler unit (Lachrom Elite®, Hitachi), an L-2130 pump (Lachrom Elite®,

Hitachi) and an Intelligent Fluorescence Detector JASCO FP-920. The column used for the analysis was a C18 X-Bridge™ HPLC (Waters) column with 5 µm particle size, 2.1 mm internal diameter and 100 mm lenght. The results were acquired and processed using the EZ Chrom Elite software. The mobile phase consisted of a mixture of acetonitrile:water 20:80 (v/v) supplemented with 0.1% (v/v) formic acid and 0.2% (v/v) PIC B7, which was run at a 0.25 mL/min flow rate. The injection volume for each standard and sample was 10 µL and the run time was 8 min. LVX was detected by fluorometry (λ_{ex} = 290 nm; λ_{em} = 460 nm).

A 2.2.3 – Preparation of stock solutions, calibration standards and quality controls (QCs)

Stock solutions of LVX (5 mg/mL) were prepared by dissolving 50 mg of LVX in 10 mL of PBS at pH 7.4, and stored at -20 °C. Two working standard solutions (500 µg/mL and 10 µg/mL) containing LVX were obtained by further dilution of the stock solution in PBS (pH 7.4) in the day of the experiment. Seven calibration standards (0.156, 0.312, 0.625, 1.25, 2.5, 4 and 5 µg/mL) were also freshly prepared in PBS (pH 7.4) by appropriate dilution of working standard solutions and of sequential dilution of calibration standards. QCs (0.156, 0.312, 2.5 and 5 µg/mL) were also considered for assuring the performance of the method.

A 2.2.4 – Sample preparation

LVX content of chitosan MS

For DL determination of chitosan MS, 10 ± 1 mg of LVX loaded-MS were added to 20 mL of 0.1 M hydrochloric acid (3 h, 300 rpm) in order to extract the LVX [7]. An aliquot of 1 mL was collected and centrifuged (3500 rpm, 5 min) prior to further dilution in PBS for LVX quantification.

LVX determination in NGI studies with chitosan MS

NGI studies were performed for MMAD determination. For LVX-loaded chitosan MS, the powder deposited in each stage of the NGI and in the inhaler, adapter and induction port was collected with appropriate volumes of 0.1 M hydrochloric acid to extract the

LVX. After this step, procedure is similar to the one described above for LVX content determination.

LVX released from in vitro release studies with chitosan MS and PLGA MS

For both chitosan MS and PLGA MS, the release studies were carried out in PBS, pH 7.4, at 37 °C and under sink conditions. Briefly, an aliquot was collected at pre-determined time points and centrifuged. An aliquot from supernatant was then kept and appropriately diluted in PBS pH 7.4 for LVX determination. For further details see appropriate sections in Chapter 4 and 5.

A 2.3 – Method validation

The HPLC method was used for LVX determination:

a) in chitosan MS (drug content);

b) in the powder recovered from NGI experiments with chitosan MS;

c) in the *in vitro* release studies with the chitosan MS and PLGA MS.

Once a similar method has already been developed and validated for LVX quantification by HPLC, partial validation was considered at this point and included the parameters that follow.

A 2.3.1 – System suitability

This parameter was evaluated by injecting five times the standard solution 5 µg/mL before starting each run. A well defined and symmetric peak was observed and peak areas and retention time compared between experiments to assure the reproducibility of the system suitability.

A 2.3.2 – Selectivity

This parameter is related to the ability of an analytical method to differentiate the analyte of interest from other components of the samples and from the matrix [4]. Unloaded MS samples (blank MS) were included in the different runs to check the eventual interference

of the polymer/MS components in the LVX peak. Hydrochloric 0.1 M samples were also included to check the presence of interfering peaks. No interference or additional peaks were observed. Thus, the method was considered specific.

A 2.3.3 – Precision and accuracy

Accuracy refers to the closeness of the determined value obtained by the method to the nominal concentration of the analyte and it is expressed in percentage (Bias (%) = (measured concentration/ nominal concentration) x 100). Concerning the precision, it describes the closeness of repeated individual measures of analyte and it is also expressed in percentage as the relative standard deviation (RSD (%)). For both bias (%) and RSD (%), they should not exceed 15 %, except for the lower limit of quantification (LOQ), for which they should not exceed 20 % (see Appendix 3 for details on LOQ approaches) [4].

Precision and accuracy were assessed intra-day and inter-day (from three consecutive days) with four QCs prepared according to the procedure described above.
Repeatability assays were performed with six replicates of each concentration (0.156, 0.312, 2.5 and 5 µg/mL). For intra-day precision and bias, it was evaluated in each day, while for inter-day evaluations, results were compared between the three consecutive days. Results from within-run precision and accuracy are included in Tables A 2.1, A 2.2 and A 2.3 and from between-run analyses in Table A 2.4.

Table A 2.1 – Within-run precision and accuracy for the first day (n=6) of repeatability assays, for validation of LVX determination in PBS pH 7.4 samples.

Nominal concentration (µg/mL)	Mean measured concentration (µg/mL)	SD	RSD (%)	Bias (%)
0.156	0.160	0.003	2.18%	2.40%
0.312	0.314	0.006	2.07%	0.56%
2.5	2.485	0.020	0.79%	-0.61%
5	5.092	0.143	2.81%	1.84%

Table A 2.2 – Within-run precision and accuracy for the second day (n=6) of repeatability assays, for validation of LVX determination in PBS pH 7.4 samples.

Nominal concentration (µg/mL)	Mean measured concentration (µg/mL)	SD	RSD (%)	Bias (%)
0.156	0.154	0.002	1.49%	-1.58%
0.312	0.307	0.004	1.19%	-1.67%
2.5	2.435	0.020	0.82%	-2.59%
5	4.931	0.060	1.22%	-1.38%

Table A 2.3 – Within-run precision and accuracy for the third day (n=6) of repeatability assays, for validation of LVX determination in PBS pH 7.4 samples.

Nominal concentration (µg/mL)	Mean measured concentration (µg/mL)	SD	RSD (%)	Bias (%)
0.156	0.158	0.001	0.37%	1.56%
0.312	0.318	0.005	1.49%	1.98%
2.5	2.511	0.014	0.56%	0.44%
5	5.039	0.027	0.53%	0.79%

Table A 2.4 – Between-run precision and accuracy (n=18) of repeatability assays, for validation of LVX determination in PBS samples.

Nominal concentration (µg/mL)	Measured mean concentration (µg/mL)	SD	RSD (%)	Bias (%)	Average RSD (%)*
0.156	0.157	0.001	0.92%	0.79%	1.35%
0.312	0.313	0.006	1.87%	0.29%	1.58%
2.5	2.477	0.003	0.14%	-0.92%	0.72%
5	5.021	0.060	1.19%	0.42%	1.52%

*mean of RSD (%) from the three days.

All the results from intra-day and inter-day analyses indicated that the method is reliable, accurate and reproducible, since neither RSD (%) nor bias (%) exceed 15 %, being in accordance with the recommendations [4].

A 2.3.4 – Linearity

For the linearity assessment of the method, four calibration curves were constructed with seven calibration standards (0.156, 0.312, 0.625, 1.25, 2.5, 4 and 5 µg/mL). This parameter was calculated resorting to the calculation of the regression line by the method of the least squares. Calibration curves were represented as the peak area versus the standard concentrations and analyzed by the Microsoft Excel® software (Figure A 2.1).

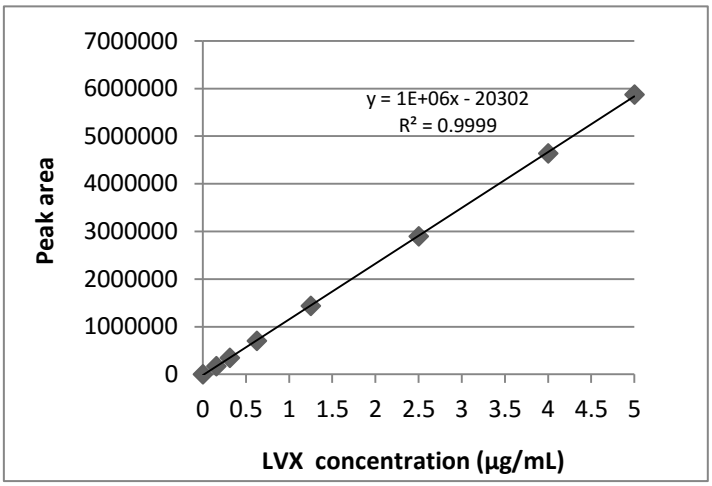

Figure A 2.1 – Linearity study with representation of the LVX calibration curve.

Table A 2.5 – Results from calibration curves performed (n=4) and respective regression coefficients (R^2).

Calibration curve	Slope	Intercept	Coefficient (R^2)
1	1160394	-12415	0.9999
2	1189960	-10313	0.9998
3	1183424	-10676	0.9999
4	1166512	-11314	0.9990
Mean	1175073	-11180	0.9996
SD	13906	921	0.0004
RSD (%)	1.18%	-	0.04%

Table A 2.6 – Back-calculated concentrations (µg/mL) of the calibration standards and between-run precision and accuracy of the method.

	Calibration standards (µg/mL)						
Curve	**0.156**	**0.312**	**0.625**	**1.25**	**2.5**	**4**	**5**
1	0.157	0.309	0.615	1.248	2.507	4.007	5.072
2	0.158	0.304	0.622	1.260	2.508	3.973	5.066
3	0.158	0.307	0.619	1.242	2.494	4.022	5.089
4	0.159	0.308	0.600	1.207	2.444	4.196	5.205
Mean	0.158	0.307	0.614	1.239	2.488	4.050	5.108
SD	0.001	0.002	0.010	0.023	0.030	0.100	0.065
RSD (%)	0.41%	0.68%	1.55%	1.87%	1.21%	2.46%	1.28%
Bias (%)	1.26%	-1.63%	-1.72%	-0.85%	-0.47%	1.24%	2.16%

Results from calibration curve analysis demonstrate that the method is linear since the coefficient, R^2, was at least 0.999 with very low RSD (%) values [8]. In addition, the back-calculated concentrations of the calibration standards presented RSD (%) and bias (%) values always lower than 15%, indicating the compliance with the recommendations (Tables A 2.5 and A 2.6) [4].

A 2.4 – Conclusion

The HPLC method was successfully validated for drug content evaluation, as well for determination of LVX released from the MS using *in vitro* release studies and of LVX deposited in NGI apparatus. It was specific, linear, accurate and reproducible, as demonstrated by the results obtained with the validation procedure.

A 2.5 – References

1. Lalitha Devi M, Chandrasekhar KB (2009) A validated stability-indicating RP-HPLC method for levofloxacin in the presence of degradation products, its process related impurities and identification of oxidative degradant. Journal of Pharmaceutical and Biomedical Analysis 50 (5):710-717.

2. Kassab NM, Amaral MSd, Singh AK, Santoro MIRM (2010) Development and validation of UV spectrophotometric method for determination of levofloxacin in pharmaceutical dosage forms. Química Nova 33:968-971.

3. Salem AA, Mossa HA (2012) Method validation and determinations of levofloxacin, metronidazole and sulfamethoxazole in an aqueous pharmaceutical, urine and blood plasma samples using quantitative nuclear magnetic resonance spectrometry. Talanta 88:104-114.

4. EMA (2011) Guideline on bioanalytical method validation. Committee for Medicinal Products for Human Use, European Medicines Agency, London.

5. FDA (2015) Analytical Procedures and Methods Validation for Drugs and Biologics - Guidance for Industry. Food and Drug Administration, Center for Drug Evaluation and Research (CDER) and Center for Biologics Evaluation and Research (CBER).

6. Shabir GA (2003) Validation of high-performance liquid chromatography methods for pharmaceutical analysis: Understanding the differences and similarities between validation requirements of the US Food and Drug Administration, the US Pharmacopeia and the International Conference on Harmonization. Journal of Chromatography A 987 (1–2):57-66.

7. Osman R, Kan PL, Awad G, Mortada N, El-Shamy A-E, Alpar O (2013) Spray dried inhalable ciprofloxacin powder with improved aerosolisation and antimicrobial activity. International Journal of Pharmaceutics 449 (1–2):44-58.

8. Shabir GA (2004) A Practical Approach to Validation of HPLC Methods Under Current Good Manufacturing Practices. Journal of Validation Technology.

Appendix 3

METHOD VALIDATION FOR LEVOFLOXACIN DETERMINATION IN BRONCHO-ALVEOLAR LAVAGE FLUID BY LC – MS/MS

A 3.1 – Introduction

Distinct polymeric formulations were developed and previously characterized, as stated in Chapter 4, for LVX-loaded chitosan MS and in Chapter 5, for LVX-loaded PLGA MS. Optimization approaches allowed to select two systems for further analyses and for *in vivo* studies, which were carried out to confirm the performance of the formulations and are described in Chapter 6. For the referred *in vivo* assessments, Sprague Dawley® rats were used and blood and BAL sampling performed at pre-determined time points. Briefly, BAL sampling procedure is the administration of 1 mL of saline at 37 °C through the trachea and using a catheter (50 mm deep) followed by rapid aspiration via the same catheter (more details in Chapter 6). LVX determination in BAL is of major importance once it is used to estimate the LVX concentration in ELF. As already described, the urea is measured in both plasma and BAL and, considered as a marker, allows determining the dilution factor to which ELF was subjected during the BAL procedure. Urea measurements in plasma and BAL consist in well defined procedures already validated [1]. However, for LVX determination in BAL, there are few data regarding the analytical method. Therefore, a rapid and simple method for LVX determination in BAL, using ciprofloxacin (CIP) as internal standard (IS) and a LC-MS/MS system was developed and validated, as described in this Appendix. Validation procedure was based on FDA regulations and EMA guidelines for "analytical method validation" and according to Good Laboratory Practices [2,3]. A number of parameters were assessed and included: suitability, selectivity, precision and accuracy, linearity, effect of dilution and stability. Some details about parameters not yet described in Appendix 2, will be included here.

A 3.2 – Materials and methods

A 3.2.1 – Materials

LVX hemihydrate was kindly provided by Tecnimede S.A. (Portugal). CIP (solution for injection, bag for infusion 2 mg/mL) was purchased from Panpharma S.A. (France). Sodium chloride (0.9% NaCl solution for injection) was obtained from C.D.M. Lavoisir (Laboratoires Cbaix et Du Marais, France). Formic acid (99–100%, AnalaR, NormaPur) and methanol of HPLC grade were obtained from VWR® (France). Acetonitrile of HPLC grade was purchased from Carlo Erba reagents (France). All other chemicals were of

analytical grade or equivalent. Purified water was produced using a MilliQ Gradient® Plus Millipore system.

A 3.2.2 – LC-MS/MS instrumentation and conditions

The LC-MS/MS system consisted of a Waters Alliance 2695 separations module equipped with a binary pump and an autosampler thermostatically controlled at 4 °C, and of a Waters Micromass® Quattro micro API triple quadrupole tandem mass spectrometer. The mass spectrometer was operated in the positive-ion mode. Ions were analyzed via multiple reaction monitoring (MRM) employing the transition of the $[M + 2H]^{2+}$ precursor to the product ions for analyte and IS (see transition ions in Table A 3.1). Optimal MS/MS set up parameters are included in Table A 3.2.

Table A 3.1 – Transitions ions for LVX and CIP (IS).

Transition (m/z)	Compound	Internal standard	Dwell time (ms)
362.2 → 318.2	LVX		500
332.2 → 314.2		CIP	500

Table A 3.2 – MS/MS set up parameters for LVX analysis in BAL.

	LVX	**CIP**
Ion spray voltage (kV)	3.25	3.25
Cone potential (V)	25	25
Extractor (V)	2	2
RF lens (V)	0.1	0.1
Source temperature (°C)	120	120
Desolvation temperature (°C)	350	350
Cone Gas (N_2) flow (L/h)	10	10
Desolvation Gas (N_2) flow (L/h)	600	600
LM 1 resolution	13.5	13.5
HM 1 resolution	13.5	13.5
Ion Energy 1	0.5	0.5
Entrance	0	0
Collision energy	20	20
Exit	1	1
LM 2 Resolution	13.5	13.5
HM 2 Resolution	13.5	13.5
Ion Energy 2	2	2
Multiplier (V)	750	750

For the reversed-phase chromatography, it was performed with a Phenomenex Jupiter TM C18 300 Å column (5.0 µm, 50 x 2.1 mm). The mobile phase was composed of 0.1% (v/v) formic acid in acetonitrile and 0.1% (v/v) formic acid in water (25:75 (v:v)). The flow rate was 0.20 mL/min and the injection volume 20 µl. All data were acquired and analyzed with the MassLynx Version 4.0 software.

A 3.2.3 – Preparation of stock solutions, calibration standards and quality controls

Stock solutions of 1mg/mL LVX were prepared by dissolution of 10 mg of LVX in 10 mL of methanol/water (50:50), which demonstrated to be stable at least for a period of 1 month if stored at – 20° C. Working standard solution of IS was freshly prepared each day by diluting the 2 mg/mL CIP solution in 0.1 % formic acid in water, and obtaining a 0.05 µg/mL solution.

Working standard solution of LVX (10 µg/mL) was obtained by dilution from the stock solution in methanol/water (50:50).

Eight calibration standards (400, 300, 200, 40, 20, 10, 5 and 2 ng/mL) were obtained by appropriate dilution of the working standard solution or from the dilution from themselves in NaCl 0.9 %.

Five replicates of each QC were prepared in similar way as calibration standards, included a low QC (2 ng/mL), two intermediate QCs (5 and 40 ng/mL) and a high QC (400 ng/mL).

A 3.2.4 – Sample preparation

BAL samples were centrifuged at 3500 rpm for 5 min and supernatants stored at - 20°C until analysis. Briefly, 20 µL of supernatant were added to 80 µL of IS (0.05 ng/µL) in 0.1% (v/v) formic acid, directly in the vials for analysis and mixing by suction-discharge.

A 3.3 – Method validation

The LC-MS/MS method for LVX determination in BAL samples was validated according to FDA and EMA regulations and the parameters considered were: system suitability, selectivity, precision and accuracy, lower limit of quantification, goodness of fit, dilution effect and stability.

A 3.3.1 – System suitability

This parameter was evaluated by injecting five high concentrated standards (400 ng/mL) before starting each run. The consistency of the peak of analyte and IS was verified.

A 3.3.2 – Selectivity

Blank samples (NaCl 0.9 % solution) were included in the different runs to check the eventual interference in the LVX and IS surface areas. An interference lower than 20 % of the LOQ for the analyte and 5 % for the IS is acceptable [2].

A 3.3.3 – Precision and accuracy

Precision and accuracy were evaluated intra-day and inter-day with standards prepared according to the procedure described in the section A 3.2.3. Repeatability assays were performed with 5 replicates of each concentration (2, 5, 40 and 400 ng/mL). Intra-day precision and accuracy were evaluated in each day. For inter-day assessments, the precision and accuracy were evaluated through three days. For the precision it is expressed as the RSD (%). For the accuracy, the measured concentration is compared with the nominal concentration, as a percentage (Bias, %). Accuracy and precision both within-run and between-run results are included in Table A 3.3, A 3.4, A 3.5 and A 3.6.

Table A 3.3 – Within-run precision and accuracy for the first day (n=5) of repeatability assays, for validation of LVX determination in BAL samples.

Nominal concentration (ng/mL)	Mean measured concentration (ng/mL)	SD	RSD (%)	Bias (%)
400	391.012	9.182	2.35%	-2.25%
40	34.552	1.554	4.50%	-13.62%
5	5.398	0.234	4.34%	7.96%
2	2.150	0.101	4.69%	7.50%

Table A 3.4 – Within-run precision and accuracy for the second day (n=5) of repeatability assays, for validation of LVX determination in BAL samples.

Nominal concentration (ng/mL)	Mean measured concentration (ng/mL)	SD	RSD (%)	Bias (%)
400	343.116	20.709	6.04%	-14.22%
40	36.210	0.906	2.50%	-9.48%
5	5.438	0.516	9.50%	8.76%
2	1.884	0.170	9.04%	-5.78%

Table A 3.5 – Within-run precision and accuracy for the third day (n=5) of repeatability assays, for validation of LVX determination in BAL samples.

Nominal concentration (ng/mL)	Mean measured concentration (ng/mL)	SD	RSD (%)	Bias (%)
400	357.469	5.927	1.66%	-10.63%
40	37.933	1.743	4.60%	-5.17%
5	5.319	0.114	2.14%	6.37%
2	2.192	0.140	6.38%	9.62%

Table A 3.6 – Between-run precision and accuracy (n=15) of repeatability assays, for validation of LVX determination in BAL samples.

Nominal concentration (ng/mL)	Mean measured concentration (ng/mL)	SD	RSD (%)	Bias (%)	Average RSD (%)*
400	363.866	7.767	2.13%	-9.03%	3.35%
40	36.232	0.458	1.26%	-9.42%	3.87%
5	5.385	0.207	3.84%	7.70%	5.33%
2	2.076	0.035	1.68%	3.78%	6.70%

*mean of RSD (%) from the three days.

Results from intra-day and inter-day repeatability assays demonstrated that the method is accurate and precise, once bias and RSD are lower than 15 % for all the analyses. Actually, a maximum of 15 % of bias/ RSD is acceptable and for the LOQ, 20 % is accepted [2].

A 3.3.4 – Lower limit of quantification

Several approaches can be applied for LOQ determination. The most practical approach and the one applied in this dissertation is the LOQ based on precision and accuracy (bias) data. The LOQ is defined as the lowest concentration of a sample that can still be quantified with acceptable precision and accuracy [4].

The LOQ for LVX in BAL samples was found to be 2 ng/mL, i.e., the lowest concentration still determined with acceptable precision and accuracy.

A 3.3.5 – Linearity

Linearity of the method was evaluated over the range 2 – 400 ng/mL of LVX. The calibration curves (n=4) were determined by quadratic regression analysis, $y = a + bx + cx^2$. The ratio of LVX peak area to IS peak area was plotted versus the calibration standards concentrations. Results are included in Table A 3.7 and A 3.8.

Table A 3.7 – Results from calibration curves performed (n=4) and respective regression coefficients (R^2).

Calibration curve	Slope (b)	Intercept (a)	Coefficient (R^2)
1	0.00869668	-0.0005588	0.99587
2	0.00960	-0.0003683	0.99373
3	0.01000	-0.0026639	0.99691
4	0.00962	0.0011366	0.99146
Mean	0.00948	-0.00061	0.99449
SD	0.00055	0.00156	0.00242
RSD (%)	5.83%	-	0.24%

Table A 3.8 – Back-calculated concentrations (ng/mL) of the calibration standards and between-run precision and accuracy of the method.

	Calibration standards (ng/mL)							
Curve	**400**	**300**	**200**	**40**	**20**	**10**	**5**	**2**
1	380.001	315.844	206.710	35.907	20.290	10.073	5.355	1.947
2	396.556	290.901	215.195	36.529	19.055	11.321	4.857	1.987
3	398.775	301.156	202.515	37.585	19.492	10.064	5.515	1.926
4	369.517	328.325	205.437	35.504	18.787	10.745	5.483	1.915
Mean	386.212	309.056	207.464	36.381	19.406	10.551	5.302	1.944
SD	13.930	16.426	5.445	0.906	0.657	0.604	0.305	0.032
RSD(%)	3.61%	5.31%	2.62%	2.49%	3.39%	5.73%	5.75%	1.63%
Bias(%)	-3.45%	3.02%	3.73%	-9.05%	-2.97%	5.51%	6.05%	-2.81%

Results from linearity evaluation demonstrated a R^2 always higher than 0.99 and bias (%) of back-calculated concentrations lower than 15 %, confirming that the method is linear.

A 3.3.6 – Dilution effect

The influence of the dilution (dilution factor of 1/100) with NaCl 0.9% (the matrix for BAL) was assessed to assure that the dilution of BAL samples allows concentration determinations with precision and accuracy. Results are included in Table A 3.9.

Table A 3.9 – Evaluation of the influence of dilution by repeatability assays (n=5).

Nominal concentration (ng/mL)	Measured concentration (ng/mL)	Mean (ng/mL)	SD	RSD (%)	Bias (%)
10000	11151.460	11117.60	1142.538	10.28%	11.18%
	11869.310				
	12407.020				
	9432.050				
	10728.140				

Results from repeatability assays demonstrate that dilution can be performed once bias and RSD values are lower than 15%.

A 3.3.7 – Stability

Stability tests were performed by using repeatability assays of two QCs (5 and 400 ng/mL) under distinct conditions, which correspond to those that samples can be subjected to during the studies and include: freeze and thaw stability; short term stability at room temperature (~ 25 °C) and auto-sampler stability (4 °C), as is referred in the EMA guidelines [2]. Long-term stability was not considered taking into account that studies were performed in the few days after the BAL sampling. Results are included in Tables A 3.10, A 3.11 and A 3.12.

Table A 3.10 – Freeze and thaw stability results after three freeze-thaw cycles (n=5).

Nominal concentration (ng/mL)	Mean measured concentration (ng/mL)	SD	RSD (%)	Bias (%)*
400	365.345	24.053	6.58%	-8.66%
5	5.446	0.223	4.09%	8.93%

*compared to the nominal concentration

Table A 3.11 – Auto-sampler stability results after 24 h in the autosampler (T = 4° C), (n=5).

Nominal concentration (ng/mL)	Mean measured concentration (ng/mL)	SD	RSD (%)	Bias (%)*
400	349.104	18.325	5.25%	-12.72%
5	5.025	0.391	7.79%	0.50%

*compared to the nominal concentration

Table A 3.12 – Short term stability results after 24 h at room temperature (n=5).

Nominal concentration (ng/mL)	Mean measured concentration (ng/mL)	SD	RSD (%)	Bias (%)*
400	348.328	13.548	3.89%	-12.92%
5	5.942	0.030	0.50%	18.84%

*compared to the nominal concentration. For standard 5 ng/mL, bias was 9.27 %, when compared with the mean measured concentration from the reference sample.

The results may infer that the analyte is stable under the studied conditions, once the results denoted the precision and accuracy of the results [2,3,5].

A 3.4 – Conclusion

A specific, linear and reproducible method for measuring LVX in BAL samples was developed and validated over the range 2 – 400 ng/mL. It was successfully applied to the BAL centrifuged samples collected from the Sprague-Dawley rats used in the *in vivo* studies, as described in Chapter 6.

A 3.5 – References

1. Gontijo AVL, Brillault J, Grégoire N, Lamarche I, Gobin P, Couet W, Marchand S (2014) Biopharmaceutical Characterization of Nebulized Antimicrobial Agents in Rats: 1. Ciprofloxacin, Moxifloxacin, and Grepafloxacin. Antimicrobial Agents and Chemotherapy 58 (7):3942-3949.

2. EMA (2011) Guideline on bioanalytical method validation. Committee for Medicinal Products for Human Use, European Medicines Agency, London.

3. FDA (2015) Analytical Procedures and Methods Validation for Drugs and Biologics - Guidance for Industry. Food and Drug Administration, Center for Drug Evaluation and Research (CDER) and Center for Biologics Evaluation and Research (CBER).

4. De Bièvre P, Günzler H (2005) Validation in Chemical Measurement. 1 edn. Springer-Verlag Berlin Heidelberg, Berlin.

5. FDA (2001) Guidance for industry: Bioanalytical Method Validation.

“It’s the little details that are vital. Little things make big things happen.”

John Wooden